On the plastic behaviour of multi directional epoxy-bolted CFRP laminates

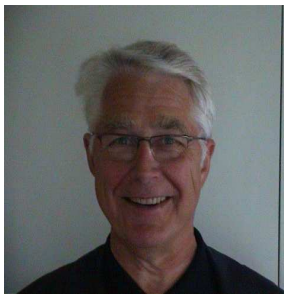

Aage P. Jensen
Ph.D., Associate Professor
Technical University of Denmark Building 118, DK-2800 Lyngby
aapj@byg.dtu.dk

Ervin Poulsen
Professor Emeritus of C.Eng.
8 Skovbrynet, Nodebo DK-3480 Fredensborg
ervin-poulsen@get2net.dk

ABSTRACT

The second generation of CFRP laminate has recently been developed. It is a multi directional CFRP laminate, i.e. a laminate with carbon fibres having several directions other than the first generation. The paper describes the laboratory tests carried out in order to develop anchorage devices for such multi directional CFRP laminates which are epoxy-bonded and bolted or nailed to the concrete substrate for the purpose of strengthening against failure caused by bending. The tests were carried out at the Technical University of Denmark, IABM and BYG · DTU.

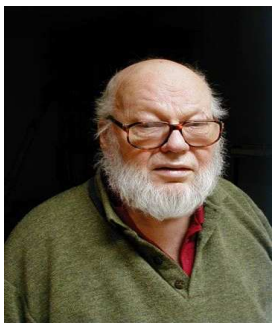

Key words. Multi directional CFRP laminates. Anchorage by bolts. Test methods.

1. INTRODUCTION

Strengthening of RC structures by means of external bonded reinforcement has been used for many years. However, it was the use of carbon fibre reinforced polymer laminates which really accelerated the application.

The first CFRP laminates used as external bonded reinforcement were composed of uni directional fibres bonded together with epoxy or vinyl ester resin. These CFRP laminates have a smooth surface and are produced in widths of 40 mm to 120 mm. The thickness is typically 1.2 mm to 1.4 mm. These CFRP laminates have a very high tensile strength, but since the fibres are parallel, the tensile strength perpendicular to the longitudinal axis is very low. Thus, they cannot be anchored with bolts or nails to the concrete substrate. Therefore, special anchoring devices have to be developed, cf. *Poulsen* [1].

2. NEW CFRP COMPOSITES OF TRADECC

The anchoring of the first generation of CFRP laminates by special anchoring devices is rather time consuming and expensive. Therefore, TRADECC has developed new CFRP laminates which contain fibres in the plus and minus 45° direction, besides the longitudinal direction. These CFRP laminates are manufactured on request in a width of 50 mm to 600 mm and an effective thickness of 1.0 mm to 30 mm. The length is available according to request. A scrim cloth (peel tape) protects both surfaces, cf. Figure 1. The packing depends on the length and thickness of the laminates.

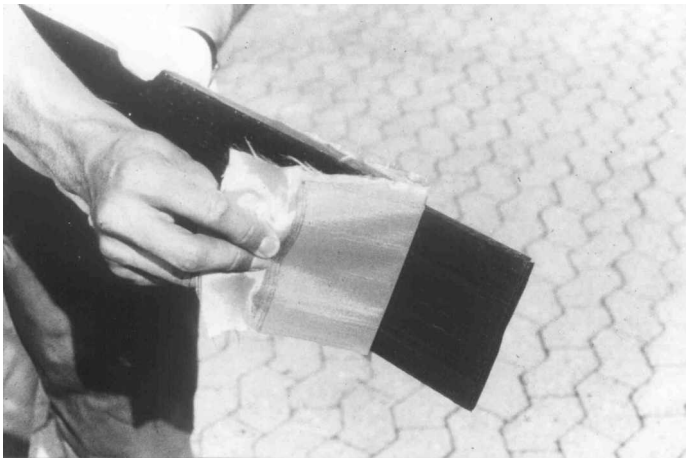

Figure 1 - A scrim cloth (peel tape) protects the surface of the CFRP laminate.

2.1 PC CarboComp Plus laminates

The laminates described above are PC CarboComp Plus and have the following advantages:

- They can be anchored to the concrete substrate with bolts and nails. The stresses in the bored longitudinal fibres are transferred to the adjoining fibres by the fibres in the plus and minus 45° direction. The anchoring increases the bearing capacity and allows a higher load than the first generation CFRP laminates, all other being equal, since the embedded strength of the anchoring bolts have a plastic failure, cf. Figure 2 and 3. Therefore, the partial safety factor is considerable lower than that of a brittle failure; cf. *DS 411:1999* [2].
- They are produced in the width of the beam so the contact surface is maximum and only one laminate is required.
- They have a rough, clean surface (the scrim cloth is easily peeled of), cf. Figure 1, so there is no need for high pressure blasting or degreasing before gluing.

The width of a standard PC CarboComp Plus laminate is 100 mm and the effective thickness of the laminate is 1.0 mm.

Figure 2 - Shear failure of CFRP laminate.

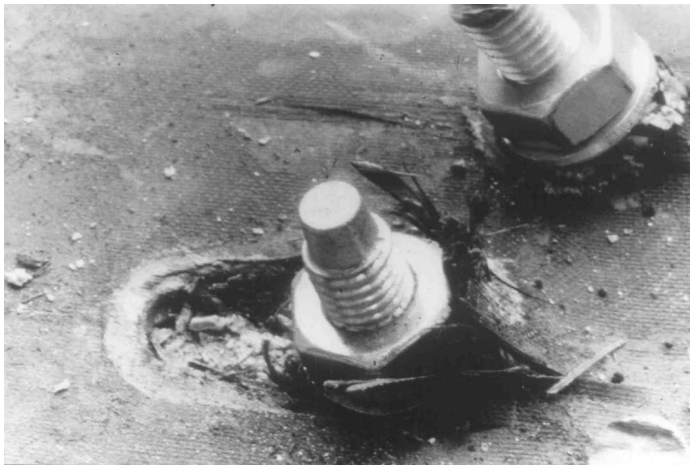

Figure 3 - Plastic failure of bolts after testing the beam.

2.2 Properties of PC CarboComp Plus laminates

The main properties of PC CarboComp Plus laminates are as shown in Table 1.

Table 1 - Properties of PC CarboComp Plus laminates

Properties	Values
Tensile strength	> 2850 MPa
Modulus of elasticity	> 175 GPa
Maximum elongation	≈ 1.65 %
Density	≈ 1600 kg/m^3
Water absorption	< 0.1 %
Application temperature	From – 40 ^{O}C to + 130 ^{O}C

3 EXPERIMENTAL DATA

In order to study the anchorage of PC CarboComp Plus laminates to concrete substrate by means of epoxy and bolts, tests were carried out at the Technical University of Denmark, IABM DTU. From earlier tests on bolted connections of multi directional CFRP laminates it was expected that the failure of bolted connections due to fail of the embedded strength had a plastic behaviour, cf. *Croes et al.* [3] and *Turvey et al.* [4]. The following presentation is based upon work of *Beck & Jacobsen* [5].

3.1 Single bolt test set-up

The aim of these tests was to determine the embedded strength of the multi directional CFRP laminates (the bearing failure) versus the diameter of the bolt and the distance from the bolt to the end of the CFRP laminate, applying two widths of the laminates, 100 mm and 50 mm.

The bolt was fixed in a predrilled hole of the laminate. Various versions of the joint were pre-tested before the final selection of the joint. Then, the tests were carried out by prestressing the bolts by means of a nut and washer on both sides of the laminates, applying a controlled torque of 10 kpm. This arrangement was necessary in order to keep the laminate in a plane position as is the case when glued and bolted to the concrete substrate. The tensile force was transmitted through the bolt to the CFRP laminates by means of a U-shaped fork.

3.2 Failure of embedded strength

The PC CarboComp Plus used had an effective thickness of 1.0 mm and a width of 50 mm and 100 mm. The distance from the bolt to the end of the CFRP laminate was 25 mm, 50 mm, 75 mm and 100 mm. There was no significant influence of the width and the distance from the bolt to the end of the laminate. There was an excellent plastic behaviour of the failure. However, in order to achieve a decent long plastic behaviour it was concluded that the minimum distance from the bolt to the end of the laminates ought to be 50 mm. Tests results are shown in Table 2. It may be detected that the characteristic value (i.e. 5 % fractile) is approx. 1000 MPa, almost independent of the diameter of the bolts in these tests, i.e. from ∅ 10 mm to ∅ 24 mm.

Table 2 – Embedded strength of CFRP laminates loaded by embedded bolts vs. bolt diameter.

Properties	Units	∅10 mm	∅16 mm	∅20 mm	∅24 mm
Nos. of tests	Nos.	36	27	21	20
Mean value	MPa	1514	1328	1687	1830
Deviation	MPa	242	194	418	331
5 % fractile	MPa	1023	967	1039	1186

3.3 Tests of PC CarboComp Plus laminates bolted to concrete substrate

To study the interaction of an epoxy-bolted PC CarboComp Plus laminate the test set-up shown in Figure 4 was used. Tests results showed that the embedded failure of the laminate is plastic while the failure of concrete is brittle. It was also documented that the HILTI design of bolts embedded in concrete could be used.

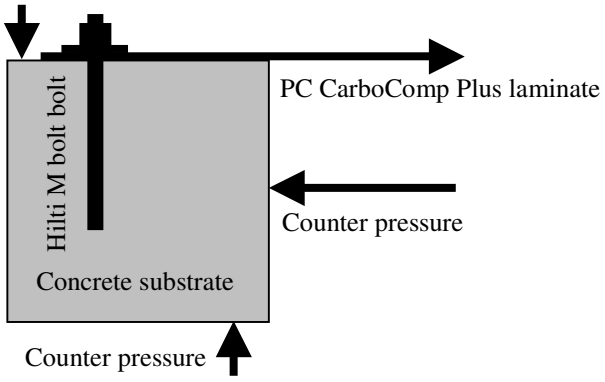

Figure 4 – Test set-up for a single bolt anchored to the concrete.

4 CONCRETE BEAMS

In concrete beams strengthened by an external bonded carbon fibre laminate, debonding of the laminate usually takes place at a sudden when the beam is loaded by an increasing load. The sudden debonding is caused by an unstable crack between the laminate and the substrate, cf. *Neubauer et al.* [6]. The debonding results in an undesirable drop in the bearing capacity of the beam and ways to avoid it should be looked for.

One way to escape the drop in the bearing capacity might be to use a CarboComp Plus laminate anchored to the beam by bolts as demonstrated above. When debonding takes place it is supposed that the bolts will assure a continuation of the connection between laminate and

substrate and since the laminate 'yields' under a constant load it might be expected that the load on the beam also will be constant even for considerable deflections.

In order to test such an idea and to obtain information about the influence of the bolt pattern and the number of bolts necessary a number of 10 beams were tested. Two of the beams were tested in a pre-testing series.

In simple supported beams strengthened by e.g. a Sika CarboDur laminate the laminate is supposed to be self-anchored by extended ends of the plate, cf. *Neubauer* [7]. With such a focus on the end of the plate and with the conception that debonding often starts at the ends of the plate it was decided to place all bolts at the ends of the laminate and only vary the number of bolts.

4.1 The pre-testing beams

Testing was carried out of 2 Nos. 3000 mm long RC beams, cross-section 300 × 300 mm, each strengthened by a single 100 × 2.0 mm multi directional laminate from TRADECC in Belgium. The beams were tested by an Amsler beam test rig. The beams were simply supported and loaded by two equal forces at the middle of the span. The strengthening of the beams was as follows:

- The CFRP laminate of one of the beams was, besides being glued to the substrate by epoxy adhesive anchored to the substrate by five HILTI stainless steel bolts, ∅ 10 mm M bolts, in one end of the CFRP laminate and seven bolts in the other. The bolts were placed into holes ∅ 12 mm, drilled into the substrate and injected with a HILTI adhesive. Each nut was tightened by a torque of 5 kpm.
- The CFRP laminate of the other beam was, besides being glued to the substrate by epoxy adhesive anchored to the substrate by 37 HILTI stainless steel nails, ∅ 3.7 mm Kwik DNH, in both halves of the CFRP laminate. The laminate was predrilled with a ∅ 5 mm drill and fixed by means of powder actuated nails.

Epoxy bonded CFRP Laminate Anchored by Bolts. According to the evaluation the used method of design has been satisfactory in coordination with the observations made. The load-deflection diagram showed a remarkably long plastic branch (with a constant load bearing capacity) so that it is possible to count on a warning, plastic failure. Due to the test set-up the anchorage was not loaded to failure.

The beam was designed so the anchorage was the weakest link. The failure mode of the anchorage was a 'yielding' of the anchorage, yielding of the embedded bolts and 'yielding' as a result of the embedded strength of the CFRP laminate. The test was cut off by a deviation of the anchorage of approx. 40 mm compared to the substrate.

This testing documents that it is possible to obtain a plastic failure (with warning) of an epoxy-bonded anchorage, bolted to the substrate. This means, that it is possible to harmonize a strengthening of a RC beam (or a RC slab) with epoxy-bolted multi directional laminates so that it is not necessary to use a high partial safety factor against a brittle failure (a speciality of the Danish Code of Practice) for the reason of a tension failure in the concrete or the CFRP laminate. A low safety factor may be used, when a ductile failure is decisive.

Epoxy bonded CFRP Laminate Anchored by Powder Actuated Nails. According to the evaluation the used method of design has been satisfactory in coordination with the observations made. The load-deflection diagram was monotonously increasing with the deflection until a

brittle failure took place (i.e. an unwarning failure).

This failure occured as a sliding failure of the concrete, following a plane just below the tips of the nails. It is the plan to consider if it is possible to obtain a plastic failure by other types of nails, another thickness of the CFRP laminate or combinations.

Epoxy-nailed CFRP laminates have their advantages in the mounting. Thus, it is justified to study if it is possible to obtain a 'plastic' failure.

5. BEAM TESTS

5.1 Test specimens

A test program consisting of 8 test beams of length 4.5 m was carried through by students, cf. *Olsen et al*. [8] under supervision of the authors. The beams had all the same dimensions and were reinforced by two rebars, 2 ∅16 mm as shown in Figure 5. Despite one beam all beams were also reinforced by an externally bonded multi directional CFRP plate 1×100 mm. The plate was in its full length glued to the beam by an epoxy adhesive and further fixed to the beam by a number of bolts, ∅10 in both ends. To secure that failure took place at end (A) two more bolts were added in end (B) than in end (A). The bolts in end (A) were placed in the laminate in accordance with the pattern shown in figure 2 starting next to the end of the laminate. The bolts were placed into holes ∅12 mm, drilled into the concrete and injected by an adhesive. A torque of 5 kNm tightened each nut. In the beam with 3 bolts the laminate was further fixed by a number of powder – actuated stainless nails, ∅3.7 mm.

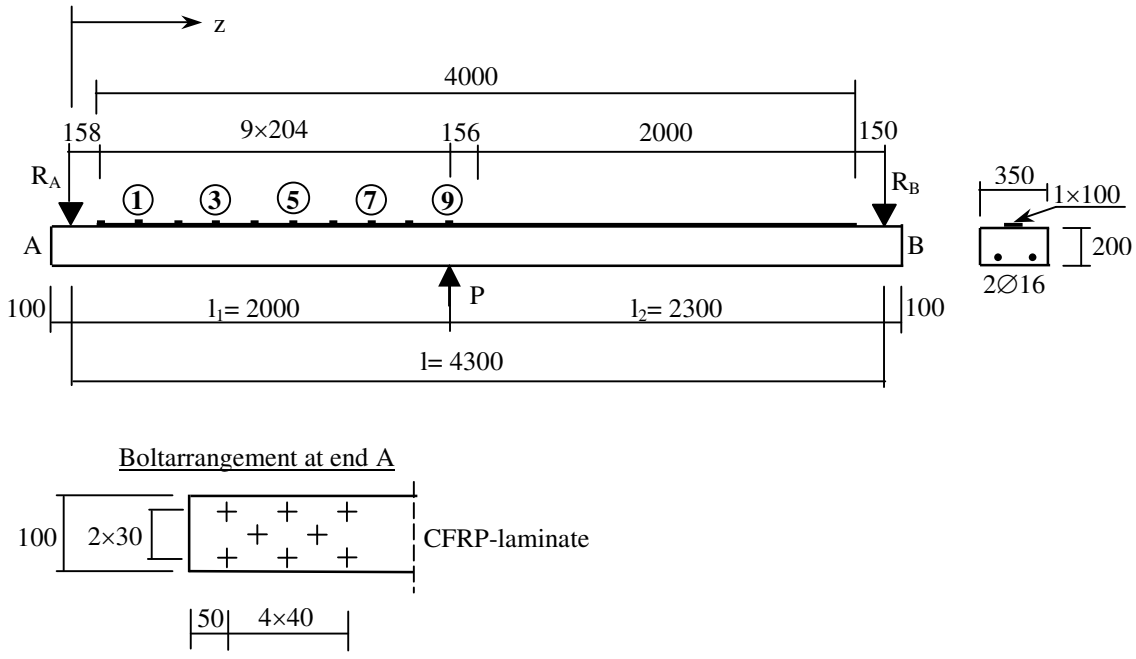

Figure 5 – Test specimen with placement of load P, CFRP-laminate and strain gauges shown. Bolts at end B(right end) are not shown.

The concrete had a compressive strength of 31 MPa. The beams were labelled no.x.x where the first digit designates the number of CFRP plates and the second digit the number of bolts at end

(A). A reference beam with no plate and no bolts is labelled no. 0.0 while the rest are labelled from no.1.0 to no.1.5 and no.1.8.

Figure 6 – Test set-up of the test beam.

5.2 Test set-up

The beams were tested in an Amsler beam test rig, cf. Figure 6. The beams were simply supported at both ends and loaded by a single force P displaced 150 mm from the middle of the beam towards end 'A' to promote failure to take place at this end. The beams were tested upside down with a load speed of 2 kN/min until debonding of the laminate and then with a speed of 1 kN/min.

The strains in the laminate were monitored by 10 strain gauges (Nos. 0 - 9) placed along the one halve part (A) of the beam, see figure 5. The deflections of the beam were monitored at both ends and at the mid-point besides at two more points in between. All tests were performed at room temperature.

5.3 Test results

The first beam to be tested was the beam with no external plate (no. 0.0). The beam behaved as expected, but the test was stopped unintentionally when yielding of the rebars started for a displacement of the mid-point of approximately 50 mm. All other beams were loaded until the deflection of the mid-point reached a value of approximately 100 mm.

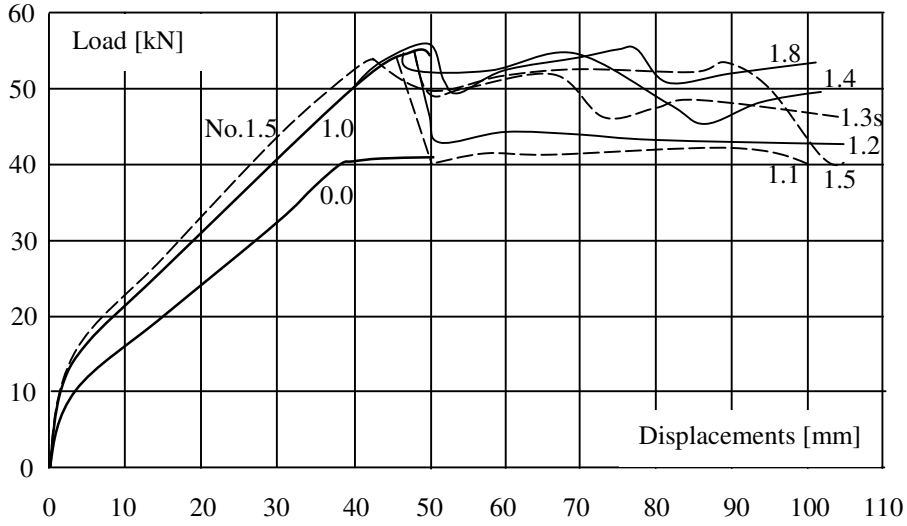

Figure 7 – Load-deflection diagrams for all test specimens.

All beams reinforced with a CFRP-laminate behaved in the same way independently of the number of bolts until debonding took place. Vertical cracks due to bending developed smoothly as expected for the increasing load the distance between two such consecutive cracks being about 70 mm in mean.

Debonding of the plates had the form of a crack in the concrete just below the plates starting from the middle of the beam and in all cases but one running towards the end 'A'. In the beam with no bolts (no. 1.0) the crack developed at a sudden with no warning while in beams with bolts at the ends debonding had a stable character in the very beginning.

In figure 7 deflections of the mid-point of the beam is shown as function of the load *P*. It is observed that:

- The maximum load is increased from 40.9 kN for the reference beam (no.0.0) to 54.7 kN for beam no.1.0 with one bonded plate and no bolts.
- The maximum load 54.7 kN is (almost) independent of the number of the bolts.
- After maximum load is reached and debonding takes place the load drops to a lower and more or less constant level depending of the number of bolts. The drop has a tendency to decrease with the increasing number of bolts.

Thus the multi directional CFRP laminate increases the maximum load on the beam with more than 30% while bolts placed at both ends of the plate have no effect. After debonding at maximum load bolts have a varying effect on the bearing capacity but the chosen bolt pattern is in all cases inadequate to keep the load at maximum level after debonding.

During loading strains along the mid axis of the plate were recorded with time intervals of 20 or 10 seconds. It turned out that even a 10 seconds interval was insufficient to catch all details of the strain distribution when debonding was about to take place at maximum load.

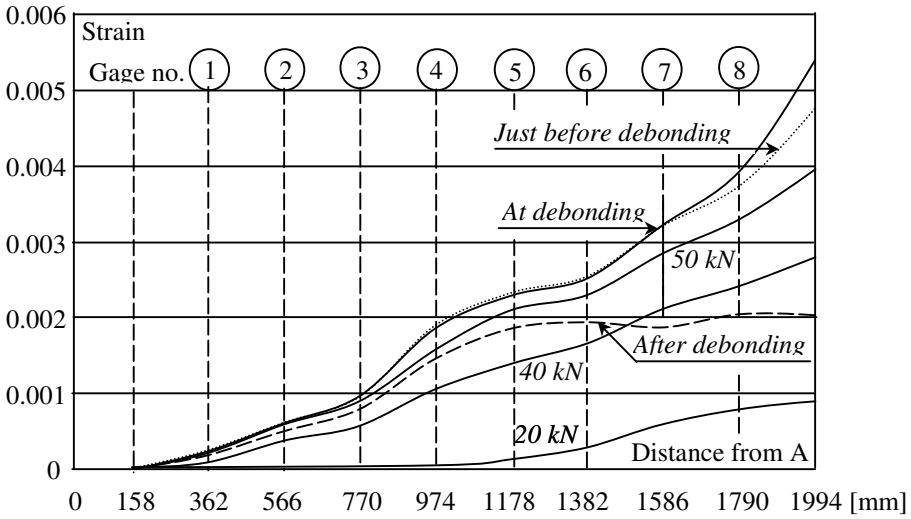

Figure 8 – Strain distribution in the plate at different load levels for beam no.1.5.

As a representative example the strain distribution for beam no.1.5 is shown in Figure 8 for different load levels. In this case the strains are recorded every 10 seconds. It is seen that independent of the load level the strains increase towards the centre of the beam as long as debonding has not started. It is further observed that the strain gradient changes along the beam and increases with the load over most parts of the beam. At debonding the strain gradient reaches its maximum next to the centre of the beam probably due to yielding of the rebars. After debonding the strains drop dramatically to an almost constant level over large parts of the beam. In several cases the plate debonds completely and is in such cases only fixed to the beam by the bolts, which carry same residual load.

In general the strain distribution before debonding is as expected. The almost linear strain distribution next to the end of the beam indicates a state with no bending-cracks in contrast to the central part of the beam where the increasing strain gradient indicates yielding of the rebars. In the transition zone between the two parts the strain gradient reaches an unaccountable level.

Since debonding is crucial for strengthening of any beam with a CFRP laminate it is of great importance to create a model that can handle the onset of debonding. A model based on fracture mechanics is proposed by *Neubauer et al*. [6], but it has a drawback with respect to simplicity.

In this study debonding always takes the form of a crack in the concrete why the reason is that the strength parameters of the concrete must govern the onset of debonding. Thus a working hypothesis might be as simple as a shear failure between the plate and the substrate and the model propose itself and takes the form illustrated in Figure 9.

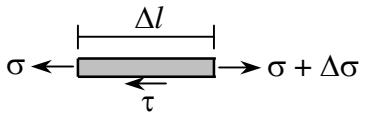

Figure 9 – Plate element of length Δl with stresses.

At two consecutive sections in the plate Δl apart, the normal stresses are σ and $\sigma + \Delta\sigma$ respectively. As long as debonding of the plate has not yet taken place the difference in the normal stresses is equilibrated by a shear stress τ along the bottom of the plate. For an even stress distribution equilibrium takes the form:

$$\Delta\sigma \times t \times b = \tau \times \Delta l \times b \tag{1}$$

or

$$\tau = t \times \frac{\Delta\sigma}{\Delta l} = t \times E \times \frac{\Delta\varepsilon}{\Delta l} \;\Rightarrow\; t \times E \times \frac{d\varepsilon}{dl} \quad \text{for } \Delta l \to 0 \tag{2}$$

where
- t is the thickness of the plate,
- b is the width of the plate,
- E is the modulus of elasticity for the laminate.

In Table 3 the maximum strain difference between two consecutive strain gauges for each beam at failure is given. It is observed that the maximum strain difference has a tendency to increase with the number of bolts with the beam without bolts as an exception. In average the strain difference $\Delta\varepsilon = 0.00130$ over a length $\Delta l = 204$ mm.

Table 3 – Maximum strain difference at failure

Beam no.	Gauge no.	Strain difference
1.0	6-7	0.00158
1.1	7-8	0.00069
1.2	7-8	0.00102
1.4	8-9	0.00110
1.5	8-9	0.00144
1.8	6-7	0.00197
Average		0.00130

Inserting into the formula above one finds that in average the maximum shear stress at debonding is:

$$\tau_{average} = 1 \times 175000 \times \frac{0.00130}{204} = 1.12 \text{ MPa} \tag{3}$$

The values of thickness t and the modulus of elasticity E are effective and minimum values respectively. The strain difference $\Delta\varepsilon$ over the length Δl represents the slope of the chord line, which is less than the maximum slope of the tangent, so for this reasons the calculated value of the average shear stress at debonding must be a minimum value, i.e. $\tau_{\text{average}} > 1.12$ MPa.

The shear strength of the concrete is difficult to access but if it is put equal to the tension strength one has according to the Danish code *DS 411:1999* [2]

$$\tau_{\max} = \sqrt{0.1\, f_c} = \sqrt{0.1 \times 31} = 1.76 \text{ MPa} \tag{4}$$

Even though there is a marked difference between the value of the average shear stress $\tau_{average}$ and the maximum shear stress τ_{max} they do not contradict each other and they are of the same order.

7. CONCLUSION

This study neither confirm nor discard the simple model proposed for the onset of debonding but show that more detailed studies are needed.

With respect to the hoped for plasticity-like behaviour of the beams after debonding the study demonstrates that a group of bolts at the ends of the plate has some effect but also that the beam soften and looses some carrying capacity after debonding. The study might indicate that a different placement of the bolts could influence the behaviour of the beam so for this reason further studies are also needed.

8. ACKNOWLEDGEMENT

The authors acknowledge the support by TRADECC, the Danish Prefab Assn., PL Beton, Spæncom, Condor Kemi, Condor Entreprise, HILTI, Germann Instruments, the staff of the laboratories of IABM and BYG·DTU at the Technical University of Denmark and the students involved.

REFERENCES

1. Poulsen. On the Anchorage of Uni Directional CFRP Laminates. *XVIII Symposium on Nordic Concrete Research.* Helsingør Denmark 2002.
2. DS 411:1999. Norm for betonkonstruktioner (Code of Practice for the structural use of concrete (in Danish but an English edition is available)). Dansk Standard. Ordrup Denmark.
3. Croes, Cuypers, Wastiels, de Roover & Vantomme. Study of Bolted Joints in Sandwich Elements With Cementious Composite Faces for Civil Applications. Composites in Constructions. Figueiras et al. Swets & Zeitinger. Lissabon Portugal 2001.
4. Turvey & Wang. Effects of temperature on the structural integraty of bolted joints in pultrusions. Composites in Constructions. Figueiras et al. Swets & Zeitinger. Lissabon Portugal 2001.
5. Beck & Jacobsen. Bolteforankring af kulfiberbånd (Anchorage of CFRP laminates by bolts (in Danish)). Bachelor Thesis, the Technical University of Denmark IABM. Copenhagen 2002.
6. Neubauer & Rostásy. Debonding mechanism and model for CFRP-plates as external reinforcement for concrete members. Composites in Constructions. Figueiras et al. Swets & Zeitinger. Lissabon Portugal 2001.
7. Neubauer. Verstärken von Betonbauteilen mit geklebte CFK-Lamellen Sika CarboDur - Einführung und Berechnungsbeispiele-. Fachseminar, Gladbeck 13 Juni 1997.
8. Olsen & Jørgensen. Forstærknning af betonplader med pålimet kulfiberbånd (Strengthening of concrete slabs by bonded CFRP laminates (in Danish)). *Bachelor Thesis, the Technical University of Denmark IABM*. Copenhagen 2003.

Mini Seminar on Form Filling Ability of Self-Compacting Concrete

Lars Nyholm Thrane
M.Sc.
Concrete Centre, Danish Technological Institute
Gregersensvej, DK-2630 Taastrup
E-mail: lars.nyholm.thrane@teknologisk.dk

Abstract

The Nordic mini-seminar "Form Filling Ability of Self-Compacting Concrete" took place on 3-4 November 2003 at the Danish Technological Institute in Taastrup, Denmark. The mini-seminar gathered 12 participants from Finland, Sweden, Norway and Denmark. The objective was to present and discuss recent developments of Self-Compacting Concrete in the Nordic countries. In general, the seminar included results and observations on the effect of fresh concrete behaviour, casting technique, and organisation on site on the filling ability, passing ability, and surface quality. The seminar had participants from the industry, working with SCC at full-scale, as well as participants working with SCC at a research level. The seminar included presentations from each participant, based on short papers, and discussions. This paper summarises the outcome of the seminar.

Key words: Filling ability, Passing ability, Rheology, Blowholes.

1 INTRODUCTION

Since Self-Compacting Concrete was introduced approximately 20 years ago, it has developed differently across country borders. SCC has become a focus area at many research institutes, but the industrial application of SCC has varied. Sweden, Japan and Holland were among the pioneers to introduce SCC in different full-scale applications whereas other countries were more conservative in the use of SCC [4,5,6]. For instance, it was only applied in horizontal castings such as floors and slaps.

SCC is defined as a concrete that is able to fill a form without the use of vibration for compaction of the concrete [1]. Depending on the type of application, the required performances of fresh SCC may vary significantly and the challenges are not the same.

In general, it seems that SCC has replaced conventional types of concrete in specific types of horizontal castings, both in-situ and in prefabrication. The form geometry and reinforcement configuration seldom impose casting difficulties that will require SCC with high flow properties e.g. slump flows above 600 mm. This has a positive effect on the segregation resistance and enables a better control of the moving front of the concrete. The segregation resistance often seem to increase when the slump flow decreases. Challenges include the choice of surface finishing procedure e.g. handling of covering, smoothing, glazing, and grinding in order to

reduce surface defects such as cracking and folding. For instance, it may be a problem to cast industrial floors with a low levelling tolerance.

For vertical applications, including complicated elements and civil engineering structures, improvements are still needed to achieve the required performances of SCC, which are a proper filling ability, passing ability and high segregation resistance. One of the main challenges is the combined control of flowablity and segregation resistance, hereunder the ability to produce SCC with a low sensitivity to variations in the mix composition (high robustness). Other challenges related to the casting of SCC include control and monitoring of the form filling, form pressure and surface quality.

Despite the challenges of SCC, the potential for improving the productivity, homogeneity, architectural design, and working environment seem to raise positivism. As an example of the need to improve the architectural design of future concrete structures, Svend Röttig, presented the idea of "Industry and Individualism" [*Svend Röttig, A*]. Svend believes that the individual expression will face a comeback for which reason the architects must have more options and larger degrees of freedom. Figure 1 shows some examples of future concrete structures.

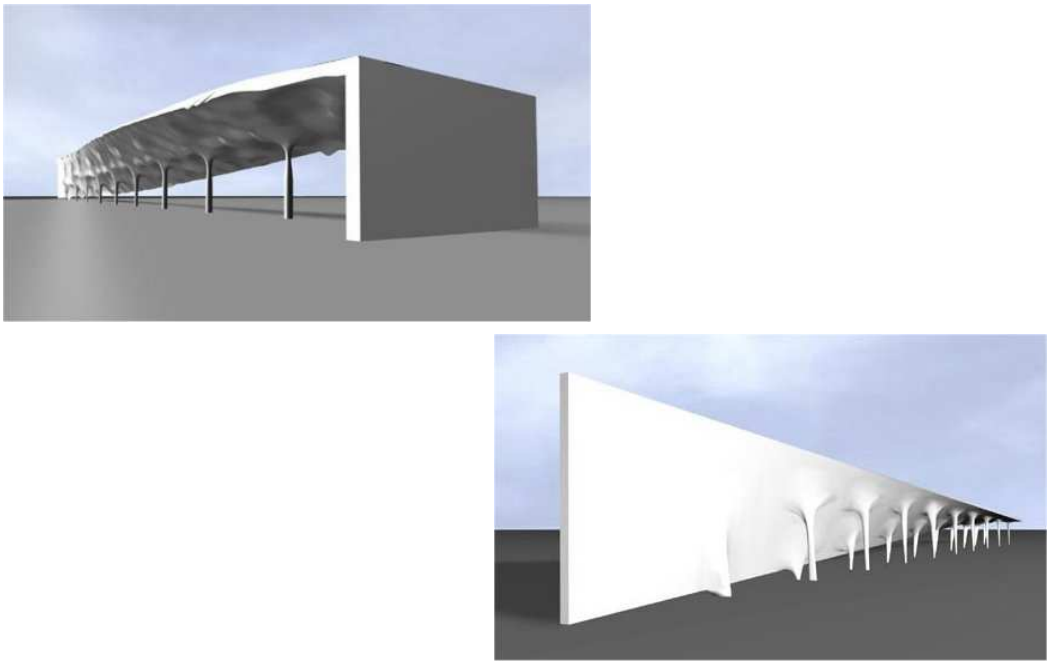

Figure 1 - Examples of future concrete structures [Svend Röttig, A].

The seminar included presentations on the fresh properties of SCC, surface quality of vertical structures, and examples of application including the form filling ability of SCC.

The behaviour of SCC is influenced by many factors, which can make it difficult to generalize results and observations. Especially, when concerned with full-scale applications the difference in mix design, constituent materials, production, transportation, casting technique and staff performance may influence the extent to which it is possible to generalise from the observed behaviour. However, the results may show a trend in some direction.

To facilitate the future development of SCC it may be important to describe and understand the governing physical and chemical properties behind the observed behaviour whether it is flow behaviour, air content, filling ability, passing ability, segregation resistance, or surface quality.

The rheological properties, plastic viscosity and yield stress, are independent physical parameters, which describe the flow properties and enable comparison and understanding of the observed behaviour between different concrete mixes [2, 3]. For instance, the rheological properties may describe why some constituent materials have a positive effect on the segregation resistance, hereunder the robustness (see section 2), and why segregation caused by dropping height during casting is observed in some applications presented from Denmark and not in the applications presented from Sweden (see section 4).

Furthermore, a rheological approach enables the calculation of SCC flow and thereby an assessment of the form filling ability as well as, for instance, determination of the yield stress and plastic viscosity from the slump flow tests (see section 2). Composite models on the effect of constituent materials on the rheological properties can then be used to assess the behaviour of SCC.

For the effect of time on the rheological properties and air void content, it is important to understand the chemical properties of superplasticizers as well as the effect of temperature (see section 2).

The rheological properties may also determine the rate of air void transportation in the fresh concrete. In combination with the casting rate this may result in migration of entrapped air voids to the surface and thereby the creation of blowholes. However, mix composition, flow behaviour during form filling, type of form work, and form work oil may also influence on the surface quality (see section 3).

In general, the early age and hardened properties of SCC were not included in details in the seminar, besides from the surface quality of vertical structures. However, Jan Erik Jonasson did present results from the modelling of deformations caused by thermal dilation and autogenous shrinkage and thereby stresses and risk of cracking [*Jan Erik Jonasson et al., B*]. Also, the effect of different surface finishing procedures in horizontal castings was not dealt with in detail.

The participants in the seminar included building owners, contractors, ready-mix/prefab/cement manufacturers, and research workers.

2 FRESH SCC PROPERTIES

The required fresh properties of SCC may vary significantly depending on the type of application. However, in every case it is important to be able to produce stable mixes that retain a satisfactory consistency and air content from the time of mixing to the time of use. The mix design, transportation time, type of casting, and temperature may influence on the fresh properties of SCC. The flow properties may be measured according to empirical test methods such as the slump flow and L-box test or by rheometers providing the rheological properties.

2.1 Flow properties and Stability

For consistency over time, Jan Erik Jonasson, presented results from a comprehensive pre-testing procedure prior to the first use of SCC for railway structures in Sweden [*Jan Erik Jonasson et al., B*]. Test results showed that the slump flow development over time seems more dependent on the mix composition than the period of transportation, for instance, some

plasticizers will increase the slump flow over time. Furthermore, the slump flow tended to decrease when the temperature was above 17°C and increase when it was below 12°C.

Finn Coch and Nina Linn Gundersen presented investigations on the robustness of three mix designs with different stabilising alternatives [*Finn Coch et al., F*]. Each mix design was tested at three water/binder ratios, approximately 0.54, 0.57, and 0.60. The three alternatives consisted of

- 65 % sand (2% air, 0 % limestone filler)
- 6 % air (55 % sand, 0 % limestone filler)
- 30 % limestone filler (2 % air, 55 % sand).

The results showed that the mixes with limestone filler followed by the mixes stabilised by air achieved the most satisfactory flow properties and segregation resistance. The mixes with the highest amount of sand were very sensitive to small variations in the water content.

Variations in the flow behaviour correspond to a variation in the rheological properties. To correlate test methods like the slump flow with rheological properties, the author, presented some initial results from numerical simulations of the slump flow test and L-box [*Lars Nyholm Thrane, H*]. The simulation of the slump flow and L-box test is part of a project with the aim of simulating form filling. A correlation between the slump flow results and the rheological properties may provide an alternative to viscometers for the yield stress and plastic viscosity determination. The experimental slump flow results depend not only on the rheological properties of the concrete but also the properties of the testing equipment, cone orientation, and lifting speed, which is possible to include in the modelling of SCC flow, however it makes experimental comparison of slump flow results (D_{max} and T50) difficult. By a controlled testing procedure it will be possible to determine the rheological properties from the experimental slump flow values D_{max} and T50. For instance, the correlation show that the T50 value depend on both the yield stress and plastic viscosity.

2.2 Air Void Stability

Ib Lauridsen presented measurements of the air content of 120 different SCC batches produced over a period of one year at the prefab plant Byggebjerg Beton A/S [*Ib Lauridsen et al., G*]. The results showed a tendency for the air content to decrease when the temperature increases. During the winter, hot water is added to keep the temperature at the preferable temperature. However, during the summer the temperature of the constituent materials can be very high, for which reason difficulties with keeping the right amount of air volume content may be encountered and considerable amounts of extra air entraining agents are often needed.

Jan Erik Jonasson presented results on the effect of transportation and pumping on the air content [*Jan Erik Jonasson et al., B*]. In general, relative to the air content just after mixing, the air content increased with an average of 0.6 percentage units during transportation and decreased with an average of 1.3 percentage units after pumping. The total decrease is somewhat lower than the general experience from the Swedish National Road Administration, which is a decrease after transportation including pumping with an average of 1.5-2.0 percentage units.

3 SURFACE QUALITY OF VERTICAL STRUCTURES

A surface of high quality is often regarded as a surface with no pores, casting defects or colour variation. The Finnish Instruction BY-40 provides an example of how to assess and classify the surface quality and this was presented and applied by Mirva Kinnunen in a study on the surface quality of SCC structures [*Mirva Kinnunen, I*].

The way to achieve a high surface quality is often a complex matter and may be influenced by the rheological properties, temperature, casting rate, mix composition, air content, type of form and form oil. Therefore, it is a difficult task to estimate whether SCC structures achieve will or will not higher quality surfaces.

3.1 Effect of Rheological Properties, Casting Technique, and Mix Composition

The rheological properties of SCC may control the transportation of air voids in the fresh concrete. In combination with the casting technique (type, placement and rate) it may determine whether the air voids migrate to the open air or the surfaces of the formwork. However, the mix composition itself may have an absolute effect on the surface quality.

Observations made by Ib Lauridsen in the manufacturing of L-elements gave further evidence to the importance of adjusting the filling rate according to the consistency and air volume content of the concrete [*Ib Lauridsen et al., G*]. If the flow properties are suddenly reduced, they have to decrease the filling rate to allow air bobbles to escape.

For the combined effect of casting and rheological properties, Jonas Carlwärd showed some examples from casting of walls from a bucket placed in the mid section and it resulted in a disturbed zone containing numerous surface pores, especially in the case of an SCC with a low viscosity [*Jonas Carlswärd et al., C*]. An example of this is shown in figure 2.

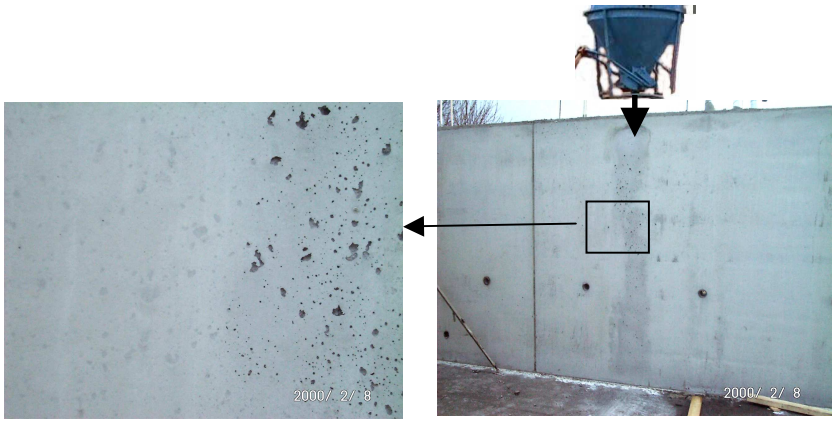

Figure 2 - Example of a wall cast with SCC in Stockholm [Jonas Carlswärd et al., C]

This may probably be due to the last placed concrete penetrating the concrete of low viscosity and thereby transporting air bubbles into the previous layers.

Mirva Kinnunen showed that more water and less superplasticizer had a positive effect on the surface quality [*Mirva Kinnunen, I*]. A possible reason for this could be that increased amounts of water reduces the plastic viscosity and yield stress and thereby increase the rate of

transportation in the concrete, whereas some superplasticizers may only reduce the yield stress [*2*].

However, the observations presented by Jonas Carlswärd showed that increased amount of water may reduce the amount of visible pores, but it seemed that the number of pores covered by a thin layer of paste had increased significantly [*Jonas Carlswärd et al., C*]. Furthermore, it seemed that an increased coarse aggregate content could significantly reduce the number of blowholes as well as positive results had been observed at some job sites when using air entrainment and silica fume. However, variations in the limestone filler amount did not have a noticeable effect on the quality of the surfaces.

Besides the effect of entrapped air, Hans Erik Gram, suggests that bleeding and transport of water to the mould surface may also result in blowholes, especially at higher w/c ratios and under cold weather conditions, which prolong the setting time [*Hans-Erik Gram, J*].

From observations of the form filling behaviour and surface quality it seemed that continuously shearing of the concrete along the surface of the formwork can have a positive effect on the surface quality compared with, for instance, no-flow zones where blowholes were clearly observed [*Lars Nyholm Thrane, D*]. This may be due to paste being generated to the surface.

Finally, the formation of so-called inward bends in civil engineering structures was presented by Hans Erik Gram [*Hans-Erik Gram, J*]. They seem to occur when it is not possible to close the gap formed between two casting layers or in-between a casting layer just at the mould. Normally, this is only a surface defect with a deepness of a few millimetres.

3.2 Effect of Formwork and Form oil

The type of formwork may influence the surface quality depending on the properties of the formwork. As mentioned by Jonas Carlswärd, air-proof formwork may result in air or water filled pores, which may be trapped in the contact area between concrete surface and form skin. Examples of this could be impermeable plywood or steel [*Jonas Carlswärd et al., C*].

Likewise, Mirva Kinnunen, presented results where lesser pores were observed when applying plywood that was not film covered, though, it was a bit dustier [*Mirva Kinnunen, I*]. Furthermore, application of wooden board moulds resulted in uneven and rough surfaces.

For the effect of form oil, it seemed that the amount of oil is more critical than the type of oil, where large amounts of oil will increase the porosity [*Mirva Kinnunen, I*].

4 EXAMPLES OF APPLICATION

Interesting results and observations on the combined effect of flow properties, casting technique, and staff performance on site on the form filling behaviour were presented.

The casting procedure and mix design requirements are dependent on the type of application. Therefore, this section has been divided into horizontal and vertical castings including in-situ, prefabrication, civil engineering structures, and laboratory experiments.

4.1 Vertical Casting

4.1.1 Pre-fabrication

Ib Lauridsen presented observations from casting of vertical elements for agricultural purposes [*Ib Lauridsen et al., G*]. Over a period of 3 years SCC has replaced conventional concrete in the production of the L-elements, slaps and sandwich elements. However, for the vertical casting of the L-elements they have developed new types of formwork in order to eliminate the surface finishing procedure. Figure 3 shows and describes the form filling procedure applied for L-elements turned upside down. The target slump flow value is approximately 650 mm.

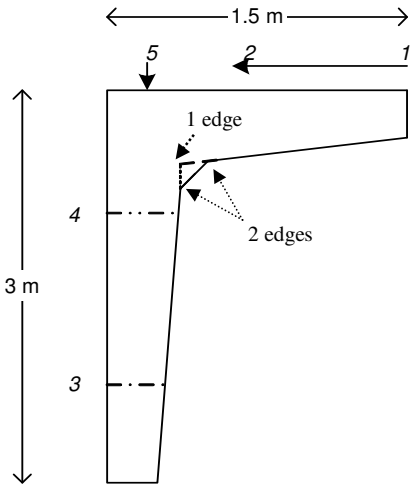

Casting Technique

Casting starts at 1. The bucket is moved to point 2, approx. 10 cm from the bend. Filling continues with the bucket fixed in this position. The concrete flows down the slope, until it reaches a height of 1/3 times the height of the element (3). Then the casting rate is reduced, until a height of 2/3 times the height of the form is reached (4). Now, the bucket is placed right above the vertical part of the element and the rest of the form is filled (5).

Bend with two edges

Final element (one edge)

Figure 3 - Casting of L-elements and pictures of the bend and final element [Ib Lauridsen et al., G].

This filling procedure has proved positive in respect of homogeneity and surface quality. A direct drop through the reinforcement has shown to increase the risk of segregation. Therefore, the casting intends to let the concrete slide slowly over the edge and preferable also more edges, as it is the case in some of the L-elements with two edges. Given the form geometry, reinforcement configuration, casting technique and flow properties tests have shown that the maximum size aggregate should not exceed 8 mm in order to avoid blocking of aggregates. The minimum space between reinforcement is approximately 20 mm corresponding to 2.5 times the maximum size aggregate.

4.1.2 Civil-Engineering Structures

Kjell Wallin presented results from the first use of SCC for railway structures in Sweden, a tunnel lining in Stäket, with importance to the effect of organisation and performance on-site [*Kjell Wallin et al., K*]. The results presented by Jan Erik Jonasson were from the prior pre-testing procedure [*Jan Erik Jonasson et al., B*]. The total length and diameter of the tunnel is 150 m and 12.5 m, respectively. SCC was cast from the middle of the formworks, which were 13 m long. In order to achieve a complete form filling, including flow in narrow sections near the end of the formwork, it was important that each batch obtained the required flow properties. The results showed that it was possible to obtain a satisfactory consistency over time by having

a strict delivery control of every truck batch, and direct contact between the quality control man on site and the ready mix factory. In this way continuously corrections could be made and in this way it was possible to obtain a complete form filling. However, though the manpower during casting was significantly reduced, the number of persons involved in the quality testing had to be increased.

Thomas Österberg made the same observations during the Sodra Lanken Project where SCC was used to cast a concrete rock lining [*Thomas Österberg, E*]. The results showed that about 30 % of the arriving batches had to be corrected to keep within the desired slump flow range of 720 to 770 mm. The reason for using SCC was the complexity of the formwork and reinforcement, which made it impossible to carry out manual vibration. The rock lining was divided into wall and top arch sections, respectively. In the wall sections (h = 5 m, l = 9 to 16 m, t = 0.8 m), the dropping height was kept within the range of 0.7 to 1.5 m. In order to limit the form pressure, a casting rate of 1 m/h was chosen for the concrete to develop a thixotropic behaviour. It resulted in form pressure measurements of 15-18 kPa compared to the hydrostatic pressure of approximately 23 kPa. To secure a complete filling of the arches (l = 8-9 m, span = 12 m) it was decided to pump through 6 valves. Continuous surveillance of the concrete flow made it possible to adjust the casting process, if necessary.

For the wall section, observations indicated a satisfactorily form filling ability, passing ability and segregation resistance. However, some minor surface areas with increased porosity and fold structures between the concrete layers were observed. For the top arches, the homogeneity was better than for those cast when using conventional concrete and vibration.

4.1.3 In-Situ Applications other than Civil Engineering

Jonas Carlswärd presented full-scale studies of SCC for housing applications in Stockholm [*Jonas Carlswärd et al., C*]. The form filling ability and surface quality of several walls were observed.
In most cases, SCC was placed from the top of the formwork, which introduced a free falling height of 2.5 m. Unlike the observations made by Ib Lauridsen, the free fall did not result in any clear signs of segregation and, in general, form filling did not seem to be a problem in simple geometries with a very light reinforcement. This included also SCC with somewhat lower slump flow values of approximately 570 mm, however, more work was required to level off the upper surface in case of a stiffer consistency. Therefore, the problem was not to achieve a proper form filling ability, passing ability and segregation resistance but more about adjusting the casting technique to avoid surface defects (see section 3).

The author presented two laboratory experiments that had been carried out in vertical form (l = 3 m, h = 1.20 m, t = 0.3 m) [*Lars Nyholm Thrane, D*] to identify the flow characteristic of SCC and the effect of flow properties, casting technique and reinforcement configuration. The concrete was pumped from the bottom lower corner at a rate of 10 m/h and reinforcement was included in one of experiments. To improve identification of the flow (i.e. dead zones, plug flow, blocking etc.) one side consisted of a transparent acrylic plate and it has shown valuable to change between normal grey concrete, and a pigmented (red) concrete during the filling process. Monitoring equipment included 80 thermal detectors for the free surface detection, electromagnetic tags for particle tracing, and form pressure measurements. The flow behaviour seemed to consist mostly of laminar flow, somewhat more turbulent flow around the inlet, and plug flow along dead zones near the end of the form. Reinforcement introduced a constraint to

the flow domain, which reduced the horizontal movement of the concrete. Reinforcement gap sizes varied between 1.5 and 3 times the maximum size aggregate of 25 mm. Some blocking occurred at 1.5 times the maximum size aggregate. Figure 4 shows an example of the difference in free surface position during casting of the wall with and without reinforcement.

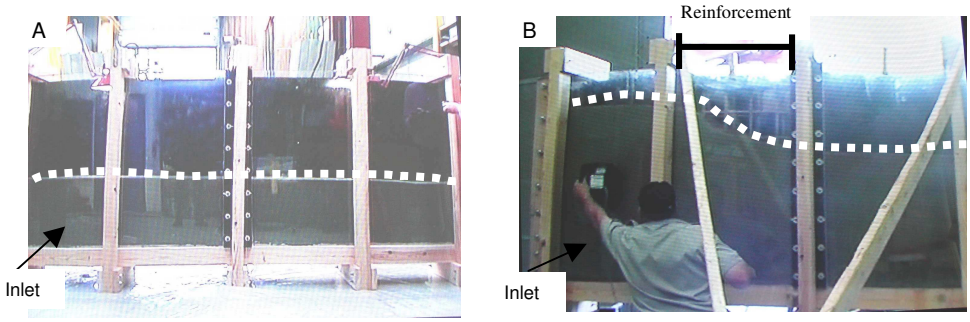

Figure 4 - Example of free surface position during casting in a wall form with and without reinforcement (A and B). The reinforcement is placed in ¼ of the form [Lars Nyholm Thrane, D]

As expected, the form pressure measurements corresponded to hydrostatic pressure. The results also showed that particle tracing is possible.

4.2 Horizontal Casting

4.2.1 Pre-fabrication

Svend Röttig presented an example from a Danish prefab manufacturer of pre-stressed beams with a TT - shaped cross section [*Svend Röttig, A*]. The width of these elements is 2.4 m and the clear span can be up to 36 m. Casting is performed from buckets and to obtain a complete form filling they aim at a slump flow value of approximately 670 mm. For this type of element the surface finishing consists only of ordinary smoothing and, in general, the number of blowholes were decreased compared to when using conventional concrete. Also, the period of casting, manpower, and noise were reduced significantly.

Ib Lauridsen presented the procedure they apply in horizontal castings and some of the issues they keep in mind during casting [*Ib Lauridsen et al., G*]. Pictures from the casting and finishing procedure are shown in figure 5.

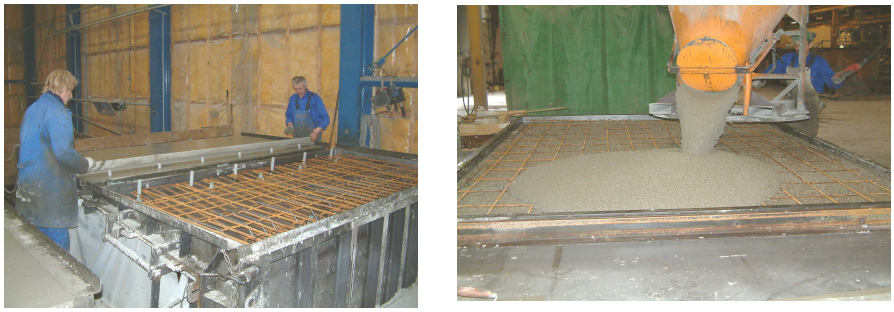

Figure 5 - Example of a horizontal casting, finishing (left) and filling (right) [Ib Lauridsen et al.,G].

In general, to avoid castings joints, they attempt to cast the concrete as quickly as possible and by moving the bucket from side to side in the longitudinal direction. However, it is not always possible to carry out the casting in this way, and in one stream. Therefore, if a break between two batches occurs the new batch should overlap the existing concrete by casting it a little behind it. However, significant setting or loss of workability of the existing concrete must not have occurred. Also, care is taken in the choice of spacers with respect to the maximum size aggregate. Normally the open space between obstacles should not be less than 2 times the maximum size aggregate. Furthermore, increased risk of blocking is observed when using crushed aggregate and when the distance is increased between the moving front of the concrete and the casting position.

4.2.2 In-Situ

Jørgen Skaarup presented experiences from manufacturing and application of SCC [*Jørgen Skaarup, L*]. For the most part SCC is used for horizontal applications and the presentation was combined with an excursion to a job site showing a typical type of application with SCC, in this case the casting of a floor at a sports arena. Some pictures from the job site are shown in figure 6.

Figure 6 - Pictures from the excursion to a job site in Ishøj, Denmark [Pictures taken by Kjell Wallin].

In the manufacturing of SCC it is equally important to be able to produce SCC with a high robustness and at a cost that is not excessively above that of conventional concrete. Therefore, it is often chosen to keep slump flow values between 550 and 600 mm, which have proved very appropriate for many types of horizontal castings. At the job site the concrete was cast by pumping and levelling was performed with the use of drain pipes.

5 SUMMARY

This paper has summarized the results and observations presented and discussed during the seminar with emphasis on the fresh properties of SCC, surface quality of vertical structures, and examples of application.

In short, the results and observations are summarized below.

For the fresh properties of SCC results and observations showed that

- flow properties over time is more dependent on the mix composition e.g. superplasticizers than the period of transportation
- to increase the robustness of SCC at w/b ratios of approximately 0.54-0.60, limestone filler was a better alternative compared to increased air content, and increased amount of sand
- the rheological properties can be used to calculate SCC flow and e.g. determine the yield stress and plastic viscosity from the slump flow values D_{max} and T50
- the air void stability depend on temperature, transportation, and pumping.

For the surface quality, observations gave further evidence to the importance of adjusting the casting rate according to the rheological properties in order to avoid entrapped air migrating to the surface. However, observations indicated that mix composition, bleeding water, and flow behaviour during form filling i.e. shearing at the walls may also influence on the surface quality. Finally, impermeable types of formwork and large amount of form oil increase the risk of getting a poor surface quality.

The examples of application showed that it is possible to apply SCC in both horizontal and vertical applications. In order to make SCC a success, especially in complicated formworks, the organisation and performance of the staff is an important factor. To obtain the proper form filling ability, the required flow properties need to be obtained. Observations showed that by having a strict delivery control of every truck batch, and direct contact between the quality control man on site and the ready mix factory, it was possible to obtain a satisfactory consistency over time. Furthermore, continuously surveillance of the concrete flow and form pressure during the form filling process will enable adjustment of the casting process, if necessary. However, there is still a need to understand the effect of casting and rheological properties on the segregation and blocking resistance of SCC.

Ongoing co-operative projects and networks are being carried out. The Danish SCC-Consortium (www.scc-konsortiet.dk) is an example of a three-year project where the general scopes are to improve the working environment and the productivity in the construction industry. The means is to make SCC the most used type of concrete. 17 parties are included in the Consortium and the budget is approximately 2.8 million EUR. The Nordic SCC Net an example of a Nordic network including 16 different parties (www.nordicscc.net).

For further information about the seminar, please contact the author or any of the other participants at the seminar.

6 LIST OF PRESENTATIONS/PAPERS, persons in italic participated in the seminar

A: *Svend Rôttig*: "Form Filling with SCC – A Major Breakthrough"
B: *Jan-Erik Jonasson*, Sofia Utsi, *Kjell Wallin*: "Form Filling with use of SCC in a Tunnel Lining - Results from Testing Procedure"
C: Jonas Carlswärd, Mats Emborg, "Use of SCC for housing applications – Experience form case studies in Stockholm"
D: Lars Nyholm Thrane: "Form filling with SCC in a vertical form – Results from Experiments"
E: Thomas Osterberg, "The use of SCC in the Sodra Lanken Project"
F: Finn Coch and Nina linn Gundersen, "Robustness of SCC with w/b 0.6"
G: Ib Lauridsen and Lars Nyholm Thrane, "Use of SC in Prefabricated Concrete elements – Examples and observations"
H: Lars Thrane, "2-D simulations of Test methods – Initial Results"
I: Mirva Kinnunen, "Surface Quality of Vertical Structures Cast with SCC In-situ"
J: Hans Erik Gram, "Possible Reasons for Surface Defects on Structures made of SCC"
K: Kjell Wallin, Jan-Erik Jonasson, Sofia Utsi, "Form Filling with Use of SCC in a Tunnel Lining - Organisation and Performance on site"
L: Jørgen Skaarup: "Manufacturing and Application of Self Compacting Concrete" (only presentation)

7 REFERENCES

1: Skarendahl, A. (2003). "The Present – The Future". *Proceedings of the 3rd International Rilem Symposium on SCC, Reykjavik, Iceland.*
2: Wallevik, O. (2003). "Rheology – A Scientific Approach to Develop Self-Compacting Concrete", Proceedings of the 3rd International Rilem Symposium on SCC, Reykjavik, Iceland.
3: Bird, R. B, Armstrong, R. C, Hassager, O. (1987). "Dynamics of Polymeric Liquids – Volume 1, Fluid Mechanics", A Wiley-Interscience Publication, John Wiley & Sons.
4: Emborg, M., Hedin, C. (1999). "Production of self-compacting concrete for civil engineering – case studies", Proceedings of the 1st International Rilem Symposium on SCC, Stockholm, Sweden.
5: Okamura, H., Ouchi, M. (1999). "Self-compacting concrete – Development, present use and future", Proceedings of the 1st International Rilem Symposium on SCC, Stockholm, Sweden.
6: Walraven, J. (2003). "Structural Aspects of Self-compacting concrete", Proceedings of the 3rd International Rilem Symposium on SCC, Reykjavik, Iceland.

PULL-OUT TESTS FOR REINFORCED AUTOCLAVE AERATED CONCRETE

Jukka Lahdensivu
Lic. Tech., Senior Research Scientist
Tampere University of Technology
E-mail: jukka.lahdensivu@tut.fi

ABSTRACT

The reinforcement of Autoclave Aerated Concrete (AAC) slab consists of main bars and transversal bars. The function of transversal bars is to be anchor for main bars. The transversal bars are welded to the main bars. Based on these tests, type and thickness of the corrosion protection of the reinforcement affects the anchor capacity considerably. Cement based corrosion protection has a good contact with steel bars and AAC. Cement based corrosion protection increased the transversal bars total diameter by 3-4 mm. Bitumen based corrosion protection is thin and it has poor contact with steel bars. Transverse compression eliminates cracking of specimens effectively. Small transverse pressure is adequate to eliminate cracking. In normal structures there is always enough contact pressure on support area.

Keywords: Autoclave Aerated Concrete, AAC, anchor capacity, cement based corrosion protection, transverse pressure

1. INTRODUCTION

1.1 Background

Reinforced Autoclaved Aerated Concrete (AAC) slabs are commonly used in industrial halls and single houses. In industrial halls roofs and external walls are sometimes made by AAC slabs. Also in single houses made by AAC, reinforced AAC slabs are commonly used in roofs, base floors and baffle plates.

AAC slabs are manufactured in a casting and autoclaving process. Dimensions of typical AAC slab are: width 600 mm, height 200 mm and length 4000-6000 mm. The reinforcement of AAC slab consists on main bars and transversal bars. The function of transversal bars is to be anchor for main bars. Transversal bars are welded to main bars. In the basic reinforced AAC slab used in Finland there are usually five transversal bars on the first quarter of the slabs length, and typically four transversal bars in the middle of the slab depending on the length of the slab.

There are two different methods in use for corrosion protection of the reinforcement: Bitumen based coating and cement based coating. Bitumen based coating is most commonly used in Europe.

The committee behind CEN TC177/WG1 is preparing a harmonised product standard prEN 12602 [1] for reinforced AAC components. In its Annex A, design rules are also given for calculation of anchorage capacity of the reinforcement in AAC components. The formula A.48

for the calculation of the anchorage capacity of the transversal bars without taking bond of the longitudinal bars into account seems to give too conservative anchorage capacity values for transversal bars at the support. In addition the formula is developed for bitumen based corrosion protection coating of the reinforcement. Cement based coating used e.g. in Finland may result in different behaviour since this coating is normally much harder than bitumen based coating.

In standard prEN 12602 formula A.48 is:

$$f_{1d} = 1{,}5\ m\ (e/Ø_t)^{1/3}\ f_{ck}/\gamma_c$$

$$\leq 2{,}7\ f_{ck}/\gamma_c \qquad (1)$$

where

- f_{1d} design bearing strength of AAC
- m is a factor for consideration of existing transverse compression (e.g. support pressure) in the anchorage zone, to be taken as $m = 1 + 0{,}3\ n_p/n_t$
- e is the distance of the axis of the transverse bars in the anchorage zone to the nearest surface of the component
- $Ø_t$ is the diameter of the transverse anchorage bars
- f_{ck} is the characteristic compressive strength of AAC
- γ_c is the partial safety factor of AAC for brittle failure
- n_p is the number of transverse bars within zone of transverse pressure (e.g. at the support)
- n_t is the number of transverse bars between the sectin concerned and the end of component.

1.2 Objective

The objective was to examine the anchorage capacity of the last transversal bar in AAC components when the transversal bar is under transversal pressure from the support using pull-out test specimens.

In this research the transverse pressure of the test specimen, the length of the transversal bar, the number of longitudinal bars and the material of corrosion protection of bars were varied. The bond of the longitudinal bar was eliminated in all cases.

2. TEST SPECIMENS

2.1 Preparation of the test specimens

In the same mould (mould 1) two similar AAC components with the dimensions of 250 x 620 x 5400 mm^3 were produced in the normal production line. AAC blocks 250 x 200 x 620 mm^3 were produced at the other end in the same mould. From one of these blocks three cubes 100 x 100 x 100 mm^3 were prepared for compressive strength testing and from another block three cubes were used for the estimation of the moisture content during testing.

Seventeen pull-out test specimens (tests 1 – 4) with the dimensions of 250 x 200 x 200 mm^3 were prepared from the first AAC component which were first cut to 800 mm long parts. The thickness of the AAC component was 250 mm which was 50 mm wider than the thickness of the pull-out test specimens. When preparing test specimens this extra 50 mm was removed by cutting so that the longitudinal bar was in the middle of the test specimen. The width of the AAC

component was 620 mm which was 20 mm more than what was theoretically needed for the cutting of the test specimens. This also helped for the adjustment of longitudinal cutting of AAC component so that the longitudinal bar was exactly in the centre of the test specimen.

Supports of the reinforcement cage in the mould were placed near the transverse cutting points of the AAC component so that they did not cause any interference to the test specimens.

The bonding between longitudinal bars and corrosion protection coating was eliminated by mould oil in all specimens main bar or main bars.

Nine pull-out specimens were produced from the second AAC component (test 6). The preparation was similar as for tests 1 - 4, except that the dimensions of the specimens were 250 x 200 x 150 mm^3 and the reinforcement of the specimens were eccentric.

Specimens with bitumen based corrosion protection (test 5) were made afterwards in another mould (mould 2). The preparation was the same as for tests 1 – 4.

The test specimens (pull-out specimens and cubes from both moulds) were stored in conditions Rh 10-12 % and temperature +20 °C ± 2 °C until the moisture content was near equilibrium.

The variables and marking of the test specimens were the following:
- Steel grade of the transversal bar: V1 (f_{yk} = 400 MPa)
- Steel grade of the main bar: V1 (f_{yk} = 400 MPa)
- Length of the transversal bar: 40, 60 or 80
- Transverse pressure: I (0 MPa), II (0,25 MPa) or III (0,5 MPa)
- No cross bar: T
- Cubes for compressive strength test: K
- Test specimens in a sample: A, B or C
  A = from the top of the mould
  B = from the middle of the mould
  C = from the bottom of the mould
- Eccentric steel bars: E

3. EXECUTION OF TESTS

3.1 Pull-out tests

The following pull-out tests were executed:

a. Standard test specimens (centric reinforcement)
- transversal bar ø7 mm with cement based corrosion protection, length 60 mm
- main bar ø7 mm, no bond with AAC
- transverse pressure 0 MPa, 0,25 MPa or 0,5 MPa
- AAC 450 kg/m^3 and compressive strength, see Table 1

b. Two main bars (centric reinforcement)
- transversal bar ø7 mm with cement based corrosion protection, length 80 mm
- two main bars ø7 mm, no bond with AAC
- transverse pressure 0,5 MPa
- AAC 450 kg/m^3 and compressive strength, see Table 1

Two main bars were welded together with an transversal bar. The main bars were fixed in pulling machine.

c. Main bar without transversal bar (centric reinforcement)
- main bar ø7 mm, no transversal bar, no bond with AAC
- transverse pressure 0 MPa
- AAC 450 kg/m^3 and compressive strength, see Table 1

Test 3 was made to verify that the bond between longitudinal bars and corrosion protection coating was really eliminated.

d. Shorter transversal bar (centric reinforcement)
- transversal bar ø7 mm with cement based corrosion protection, length 40 mm
- main bar ø7 mm, no bond with AAC
- transverse pressure 0,5 MPa
- AAC 450 kg/m^3 and compressive strength, see Table 1

e. Different corrosion protection (centric reinforcement)
- transversal bar ø7 mm with bitumen based corrosion protection, length 60 mm
- main bar ø7 mm, no bond with AAC
- transverse pressure 0 MPa
- AAC 450 kg/m^3 and compressive strength, see Table 1

f. Eccentric steel bars
- transversal bar ø7 mm with cement based corrosion protection, length 40 mm
- main bar ø7 mm, no bond with AAC
- transverse pressure 0 MPa, 0,25 MPa or 0,5 MPa
- AAC 450 kg/m^3 and compressive strength, see Table 1

Note: After testing it was found out that the transversal bar was unintentionally located closer to the nearest surface of the test specimen compared to the longitudinal bar. The original plan was the other way round.

One sample included generally three test specimens (tests) taken from the top, from the middle and from the bottom of the mould.

3.2 AAC compressive strength test specimens

AAC compressive strength was tested from cubes 100 x 100 x 100 mm^3.

A sample included generally three cubes (tests) taken from the top, from the middle and from the bottom of the mould. AAC compressive strength was tested from all batches (mould 1 and 2).

3.3 Summary of the tests

1. Standard tests	3 x 3 =	9 tests	3 samples
2. Two main bars	2 tests		1 sample
3. Main bar without cross bar	3 tests		1 sample
4. Shorter cross bar	3 tests		1 sample

5. Different corrosion protection	3 tests		1 sample
6. Eccentric steel bars	3 x 3 =	9 tests	3 samples
Total number of pull-out tests		29 tests	
7. AAC compressive strength from cubes		3 tests	2 batches

In addition cubes were prepared for the estimation of the moisture content during pull-out test according to EN 678.

Pull-out tests were carried out in the laboratory of Structural Engineering during 24.-26. February and 15. April 2003.

A special test rig was made for these tests. The test rig and the working principle is shown in Figure 1.

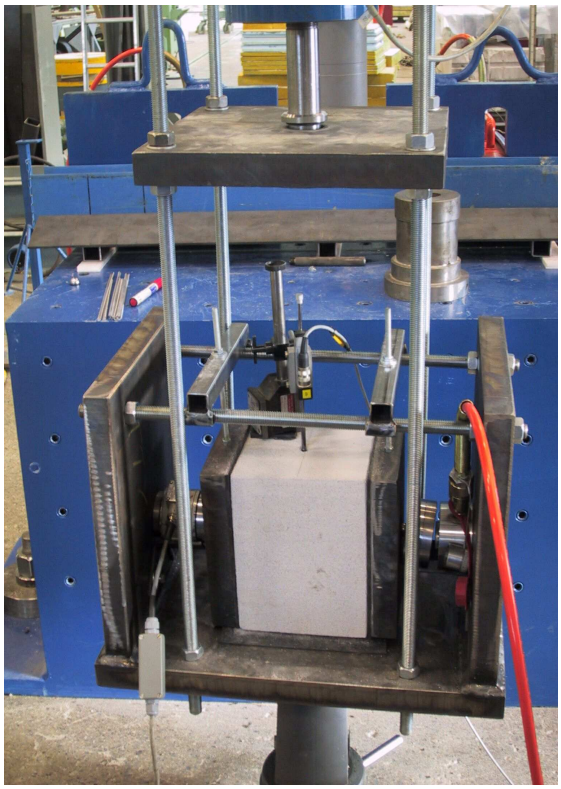

Figure 1. Test rig for pull-out tests.

All pull-out tests were carried out by displacement control. The steel bar of the specimen was connected to solid chin and the whole test rig with specimen was moved up. Displacement speed was 1 mm in 52 seconds. The displacement of steel bar and test rig, tensile force and transverse force were controlled in the tests.

The uniform transversal forces were 0 kN, 12,5 kN ± 4 % or 25,0 kN ± 2 % which caused uniform transversal pressure of 0 MPa, 0,25 MPa or 0,5 MPa respectively.

4. RESULTS

The test results are shown in Tables 1 to 5.

Compressive strength, density and moisture content of AAC are presented in Table 1. There is difference between top, middle and bottom of the mould in AAC strength. Also moisture content and density influence the strength of AAC as shown in table 1.

Table 1. Compressive strength, density and moisture content of AAC.

Specimen	Test	Mould	Comp. strength f_{cm} [MPa]	Density [kg/m^3]	Moisture % by weight
KA	1 – 4, 6	1	4,07	433	1,56
KB	1 – 4, 6	1	4,26	443	1,56
KC	1 – 4, 6	1	4,41	448	1,56
KA	5	2	3,00	466	4,60
KB	5	2	3,10	466	4,60
KC	5	2	3,30	448	4,60

In Tables 2-5 peak force and equivalent displacement of the steel reinforcement are presented. The bearing strength $f_{cb,u}$ in front of transversal bar is calculated from peak force by dividing it by the transversal bar area, 280 mm^2 (7 mm x 40 mm), 420 mm^2 (7 mm x 60 mm) or 560 mm^2 (7 mm x 80 mm) depending on the diameter and length of the transversal bar. In Figure 2 there is an example of force-displacement curve.

Factor $f_{cb,u}/f_{cm}$ is calculated by dividing bearing strength by compressive strength.

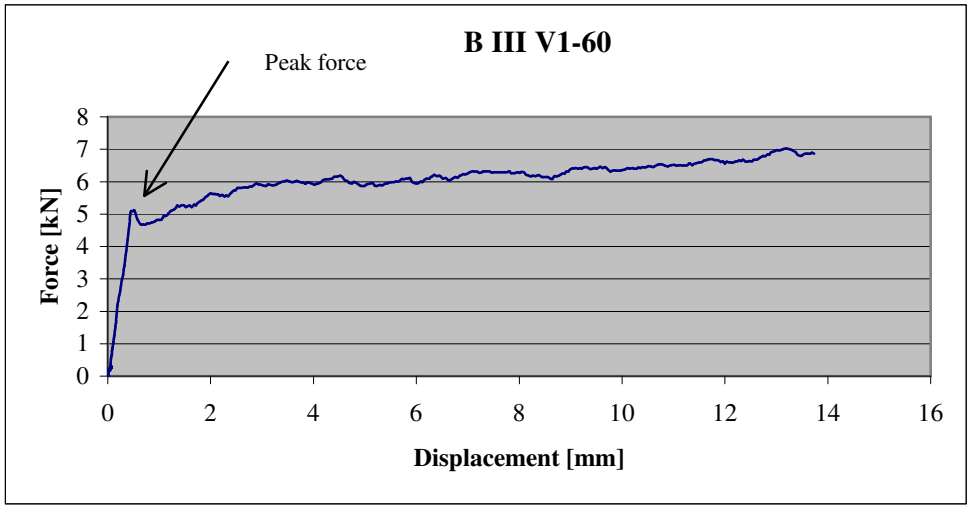

Figure 2. An example of force-displacement curve.

Table 2. Results of tests 1 , 3 and 4: Centric reinforcement, cement based coating.

Specimen	Test	Peak force [N]	Displacement [mm]	Transverse force [kN]	Bearing strength $f_{cb,u}$ [MPa]	$f_{cb,u}/f_{cm}$
A T	3	831,6	0,387	0		
B T	3	481,8	0,077	0		
C T	3	480,7	0,253	0		
A I V1-60	1	4964,4	0,661	0	11,82	2,90
B I V1-60	1	4631,3	0,375	0	11,03	2,59
C I V1-60	1	8847,2	0,276	0	21,06	4,78
A II V1-60	1	5264,4	0,711	12,8	12,53	3,08
B II V1-60	1	4620,1	0,372	13,0	11,00	2,58
C II V1-60	1	7117,0	0,248	13,0	16,95	3,84
A III V1-60	1	5151,0	0,370	25,8	12,26	3,01
B III V1-60	1	5111,3	0,515	25,4	12,17	2,86
C III V1-60	1	6543,8	0,278	25,1	15,58	3,53
A III V1-40	4	7301,3	0,150	25,1	26,08	6,41
B III V1-40	4	2830,4	0,436	24,6	10,11	2,37
C III V1-40	4	3800,7	0,329	24,5	13,57	3,08

In all specimens of test 1 and 4 where the transversal bar length was 60 mm or more transversal bars were found to be bent at the end of tests, see Figure 3. Transversal bars with length 40 mm stayed straight during the test.

In specimens B I V1-60, C I V1-60 and C II V1-60 the corrosion protection coating was broken when the test was stopped so that part of it was still attached to the AAC behind transversal bar, see Figure 5. Smaller parts of the corrosion protection coating were broken also in specimens A II V1-60, A III V1-60, B II V1-60 and C III V1-60.

Table 3. Results of test 2: Two longitudinal bars, centric reinforcement, cement based coating.

Specimen	Peak force [N]		Displacement [mm]		Transverse force [kN]	Bearing strength $f_{cb,u}$ [N/mm^2]	$f_{cb,u}/f_{cm}$ [1)]
	bar 1	bar 2	bar 1	bar 2			
B III V1-80	11631,0	16017,0	0,077	0,375	24,9	20,80	4,88
C III V1-80	9572,0	9572,0	0,653	0,518	24,2	17,09	3,88

[1)] The bearing strength is calculated by dividing the smaller failure force by the transversal bar area (560 mm^2).

In both specimens of test 2 the transversal bars were bent when the test was stopped.

Figure 3. Bending of a 60 mm long cross bar when the test was stopped.

Table 4. Results of test 6: Eccentric reinforcement, cement based coating.

Specimen	Peak force [N]	Displacement [mm]	Transverse force [kN]	Bearing strength $f_{cb,u}$ [N/mm^2]	$F_{cb,u}/f_{cm}$	Eccentricity[2)] [mm]
EA I V1-60	4531,5	0,242	0	10,79	2,65	22,6
EB I V1-60	4529,7	0,177	0	10,79	2,53	23,9
EC I V1-60	4983,3	0,029	0	11,87	2,69	21,8
EA II V1-60	5506,4	0,188	12,4	13,11	3,22	24,7
EB II V1-60	4735,9	0,156	12,5	11,28	2,65	25,6
EC II V1-60	8020,9	0,132	12,7	19,10	4,33	25,6
EA III V1-60	5861,6	0,300	25,4	13,96	3,43	26,6
EB III V1-60	3594,8	0,481	25,5	8,56	2,01	26,0
EC III V1-60	7608,0	0,709	25,0	18,11	4,11	24,5

[2)] Distance from the surface of the test specimen to the centre of the transversal bar.

In test 6 cracks appeared after 2 mm displacement of the reinforcement in the specimens without transverse force, see Figure 4. The other specimens had no cracks. In all specimens with transverse pressure the transversal bars were generally bent when the test was stopped. In specimens without transverse pressure the transversal bars stayed straight during whole test.

Figure 4. Cracking after 2 mm displacement in those specimen with eccentric reinforcement and without transverse force.

Table 5. Results of test 5: Centric reinforcement, bitumen based coating.

Specimen	Peak force [N]	Displacement [mm]	Transverse force [kN]	Bearing strength $f_{cb,u}$ [N/mm^2]	$f_{cb,u}/f_{cm}$
A V1-60	2342,3	0,348	0	5,58	1,86
B V1-60	2738,7	0,256	0	6,52	2,10
C V1-60	2601,4	0,288	0	6,19	1,88

In all specimens of test 5 transversal bars stayed straight during whole test.

Figure 5. The corrosion protection coating (cement based) was broken when the test was stopped so that part of it was still attached to the AAC behind cross bar.

5. DISCUSSION

Cement based corrosion protection on steel bars had good contact with transversal bars and AAC. Bitumen based corrosion protection had good contact with AAC but poor contact with transversal bar. The bonding between longitudinal bars and corrosion protection coating was eliminated by mould oil in all specimens. Debonding of the longitudinal bars was found to be effective, the average peak force was less than 10 % of average peak force of standard tests without transverse pressure (test 1).

The cement based corrosion protection increased the transversal bars total diameter with 3-4 mm. The transversal bars with length 40 mm stayed straight during the test. Longer transversal bars were normally bent when the test was stopped. In test 5 the corrosion protection was bitumen based and all transversal bars remained straight. It was due to smaller bearing area.

In most cases the peak load occurred between 0,2 – 0,5 mm displacement. After the peak force the force could increase considerably. This was not the case for highest peak forces and for tests with eccentric reinforcement and without transverse force.

Only in the three specimens with eccentric reinforcement and without transverse force cracking occurred. After peak force the force decreased quite rapidly.

The failure mode was ductile except when cracking appeared.

6. CONCLUSIONS

Based on these tests it can be concluded that type and thickness of the corrosion protection affects the test results considerably. Cement based corrosion protection has a good contact with steel bars and AAC. The cement based corrosion protection increased the transversal bars total diameter by 3-4 mm. The bitumen based corrosion protection is thin and it has poor contact with steel bars.

Transverse compression eliminates cracking of specimens effectively. 0,25 MPa transverse pressure is adequate to eliminate cracking. In normal structures there is always enough contact pressure on support area in the serviceability limit states.

Normally the bearing strength $f_{cb,u}$ in front of transversal bar is calculated based on transversal bar diameter. Based on these tests, one can increase the transversal bar diameter taking into account the cement based corrosion protection layer or one can allow higher $f_{cb,u}/f_{cm}$ for transversal bars with thick cement based corrosion protection. This means that we have to pay attention to the manufacturing process of cement based corrosion protection layer.

REFERENCES

1. prEN 12602, Prefabricated reinforced components of autoclaved aerated concrete. European standard 2003.

Implementing Environmentally-friendly and Durable Concrete to Finnish Practice

Erika Holt
Ph.D., Researcher
VTT Building and Transport
Technical Research Centre of Finland
P.O. Box 1800, 02044 VTT, FINLAND
e-mail: erika.holt@vtt.fi

Tuula Råman
M.Sc. Tech, Production manager
Lafarge Tekkin Oy
Sinikalliontie 9, 02630 Espoo, FINLAND
e-mail: tuula.raman@lafarge-tekkin.com

Leif Wirtanen
Lic.Sc. Tech.,Researcher
Building Materials Technology
Helsinki University of Technology
P.O. Box 2100, 02015 HUT, FINLAND
e-mail: leif.wirtanen@hut.fi

Mika Tulimaa
M.Sc., Researcher (until 31.12.2003)
Building Materials Technology
Helsinki University of Technology
P.O. Box 2100, 02015 HUT, FINLAND
e-mail: mika.tulimaa@hut.fi

ABSTRACT

Producing durable concrete that is environmentally-friendly has been the goal of recent Finnish research. Extensive testing was done on about 40 mixtures containing up to 10 % silica fume, 60 % fly ash, and/or 70 % blast furnace slag. Laboratory and field station tests were conducted, along with coring from existing structures and making applied tests in local factories. Models were developed to assess deterioration tendencies and recommendations were provided for industry. This paper provides an overview of the project results and shares how some of the research results have been implemented by Finnish industry.

Key words: environmentally-friendly, slag, fly ash, silica fume, frost durability, field stations.

1. BACKGROUND

Two projects have been underway in Finland addressing the goal of producing environmentally-friendly high performance concrete (HPC) that is durable and economically feasible. This paper provides some general information about both projects, such as describing the tasks involved, the materials and test methods used, and how the results have been implemented to practice by industry. More specific results are provided for a few parts of the laboratory testing results, as merely an example of the investigations. The goal of this paper is to provide the reader with an overview of the importance in Finnish research on environmental aspects of concrete technology.

The first project, titled CONLIFE, was part of the EU 5th Framework programme for Competitive and Sustainable Growth, in cooperation with 10 other partners from 7 countries. The second project was a Finnish domestic project involving 9 industrial partners (such as cement manufacturer, ready-mix companies, precast companies and building material manufactures). Both projects began in 2001 for duration of three years. The EU-project investigated high strength concrete (> 60MPa) with materials from across Europe, while the domestic project tested normal strength concrete (30-60MPa) and used local materials. Through-out this paper, both projects will be described, first on the domestic level and then on the European level.

The main goals of the projects were to:

- Design mixtures that would be environmentally-friendly and economically feasible by replacing some of the cement with mineral additions. (fly ash, silica fume, ground granulated blast furnace slag)
- Investigate the durability of these concretes.
- Evaluate freeze-thaw test methods and compare the Scandinavian Slab [1], the German CIF/CDF [2, 3] and the Finnish SFS test methods [4].
- Correlate accelerated laboratory tests (such as freeze-thaw and carbonation) with real-time field exposure tests.

All of these above mentioned goals were equally important and the projects tried to quantitatively assess how the goals were met. Both projects also had the general goal of addressing how the concrete industry can meet some of the demands implicated from the Kyoto Protocol [5]. In the domestic project an additional criteria was also considered with evaluation of the durability performance for conventional curing compared to heat-treatment of the concrete. This was done to address how the use of mineral admixtures may affect industrial applications where production cycle time is critical. The European project had conventional curing of all samples and also some mixtures were deliberately produced with poor durability. It was intended from the onset of the EU-project to have a wider range of performance in these HPC mixtures to allow for better modelling of deterioration. The modelling of results is reported in a 150 page document within the European deliverables package [6] which can be downloaded from the project web-page.

There are many reasons why these types of projects related to environmentally-friendly constructions are important, which will be addressed in Chapter 2. Overall, it is known that in the future there are various implications that will affect our field, including the changing trends in construction, need for technical development, and changes in mix design caused by altered

types of aggregates, additions, cement. etc. The differences in concrete types will be related to aspects such as:

- Worse quality materials become more available and economic more feasible (i.e. unstable ashes),
- Need to use crushed aggregate as natural materials are less available and/or too costly,
- Greater variety of concrete types, allows input of lower-grade material in some applications.

Both projects followed the same work structure. The first part of the projects included extensive literature reviews of past studies, which are detailed within the database and reference lists of the project reports [6, 7]. The projects tried to incorporate the latest know-how, test methods and assessment tools from the various other research projects that have been done in this area. The next tasks of the project included sampling from existing field structures, which is briefly described in Chapter 3. The middle part of the work involved casting concrete for accelerated lab testing and placement at field stations for real-time evaluations. There were two field stations used in Finland, and an additional 8 stations around Europe. One part of the domestic project was carried out in two factories, where concrete products were made directly in the production chain for durability testing. The last part of the projects covered the modelling of durability of environmentally-friendly concrete. Finally, manuals were written for industrial applications to provide guidelines for producing environmentally-friendly and durable concrete.

2. ENVIRONMENTAL CONSIDERATIONS

Both projects have impact to the increasing awareness about preserving the Earth's environmental biodiversity. Tools such as life cycle inventory (LCI) and life cycle assessment (LCA) analysis which have been developed in accordance with ISO 14040 standards provide means to quantify the environmental burden that results from a material or production process [8]. These tools were used for evaluation in this study, both for assessing the environmental impacts of laboratory mixtures and factory products.

The importance of environmental protection has received greater emphasis since 1997 when the Kyoto Protocol was established at the United Nations Framework Convention on Climate Change. So far, some 178 countries have signed the treaty, including all the major industrialised countries except the United States. The treaty calls for a worldwide reduction of emissions of carbon-based gases by an average 5.2 percent below 1990 levels by 2012. Different countries have adopted different targets, including the EU commitment to cut emissions by eight percent [5].

The European Commission decided on the practical goal in its so called Green Paper in May 2000 and prepared the rules for the emission directive by 2003. The burden sharing between the EU countries was decided in this connection. In each EU country the target quota of the directive is divided between the main industrial branches (production of energy, ferrous metals, pulp and paper and construction industry). Each branch will again negotiate limits for individual plants and companies.

For the concrete and cement industry the effect of the emission directive are considerable, because:

- CO_2-emission / ton of products is high (60 % comes from limestone and 40 % from energy).
- The price of the product / ton is relatively low.
- In the European cement industry, decreasing energy consumption has been a major topic since the 1970´s; additional decreases are expensive.
- There is a risk of increasing competitive imports from outside Europe.
- Business fluctuation is high and investments expensive.

In the materials technology of cement and concrete these reasons seem to lead to actions such as the need for minimizing the amount of clinker in cement, coarsening of clinker (because of rise of the price of electricity for grinding) and lowering the cement clinker content in concrete. A general way of aiming towards the goal is to use more mineral additives and also chemical admixtures, but at the same time to ensure an adequate or even extended service life.

Life cycle assessment (LCA) is a useful tool for studying environmental impact. LCA is a "cradle to grave" approach for understanding the environmental consequences of technological choices. It is a structured method for measuring, analyzing and reporting physical inflows of natural resources (including energy and raw materials) and products utilized, and outflows of wastes generated and released into the environment for a process at different stages throughout their life cycle. A methodological framework for LCA has been established by the Society for Environmental Toxicology and Chemistry (SETAC) and forms the basis of ISO Standards 14040-14043 which are now widely employed by LCA practitioners. A complete LCA consists of four steps which include: 1) Goal Definition and Scoping, 2) Inventory Analyses, 3) Impact Assessment, and 4) Improvement Analysis. LCA was used to assess the laboratory and factory tests, as described in Chapter 7.

3. FIELD ASSESSMENTS

The first results of the projects were obtained from sampling 11 Finnish field structures, ranging in age from 20 years to new constructions [7]. In the CONLIFE project, another 50 structures were sampled from around Europe and all of the results were documented in other publications [6, 9].

For the European project, the compressive strength of the cores ranged from 75 to 130 MPa and some of the mixtures contained silica fume. The compressive strengths of the domestic project's cores were around 60 MPa and all of the designs included mineral additions (such as 70 % blast furnace slag or 25 % fly ash). All of the structures were performing well in the field, though some of them showed unsatisfactory durability when subjected to further accelerated laboratory tests. In all cases of poor frost resistance, the concrete did not include air entrainment. The results from field sampling contributed to the later analysis and modelling of durability in combination with the laboratory and factory tests. The results are too extensive to go into full detail here, but are included in other reports from the projects [6].

4. LABORATORY TESTING

4.1 Materials

Domestic Project
For the casting of laboratory and field station specimens, the goal was to produce concrete in the compressive strength class (cube) range of 30-45 MPa that would be applicable for either ready-mix or pre-cast production. There were 8 primary mix designs used:

- 2 reference mixtures
- Mixtures containing 20, 40 or 60 % class C fly ash
- Mixtures containing 25, 50 or 70 % ground blast furnace slag

Finnish cements of types CEM IIA 42.5R and CEM IIA 52.5R were used, with cement amounts of 250 to 340 kg/m^3. The water amount ranged from 145 to 180 kg/m^3, with water-to-binder ratios from 0.50 to 0.65. All aggregates were natural Finnish granite, with a maximum size of 16 mm. Superplasticizer and air entrainment agents were used to obtain a target slump of 50-100 mm and an air content of 6 %. When cement was replaced by mineral additions, the assumed activity index for replacement was 0.3 for fly ash and 1.0 for slag.

The Finnish concrete code (Betoninormit 2000 [10]) allows the use of blast furnace slag up to 350 % of the cement amount and a maximum amount of 60 % of class-A fly ash when the cement is of class CEM I (Portland cement). This corresponds to 78 % of blast furnace slag and 38 % of fly ash when calculated from the total binder amount. In other cement classes, the amounts of fly ash allowed are smaller.

European Project
Similar to the domestic project, samples were prepared for both laboratory testing and field station placement. In the Nordic region and thus the concretes evaluated in Finland, the mixtures were made from Danish cement of Type CEM I 52.5R. The water amount remained constant at 150 kg/m^3, with water-to-binder ratios (w/b) of 0.30, 0.35 and 0.42. When cement was replaced by mineral additions, the activity index for replacement was 0.4 for fly ash, 2.0 for silica fume and 0.6 for slag, in accordance with EN206-1 guidelines [11]. All aggregates were German basalt, with a maximum size of 16 mm. One superplasticizer was used to obtain a target slump flow of 500 mm. Air entrainment was used in the mixtures with a w/b of 0.42, so that the target air content was 5 %. The mixtures with lower w/b ratios (0.30 and 0.35) were non-air entrained. The target compressive strength was over 60 MPa and the 22 mix designs included the following factors:

- 2 reference mixtures without mineral additives
- 6 plain mixtures (7 % silica fume) at 3 w/b ratios, with and without air entrainment
- 6 mixtures with fly ash (10, 20 or 40 %) and 7 % silica fume together
- 4 mixtures with ground blast furnace slag (30 % typical slag with silica fume or 7 % extra fine slag without silica fume)
- 4 mixtures with varying silica fume (3 and 10 %).

4.2 Testing Methods

Domestic Project: Laboratory testing
Approximately 30 samples were made for every concrete mixture and all mixtures were cured in a normal curing environment and by heat-treatment. The normal curing environment was 20±2°C and >95 % RH. The heat-treatment was done to simulate pre-cast factory conditions, with storage at 50°C for 2 days followed by normal curing. All samples were cured for 91 days prior to laboratory tests or field placement. In some cases the samples were stored in a drier climate (20±2 °C and 65 % RH) prior to testing, as specified in standards. Table 1 gives an overview of the long-term tests performed based on the standards.

Table 1 - Long-term tests conducted

Lab Tests		Notes
Compressive Strength [12]		2, 7, 28, 91, 365 days
Freeze-thaw:	Slab [1, 2]	deicing and plain water both
	CIF [1, 3]	plain water only
	SFS 5449 [4]	deicing only
Pore Characterization:	Capillary Water Uptake [13]	Fagerlund method
	MIP [14]	
	Thin-sections [15]	
Field tests	freeze-thaw [1, 2]	non-saline environment
	carbonation [16]	
Factory tests	Roofing tile QC [17, 18]	

Domestic Project: Factory and field testing
Tests on stiff types of concretes were done primarily at factories. Stiff types of concrete are mixtures with no workability which are vibrated and/or compacted into products, such as paving stones and roofing tiles. These tests were done with the use of fly ash, slag and crushed aggregate.

All mixtures cast in the laboratory were placed at 2 field stations in the cities of Sodankylä and Espoo for real-time exposure. The field stations have the following properties:
Sodankylä, Finland field station:

- 150 km north of Arctic Circle and city of Rovaniemi
- Latitude 67°22'N, Longitude 26°39'E
- Elevation =55 m above sea level
- Average weather conditions: winter -13.1°C and summer +12.4°C

Espoo, Finland field station:

- Located along seashore in neighbourhood of Otaniemi, near VTT
- Latitude 60°11'N, Longitude 24°50'E
- Elevation = 0 m above sea level
- Average weather conditions: winter -3.8°C and summer +15.9°C

European project
Over 100 samples were made for every concrete mixture and distributed around the Nordic countries for testing starting at the age of 28 days. All mixtures were cured in the normal

environment of 20±2°C and >95 % RH unless otherwise specified by the standards. The lab and field test methods were similar to those listed in Table 1 though no factory tests were performed. The frost testing included cycles of both ±20 °C and ±40 °C and went for double the duration as specified in the standards (i.e. Slab test to 112 cycles). Additional tests included assessment of acid resistance, chloride resistance, cyclic temperature attack, drying and autogenous shrinkage. The field station placements were done only at Sodankylä and then another 8 field stations around Europe (2 in each country: Iceland, Sweden, Germany, Italy). The results of these additional lab and field tests are reported elsewhere [6].

5. TEST RESULTS

5.1 Domestic project

Figure 1 shows some of the trends from the compressive strength testing. The effect of heat-treating at the start of curing can be seen from these figures. The cases where the heat-treatment improved the strength was at the age of 7 days for mixtures containing mineral additives, such as 40-60 % fly ash and 25 to 70 % slag. The heat-treatment had a greater impact on mixtures containing a higher amount of additions, as expected. At 91 days there was always a lower strength in the heat-treated samples compared to the normal cured specimens. The deviant strength development of concretes that have a higher addition of mineral admixture derives from the fact that at seven days the chemical reactions of neither fly ash nor slag have yet contributed to the full-scale strength development compared to normal cured concretes. On the other hand, the heat-cured concretes benefit from the heat-treatment and gain more strength at early ages because of the accelerated fly ash and slag chemical reactions. By the age of 91 days the situation has turned vice versa and the slow strength development of normal cured concretes has bypassed the strength development of the heat-treated concretes.

The strength levels at 7 and 91 days for both concrete types (containing fly ash and slag) at high levels of substitution indicate that the activity indexes of both mineral admixtures was incorrectly wrong. The activity of fly ash (0.3 at 91 days) was assumed too low. Therefore the cement amount is relatively high, also in the mixture with a high addition of fly ash, which contributes to the higher strength level at 7 days compared to slag concretes which had relatively low amounts of cement in the high substitution mixes. For slag concretes, the activity was assumed to be 1.0 at 91 days. The correct activity values for fly ash and slag at 91 days should have been 0.5 and 0.8, respectively.

When conducting frost-tests, none of the mixtures showed internal damage after 56 freeze-thaw cycles in either the slab or CIF test when evaluated using ultrasonic transit time. As expected, no mixtures showed scaling damage when plain water was used as the testing liquid. The results of testing after 56 freeze-thaw cycles using de-icing salt agent as the testing liquid are presented in Figure 2. For the mixtures containing fly ash (Figure 2a), there was an increase in the scaling with higher amounts of additions, beyond the acceptance limit of 1.0 kg/m^2. Similar results were found from the CIF testing.

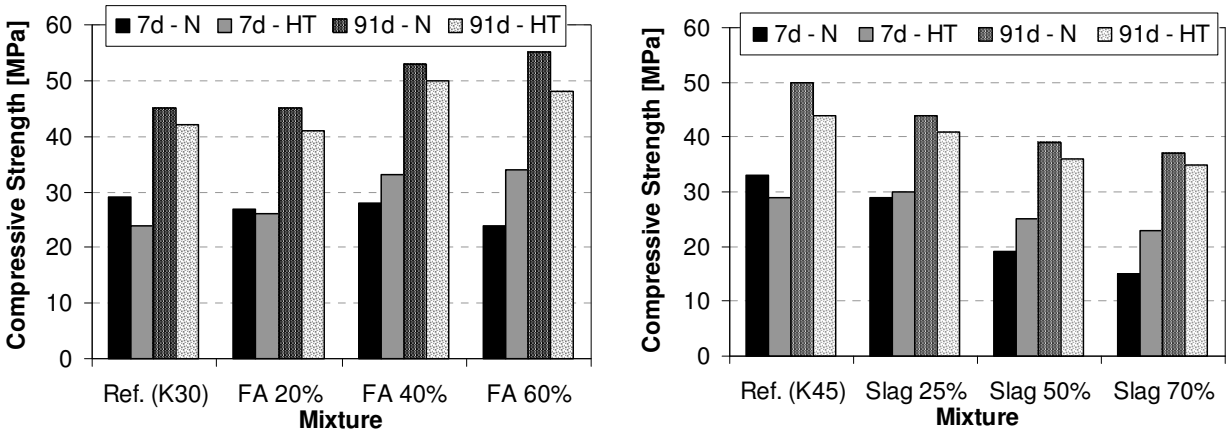

(a) Fly ash mixtures *(b) Blast furnace slag mixtures*

Figure 1 - Compressive strength results for normal cured (N) and heat-treated (HT) mixtures at 7 and 91 days. Reference mix labels of K30 and K45 refer to strength class.

The mixtures containing slag showed the same trend of increasing scaling with higher addition amounts (Figure 2b), though in all slag mixtures the scaling limit was not reached. The fly ash mixtures were only tested for normal cured samples, while the slag mixtures were tested for both curing regimes. The only difference was seen at the high addition of 70 % slag, where the heat-treated specimens showed less deterioration. None of the slag mixtures tested with plain water showed scaling greater than 0.05 kg/m^2.

The reference K45 mixture had extremely high scaling for the heat-treated specimen. The same results were seen in the Finnish SFS test, where the heat-treated mixture had three times greater volume loss than the normal cured samples. The capillary water uptake of this mixture was also much higher than the other mixtures. The thin-section microstructural evaluation of this heat-treated mixture revealed the satisfactory air content (total air = 7.4 %, specific surface = 31 mm^2/mm^3 and 0.14 mm spacing factor), with a very high degree of hydration though the air voids were somewhat inhomogeneous and contained calcium hydrates. The Mercury Intrusion Porosimetry (MIP) investigations also showed that the heat-treated specimens had a lower mesoporosity (pore radius ~ 100-10000 nm) than the regular cured specimens. Further investigations have been underway to examine the high deterioration of this mixture.

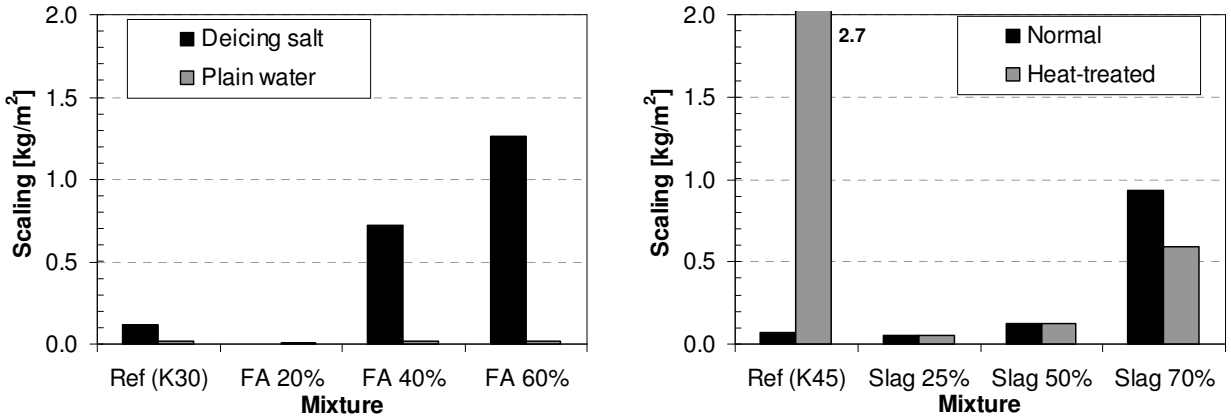

(a) Fly ash mixtures, normal curing *(b) Slag mixtures, deicing salt*

Figure 2 - Freeze-thaw results from slab test, with plain and de-icing salt exposure for different curing methods. Testing after 56 freeze-thaw cycles, with 91 days curing prior to testing.

5.2 European Project

Only a few key results from the CONLIFE EU-project will be given here, as additional results are well documented in other publications [6]. Figures 3 to 5 gives samples of the results from the slab freeze-thaw test [1] after 112 ftc at ±20°C, for pure frost and frost-salt testing respectively. On the graphs the surface scaling (y-axis) is compared to the internal damage measured by relative dynamic modulus (RDM, on the x-axis). A mixture having either a RDM value below 80 % or scaling greater than 1000 g/m^2 was considered failing.

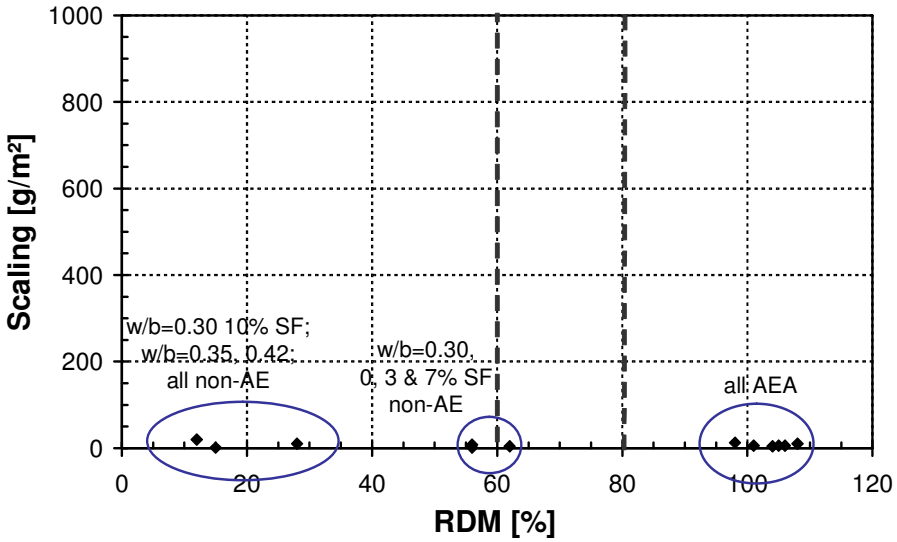

Figure 3 – Slab pure frost freeze-thaw test results (112 cycles) for mixtures with varying amounts of silica fume (SF) and air entrainment (AEA). [6]

The results in Figure 3 show that for pure frost, internal damage was the controlling deterioration mechanism. This held true for all HPC mixtures tested, as no mixtures had severe scaling. As expected, all of the mixtures that were non-air entrained (non-AE) failed the test and more severely as the w/b ratio increased from 0.30 to 0.42.

Additional results showed a high dependence between the amount or rate of capillary water uptake and the time until the concrete started to show internal damage. Some modelling was done on these correlations and is elaborated on in the reports [6]. And example of this type of modelling can be seen in Figure 4, where the progress of internal damage (Relative Dynamic Modulus - RDM) over the test duration inversely mirrors the moisture uptake. These results are for mixtures containing 7 % silica fume. The results showed that the non-air entrained (no-AE) mixture at a w/b of 0.42 had the earliest onset of frost damage while also having the highest amount and greatest rate of water uptake. The air-entrained mixture (AE) at the w/b of 0.30 showed no internal damage after 112 cycles and the moisture uptake remained very low through the whole test duration. The results lead to the conclusion that the time until a critical degree of water saturation is reached is an important factor when assessing pure frost damage.

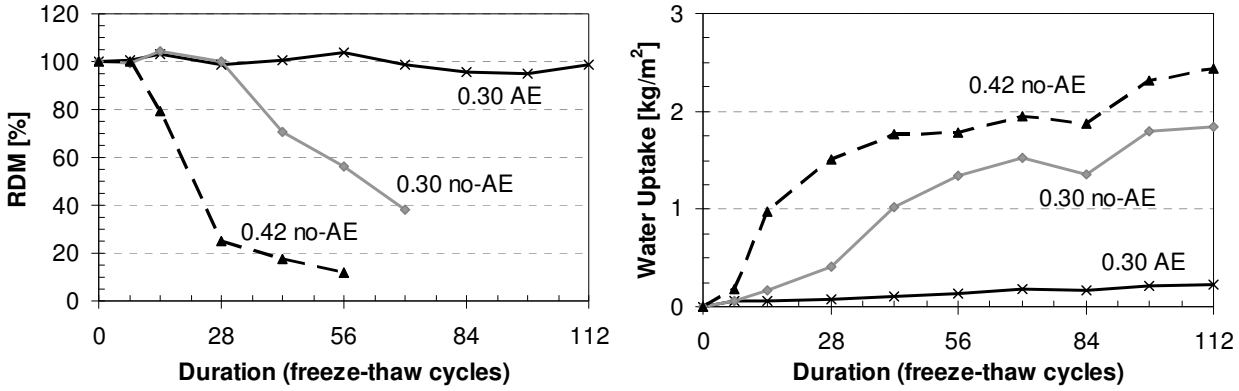

(a) *(b)*

Figure 4 – Progress of (a) internal damage (RDM) and (b) moisture uptake over time during pure frost freeze-thaw tests.

Another freeze-thaw condition includes the consideration when deicing solution is present, as given in Figure 5. The results show that both internal damage and scaling can occur in the frost-salt tests. In these mixtures and others within the test program, the results ranged from no damage (such as with the air entrained mixtures), to mixtures with full loss of RDM and medium to high scaling (such as in the non-air entrained mixtures). Typically the acceptance criteria for durability of concrete exposed to frost-salt with deicing solution is based on scaling alone. These results showed that for high strength concrete the criterion of internal damage (RDM) is also important since some mixtures had severe internal damage (low RDM) but also low scaling. Further analysis of these and other frost-testing results can be found in the European project reports [6], including comparisons to the existing trends as reported by other research.

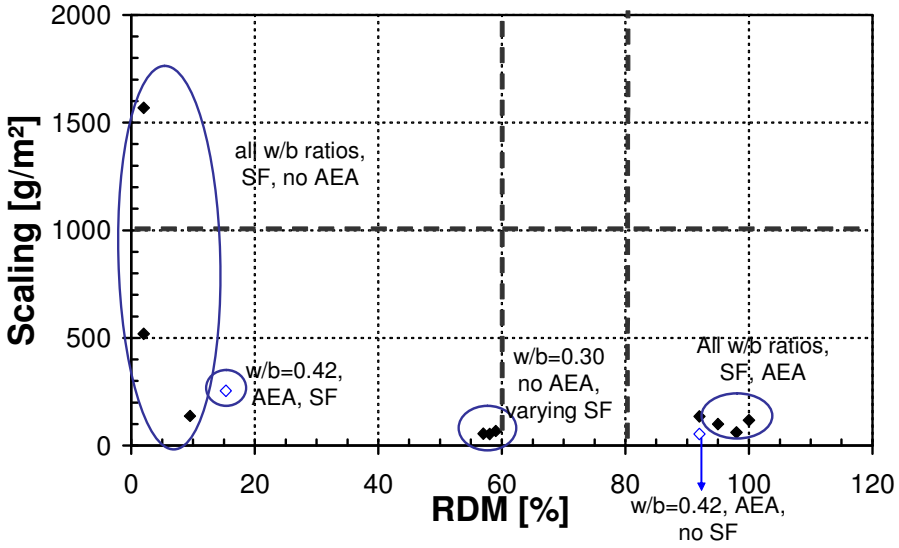

Figure 5 – Slab frost-salt test results (112 cycles) for mixtures with and without silica fume (SF) and air entrainment (AEA).

Figure 6 shows a comparison of laboratory and field results after frost exposure of a mixture at the Sodankylä, Finland test station with a -40°C test environment. These results are for a non-durable mixture having a w/b of 0.42, containing 7 % silica fume and non-airentrained. It is seen that there is a good correlation of the results, with failure indicated by the drop in RDM

below 80 % which indicates internal damage. This deterioration level in both the laboratory and field tests occurred after less than 100 freeze thaw cycles (ftc), or within the first winters.

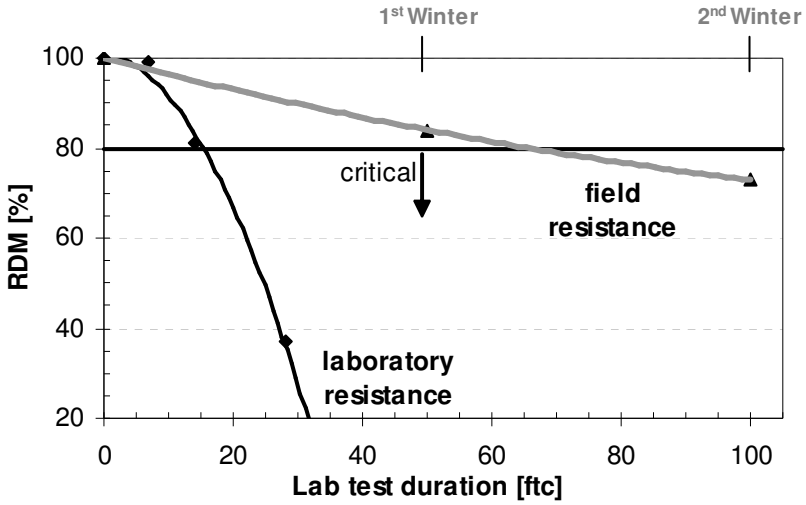

Figure 6 – Comparison of results of lab test and field exposure for a non-durable mixture at Sodankylä field station.

Subsequent healing of the field samples in the summer provided a longer life, yet the sample continued to deteriorate with additional freeze-thaw cycles in the next winters. It is important to continue these types of long-term field tests to assess the applicability of accelerated lab testing for service life predictions.

6. SERVICE LIFE ASSESSMENT

The results of these studies have shown that the use of more environmentally friendly concretes containing high amounts of mineral additives is feasible. It is possible to ensure these mixtures' durability and applicability in severe environments. The results from the domestic project freeze-thaw tests were evaluated in comparison to the Finnish acceptance criteria, which are also a part of the EN206 Finnish Annex [11], as given in Table 2. The criteria in this table are the mass loss due to scaling (m) and internal damage as assessed by the relative dynamic modulus (RDM). For exposure to deicing agents, there is no internal damage requirement since the scaling is the deciding factor. Similar criteria are also defined for the CIF/CDF and Finnish SFS freeze-thaw test methods.

When combining the accelerated material laboratory tests with evaluation of a concrete structure's geography, construction and other parameters, it is possible to estimate the service life design of the structure. Based on the material lab results alone, the mixtures containing up to 60 % fly ash or 70 % slag would be suitable for both XF1 and XF3 for a 200 year service life since the scaling was so low. None of the fly ash mixtures would be suitable for XF2 and XF4 classes (deicing salt exposure). The mixtures containing 25 % slag would be suitable in class XF2 for 200 years or XF4 for 100 years, while the 50 % slag mixtures have a shorter life-time expectation of 100 years and 50 years for the respective classes.

Table 2 - Finnish concrete structural service life from results of slab test for EN206 exposure classification [11]

Exposure Class		Scaling (m_{cycles}) and Internal Damage (RDM) Service life (years)		
		50	100	200
XF1	Moderate saturation, plain water	$m_{56} \leq 500$ g/m^2 $RDM_{56} \geq 67$ %	$m_{56} \leq 200$ g/m^2 $RDM_{56} \geq 75$ %	$m_{56} \leq 100$ g/m^2 $RDM_{56} \geq 85$ %
XF3	High saturation, plain water	$m_{56} \leq 200$ g/m^2 $RDM_{56} \geq 75$ %	$m_{56} \leq 100$ g/m^2 $RDM_{56} \geq 85$ %	$M_{112} \leq 100$ g/m^2 $RDM_{112} \geq 75$ %
XF2	Moderate saturation, deicing agent	$m_{56} \leq 500$ g/m^2	$m_{56} \leq 200$ g/m^2	$m_{56} \leq 100$ g/m^2
XF4	High saturation, deicing agent	$m_{56} \leq 200$ g/m^2	$m_{56} \leq 100$ g/m^2	$M_{112} \leq 100$ g/m^2

The criteria in Table 2 are empirically established, based on experience from concrete with traditional constituents. Long-term field exposure to assess strength, frost-resistance and carbonation are still underway. With these and other real-time assessments it will be possible to further verify or adjust the Finnish acceptance criteria, so also the new environmentally-friendly concrete types with mineral additions can be dealt with.. The specimens remain at the field stations and will be continuously evaluated after this project. After the first winter, the samples had been subjected to approximately 42 freeze-thaw cycles at the Sodankylä (northern) site and 54 freeze-thaw cycles and the Espoo (seashore) site.

The results from factory testing and analysis are described in the next section. The results of modelling and guideline development are still underway and will be presented to industry in early 2005.

7. IMPLEMENTATION OF THE RESULTS BY INDUSTRY

The issue of the environment and the need for sustainability are playing part in political life with attendant effects on economic decisions and on the business. Industry will succeed in the long run only if the actions respect the common interest.

In the domestic project, the project aims were driven by industrial partners. The results from the earlier parts of the domestic project and information gained from the European project were directly applied in domestic factory tests. An emphasis was put on ensuring environmentally-friendly products that would maintain their outstanding durability. One factory where tests were conducted was at Lafarge Tekkin Oy. This company is the Finnish operating company of Lafarge Roofing, which is a division of Lafarge Group. Lafarge is committed to continuous environmental performance improvement and Lafarge environmental policy is supplemented with clear environmental objectives.

At Lafarge Tekkin Oy, LCI and LCA assessments have been used to provide information of the environmental impact of concrete roof tile manufacturing. This covers acquisition and processing of raw material, transportation of finished products, performance in service and disposal at the end of service life. In the assessments, the materials used, energy and the

emissions to the environment were determined both quantitatively and qualitatively and the impacts of these have been assessed in relation to the ecological system, human health and raw material consumption.

The results shown in Table 3 reveal that the biggest environmental impact of concrete tile production process is from manufacturing of cement. The right side of the table gives the relative effect, or change, in both emissions and fuel consumption within the 5 year improvement phase. The other significant impact, albeit to lesser extent, is from transportation. No toxic substances are emitted in the tile manufacturing process. The calculations correspond to an average tile weight of 4.2 kg, and their consumption during use is 9.5 to 11 tiles/m^2.

Table 3 - The environmental effects of changing roofing tile production process over 5 years.

Emissions (g/tile)	1997	2002	Change (%)
CO_2	632	589	7
CO	2.6	0.5	82
NO_x	3	2	18
SO_2	1.3	0.6	50
VOC total	1.0	2.1	-100
Heavy metals	0.0001	0.0002	- 24

Fuels (MJ/tile)	1997	2002	Change (%)
Non renewable fuel	6.7	5.5	18
Renewable fuel	0.28	0.47	-66
Inherent energy	2.1	1.8	14

In the domestic project, Lafarge Tekkin tiles containing high amounts of mineral additions were studied. Tests were done on three sets of tiles that were approximately 10 years old and contained up to 30 % fly ash or 45 % slag. The tiles were tested following EN490 and EN491 standards [17, 18] for transverse strength, permeability and freeze-thaw testing. All of the results were good, as the characteristic transverse strength was about 5 kN while the requirement is > 2 kN. After freeze-thaw testing there was no significant reduction of the strength or any change in the permeability.

The microstructure of the tiles was investigated by means of MIP [14] and polarisation microscopy, using thin sections [15]. The MIP results showed the total porosity of all three sets of tiles was about 11 %, with a specific surface of 3.4-3.9 m^2/g and a bulk density of 2.2 g/cm^3 in all three sets. A sample MIP result is given in Figure 7 and a sample photo of the microstructure is shown in Figure 8. The results from the microscopy investigations showed:

- The aggregate was quartz rich sand with a maximum size of 2 mm.
- The binding agent was cement with addition of fly ash (20-30 %) in Tiles A and C and slag (40-50 %) in Tiles B.
- The structures were homogeneous and dense (as seen in Figure 8).
- The air content in Tiles C (25% fly ash) was a bit higher than in Tiles A (30 % fly ash) and Tiles B (45 % slag)
- The carbonation depth was 2-3 mm.
- There were no frost cracks in the tiles.

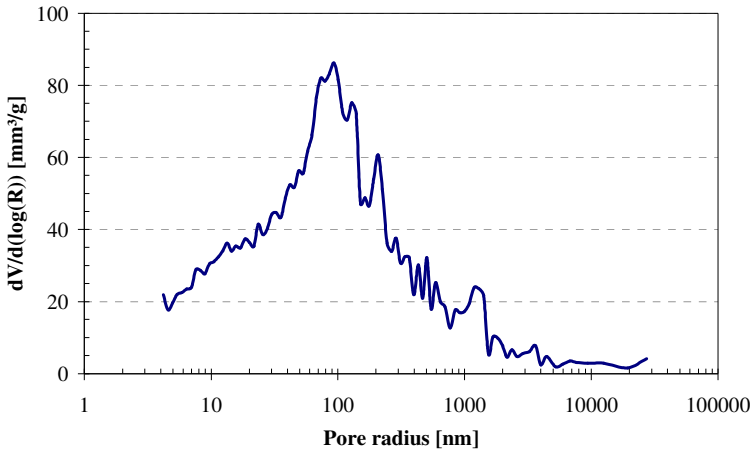

Figure 7 – Pore size distribution by MIP for Tiles C with 25 % fly ash. 11.7 % total porosity.

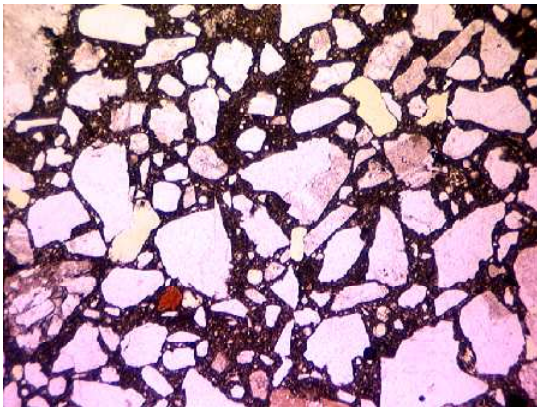

Figure 8 - Thin-section of Tiles C with 25 % fly ash, showing homogeneous and dense structure. Micrograph height is 2.7 mm.

At Lafarge Tekkin the combination of field core sampling and laboratory studies along with LCI results have been used to provide information on environmental impacts of concrete roof tile manufacturing. Based on the combined results it is possible to set priorities for making environmental improvements to reduce burdens. The concrete tile producer has done the basic recipe for development work. Further developments and many improvements have been made based on the results achieved in the domestic project. This project has successfully combined the results from R&D work with implementing the results into production of concrete roof tiles and other products.

8. SUMMARY

The wide range of test results in both projects showed that the goals of the projects were met. Economic and environmental LCA analysis showed the benefit of utilizing mineral additives, while maintaining concrete durability [6]. The durability performance covered pure frost, frost-salt, chloride ingress, acid attack and shrinkage cracking considerations. The test methods for freeze-thaw durability were compared and recommendations were shared with Finnish industry about testing methods used in the future. Initial indications show that the field station results can be correlated to accelerated lab tests, though the studies should continue for many years to gain more understanding.

Overall, these two projects have successfully shown how concrete can be made more environmentally-friendly and still maintain outstanding durability characteristics. Reviews of in-service structures, accelerated laboratory tests, real-time field tests and factory development

work have all yielded informative results that have helped to form guidelines for the Finnish industry. It is possible to increase the amount of mineral additives in the mixtures and achieve the desired strength level and reasonable strength development while still obtaining good frost resistance. Providing a proper air void structure also proved to be significant in ensuring frost resistance.

Regarding the involvement of industry in Finnish research, their environmental optimism is part of today's development work. The environmental work carried out at e.g. Lafarge Tekkin Oy is part of the continued development taking place in the Finnish concrete industry and the entire construction field. Development has occurred and is ongoing, albeit slowly. A processed way of working, reviews covering larger entities and the entire life span of the product, and the inclusion of the entire product chain constitute the way forward in environmental work. Quality and environmental systems are good tools aiding the technical implementation of different issues. The environmental strategies emphasize preventive action and ecologic competitive ability. Environmental operations are developed by taking into account legislative demands, the expectations of society, technological development and increases in information.

REFERENCES

1. prEN 12390-9, "Testing hardened concrete – Part 9: Freeze-thaw resistance - Scaling," Draft European Standard, Brussels, 2002.
2. RILEM TC 176-IDC, "Slab Test – Freeze/Thaw Resistance of Concrete – Internal Deterioration," Materials and Structures, 2001, Vol. 34, pp. 526-531.
3. RILEM TC 176-IDC, "CIF-Test – Capillary suction, Internal damage and Freeze thaw test," Materials and Structures, 2001, Vol. 34, pp. 515-525.
4. SFS 5449 "Concrete. Durability, Frost-salt resistance," Finnish Standards Association SFS, 1988.
5. The Convention and Kyoto Protocol, web page of the United Nations Framework Convention on Climate Change,http://unfccc.int/resource/convkp.html, 2004.
6. Deliverable Reports D1 to D10, CONLIFE: Life-time prediction of high-performance concrete with respect to durability, EU 5th Framework Project G5D1-2000-25795, http://fasae.ibpmw.uni-essen.de/euproject/, 2004.
7. Tulimaa, M., Holt, E., Wirtanen, L., Kukko, H., Penttala, V., Environmentally friendly and durable concrete (in Finnish), Helsinki University of Technology, Building Materials Technology, To be published spring 2005.
8. Häkkinen, T. et al., "Environmental Profiles of Building Products and the Principles for Assessment," VTT Research Notes 1836, Technical Research Centre of Finland, Espoo, 1997, 138 p.
9. Nordic Concrete Federation: "Durability of Exposed Concrete Containing Secondary Cementitious Materials," Proceedings of workshop in Hirtshals, Denmark, 21-23 November 2001.
10. Betoninormit 2000, BY 15, RakMK B4, Suomen Betonitieto Oy, 2000.
11. EN 206-1, Annex A "Concrete – Part 1: Specification, performance, production and conformity," European Standard, draft Finnish National Annex, 2004.
12. EN 12390-3: "Testing of hardened concrete – compressive strength testing of specimens, European Standard, 2002.
13. Fagerlund, G., "The critical degree of saturation method of assessing the freeze/thaw resistance of concrete," Materials and Structures, Vol. 10, No. 58, 1977, pp. 217-229.

14. Cook, R.A. and Hover, K.C., “Mercury porosimetry of hardened cement pastes,” Cement and Concrete Research, Vol. 29, No. 6, 1999, pp. 933-943.
15. NTBUILD 381 “Concrete, Hardened: Air Void Structure and Air Content,” Nordtest Method 1991.
16. CEN CR 12 793: “Measurement of the carbonation depth of hardened concrete,” 1997.
17. prEN490 “Concrete roofing tiles and fittings for roof covering and wall cladding – Product specification,” draft European standard, 2004.
18. prEN491 “Concrete roofing tiles for roof covering and wall cladding – Test methods,” draft European standard, 2004.

Durability of High Strength Self-Compacting Concrete (HSSCC) - a study based on laboratory tests and field performance

Gísli Guðmundsson
Ph.D. Senior Research Scientist
Hönnun
Grensásvegi 1, 108 Reykjavík

ABSTRACT

The frost resistance of two non-air entrained HSSCC test samples was not very good. The samples showed poor performance when tested with water with serious internal damage. The scaling resistance was better. Both the concrete samples passed the 1 kg/m^2 criteria after 56 cycles. When tested again at the age of 5 months, the sample SCC-II failed the scaling test. This test results is backed up by evidence of surface cracking in a real structure after 290 days.

There is some evidence that the abundance of silica fume lumps are contributing to the crack formation. Some of the silica fume lumps showed signs of alkali-silica-reactions. This was not confirmed by the SEM analysis. If these samples are ASR active or become active during a freezing and thawing process it will aid to the break down of the samples.

The chloride diffusion coefficient of the concrete is relatively low and as with normal concrete it improves with the age of the concrete. The chloride content of the concrete is relatively high, much higher than in a normal concrete. More research is need to verify this behaviour in other types of SCC. If this is the case for SCC then chloride induced corrosion could be a serious problem.

The concrete which is the scope of this research is in many ways unique, therefore the conclusions can not be generalized upon all types of SCC.

Key words: freeze/thaw resistance, chloride diffusion, silica fume lumps

1. INTRODUCTION

The concept of Self-compacting concrete (SCC) was first introduced in 1988 [1]. SCC offers many new solutions to the concrete industry, due to its unique rheological properties. During the past 3-4 years the utilization of SCC in Europe has been steadily growing each year. Much effort has been on the rheological properties of SCC and less on the durability of SCC. Zhu et al. [2] studied the transport properties as well as the durability of SCC. They concluded that the chloride migration depended much on the type of solid additives used in the mix. Mörtsell and Rodum [3] compared SCC with normal concrete and found out that for variety to durability tests, SCC only showed better frost resistance of the skin surface. Makishima et al. [4] studied frost resistance of SCC. The concluded that SCC has excellent resistance to freezing and thawing, but in order to achieve long-term frost resistance, entrained air is needed. Persson [5] studied the frost resistance of SCC. In his conclusions, he found that internal damage is much less in SCC compared to normal concrete, but scaling is similar between SCC and normal concrete. Contrary to [4] no relationship between the air void content and frost resistance.

This relatively small summary of work done with respect to the durability of SCC underlines that there are many types of SCC, probably much more than there are of normal concrete. Each and every variable influences the properties of the concrete, including the durability, therefore each case must be considered separately. It can be misleading when different types of SCC are compared together or SCC is compared to normal concrete.

The scope of this research is to study the durability of self compacting concrete, mainly the freeze/thaw resistance and the chloride penetration, and to a lesser extent the interaction between sea-water and concrete (in terms of sulphate attack). This paper presented here is only focused on one type of self-compacting concrete in two particular structures which were cast in 2002.

The structures are two bridges located in the town of Borgarnes, in Western Iceland. The concrete in both the structures was used as a cover-crete, i.e. it was used to repair damaged areas in the bridge piers, see Figure 1 and 2.

The older bridge (Brakarsund) shown in Figure 1 was originally cast in the middle of last century. In 1998 it was rebuilt. In 2002 a part of the foundations were still in need of repair and in it was repaired with self compacting cover-crete, which was cast over the damaged area – SCC-I.

Figure 1. Brakarsund. The picture is taken prior to the repair in 1998. SCC was cast in 2002 in the foundation of the bridge on the near end of the bridge where the wooden moulds are. The picture is taken at low tides. The foundations were submerged in sea water within two hours.

The piers under the younger bridge (Borgarfjordur) are being damaged, the damages have been described elsewhere [6]. Prior to the repair described here, two piers have been repaired with high performance concrete [7]. In 2002 the third pier was repaired with self-compacting concrete – SCC-II [8], which is in the scope of this paper.

Figure 2. Borgarfjordur bridge. Two piers on the picture have been repaired with cover-crete. The second one was done with SCC in 2002.

Both the structure were cast with the same type of concrete. The Brakarsund repair was performed on 12-9-2002 and the repair on Borgarfjordur was done on the 24-09-2002.

1.1 Type of concrete

The concrete consists of Norwegian aggregates, cement, silica fume, which were imported to Iceland in ready-to-use big bags. The mix-design was made in Iceland and is given in Table 1 and custom made in Norway. A more detailed description of the mixture is found in [8].

Table 1. Mixing proportion of concrete, the cement and aggregates are from Norway

	kg/m^3
Cement	497
Silica fume	40
W/B-ratio	0.28
Norwegian sand	1054
Norwegian gravel	676
Glenium 51	5.29
Defoamer	yes

In the mixture the silica fume was as a dry powder, not as a slurry nor inter-grinded with the cement clinker. The big bags were emptied into concrete trucks and mixed there. Only water, super-plasticizer, defoamer and plastic fibres were added to the mixture in Iceland. All the test samples, which are described in this paper, were taken at the construction site.

The compressive strength (cylinder) was measure after 28 and 90 days and the results are given in Table 2.

Table 2. Compressive strength of the concrete, MPa. Samples were 10 by 20 cm cylinders

	28 days	90 days
SCC-I	94.3	114.6
SCC-II	107	118.2

The strength is relatively high, 28 day strength about 100 MPa. There is a significant difference between the 28 day compressive strength of samples SCC-I and SCC-II, which presumably lies with a different degree of compaction of the test samples. The 90 day strength is about 115 MPa.

The air void characteristics were measured in mix SCC-II, and the results are given in Table 3.

Table 3. Air void characteristics of SCC-II, average values are given in the lowest line. The measurements were done by point counting hardened concrete samples

Total air content, %	Spacing factor, mm	Specific surface, mm^{-1}
1.7	0.76	11
1.0	0.52	20
2.2	0.70	11
1.6	0.66	14

As expected the air void content of the concrete was relatively low, less that 2 %. The air voids are rather big and far apart.

2 TEST PROGRAM

All the test samples were cast at the construction site. The samples were cured in a standard way. After 28 days from casting, samples were tested for freeze/thaw resistance and chloride penetration and thin sections were made. Samples from SCC-II were stored in a field station outside The Icelandic Building Research Institute. After 5 months, samples were tested for freeze/thaw resistance.

In summer of 2003 cores were drilled from cover-crete in Brakarsund (SCC-I). Chloride penetration profile was established in the concrete and thin section was made of the concrete.

The frost resistance of the samples were tested according to the Swedish standard SS 13 72 44, which recently has been accepted as a European reference method. The samples were tested with 3 % NaCl and with pure water. Surface scaling was measured as well as internal damage. With the standard method, the samples are tested for 56 cycles, but theses samples were tested up to 168 cycles.

The chloride diffusion coefficient was measured according to the NT Build 492 test method.

Grinding of the cores and the chloride analysis were carried out as described in [9].

2.1 Results of Freeze/thaw testing

In Figure 3 are given the scaling values after testing with 3 % NaCl.

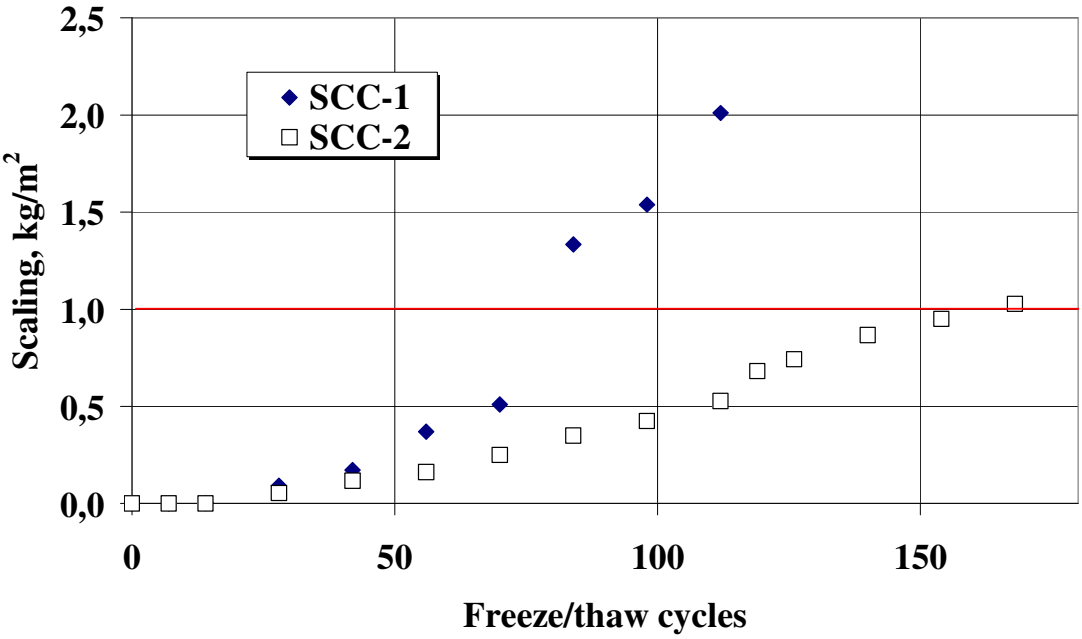

Figure 3. Measured scaling in standardized freeze/thaw testing on 28 day old samples. The samples were tested with 3 % NaCl solution. The solid line shows the limit (1 kg/m^2) after 56 cycles.

Both the samples passed the criteria of scaling less that 1 kg/m^2 after 56 cycles. The tests were continued beyond 56 cycles. The scaling continued in both the samples. Sample SCC-I had a sudden increase in scaling between 70 and 84 cycles, where the scaling rose from 0.5 up to 1.3 kg/m^2. The measured scaling in sample SCC-II was much less than in sample SCC-I and it was not until after 168 cycles when the measured scaling was more than 1 kg/m^2.

The ultrasonic pulse transmit time (UPTT) was measured using 55 KHz conic transducers [10]. The UPTT measurements are used to detect internal cracking during freeze/thaw testing. The measurements were carried out at the same time when the scaling was measured. The measured values are reported as relative to the initial value. Generally, the acceptance criterion is if the measured value is less that 120 % after 56 cycles. In Figure 4 are shown the results of the measurements on the 28 day samples.

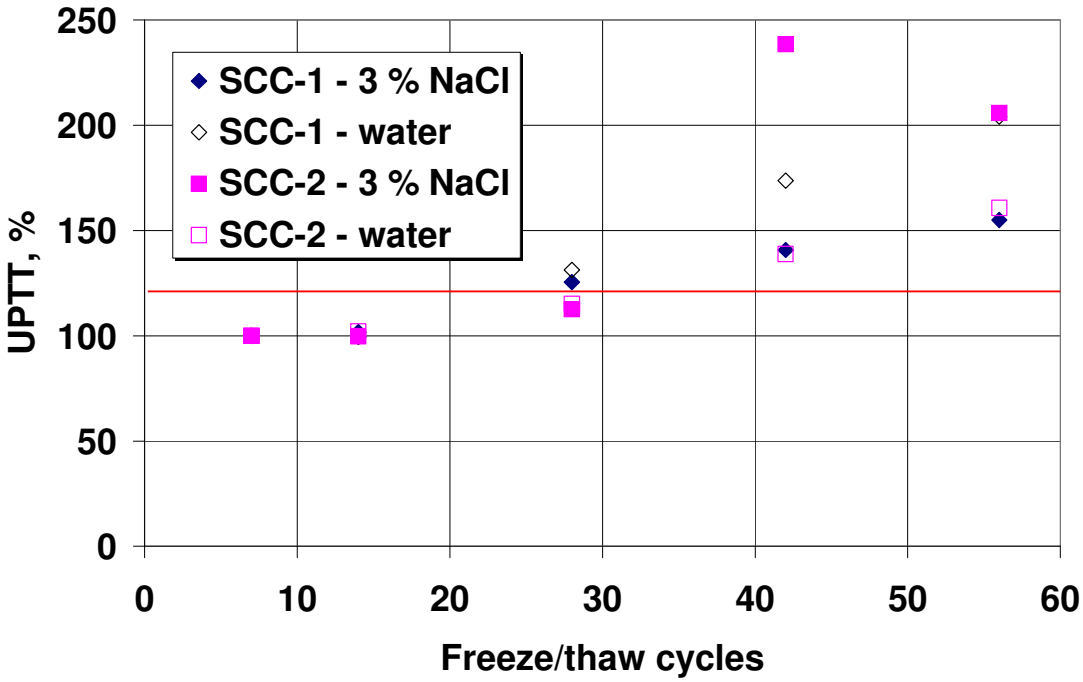

Figure 4. Freeze/thaw internal damage (UPTT) with 3 % NaCl and water. The acceptance criterion is shown as the solid line.

There is not much difference between sample SCC-I and SCC-II and also not much different if the freezing medium is water or 3 % NaCl-solution. It seems that the 120 % criterion is achieved after 28 cycles in both samples regardless of which freezing media is used.

Water uptake and length change during the freeze/thaw cycles were also monitored. The results show that the samples take up relatively high amount of water and the dilation measurements indicate that the sample expanding. These results, combined with the UPTT measurements, shown in Figure 4, indicate that internal damage is severe in these samples.

Samples of SCC-II which were stored in a field station outside the IBRI were tested at an age of 5 months. The measured scaling is shown in Figure 5, for comparison the scaling values of the 28 day old samples are also shown.

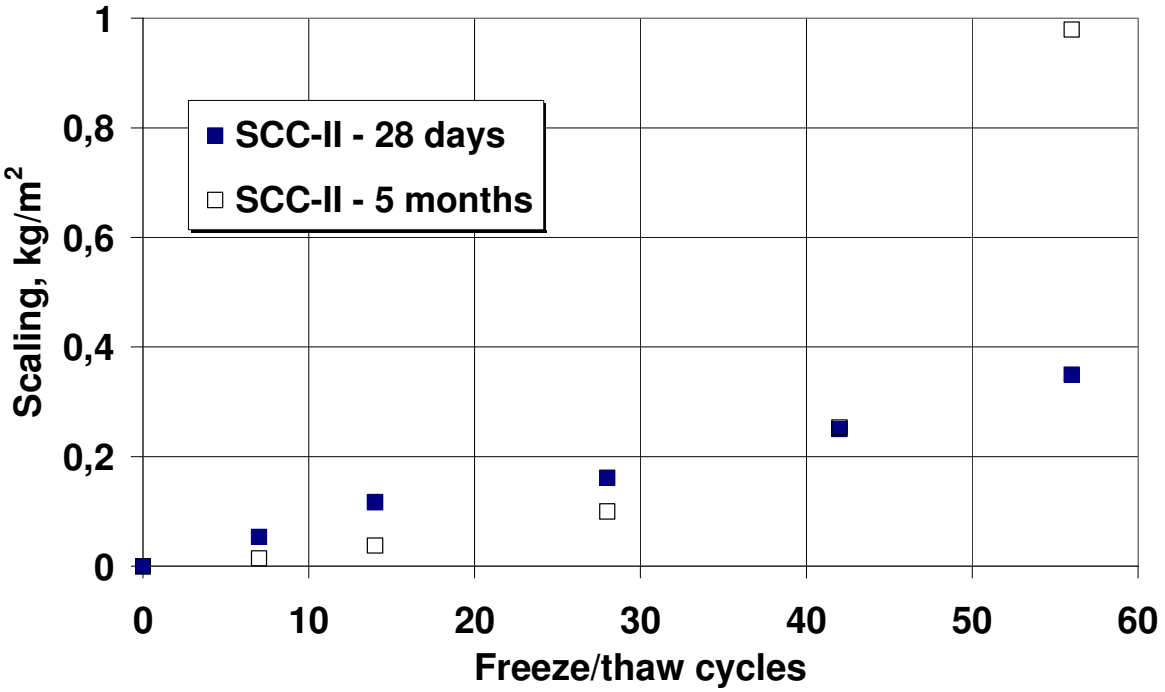

Figure 5. Measured scaling (3 % NaCl) in standardized freeze/thaw testing on 5 months old samples and for comparison the result of measurements on 28 day old samples. The scaling values at 42 freeze/thaw cycles are the same for both the samples.

The frost resistance has reduced during storage in field station, compared to the 28 day sample. Presumably the environmental conditions in the field station can not be the main reason for this increase, due to the short time and mild climatic conditions in the field station. The scaling is now similar to sample SCC-I. One interesting feature the 5 month sample has is the sudden increase in scaling between 28 and 56 cycles. After 28 cycles the scaling is only 0.1 kg/m^2, which is generally considered very good. At the completion of the test, the value for the scaling is 1 kg/m^2. Normally, scaling increases linearly with the number of cycle. Therefore, the acceptance criterion for 28 cycles is 0.5 kg/m^2. This sample does not mimic such behaviour.

When the 5 months old samples were tested with water, the sampled failed the test in a similar manner as the 28 day old sample, see Figure 4. At the end of the test, after 56 cycles, the slabs were cut in to 3 bars, 5 by 5 by 15 cm. The bars were broken in 3-point bending test and then the compressive strength was measured on each half (IST EN 196-1:1994). The results are given in Table 4, and for comparison values for a reference sample which was stored in a fog room are also given.

Table 4. Strength of sample SCC-II after the freeze/thaw test with water, for comparison is a reference sample, which was stored in a fog chamber

	Compressive strength, MPa	Flexural strength, MPa
SCC-II after test	67.4	1.8
SCC-II reference	117.2	11.4

The samples did not show any sign of deterioration after the freeze/thaw test, yet the strength has been reduced by more than one log unit.

2.2 Results of Chloride penetration

The chloride diffusion coefficient was determined with the NT Build 492 test method. The diffusion coefficient was measured in 2, 22 and 290 days old samples in concrete SCC-I. The 290 day old sample was taken from the structure. In concrete SCC-II, the diffusion coefficient was determined in 10 and 29 day old samples. The results of the measurements are given in Table 5.

Table 5. Diffusion coefficient as determined in NT Build 492

	Diffusion coefficient, m^2/sec
SCC-I – 2 days	$1.55 * 10^{-11}$
SCC-I – 22 days	$1.25 * 10^{-12}$
SCC-I – 290 days	$4.11 * 10^{-13}$
SCC-I – 290 days[1]	$3.16 * 10^{-13}$
SCC-II 10 days	$2.28 * 10^{-12}$
SCC-II 29 days	$2.11 * 10^{-12}$

The diffusion coefficient improves greatly in sample SCC-I between 2 and 22 days or almost by one log unit. The improvement continues as the concrete ages, at 290 days the chloride diffusion coefficient is lower than 28 day diffusion coefficient.

Chloride penetration profile was measure in the samples which were taken from Brakarsund after 290 day service. The chloride profile is shown in Figure 6 and the diffusion coefficient which was calculated from the data, using Ficks second law of diffusion [11] is given in Table 5.

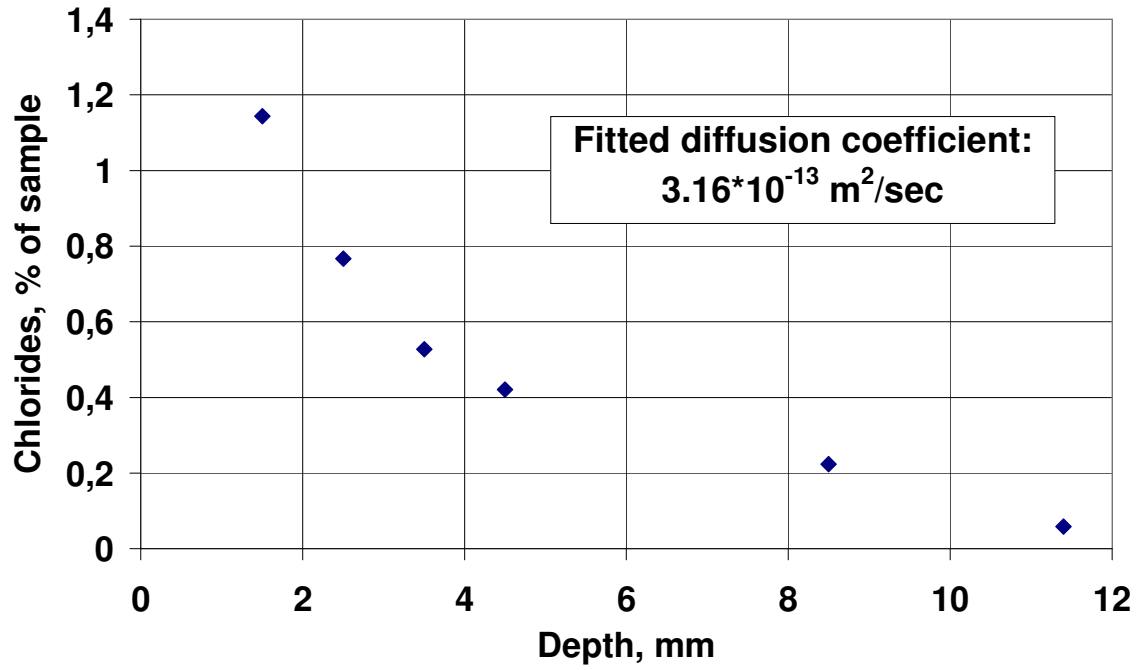

Figure 6. Chloride penetration profile in SCC-I after 290 day service. The concrete was submerged in sea-water after 2 hours from casting.

[1] value derived from chloride penetration

The chloride content of the sample is very high, in a normal concrete the chloride surface content is usually between 0.4 and 0.6 % of concrete weight, but in SCC-I it is close to 1.4 % of concrete weight.

For the 290 day samples, there is a very good agreement between the measured diffusion coefficient according to test method NT Build 492 and the calculated one from the data in Figure 6. The difference is within the error of the measurements.

2.3 Microscopic analysis

Thin sections were made for samples from SCC-II, the samples which were stored in the filed station outside IBRI for 5 months. The thin sections were made from reference samples and samples which were tested in the freeze/thaw (both with water and 3 % NaCl solution). Finally, thin sections were made from samples from SCC-I structure an after exposure for 290 days (Brakarsund).

The reference concrete (SCC-II) is characterized with relatively thick interfacial transition zone (ITZ) between the aggregates and the cement paste, see Figure 7.

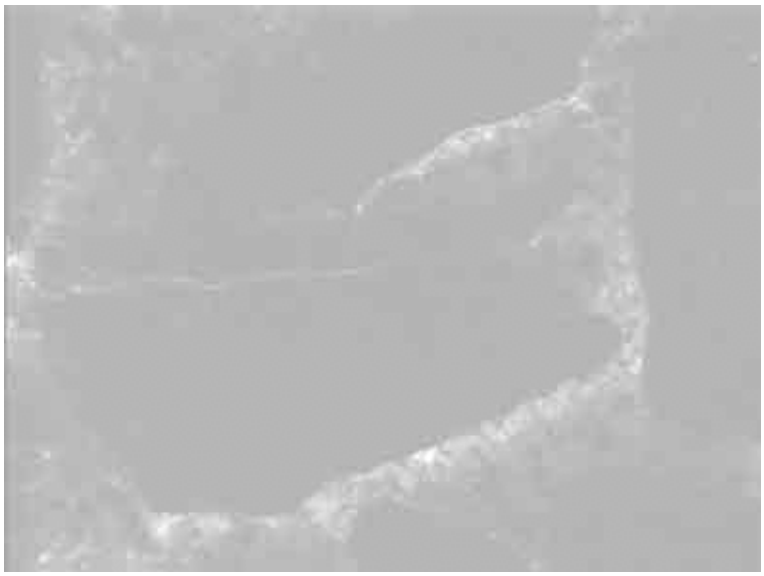

Figure 7. Microphotograph taken with Mercury fluorescence light. Aggregates are opaque and the relatively dense cement paste is dark. The bright areas are relatively open ITZ around aggregates. The frame is 1.36 by 1.04 mm.

The ITZ is also visible with the SEM, see Figures 8 and 9.

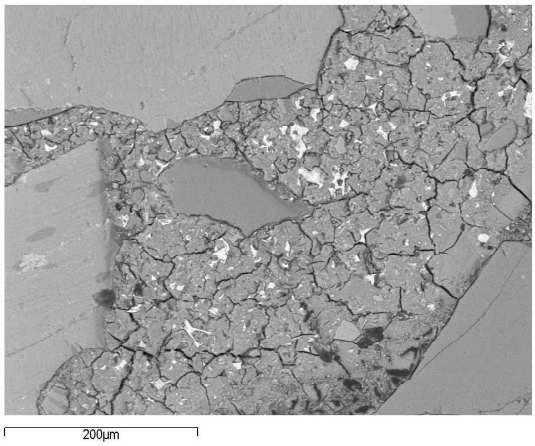

Figure 8a. SEM Microphotograph

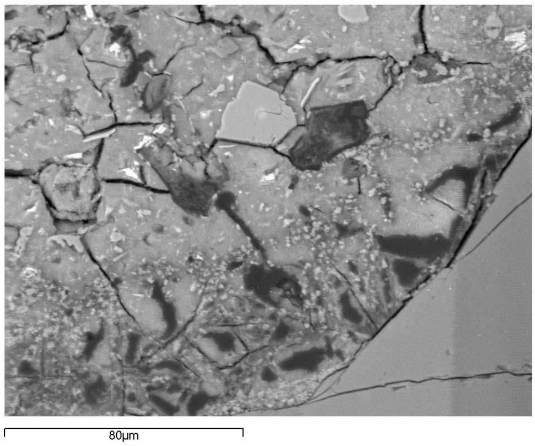

Figure 8b. SEM microphotograph of enlarged area of Figure 8a. The dark areas are empty voids. The relatively small bright spots are unidentified silicates.

The ITZ are characterized with relatively open structure, as can be seen in Figure 8b and abundance of relatively small unidentified silicates. The chemical composition of these silicates was very variable and at least few analyses showed granitic origin (colloidal particles).

Another characteristic feature of this concrete is the existence of Portlandite crystals ($Ca(OH)_2$). Portlandite can be seen in Figure 9 and it is commonly found thru out the samples. It seems that Portlandite is not found within the ITZ.

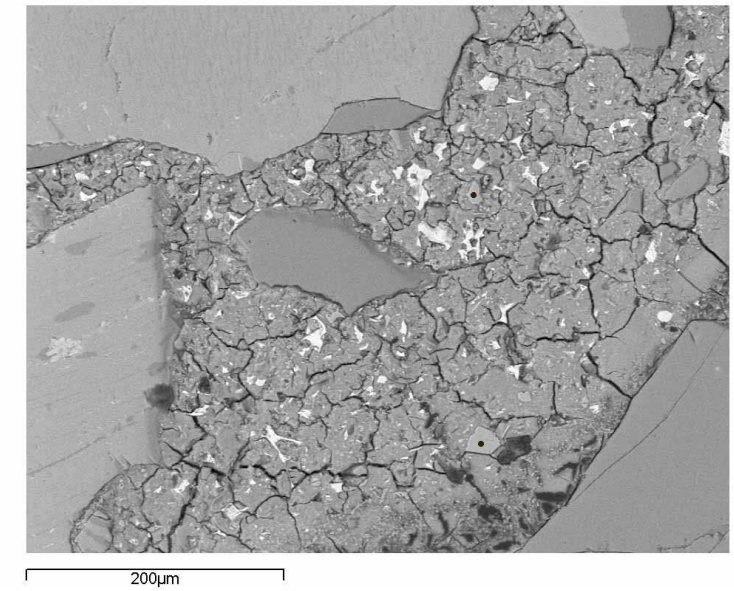

Figure 9. SEM microphotograph. The black dots show two Portlandite crystals which where identified with the SEM. Such phases are common in the Figure as well as all the sample.

Since this is a silica fume blended concrete, the silica fume should react with Portlandite to produce cement paste, hence the pozzolanic reaction. The presence of Portlandite suggests that the pozzolanic reaction was hindered.

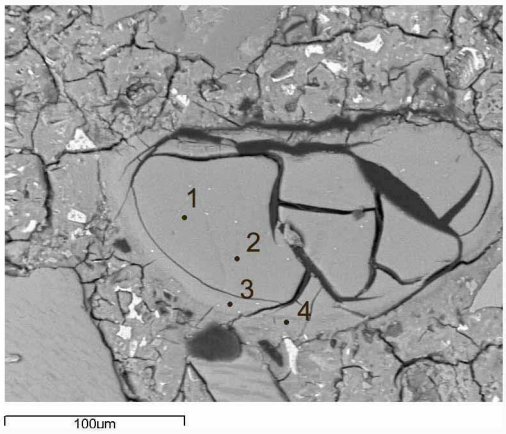

Figure 10. SEM microphotograph of silica fume lump and chemical compositions of four points, see Table 6. Point 4 is outside the silica fume cluster

Table 6. Chemical analysis of silica fume cluster show in Fig. 10, wt %

	1	2	3	4
SiO_2	68.72	63.64	62.89	52.51
Al_2O_3	0.4	0	0	1.25
Fe_2O_3	0	2.06	0.35	0.76
MgO	0.71	0.49	0.46	1.01
CaO	10.87	10.46	17.45	20.79
Na_2O	0.59	0.59	0.49	1.25
K_2O	2.71	2.52	2.01	3.14
SUM	84.0	79.8	83.7	80.7

Chemical composition of 4 points is given in Table 6. Of the four points, three are inside the silica fume lump; thereof two in the interior of the lump (1 and 2) and one close to the cement paste (3), and finally one is outside the silica fume lump (4). Inside the silica fume lump the SiO_2 content is as high as about 69 %. The calcium content is relatively high, about 11 % and it increases towards the cement paste. At the rim of the silica fume lump, the calcium content is about 17 %, compared to about 21 % in the cement paste (point 4). The potassium content of the silica fume lump is relatively high. The sodium equivalent of the silica fume is about 2.15 %. This is also the case for the cement paste, which has also relatively high sodium equivalent content. The sodium equivalent is about 3.32 %. For the average cement paste the sodium equivalent is about 0.8 %.

Thin sections were made from the samples which were tested in the freeze/thaw test. In Figure 11 are shown microphotographs of sample SCC-II (5 months) after being tested for 56 cycles both with water and with 3 % NaCl solution. The microphotographs are taken at 5 to 8.3 mm and at 35 to 38.3 mm below the surface.

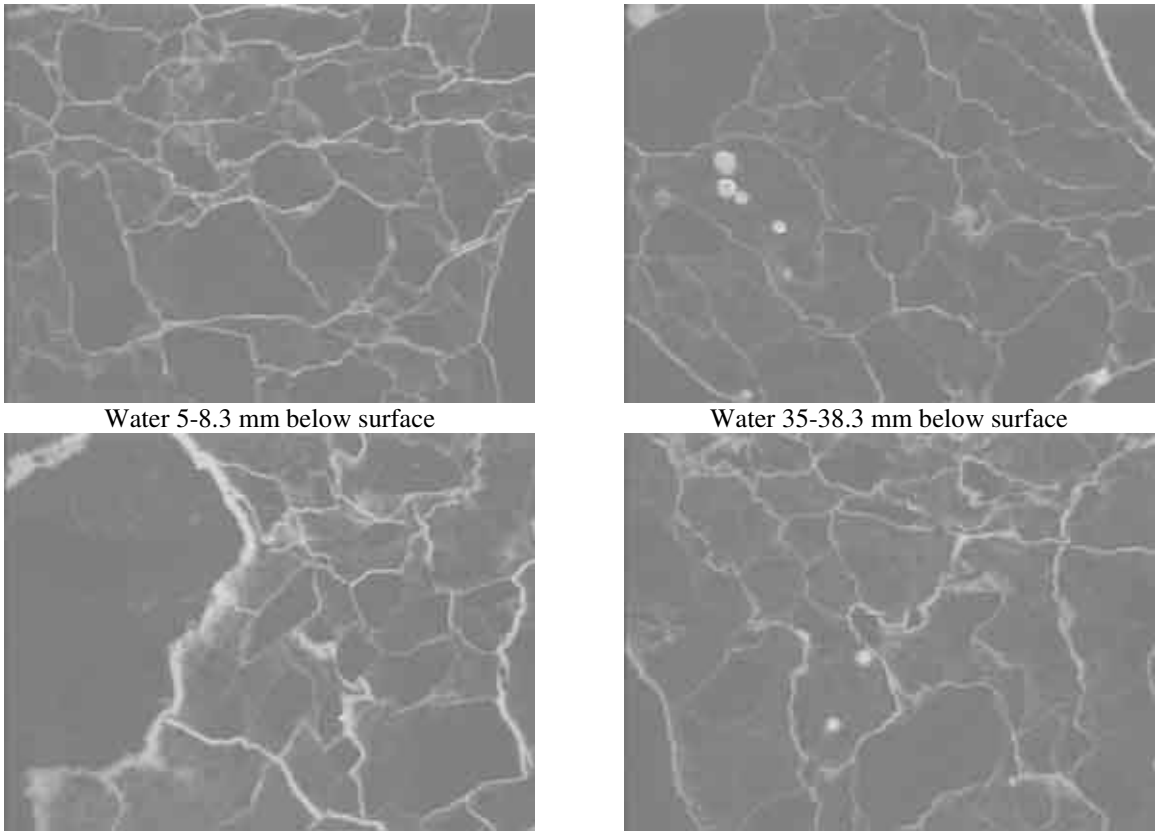

Water 5-8.3 mm below surface | Water 35-38.3 mm below surface

3 % NaCl 5-8.3 mm below surface | 3 % NaCl 35-38.3 mm below surface

Figure 11. Microphotograph taken with Mercury fluorescence light. Sample SCC-II after 56 freeze/thaw cycles. Cracks appear in bright colours. The sample in the upper two microphotographs was tested with water and the sample in the lower two microphotographs was tested with 3 % NaCl-solution. The microphotograph on the left are taken at 5 to 8.3 mm depth and the ones on the right are taken at 35 to 38.3 mm depth below the surface. Each microphotograph is 3.3 by 4.2 mm.

The samples which were tested were 50 mm thick. As expected the samples are severely cracked throughout the whole samples. The number of cracks per unit area was not worked out, but it seems to be fairly constant in the samples. It seems that the cracks are a little wider at 5 to 8.3 mm depth than at 35 to 38.4 mm depth. The cracks are also wider when tested with 3 % NaCl than with water.

Silica fume lumps are abundant in the samples (see Figure 10) and therefore it is interesting to observe how the lumps behave during the freeze/thaw testing. In Figure 12 is shown an example of one relatively large lump after the freeze/thaw test.

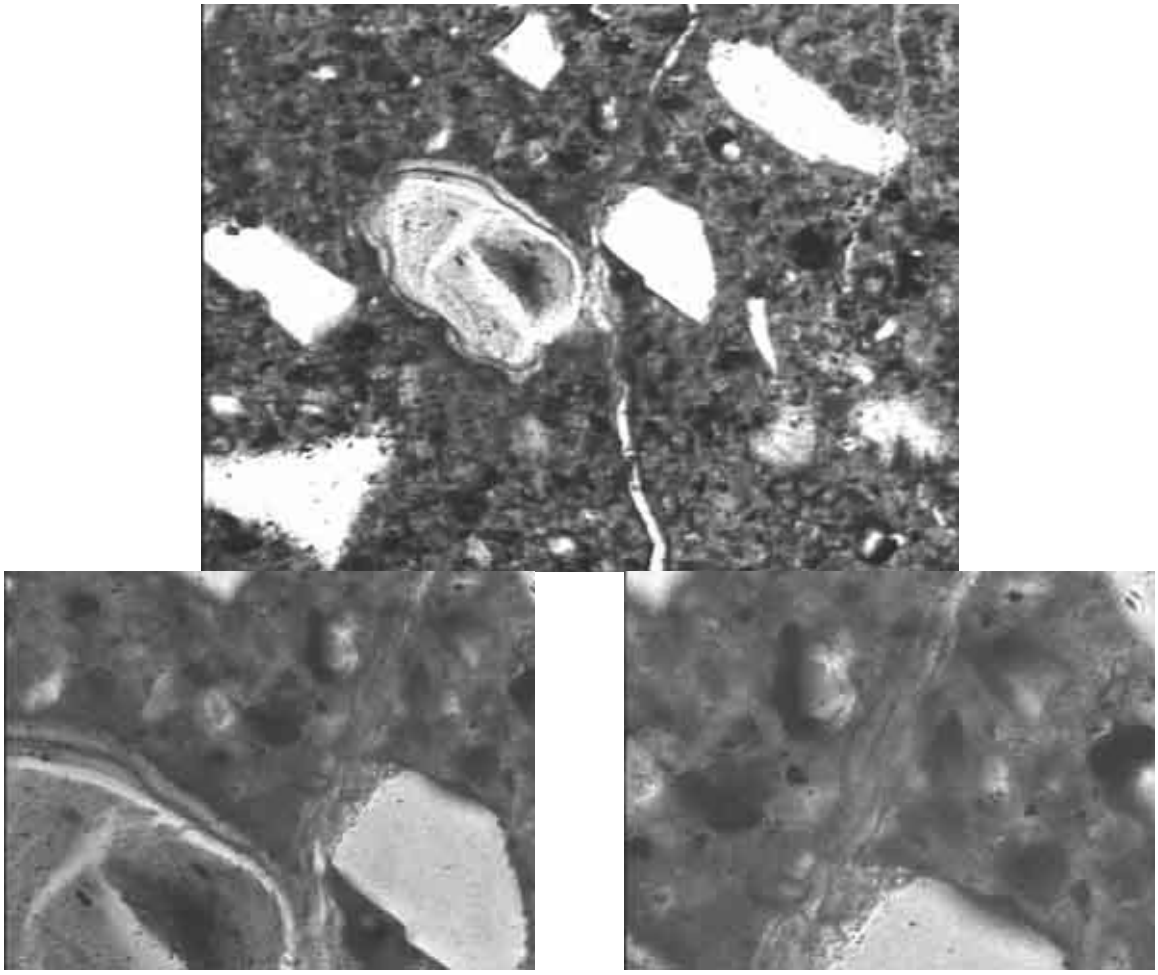

Figure 12. Microphotograph of a silica fume lump in sample SCC-II after a freeze/thaw test in 3 % NaCl. The upper micrographs show a relatively large silica fume lump and a crack penetrating the cement paste and interacting with the silica fume lump. The lower two micrographs show enlarged portions of the silica fume ump and the crack. The crack filling could be alkali silica gel. The upper photograph is 0.67 by 0.52 mm and the lower photographs are 0.34 by 0.26 mm.

The silica fume lump has partially dissolved inside and has a gel-like outer rim. Frequently cracks are associated with the lumps and in some cases the cracks looked to be filled with gel, as shown on the enlarged parts of Figure 12. With the SEM, it was attempted to analyze the composition of this gel, but it turned out to be impossible to find such gel.

The relatively wide cracks formed during freeze/thaw testing contain fine fibrous minerals, shown in Figure 13. Due to the relatively small size of these phases it was not possible to analyze the chemical composition.

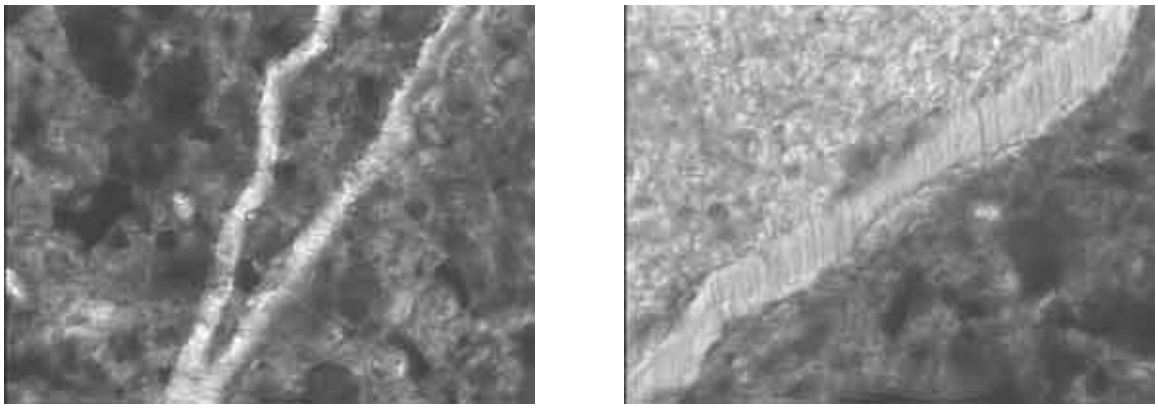

Figure 13. Microphotograph fibrous mineral in freeze/thaw cracks in sample SCC-II, tested with 3 % NaCl-solution. The left photographs is 0.67 by 0.52 mm and the right photograph is 0.34 by 0.26 mm.

Cores were taken from Brakarsund (SCC-I) in summer of 2003, after a service of 290 days. Visual observation of the structure, as well as Borgarfjardarbru (SCC-II), do not show any sings of wear. There is not scaling taking place in the concrete and no cracks were observed on the surface.

Thin section was made from the surface of the core. There are cracks present in the surface of the sample, shown in Figure 14.

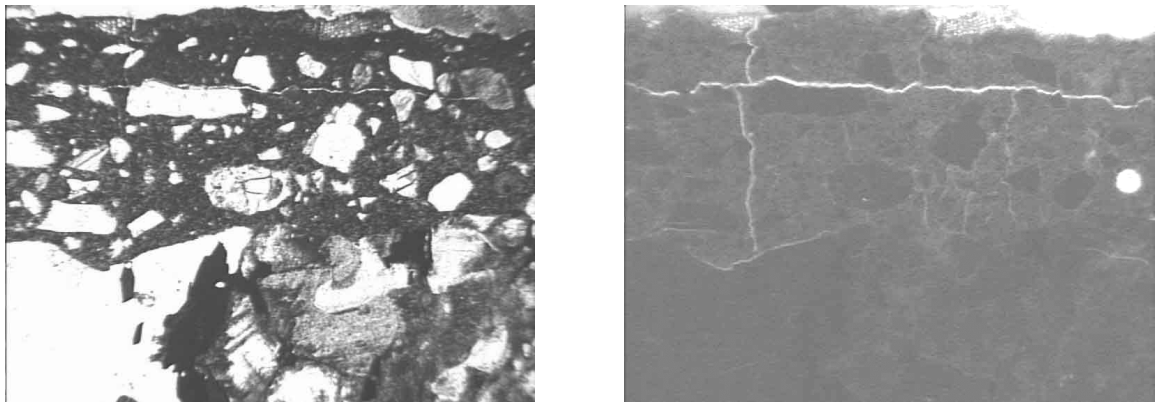

Plane polarized light Hg fluorescence light

Figure 14. Microphotograph of the surface of concrete sample from the structure Brakarsund after exposure for 290 days. Each frame is 4.3 by 3.3 mm.

The cracks from a distinct crack pattern, with cracks running parallel with the surface of the concrete and then cracks which are perpendicular to the surface. These cracks are found in the uppermost 1.5 mm of the sample. The cracks penetrate through aggregates, see Figure 15.

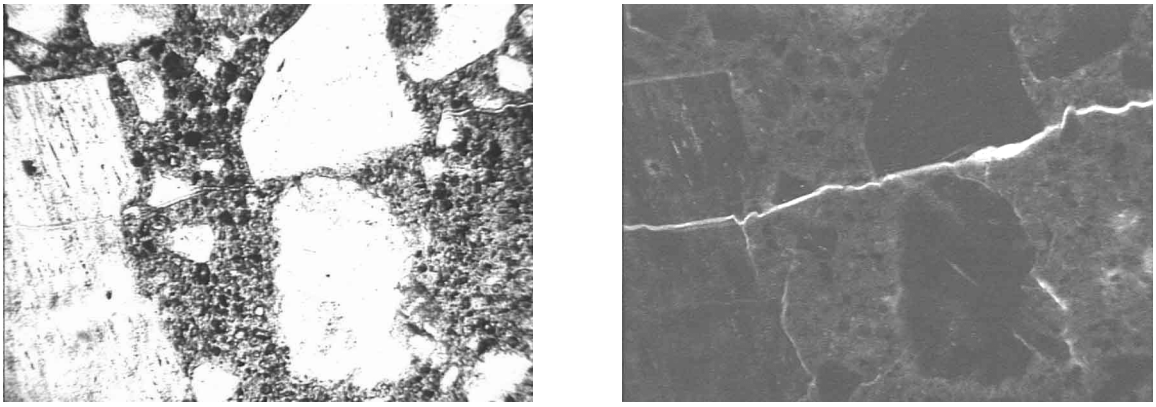

Plane polarized light Hg fluorescence light

Figure 15. Microphotograph of the freeze/thaw cracks in surface of the concrete. The crack which penetrates into the aggregate (on the left side) is at 1.5 mm depth from the surface. Each frame is 1.36 by 1.04 mm.

Silica fume lumps are frequently found in the concrete. The lumps are generally uncracked and with a solid core, see Figure 16.

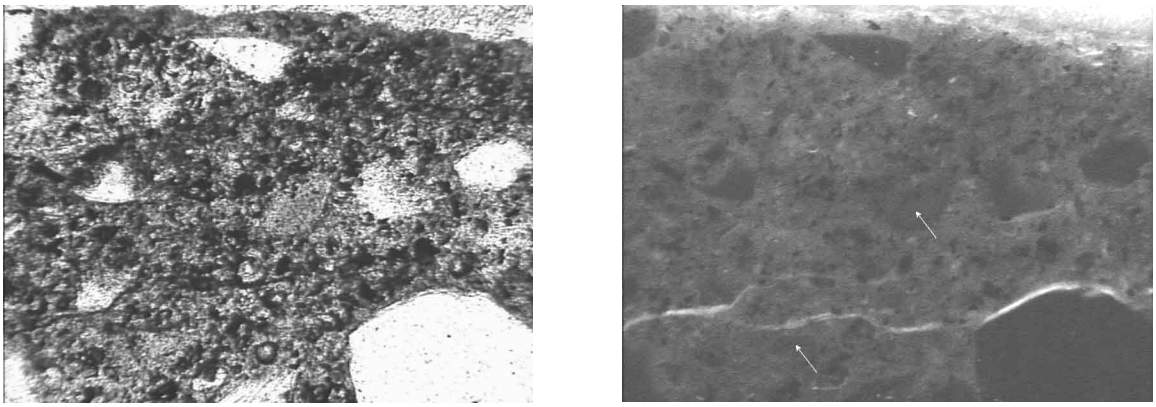

Plane polarized light Hg fluorescence light

Figure 16. Microphotograph of the freeze/thaw cracks in surface of the concrete. On each side of the crack are two solid silica fume lumps (see arrows). Each frame is 0.68 by 0.52 mm.

In Figure 16 two solid silica fume lumps can be seen (see arrow in Figure 16 b). The lumps are not associated with the crack which penetrates thru the cement paste. However, it is possible, but not common, to find broken up silica fume lump and with cracks associated with is, see Figure 17. The silica fume lump, which is shown in Figure 17, is very close to the surface.

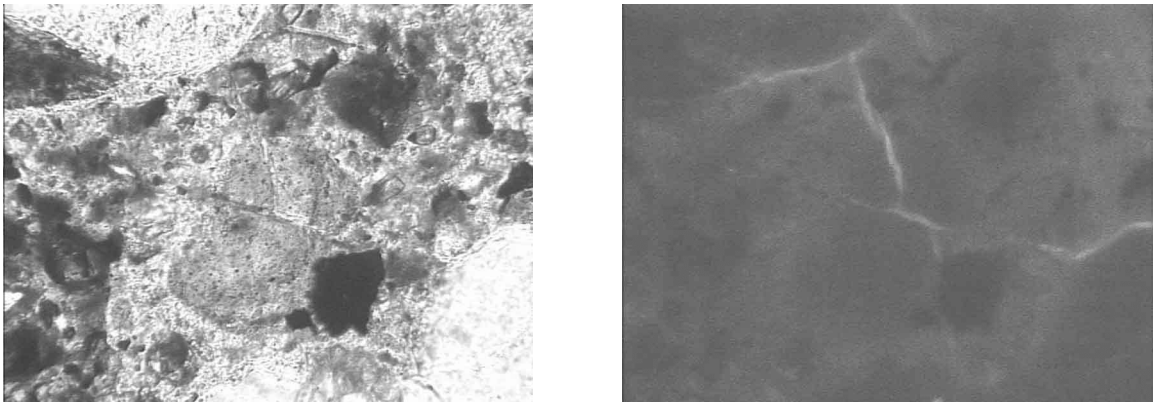

Plane polarized light Hg fluorescence light

Figure 17. Microphotograph of a broken up silica fume lump. Each frame is 0.27 by 0.21 mm.

In this concrete (SCC-I) interfacial transition zone is not as apparent, if it exist at all, as in concrete SCC-II.

3. CONCLUSIONS

The concrete which is the scope of this research is in many ways unique. Mainly since the concrete was made with foreign solid constituent, which were imported to Iceland in big bags and then mixed in concrete trucks. All the test samples were cast at the construction site.

The frost resistance of the test samples was not very good. Unpublished test results from the Icelandic Building Research Institute on similar concrete mixes, i.e. with w/b ratio of about 0.27-0.28 and non air entrained indicates that this type of concrete should be frost resistance. Therefore there should not be any need for air entrainment in this type of concrete. Samples showed poor performance when tested with water and showed serious internal damage. The scaling resistance, tested with 3 % NaCl, was better. Both the concrete samples passed the 1 kg/m^2 criteria after 56 cycles. When tested after 5 months the sample SCC-II failed the scaling test. Furthermore, the concrete in Brakarsund shows deterioration after 290 days.

The reason for the relatively poor frost resistance is not know. Based on observation in the microscope it is evident that the silica fume lumps is a contributing factor in the poor frost resistance of the concrete samples. Partially hydrated silica fume lumps contain water, which presumably is relatively loose bound. The water in the silica fume lumps will lower the frost resistance of the concrete. For the real structure, cracks are present at surface. There is some evidence that the silica fume lumps are contributing to the crack formation, since the only cracked up silica fume lump was found close to the surface (see Figure 17). Some of the silica fume lumps in the test samples showed signs of alkali-silica-reactions. This was not confirmed by the SEM analysis, since no alkali-silica gels were found in the samples, but the alkali content of the silica fume lump and adjacent cement paste was relatively high. If these samples are ASR active or become active during a freezing and thawing process it will aid to the break down of the samples.

If the silica fume lumps are a contributing factor to the poor performance of the concrete, further research is needed on how silica fume should be added to concrete. The reason for the

presence to the silica fume lumps is because the silica fume had been over densified during its production. Silica fume lumps were visible with the naked eye in the raw material.
The chloride diffusion coefficient of the concrete is relatively low and as with normal concrete it improves with the age of the concrete. The chloride content of the concrete is relatively high, much higher than in a normal concrete. More research is needed to verify this behaviour in other types of SCC. If this is the case for SCC then chloride induced corrosion could be a serious problem.

All the laboratory testing, both the freeze/thaw and chloride penetration, are supported with the field performance. Therefore, the long-term performance of these two structures is very important since it will give valuable information on the validity standardized testing on concrete.

ACKNOWLEDGEMENT

This project was partially funded by the Concrete Commission in Iceland (Steinsteypunefnd) and partially by the Icelandic Road Administration. Thanks are also due to Rognvaldur Gunnarsson and Einar Haflidason at the Public Road Administration and dr. Olafur Wallevik and Indridi Nielsson at IBRI.

REFERENCES

1. Okamura H (1997) Self-Compacting High-Performance Concrete, Concrete International, 7, 50-54
2. Zhu W, Quinn J, Bartos PJM (2001) Transport properties and durability of self-compacting concrete. Proceedings of the 2nd International Symposium on Self-Compacting Concrete, eds. Ozawa K, Ouchi M, Tokyo, Japan, 451-458
3. Mörtsell E, Rodum E (2001) Mechanical and durability aspects of SCC for road structures. Proceedings of the 2nd International Symposium on Self-Compacting Concrete, eds. Ozawa K, Ouchi M, Tokyo, Japan, 459-468
4. Makishima O, Tanaka H, Itoh Y, Komada K, Satoh F (2001) Evaluation of mechanical properties and durability of super quality concrete. Proceedings of the 2nd International Symposium on Self-Compacting Concrete, eds. Ozawa K, Ouchi M, Tokyo, Japan, 475-482
5. Persson B (2003) Internal frost resistance and salt frost scaling of self-compacting concrete. Cement and Concrete Research, 33, 373-379
6. Gudmundsson G (1997) Deterioration of concrete bridge piers in Iceland. In: mechanisms of chemical degradion of cement-based systems. Eds.: KL Scrivener and JF Young. E & FN Spoon, London, 201-208
7. Gudmundsson G, Wallevik O (2002) Concrete in an aggressive environment. Proceedings of the Minneapolis Workshop on Frost Damage in Concrete, eds.: Janssen DJ, Setzer MJ, Snyder MB, 87-102
8. Nielsson I, Wallevik O, (2003) Mix Design of HS-SCC and Practical application. In: Self-Compacting Concrete. Proceedings of the 3rd International RILEM Symposium. Eds. Wallevik O, Nielsson I, RILEM Publication, 506-513
9. Gudmundsson G, Antonsdottir V (2002) Chloride diffusion in and out of concrete made with different type binder. RILEM-workshop in Madrid 2002

10. Tang L, Bager D, Jacobsen S, Kukko H (1997) Evaluation of the Ultrasonic Method for Detecting the Freeze/thaw Cracking Concrete. NORDTEST Project No. 1321-97. SP REPORT 1997:37
11. Chatterji S (1995) On the applicability of Fick's second law to chloride ion migration through Portland cement concrete. Cement and Concrete Research, 25, 299-303

Effect of corrosion inhibitors in chloride contaminated concrete in Iceland

Gisli Gudmundsson
Ph.D. Senior Research Scientist
Hönnun
Grensásvegur 1, IS-108 Reykjavik
gislig@honnun.is

Dr. Ríkharður Kristjánsson.
Managing Director and Chief Engineer
Línuhönnun Consulting Engineers,
Suðurlandsbraut 4A, IS-108 Reykjavík,
Rikhardur@Lh.is

ABSTRACT

The use of corrosion inhibitors was studied in chloride contaminated concrete, for up to about 3 years after being applied to the structure. In order to determine the effect of the corrosion inhibitors: cores were taken from the structure, pore water was pressed out and the corrosion inhibitor content analysed; and the corrosion rate was measured in the in the treated areas and the result compared to non treated areas. This is only a part of a large project, in which different types of surface treatment were tested in order to estimate the effectiveness of preventing chloride ingress. The main objective of this research is to support the construction industry and owners of steel reinforced concrete buildings and structures by the technical and economic optimisation of the resources used to construct, monitor and maintain steel reinforced buildings and structures.

The main conclusion of this research is that the type of corrosion inhibitor tested does not offer any protection when compared to non-treated concrete.

Key words: concrete - reinforcements - corrosion - corrosion inhibitors – corrosion rate

1. INTRODUCTION

In a sound undamaged concrete, the steel reinforcement is protected against corrosion by the relatively high alkalinity of the cement paste. One can say that concrete has a built-in inhibitor against reinforcement corrosion. In spite of this, corrosion of steel in concrete takes place and is a widespread problem thru out the world, including the Nordic countries. When this happens

the built-in inhibitor has been broken down, normally due to carbonation or chloride ingress from the surface and corrosion can take place. The corrosion can occur locally (pitting) or it may be spread over a larger area.

One of the common counter-actions against reinforcement corrosion is to apply corrosion inhibitors (CI) to the concrete. Relatively many reports and scientific papers have been written on corrosion inhibitors in concrete. One of the major documents, which have been very important to this work, is the Final Report from the COST 521 Action: Corrosion of Steel in Reinforced Concrete Structures [1].

1.1 Corrosion of steel in concrete

Once corrosion has been initiated, the rate will depend on many things, which will make the corrosion, progress very slowly up to very fast rate. Tuutti introduced a model of a corrosion sequence [2]. The lifetime model is shown in Figure 1 (chloride induced corrosion).

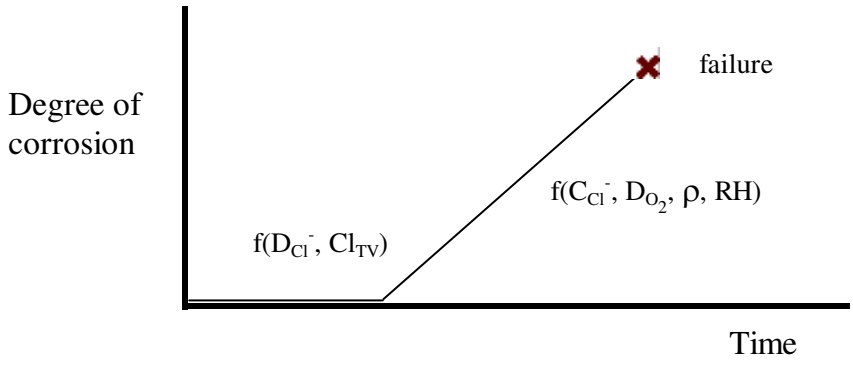

Figure 1. Corrosion rate of reinforcing steel as a function of the lifetime of the structure [2,3].

The corrosion rate depends on various parameters like the oxygen ingress (D_{O_2}), the electrical resistivity of the concrete (ρ) and on relative humidity and temperature. The length of the first period, the initiation period, depends on parameters like the chloride diffusion rate (D_{Cl^-}) and the chloride threshold values (Cl_{TV}) [3]. All the parameters are complicated and its function in concrete is by far not fully understood and it is not in the scope of this paper to deal with it. The important thing here with regards to corrosion inhibitors, is that inhibitors do or can prolong the induction period, and it is also believed that the corrosion inhibitors reduce the corrosion rate, once the corrosion has started [4].

1.2 Action of inhibitors in concrete

Ideal corrosion inhibitor has been described as: " a chemical compound, which, when added in adequate amounts to concrete, can prevent corrosion of embedded steel and has no adverse effect on the properties of concrete" [5]. Both organic and inorganic inhibitors are available. The corrosion inhibitors, which are applied to concrete, are of three types: anodic, cathodic and a mixture of both anodic and cathodic inhibitors. An anodic inhibitor is a chemical substance, which reduces the anodic reaction. This will cause the corrosion potential to shift to more positive values. It is critical to use sufficient concentration of the inhibitor, else the cathode area

will be too large and the corrosion will be accelerated at the anode site [6]. This will cause pitting. A cathodic inhibitor reduces the cathodic reactions by oxygen reduction or hydrogen discharge and it will shift the corrosion potential to negative values [7]. Most of the cathode inhibitors are sodium hydroxide or sodium carbonate based, as such when applied to concrete the pH level will be increased. Mixed inhibitors (multi-functional) reduce both the cathodic and the anodic reaction rates.

For reinforced concrete, the inhibitors are also classified according to the way they mechanically work in concrete, i.e.:

Absorption inhibitors acting as anodic, cathodic or mixed inhibitors
Film forming inhibitors, which block both the anodic and the cathodic corrosion reactions
Passivators, which lead to the passivation reactions of the steel (e.g. hydroxyl ions)

Commercial inhibitors do often contain several active compounds and the interaction between these compounds in concrete can be complicated and difficult to identify it with conventional laboratory tools.

1.3 History of inhibitors in concrete

Corrosion inhibitors have been utilised with good success in protecting steel structures (i.e. tanks, pipelines, etc.) against corrosion for many decades. As a protection for the reinforced steel in concrete the use of CI's is much more recent and the effect is not as decisive.

The utilisation of corrosion inhibitors in concrete is normally split into two categories:

surface applied inhibitors (applied to relatively old structures), and
mixed-in inhibitors (applied to fresh concrete – new structures).

Mixed in inhibitors in concrete are known from the early fifties, but it was not until the seventies when calcium nitrites were introduced, that the application of inhibitors became common practice. Since the late seventies calcium nitrates have been used successfully in the USA – in various types of structures [8].

1.4 Types of inhibitors

In products available on the market the same active substances are used in both mixed-in- and migrating inhibitors. There is of cause a fundamental difference between the two, namely the surface applied inhibitor must penetrate in to the concrete while the mixed-in inhibitor is present in the concrete. The transport mechanism of surface applied inhibitors will be dealt with separately in the paper, otherwise no general distinction will be made between the surface applied and mix-in inhibitors.

When mixed-in inhibitors are used, the inhibitor must obviously be added to the mixing water of the concrete. This can call for some concern about the dosage of the inhibitor. How much of the inhibitor is needed to protect against for instance chloride-induced corrosion, in other words some idea must be on the expected chloride level. Secondly, normally the corrosion will take place after 20 to 30 years, or even after longer time for high quality concrete, is there any

guaranty that the inhibitor is going to be active after this relatively long induction period. Is it possible that during this period the inhibitor is leached out of the concrete or it becomes chemically unstable? Thirdly, the inhibitor added to the mixing water may affect the properties of the concrete, like the air entrainment, rheology, strength, etc.

1.5 Transport of CI´s into concrete – migrating inhibitors

These substances are considered to have preventive effect against corrosion or to restore lost built-in corrosion protection. All of these are sold in aqueous solution, are easy to apply by spraying, rolling or painting the surface and furthermore all are relatively cheap. According to description of the manufactures of this type of inhibitor, the inhibitor part penetrates the concrete relatively fast by diffusion thru the vapour phase, due to the apparently high vapour pressure. The transport mechanism of certain commercial inhibitor has been studied in details by Tritthart [9,10]. His work was performed in cooperation with the producer of the inhibitor. This type of inhibitor has two active ingredients, the amino alcohol and a phosphorous compound. This inhibitor is described as fast migrating inhibitor, which is supposed to penetrate between 2 and 20 mm per day. The main conclusions from his work are that the phosphorous compound is insoluble in the pore fluid of the concrete and therefore precipitates from the pore fluid. As such it cannot penetrate in to the concrete and is presumably not useful as an inhibitor. The amino alcohol is dissolved and very mobile in the concrete. Tritthart´s idea is that the amino alcohol is transported by diffusion in solution, but at much slower rate than suggested by the producer. The main question is if the amino alcohol can alone inhibit corrosion or does it require the phosphorous compound?

The general conclusions for alkanolamines and amines based inhibitors are that the effectiveness of preventing corrosion is in question. These inhibitors have only been available on the marked for relatively short period of time and there is at the moment no good field records which support the producers claim. On the contrary, there are several carefully carried out research project which at the best question its performance

2. PROJECT INFORMATION AND AIM OF THE STUDY

The aim of this research is to study the effectiveness of corrosion inhibitors and other surface applied material (i.e. hydrophobic and surface sealing material) with Icelandic concrete. Use of de-icing chemicals (salt) is common in the Reykjavik metropolitan area. Due to this serious reinforcement corrosion (chloride induced) has taken place in structures which are under relatively heavy load of chlorides like car parks. Reinforced concrete is by far the most common building material in Iceland. Repair works on corroded reinforcements are performed to some extent annually and high amounts of money are spent on such operations. This research project is aimed towards reducing the corrosion problem of the reinforcements in concrete structures.

The ultimate goal of this study is to find the most economical and practical solution for avoiding chloride induced corrosion in the concrete. This paper deals only with one, commercially available, migrating corrosion inhibitors, amino alcohol based.

Corrosion inhibitors have not been widely used in Iceland and therefore very little experience has been gathered using corrosion inhibitors in Iceland. In recent studies high chloride content

has been found in concrete from bridges and car parks, suggesting that the rebars are in a great danger. Utilisation of corrosion inhibitors in both old and fresh concrete offers cost effective alternative to prolonged lifetime, if the corrosion inhibitors are effective in reducing chloride induce corrosion in an old concrete and to eliminate it in a new concrete.

3. RESEARCH PLAN

This research project was carried out in two car parks in Iceland. The older car park, car park K, was taken into service in 1984, the newer, car park R in 1991. The older one is very suitable for this kind of study because the rebar cover is only 2.5 cm thick. The low rebar cover and the relatively high chloride content makes this car park very suitable for this type of study. As a consequence of this situation after only 14 years of service serious corrosion had taken place in some areas of the structure. Potential mapping was carried out and revealed the rather serious conditions of the structure. Areas where the rebar corrosion was serious were repaired with new covercrete. Two areas, one in the old structure and one in the new covercrete used in this project. The areas were sectioned up into about 10 m^2 large areas. In these relatively small areas experiments are carried out on individual material. Corrosion inhibitors were tested in five of these areas.

The newer structure was made with blast furnace slag and the concrete has 40 mm thick cover. The test areas were section up in to 9 to 10 m^2 areas where the tests were conducted. Corrosion inhibitor was tested in one of these test sites.

In the both structures areas were left untreated, as a reference. Each test area included a part of the area where the cars are parked and a part of the adjacent driveway.

Prior to applying the material to the concrete, potential mapping of the surface of the concrete was carried out. Potential mapping was also carried out towards the end of the project. Cores were drilled from selected areas and chloride profiles were obtained. The pre-treatment of the concrete and the corrosion inhibitors were applied to the surface of the test sites according to instructions given by the producer.

In order to find out the effectiveness of the inhibitors and to study its depth distribution, the idea was squeeze out the pore fluid from selected samples and analyse the composition of the pore fluid. This enables one to observe how the concentration of the inhibitor in the pore water of the concrete changes with time.

In addition to these tests, the corrosion rate was measured with a Galva-Pulse instrument towards the end of the project.

4. RESULTS

Temperature and humidity measurements were carried out in the car park K over a period of one year. The concrete temperature ranges from about 6 °C during the winter up to about 20 °C during summertime. The relative humidity is much more stable and solely a function of the concrete temperature. The measured relative humidity in the concrete is on the order of 90 % and it varies only by about 1 % over temperature fluctuations of about 15-20 °C.

4.1 Chloride content

For the chloride analysis three areas in each test site were considered, an area in the driveway where the traffic is apparently most prominent, in the area around where the real wheel of the parked cars is normally located and finally in the area under the centre of the parked cars.

In Figure 2 is shown results of chloride analysis selected locations in the car park taken in 1997 and 1998. After only 14 years of service the chloride content in the concrete is relatively high and well above the critical corrosion levels in many areas.

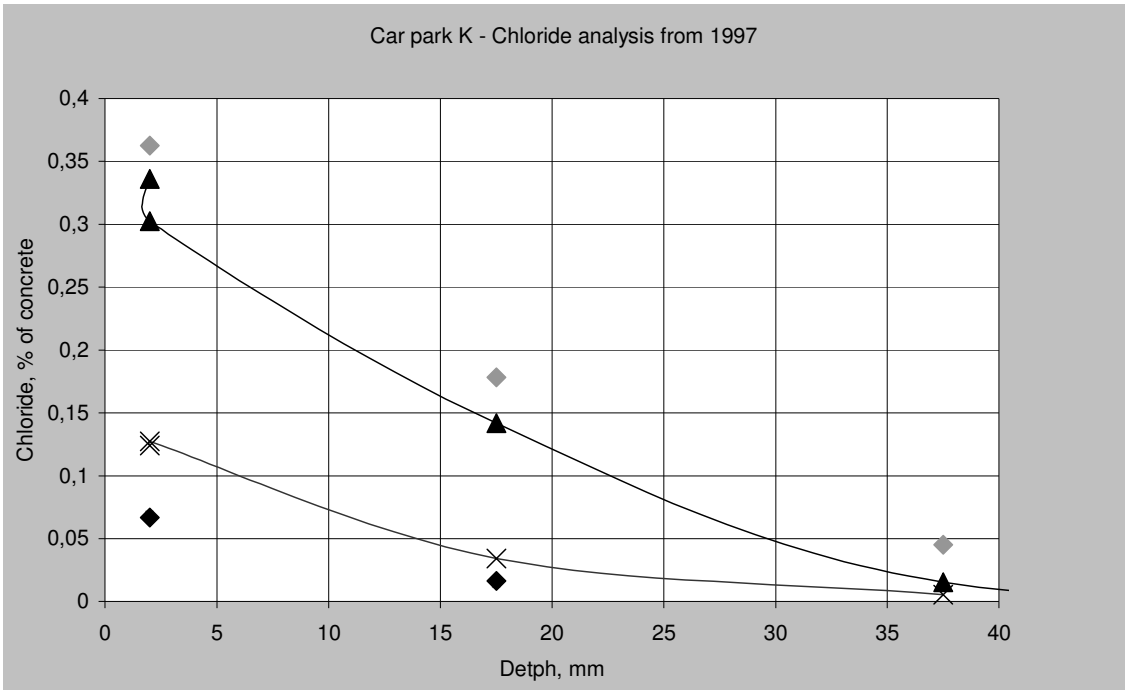

Figure 2. Selected depth profiles of chloride penetration in the car park K at various locations. The rebar cover is about 25 mm.

In Figure 3 is shown the build up of chloride in the car park over a period of 3 years, or for the duration of this study. In this case the study area (10 m^2) is one test site where corrosion inhibitor was applied to the surface. During this period considerable chloride was built up in the concrete.

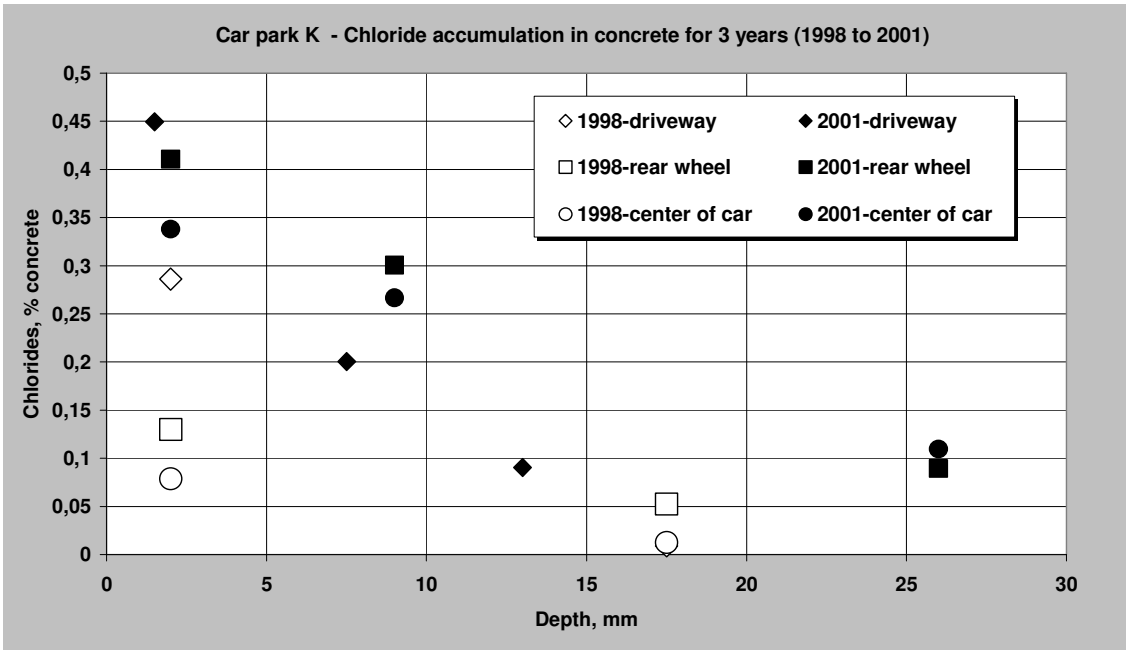

Figure 3. The Figures show the build up of chlorides in three years in car park K. The white symbols are analysis from 1998 and the black symbols are analysis from 2001. The samples were taken from a test site treated with corrosion inhibitors.

One of the results from the potential mapping measurements was that the corrosion of the reinforcements follows the traffic pattern within the car parks. Highest corrosion was measured in the driveway and in the area under the rear wheels in the parking areas. When the chloride profiles were measured it was found that the chloride content follows this pattern at depth levels close to the surface, but at greater depth this turned out not to be the case, see Figure 3.

In Figure 4 is shown the build up of chlorides in the covercrete after having been in service for 3 years. The samples taken for this study were only from the area around the rear wheel of the cars.

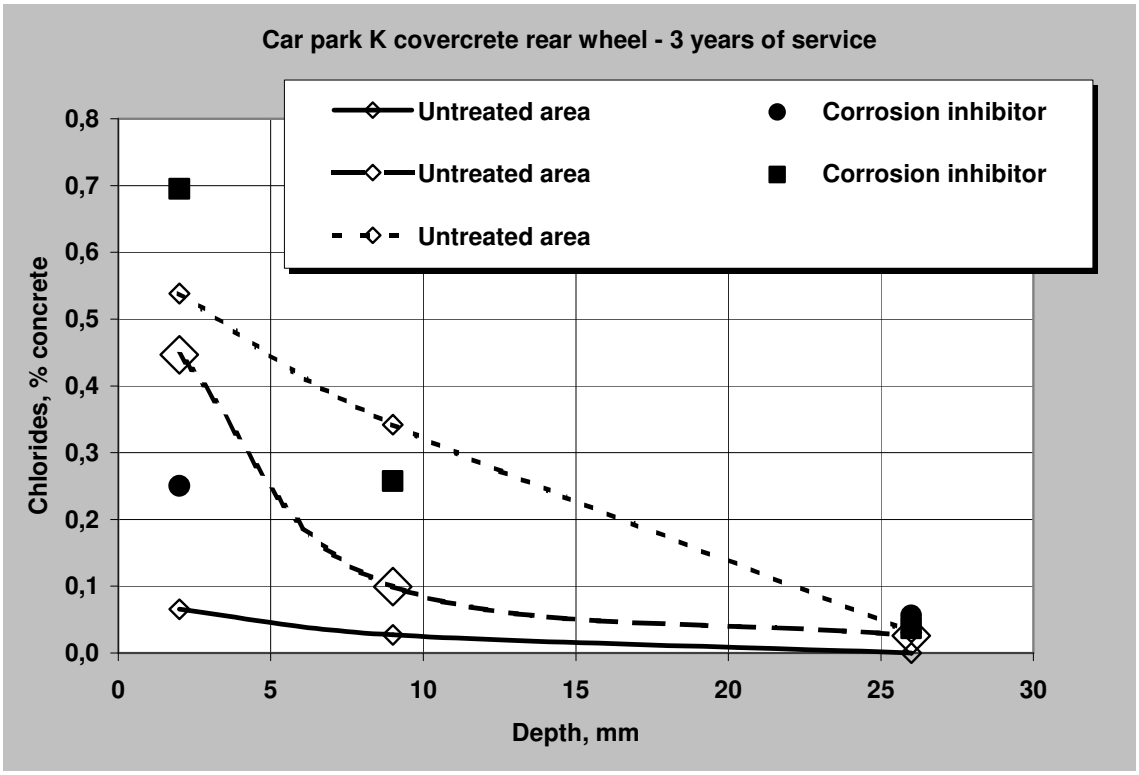

Figure 4. The figure shows the chloride build up in the covercrete after 3 years.

Although the surface content is relatively high, it does not penetrate relatively deep into the concrete, but one must bear in mind that his is only after 3 years and the quality of the concrete was good, with a w/c ratio of 0.45 and the reinforcement cover was 40 mm.

In Figure 5 is shown the chloride content in selected test sites in car park R. In 10 years of service considerable chlorides has been build up and it seems that a chloride front of 0.4 to 0.7 has penetrated down to about 10 mm depth. From this data it is anticipated that critical situations in terms of reinforcement corrosion might occur in the structure after 10 to 20 years.

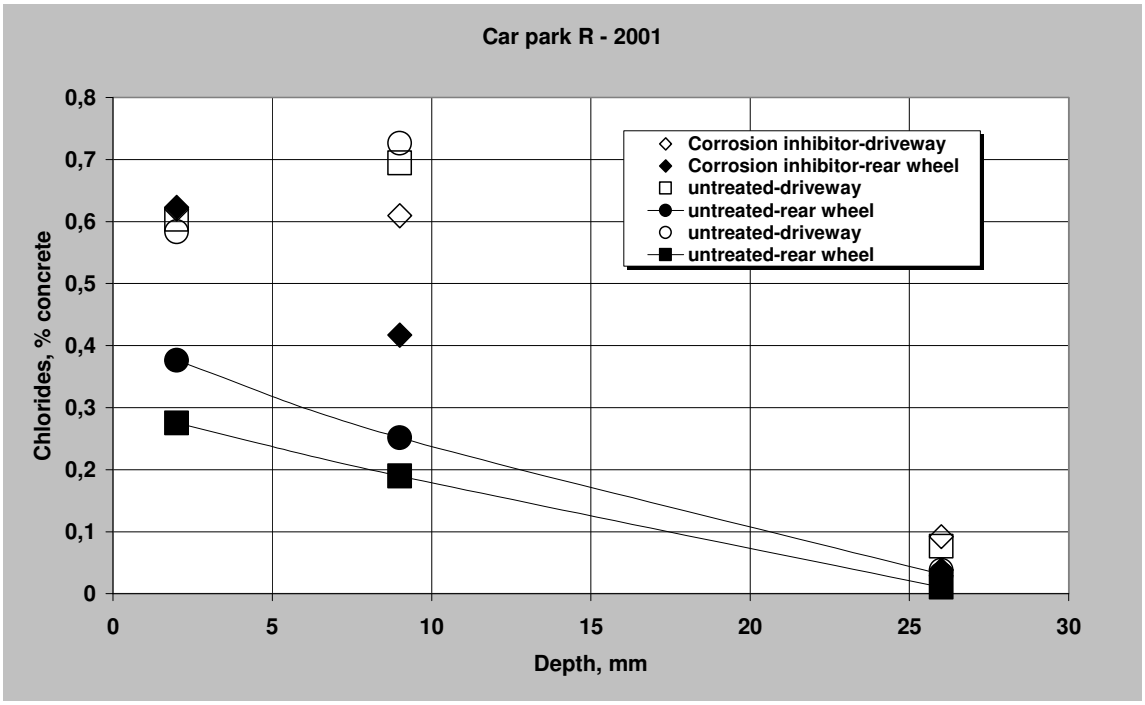

Figure 5. The build up of chlorides in car park R, after 10 years in service.

4.2 Pore water extraction, general chemistry and corrosion inhibitor content[1]

Pore water was squeezed out of some concrete cores, sampled taken 6 months after the structures were treated with the corrosion inhibitor. The chloride, OH^- and the inhibitor content was analysed in the solutions. The chloride and the OH^- content of the pore water is given in Table 1, as well as the Na and K content in core 1 (b)

Table 1. Pore solution composition of concrete samples from Iceland.

Sample	Core length (cm)	OH^- (mole/l)/pH	Cl^- (ppm)/(mole/l)	Na^+ (ppm)/(mole/l)	K^+ (ppm)/(mole/l)
R-1	0-8	0.076 / 12.88	966 / 0.027	n.a.	n.a.
K-1 (a)	0-10	0.100 / 13.00	2960 / 0.084	n.a.	n.a.
K-1 (b)	0-10	0.105 / 13.02	2080 / 0.059	3640 / 0.158	450 / 0.012
K-2	0-12	0.070 / 12.85	2480 / 0.070	n.a.	n.a.
K-2 (a)	0-5	0.072 / 12.86	5520 / 0.156	n.a.	n.a.
K-2 (b)	5-11	0.143 / 13.16	460 / 0.013	n.a.	n.a.

R=car park R. K = car park K

The first sample (R-1) is made with slag cement. It turned out to be relatively easy to press out enough solution required for the chemical analysis. For the remaining cores it was much more difficult to press out enough solution for the required chemical analysis, although the total force was as high as 2300 kN. Sample K-1 (a) gave very little pore solution, but it was possible to press about 1 ml from core K-1 (b). Due to this difficulty to press solutions out it was decided to put cores K-2 in a water bath under vacuum for 24 hrs. This procedure turned out to be very

[1] The pore water was pressed out of the cores and all the analyses, except the inhibitor analysis were carried out in Graz, Austria. The inhibitor content was analysed by the producer of the inhibitor. This work was carried out in cooperation by Professor Joseph Tritthard.

useful. From core K-2 about 3 to 4 ml were collected. Then one core from the same location (K-2 a-b) was cut up in two parts. one from the surface down to 5 cm depth (K-2 a) and one from 5 cm down to 11 cm depth (K-2 b). About 3 to 4 ml were extracted from each core.

It is very interesting that the OH^- concentration of all the pore solutions is relatively very low. This is due to the fact that the cement in the car park K contains 7.5 % silica fume and the cement in car park R is made with slag cement with 70 % slag. The effect of slag is as with silica fume to reduce the OH^- concentration of the pore water. It is also very interesting when the chloride content is relatively high, as in sample K-2 (a), the upper half of core K-2, the OH^- concentration is relatively low. When the chloride content is on the other hand relatively low, like in core K-2 (b), the lower half of core K-2, the OH^- concentration is relatively high.

One of the chemical characteristics of Icelandic cement is that the alkali content is relatively high. $Na_2O_{eq.}$ is about 1.6 and the sodium content is twice the potassium content. The alkali content of the pore solution from core K-1 was analysed. The total sodium content of the pore solution is indeed very high and much higher than the potassium content.

Obviously if is difficult to press out pore solution from concrete with silica fume. The silica fume increases the density of the cement matrix and reduces the micro-porosity of the concrete, which makes it harder to press out the pore solution. One might expect the same behaviour with slag cement, but presumably the beneficial tightening of the cement matrix by blast furnace slag is only achieved it the concrete is allowed to harden at relatively wet conditions. It was necessary to presaturate the samples under vacuum for at least 24 hrs. prior to the extraction. This saturation does not affect the OH^- concentration in the samples. It seems that the pore solution reaches equilibrium within 24 hrs. However, for the remaining of the analysis like the chloride content one must correct for this additional water.

The corrosion inhibitor content of the pore solution was analysed in samples R-2 and K-2. The results of the analysis are given in Table 2.

Table 2. Corrosion inhibitor content in pressed out pore water

Sample	Amino alcohol (ppm)	Corrosion inhibitor (inorganic content)
R-2 (0-8 cm)	8	below detection limit
K-2 (0-5 cm)	348	below detection limit
K-2 (5-11 cm)	6	below detection limit

The result of the chemical analysis clearly demonstrates that 6 months after the structures were treated with the corrosion inhibitor, the inhibitor has not reached deep into the concrete. Furthermore, the inorganic part of the inhibitor is not present in the pore solution at all. It is interesting to see that the concentration of the amino alcohol in sample K-2 is dependent on the depth profile i.e. the amount of amino alcohol is higher in the top 5 cm than it is in the lower part of the sample.

Due to the difficulty of obtaining pore solution from concrete cores and the fact that the inhibitor content is not going to be any more than it already is (see Table 2), no more attempts were made to press out pore solution. It is more likely that the effectiveness of the corrosion inhibitors will be tested by measuring the corrosion rate directly by applying techniques like the galvanostatic pulse method to the test areas.

4.3 Potential measurements

In the car park K, due to the relatively thin rebar cover and high loads of chlorides, the rebars corroded badly. Potential mapping was carried out in 1997, prior to the repair, and in 1998 in repaired areas. The corrosion map is shown in Figure 6. Generally when the measured potential is below –200 mV, corrosion is considered to be active. It is apparent that serious conditions were achieved in the concrete in some areas.

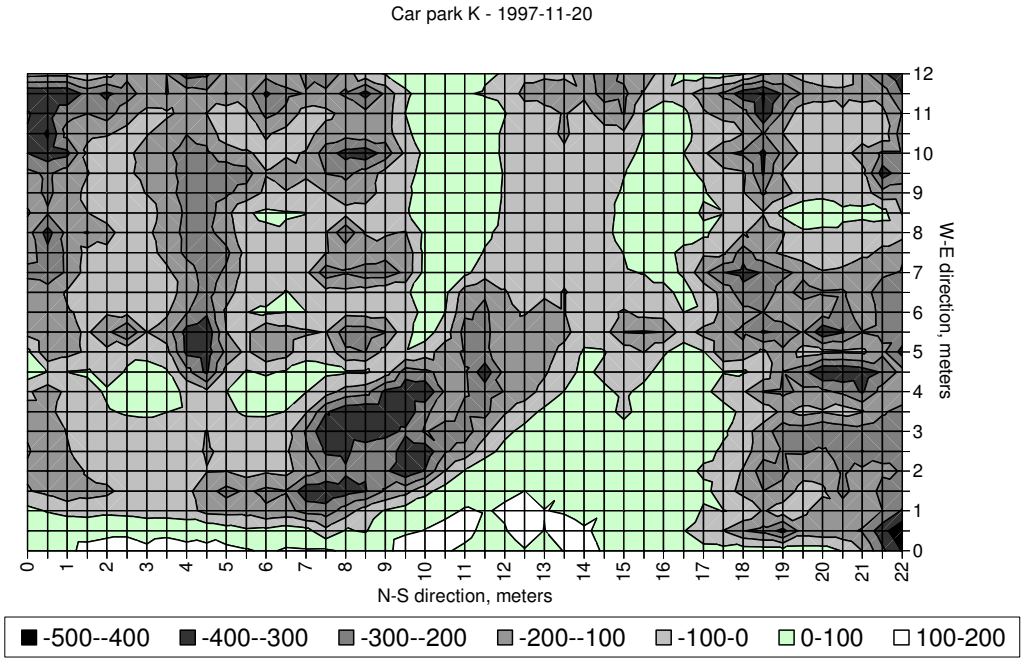

Figure 6. Results of potential measurements in car park K, taken in 1997. In this area the corrosion was very high and this area was repaired. The corrosion is apparently highest in the driveway (the curved area in the middle of the Figure) and in some of the parking areas (corroded areas with linear appearance).

The corrosion follows the driveway of the structure and it can also get relatively high in some of the areas where the cars are parked. All the area shown in Figure 6 was repaired with new covercrete. The old concrete was removed with high pressure water jetting, the corroded reinforcement bars replaced with new ones and new concrete was cast, with a concrete cover of about 40 mm.

Although potential measurements were carried out in the test areas at various time throughout the project, the results did not change much. Potential measurements are probably not were suitable/sensitive for this type of research, i.e. to distinguish between relatively small untreated and surface treated areas, in terms of activity of the surface material to fight reinforcement corrosion.

4.4 Corrosion rate Measurements

The corrosion rate was measured by a GalvaPulse instrument, which is based on the galvanostatic pulse technique [11]. These measurements were carried out in September 2000 by the FORCE Institute in Denmark. The procedure with the measurements is the same as with

potential mapping. Measuring grit is laid out on the floor and spot measurements are carried out. The test areas were measured with 0.5 m grid. The average values for each test area are given in Table 3. For car park K, at least 30 individual measurements were used to compute the average number, but for car park R only 6 measurements were available for the average calculations.

Table 3. Results of the GalvaPulse measurements. Each number for car park K is an average of at least 30 measurements, for car park R only 6 measurements were done in each area. The standard deviation is shown in the parentheses.

Test area	Corrosion rate, $\mu A/cm^2$
K-Covercrete - untreated	6.57 (9.02)
K-Covercrete - untreated	7.51 (6.55)
K-Covercrete - untreated	8.55 (8.49)
K-Covercrete - Inhibitor	7.02 (5.79)
K-Covercrete - Inhibitor	7.17 (10.06)
K-Old concrete - untreated	0.90 (0.62)
K-Old concrete - untreated	1.24 (0.44)
K-Old concrete - untreated	4.43 (4.26)
K-Old concrete – Inhibitor	2.05 (1.37)
K-Old concrete – Inhibitor	2.09 (1.36)
R – untreated	2.79 (1.71)
R – untreated	3.43 (1.89)
R – untreated	4.58 (3.68)
R – Inhibitor	4.18 (1.94)

It is obvious from Table 3 that the measured corrosion rate in the in the test areas treated with inhibitor are not any lower than in the areas that were left untreated. In the covercrete the corrosion rate measured in the non-treated areas range from 6.6 to 8.6 $\mu A/cm^2$ and in the areas treated with inhibitor the measured corrosion rate is about 7.1 $\mu A/cm^2$. Interestingly enough, in the older concrete the measured corrosion rate is generally much lower that in the covercrete. The corrosion rate in the untreated areas is between 0.9 and 4.4 $\mu A/cm^2$ and in the areas treated with corrosion inhibitor the measured corrosion rate is about 2.1 $\mu A/cm^2$. The reason for the higher corrosion rate in the covercrete than in the old concrete is unknown. In car park R the corrosion rate in the non-treated areas ranges from 2.8 to 4.6 $\mu A/cm^2$ and in the area treated with corrosion inhibitor the measured corrosion rate was about 4.2 $\mu A/cm^2$.

The results of these measurements clearly show that the corrosions rate in the areas where the corrosion inhibitor was applied to the surface three years ago is not any lower than in untreated areas. This is the case for both the structures and for a relatively new and relatively old concrete. If the inhibitors were affecting the corrosion in the treated areas one would expect the measured corrosion rate to be lowered in these areas than in the untreated areas. Since there is no real difference between the two areas one must assume that the corrosion inhibitors are not very effective in reducing the corrosion rate.

5. CONCLUSIONS

In the studied structures, which were two car parks in Reykjavik, there is considerable amount of chlorides left in the concrete each year. The chlorides originate from de-icing salts are brought into the structure with the cars that are parked in the structures. Presumably, most of

the chlorides are brought into the structures as a snow or a slurry which sticks to the cars entering the structures. Water leaks from the cars while they are driven into the parking area. There more water comes of them and the chlorides penetrate into the concrete. Due to this build up of chlorides in the floors of car parks corrosion will take place when critical chlorides levels have reached the reinforcements. In car park K reinforcement corrosion was taking place in areas where the chloride content at the reinforcement depth was about 0.1 as % of the weight of the concrete.

It is obvious that solutions are needed to solve this problem, it can not be acceptable to carry out a major repair work after only 14 years of service. One such relatively cheep solution could be corrosion inhibitors which can be applied to the surface of old structures or they can be cast in the concrete in new buildings.

In this project a penetrating corrosion inhibitor was applied to test areas, both to a old concrete with relatively high chloride content and to a new covercrete. After 6 months cores were drilled from the test areas. Pore water was pressed out and analysed for the content of the inhibitor. According to the producer the inhibitor should move very fast thru the concrete to the reinforcements where is should protect the reinforcements against chloride induced corrosion. The corrosion inhibitor content of the pore water was not measurable, which suggest that the inhibitor does not move much into the concrete. One core was analysed at depth level from 0 to 5 cm and from 5 to 11 cm. It turned out that the amino alcohol content of the pore water, which is the organic part of the inhibitor, was much higher in the upper part than the lower one. This suggests that there is some concentration gradient of the inhibitor with depth. It would have been better if thinner samples were analysed, but unfortunately pore water could not be pressed out from such relatively small concrete samples. None the less the fact that no inorganic inhibitor is found in the analysis and the organic component is in very low concentration suggest that the inhibitor did not penetrate deep into the concrete in six months.

The corrosion rate was measured in the test areas with the GalvaPulse instrument. In the two car parks total of five test areas were measured in which corrosion inhibitor was applied to the surface. The result of these measurements was compared to measurements done in untreated areas, nine untreated areas were measured. After about 2.5 years from the surface treatment the corrosion rate was measured in the test areas. The results of the measurements is that the there is no statistical difference between the untreated areas and the areas which were treated with the corrosion inhibitor. Although the measured corrosion rates are relatively low in all the areas one would expect them to be lower in the treated areas than in the untreated areas, otherwise the corrosion inhibitors offer no protection.

The general conclusion of this work is that penetrating corrosion inhibitors like the one which was tested offer no protection against chloride induced reinforcement corrosion, and therefore can not be a part of any long term strategy to increase the maintenance free time of structures which are under chloride loads. The solution to prolonged maintenance free period lies elsewhere.

REFERENCES

1. Elsener, B., 1.5 Mixed-in inhibitors, pp. 43-55 and (with Cigana, R.) 3.3 Surface Applied inhibitors, pp. 165-175. COST 521: Corrosion of Steel in Reinforced Concrete Structures, ed.: Weydert, R, 2002, 254 pp
2. Tuutti, K. Corrosion of Steel in Concrete. CBI – 4.82, 1982, 469 pp
3. Hansson, C.M., Mammoliti, L., Hope, B.B. Corrosion Inhibitors in Concrete - Part I: The principles. Cement and concrete research, 28, 1775-1781, 1998
4. Laamanen, P.H., Byfors, K. Corrosion inhibitors in Concrete – AMA (Alkanoamines) – Based Inhibitors – State of Art Report. Nordic Concrete Research, pub. no. 19, 2/1996, 29-40
5. Hope, B.B., Ip, A.K.C. The Research and Development Branch, Ontario Ministry of Transportation, Report No. ME-87-09 (1987)
6. Fadayomi, J. Corrosion inhibitors. Concrete, 1997, Sept, 21-22
7. Page, C., Ngala, V.T., Page, M.M. Corrosion Inhibitors in concrete Repair Systems. Magazine of Concrete Research, 52, 25-37, 2000
8. Berke N.S.,Weil T.G. World wide review of corrosion inhibitors in concrete. In Advances in Concrete Technology (ed. V.M. Malhotra). CANMET, Ottawa, 1994, pp. 899-1022
9. Tritthart, J. (2001) Transport of the Corrosion Inhibitor SIKA FerroGard 903 in Cement Paste and Concrete. In: COST 521 – Corrosion of steel in reinforced concrete structures. Proceedings of the 2001 workshop, Tampere Finnland, ed.: Mattila, J., 191-196
10. Tritthart, J. (2002) Transport of the Ingredience of a Corrosion Inhibitor in Cement Paste and Concrete. In: COST 521 – Corrosion of steel in reinforced concrete structures. Proceedings of the 2002 workshop Luxembourg, Luxembourg, ed.: Weydert, R., J., 233-244
11. Elsener, B., Klinghoffer, O., Frolund, T., Rislund, E., Schiegg, Y., Böhni, H. (1997) Assessment of reinforcement corrosion by means of galvanostatic pulse technique. Proceedings from Int. Conf. : “Repair of Concrete Structures”, Svolvær, Norway.

ACKNOWLEDGEMENTS

This work was funded by the Icelandic Research Council and the City of Reykjavik – Car Park division.

Field experience from investigation of more than 100 Norwegian bridges with respect to Alkali Aggregate Reactions (AAR)

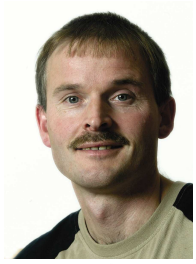

Jan Lindgård
M.Sc.Eng., Senior Research Engineer
SINTEF Technology and Society, Concrete,
NO – 7465 Trondheim, Norway
E-mail: jan.lindgard@sintef.no

Børge Johannes Wigum
Ph.D., Engineering Geologist
Hönnun Consulting Engineers, Grensásvegur 1,
IS-108 Reykjavik, Iceland
E-mail: wigum@honnun.is

Marit Haugen
M.Sc.Eng., Research Engineer
SINTEF Technology and Society, Concrete,
NO – 7465 Trondheim, Norway
E-mail: marit.haugen@sintef.no

Ola Skjølsvold
Eng., Research Engineer
SINTEF Technology and Society, Concrete,
NO – 7465 Trondheim, Norway
E-mail: ola.skjolsvold@sintef.no

ABSTRACT

A Norwegian research project (2000-2003) concerning Alkali Aggregate Reactions (AAR) has been completed. The main aims of the project were to:

- Use experience from concrete structures in the field to carry out an assessment of the current critical limits for the methods used in Norway during the last 10-15 years for evaluation of aggregates with respect to AAR.
- Give suggestions for revision of the current Norwegian guidelines for production of durable non-reactive concrete.

About 160 concrete structures, mainly bridges, were investigated in the field. Comprehensive laboratory investigations were performed on cores from about 50 of these structures.

Key words: AAR, field experience, guidelines, regulations

1. INTRODUCTION

1.1 Background

More than a decade of research and development in Norway has provided reliable and reproducible testing methods regarding AAR. This is the case both for classification of the reactivity of the aggregate itself and the potential of the reactivity of various concrete mixes. Until today a critical limit of up to 20 % reactive rock types in an aggregate is accepted for making a non-reactive concrete (measured in a petrographical analysis by use of thin sections) [1], i.e. no other preventive actions have to be carried out. A critical limit (0.10 %) is also set for the expansion in the accelerated mortar bar test, where the prisms (40·40·160 mm) are exposed in 1N NaOH at 80^{o}C for 14 days [1]. The critical limits for both methods have been valid in Norway since 1993. The reliability of the present acceptance/rejection criteria for aggregate material has been somewhat uncertain, due to a lack of correlating data from actual alkali-reaction damaged concrete structures in the field. To reduce these uncertainties, and as a basis for suggesting new critical limits, quantitative data on drilled cores from existing structures have been gathered and evaluated.

1.2 Aims of the research project

The aims of the project were to:

- Use experience from concrete structures in the field, together with quantitative measurements on concrete cores (environment, type of aggregates and mix design of concrete), to carry out an assessment of the current critical limits given by the Norwegian petrographical method and the accelerated mortar bar test;
- Find correlation between type of structure, local environment (humidity) and degree of damage in the field, with the ambition of obtaining more differentiated guidelines for production of non-reactive concrete;
- Make suggestions for revision of the Norwegian guidelines for production of durable concrete given by the Norwegian Concrete Association (NB publication No. 21, [2]).

1.3 Scope of work

A main part of the research project was to evaluate the critical limit for the petrographical analysis. As a basis for the research work the following issues were focused on:

- **Find representative structures with aggregates containing about 20 % reactive rocks**. In the South East of Norway the sand and gravel deposits contain from 10 to 30 % reactive rocks, i.e., both below and above the critical limit in Norway. Materials from these deposits are frequently used as concrete aggregate, and as a consequence, this area was selected – see Figure 1.
- **Collect relevant information**. Project information and specifications for a large number of concrete structures in South East of Norway was collected and evaluated. It was emphasised collecting information about the concrete recipes and the aggregate composition. Experience from preliminary studies showed, however, that such information received from owners, concrete- and aggregate producers was too uncertain to be used as documentation without performing supplementary laboratory investigations on drilled cores.

- **Select structures for inspection**. Based on the available documentation a total of 160 concrete structures, mainly bridges were selected for inspection. Due to variation in damage and a possible variation in concrete recipes and moisture content between different parts of the structures, only selected structure members were chosen for further investigations. A total of 80 structure members from different structures were selected, and 3 cores (diameter 100 mm and length about 300 mm) were drilled out from each of these. For 46 of these structures the cores were examined in detail in the laboratory. The cores from the remaining 32 structures were visible inspected, in addition to measurement of water content and porosity.
- **Find suitable laboratory methods**. To be able to evaluate the critical limit for the petrographical analysis it was necessary to have a sufficient degree of accuracy for evaluation of the rock composition in the concrete cores. In this project much effort was therefore paid to search for a method for separating the aggregate from concrete cores. A successful separation method would enable use of petrographical analysis as for virgin material (see chapter 3). Much effort was also paid to search for a method for describing the degree of damage in the drilled cores by use of only one parameter. Then it would be possible to make plots to investigate the correlation with other relevant parameters influenced by alkali aggregate reactions (see chapter 4).

Figure 1 – 160 structures in the South East part of Norway were selected for visual inspection.

1.4 Presentation of results from the research project

The results from the research project are presented in a main research report [3] (written in Norwegian, but including an English summary). In the succeeding chapters the following main topics from the project report are presented:

- Accuracy of the Norwegian petrographic method to quantify alkali reactive rock types in aggregates (chapter 2);
- Experience from separation of aggregates from sampled concrete cores with a new method assessed and tested in this project (chapter 3);
- Assessment of degree of damage in the plane polished sections of half-cores based on the "Crack Index Method" (chapter 4);
- Revision of the specifications and guidelines for production of AAR resistant concrete in Norway (chapter 5);
- Main conclusions from the research project (chapter 6).

In addition to the topics above and presentation of the results from the field – and laboratory investigations performed, the project report [3] includes the following main items:

- Background regarding AAR research in Norway;
- Accelerated mortar-bar testing [1] of separated aggregates from concrete cores ("pilot testing" - the results were collaborated with results obtained by testing "virgin" material from the same deposits);
- A review of more than 10 years of experience with the "Norwegian version" of the Canadian concrete prism test method;
- A brief review on international status on test methods and guidelines regarding how to minimise the risk of deleterious AAR.

It is possible to download a Norwegian "pdf-version" of the complete research report [3] by visiting the website of the **F**orum for **A**lkali aggregate **R**eactions **I**n **N**orway (**FARIN**) at; *www.this.is/ergo/efarin*. At this site you will also find more information about AAR in Norway, including a "Norwegian picture atlas" with thin section pictures of reactive rock types.

2. ACCURACY OF THE NORWEGIAN PETROGRAPHIC METHOD TO QUANTIFY ALKALI REACTIVE ROCK TYPES IN AGGREGATES

The current Norwegian petrographic method, to quantify alkali reactive rock types, is based on point counting of aggregates in thin-sections. As the method has been used as a screening engineering tool in Norway for more than a decade and has now been adopted as a RILEM method, the status of the method and its accuracy were evaluated as a part of the project [4].

The overview carried out regarding the development of the method since 1993 [1] included:

- Investigation and quantification of the micro structural features of a number of Norwegian rock samples;
- Comparison of quantitative parameters for quartz to expansion results from ultra accelerated mortar bar testing;
- Evaluation of the development of nomenclature used by operators during the years;
- Collection of petrographical results on a national level;
- Examination of annual variation of amount of reactive rocks obtained by the petrographic method;

- Evaluation of the accuracy of the method by estimating the statistical variation between operators and the statistical variation in the method itself.

The development of the petrographic method in Norway during the last decade has shown that it is possible for well-coordinated operators to obtain results with good convergence. In order to minimize the variations, the accuracy of the determination of quartz grain size appears to be essential.

Studies of petrographical results from 1993 to 2001 have enabled evaluation of variations within the same locations. In Figure 2 results from petrographical examination of natural sand aggregates from 38 Norwegian quarries are presented. Even though many locations exhibit low variations in amount of reactive rock types from year to year, some locations exhibit significant levels of variation.

Possible sources for these variations may be:
- Statistical variation in the point-counting itself;
- Variation between operators and between laboratories (samples from a given quarry may be investigated at different laboratories from year to year);
- Development of the method and development (improvement) of the operator;
- Natural geological variations in the quarry;
- Occasionally some producers have blended aggregates from more than one quarry (e.g. if the concrete producer use a blend of two sand types in the concrete mixes) before supplying the sample to the laboratory for petrographical examination (to save some money, even though the Norwegian regulations require aggregates from each quarry to be analyzed separately).

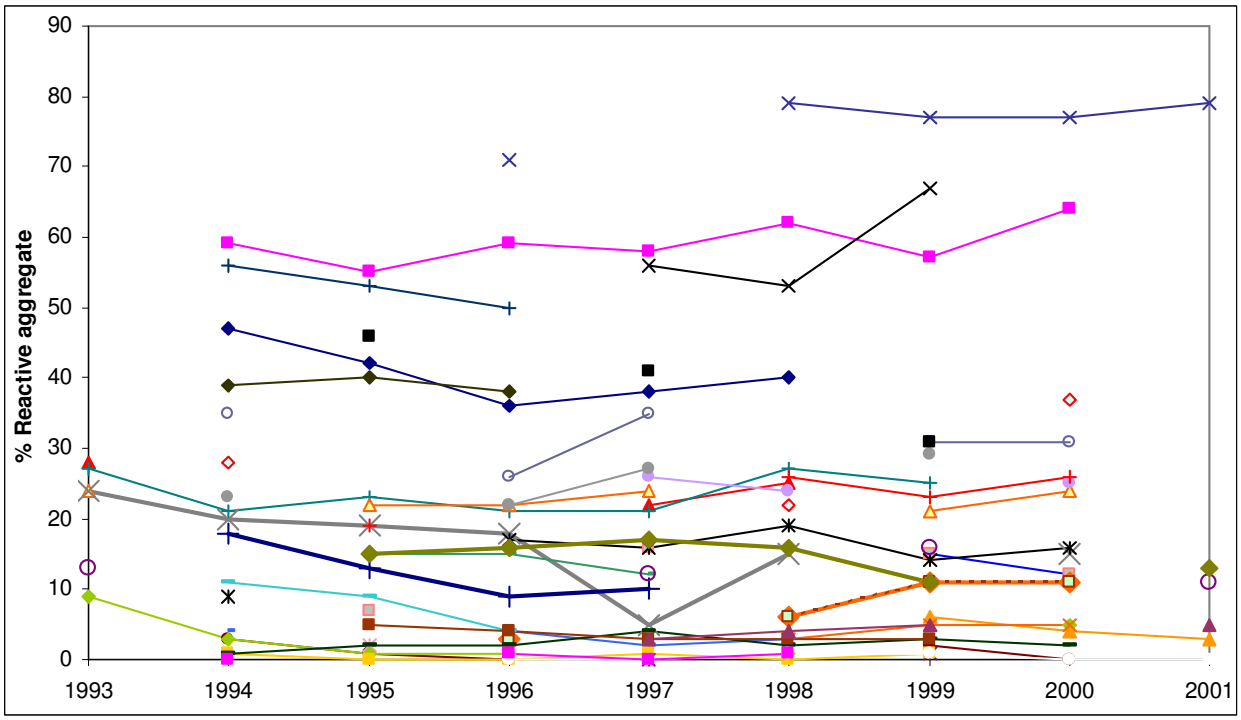

Figure 2 – Annual variation in amount of potential reactive rock types for 38 quarries with natural sand aggregate (three or more samples from each location).

It is difficult to find a fixed degree of variation due to the fact that number of parallel samples is variable. For some aggregate types the standard deviation is based upon only two measurements, while for other aggregates the standard deviation is based upon 7-8 measurements. Thus criteria to decide for one or another source of variation are either ambiguous or not accurate enough.

The theoretical degree of variation for sand aggregates, at the critical content of 20vol% reactive rock types is in the range from +2.6vol% to 2.4vol%. Experience among operators subsequent to the round robin test, implicate results in the range of ± 5vol% deviation.

It is suggested that expected degree of variation should be included in future determination and classification of the critical degree of potential alkali reactive rock types. This is also important in cases where blending of aggregates is carried out by the aggregate – or by the concrete producer in order to produce a non-reactive concrete.

3. EXPERIENCE FROM SEPARATION OF AGGREGATES FROM SAMPLED CONCRETE CORES WITH A NEW METHOD ASSESSED AND TESTED IN THIS PROJECT

3.1 Scope of work

In order to evaluate the critical limit for the petrographic analysis it was necessary to have a satisfactory degree of accuracy for evaluation of the rock composition in the concrete cores. Norwegian alkali reactive rocks are very fine grained and identification/classification is very uncertain without thin section microscopy. When concrete cores are examined with respect to cause and extent of damage and concrete composition, it has been a common practice both in Norway and internationally, to perform structure analysis; fluorescence impregnated plane polished sections of half-cores examined with a stereo microscope and thin sections examined with a polarization microscope. With this method it is possible to roughly estimate the concrete composition, but the method is too uncertain for assessment of the content of alkali reactive rocks.

In this project much effort was therefore paid to search for a method for separating the aggregate from concrete cores. A successful separation method would enable use of petrographic analysis as for virgin material.

3.2 Technique for aggregate separation

A ”separation method” developed in Canada [5] was adjusted to the available equipment at SINTEFs laboratory. In this method a water saturated core is placed in liquid nitrogen (-196ºC) before heated in a micro-wave oven (varying number of cycles). Between each cycle the concrete is hammered to loosen the stones from the paste. After sieving, sand and stone are washed in an acid solution. A more detailed description of the technique for aggregate separation and the results gained in the research project is given in [3] and [6].

Figure 3 shows a part of a concrete core (diameter 100 mm) before separation of the aggregate, in addition to the “concrete” after separation, but before washing in acid.

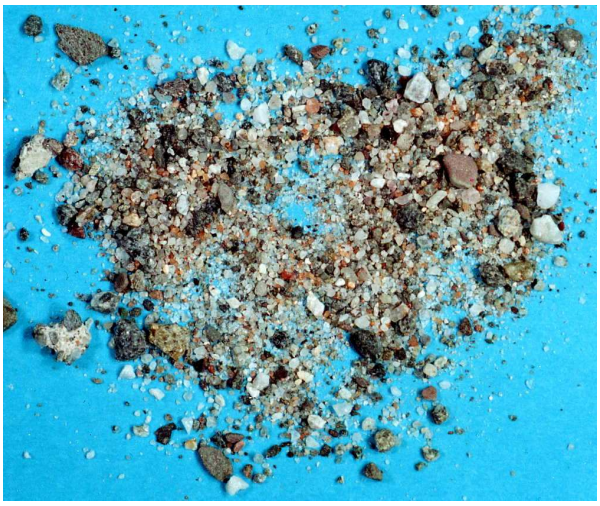

Figure 3 – Left: Part of a water-saturated concrete core before separation of the aggregate Right: The "concrete" after separation, but before washing in acid

3.3 Petrographic analysis

The petrographic analysis of the separated aggregates was performed with point counting in thin sections according to [1]. For sand both the fractions 2-4 mm and 1-2 mm were counted. Coarse gravel and crushed rock particles were crushed down before sieving out the fraction 2-4 mm, which was point counted.

In Norway it is required that the petrographic analysis should be performed by an experienced petrographer. This is important because Norwegian rocks are very varied and hence often difficult to identify and classify correctly (see [4]).

After separation of the sand and stone aggregate from the concrete, it was possible to perform petrographic analysis of this material with the same method as for a virgin aggregate. The accuracy of the analysis therefore corresponds to the accuracy of an ordinary petrographic analysis (see chapter 2).

3.4 Results and discussion

The experiences with separating aggregate from the 46 concrete cores are very good. The method is regarded as technically and economically feasible. However, the procedure demands skilled and experienced laboratory personnel. When the concrete is hammered the operator has to be very careful, due to the danger of loss of material. During the acid washing process, the operator has to be careful to obtain clean particles. If not, cement paste/mortar will cover much space in the thin sections.

The impression after point counting of about 240 thin sections (46 samples) is that the separated and sieved (and for stone also crushed) aggregate particles are very clean.

For some rock types, special requirements are necessary. Limestone particles may be dissolved by the acid during the washing process, and therefore have to be identified in advance. However, most of these coarse limestone particles were pretty clean even without washing.

Special precautions should also be taken when very weak rock types are present, e.g. phyllite. For a few aggregate types containing phyllite it was observed that the separation process could be too severe, and thus split the coarse aggregate particles into smaller particles. However, only in a few samples it was possible to identify grains from the stone fraction in the sand fraction, but in most cases this constituted a small amount. If possible these "contaminations" were corrected for by not including them in the petrographic description of the actual sand.

Another possible source of error is presence of coarse grains from the sand fraction in the stone fraction. However, this could be observed only in a few cases, and then the content of such grains was rather small.

In many cases the operator was able to recognize the origin of the aggregates (area/deposit). In most of these cases the results from the petrographic analyses of the separated material were almost identical to the results of the petrographic analyses of the virgin material, see Figure 4. This confirms that the relatively small samples used were sufficient for our purpose (i.e. to find the rock composition and the origin of the material).

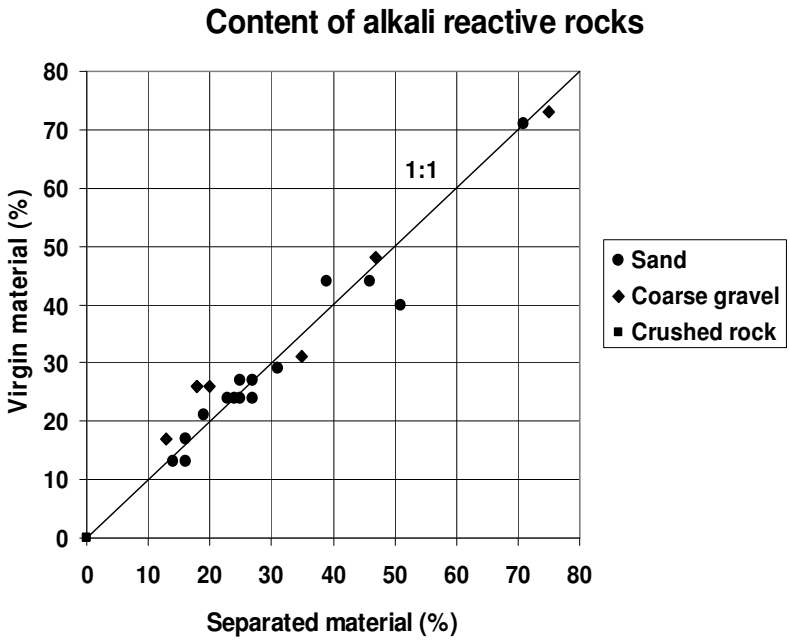

Figure 4 - Correlation between petrographical analyses on separated aggregates and virgin material, respectively

In several occasions the collected information concerning aggregate types used in the concrete structures was incorrect. This was revealed in the petrographic analyses of the separated aggregates from the concrete cores.

4. ASSESSMENT OF DEGREE OF DAMAGE IN THE PLANE POLISHED SECTIONS OF HALF-CORES BASED ON THE "CRACK INDEX METHOD"

To investigate if AAR appears in a concrete it is common to drill cores from the cracked structure and perform structural analysis (i.e. plane polished- and thin section analysis). Based on the presence of cracks in the cores the degree of damage is estimated and described, normally only verbal (for instance; "a small amount of large cracks", "some large cracks", etc.). In the present research project the aim was to describe the degree of damage in a simple quantitative way, preferably by use of only one parameter. Then it would be possible to make plots to investigate the correlation with other relevant parameters influenced by alkali aggregate reactions.

In the beginning of the project different methods were evaluated. Among these the method called the "Damage Rating Index, DRI" [5] was used in preliminary tests. A short description of the method (where 8 parameters are counted) and the results from the preliminary tests are given in [3] and [7]. This method was found to be rather elaborate and also time consuming. Not all parameters, such as "particles with reaction rim" and "air voids with gel", are directly linked to structural damage, but still contributed much to the total calculated DRI in some samples. In addition one parameter which normally is observed in Norwegian concretes damaged by AAR, is absent in the "DRI-method"; aggregates with cracks continuing from the aggregates into the cement paste. In the context of our research project it was therefore decided to focus only on the number of cracks, since rating of structural flaws were considered to be the most important measure of the "degree of AAR damage" in our structures. This could be done safely when AAR had already been detected in thin sections.

A simplified method for describing the degree of damage in plane polished sections is earlier applied in Norway [8]. In this method, named the "Crack Index method", the degree of damage due to AAR is evaluated by counting cracks in fluorescent impregnated plane polished sections (no microscope is used). Only 3 crack parameters are counted (in ultra violet lighting) within divided zones in the plane polished sections, see Figure 5:

- Number of coarse aggregates (> 4 mm) containing cracks (marked "A");
- Number of coarse aggregates containing cracks continuing from the aggregates into the cement paste (marked "AP");
- Number of cracks in the cement paste (marked "P").

Based on the preliminary results the reproducibility of the method was regarded as acceptable, and the "Crack Index Method" was chosen to be used in the research project instead of the "DRI-method". In addition to the reasons for this given above, it may be added that in our research project we were looking for harmful AAR. This means that the cracks ought to be visible by eye in the fluorescent impregnated polished sections (i.e. without using a microscope, as in the "DRI-method). Another reason is that the "Crack Index Method" is more cost effective, and it is simple to perform by a trained operator.

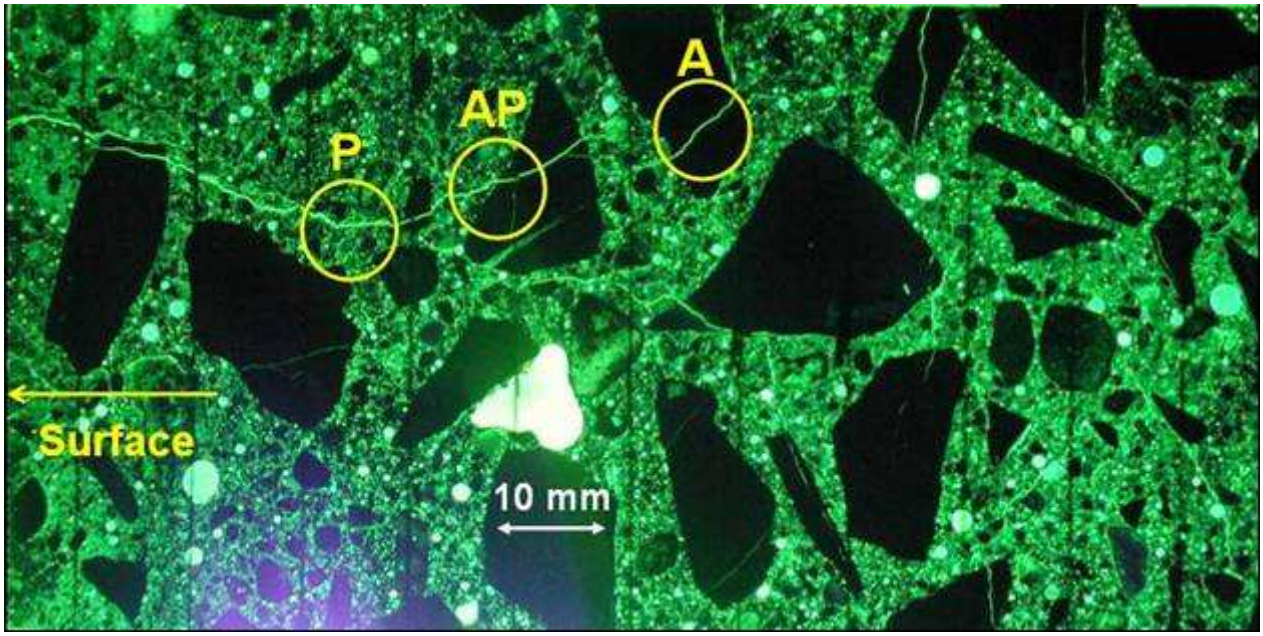

Figure 5 – Parameters counted in the "Crack Index Method" within divided zones in the plane polished sections

After counting of cracks according to the "Crack Index Method" on plane polished sections of half-cores from totally 46 concrete structures, the results were evaluated (including regression analyses). Taking into account the fact that more than 15 % of the stones contain cracks independent if AAR occurs in the concrete, it was decided to not include this parameter in the calculation of a "common crack parameter". This is also in accordance with the "DRI-method" [5], where the weight for "coarse particles with cracks" is only 0.25 out of a total of 16.25, i.e. this parameter only contributes with a weight of 1.5 % in the calculation of the DRI.

On this basis a "Crack Index" (CI) was defined as:
- [% of the stones containing cracks continuing from the aggregates into the cement paste]· **0,6**
- [amount of cracks in the cement paste given as number/cm^2 ·100]· **0,4**

By use of the measured/calculated "Crack Index", and the results from the thin section analyses (number of reacted aggregate particles and extent of gel formation), the extent of AAR in the drilled cores from the 46 concrete structures (mainly bridges) were evaluated. The observed crack widths in field on most of the structures with map cracking varied from about 0.05-0.15 mm. However, more severe damage, with crack widths > 0.35 mm, was observed on some of the structures.

The method appears to be beneficial. The "Crack Index" (CI) describes reasonably the degree of damage in the drilled concrete cores due to AAR caused by slowly reactive Norwegian aggregates. The correlation to field observations is also acceptable (a condition for this is of course that representative samples are drilled out from the structures investigated).

Reasonable correlations with other parameters connected to AAR are recognized, in particular degree of capillary suction (water content) and age of the structures where AAR is presence, see Figure 6 and 7. For most of the concrete structures with documented AAR, CI is ≥ 8. In the interval CI = 5-8, some structures have small signs of AAR, the rest have no signs of AAR. For

the structure with the extremely high CI (56), also cracks due to frost attack gave a significant contribution to the measured CI.

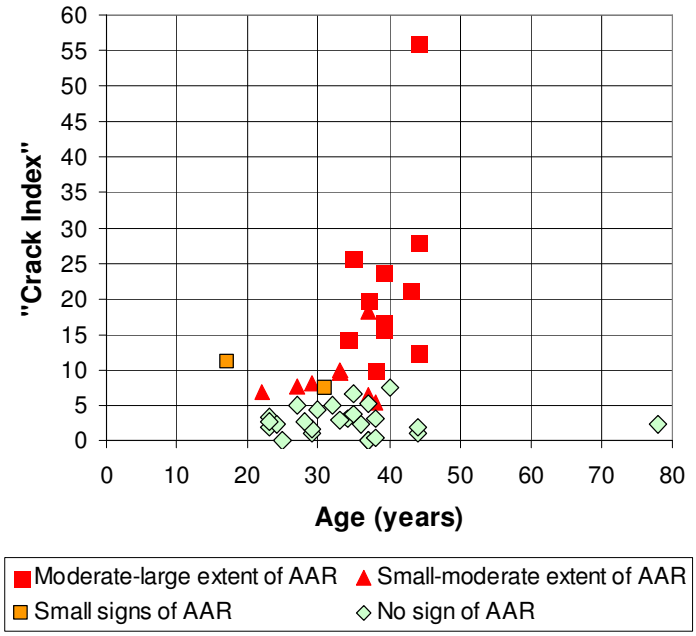

Figure 6 – "Crack Index" versus age of the concrete structures.

As can be seen from Figure 6, most of the concrete structures were from 25-45 years old. For the concretes with documented AAR, it seems like the extent of cracks in the drilled cores increases with age. This is in agreement with the experience gained after visual inspections of several hundred concrete structures in Norway. The first cracks on the surface of the structures are normally visible after 15-20 years, and the crack width normally increases with the age.

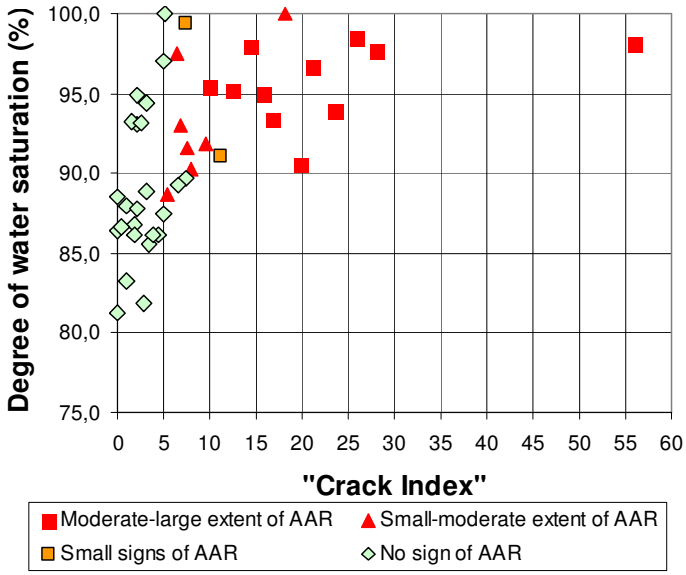

Figure 7 – "Crack Index" versus degree of water saturation in the drilled cores.

With one exception the degree of water saturation of the concretes is higher than 90vol% for all the concrete with presence of AAR. Further one the water content of the majority of the concretes with no sign of AAR in the drilled cores (and thus a low CI) is lower than 90vol%. One reason for the observed high water content in the concretes with presence of AAR is that a high water content increases the risk for development of AAR. Another reason is assumed to be that the formation of an absorbing gel due to AAR leads to an increased water content.

No good correlation was found between the observed damage due to AAR (i.e. measured CI) and the water/binder ratio or the air content of the concrete, respectively.

A more comprehensive presentation and discussion of the "Crack Index Method" and the results gained in the research project by use of this method is given in [3] and [7].

5. REVISION OF THE SPECIFICATIONS AND GUIDELINES FOR PRODUCTION OF AAR RESISTANT CONCRETE IN NORWAY

Based on the results from the research project, suggestions were given for revision of the current Norwegian guidelines for production of durable concrete given by the Norwegian Concrete Association (NB publication No. 21, [2]). Focus was made on critical limits for the three methods used in Norway for more than a decade (the methods were earlier described in [1]; revised descriptions are given in [12]):

- Petrographical analysis by use of thin sections (used for evaluation of the reactivity of an aggregate – the method is in agreement with the RILEM AAR-1 method [13]);
- Ultra accelerated mortar bar test (used for evaluation of the reactivity of an aggregate or a mix of aggregates – the method is quite similar to the RILEM AAR-2 method [14]);
- Concrete prism test (used for evaluation of the reactivity of an aggregate, a mix of aggregates, a binder or a given concrete recipe).

It seems likely that coarse aggregates lead to more damage (i.e. is more severe) than the sand fractions. Thus, more strict requirements are recommended for the coarse aggregates. However, for sand aggregates the critical limits used since the beginning of the 90'ties seem rather conservative.

Based on the new knowledge obtained from the research project as well as international research, the revision work on NB publication No. 21 (NB21) could start in late 2002. This time the publication would be given formal status as a harmonized normative reference document to the new concrete materials standard, NS-EN 206 /9/. This implies that to be in compliance with the material standard, concrete shall be composed according to the specifications in the publication. In September 2004 a revised edition of the publication /10/ was provided by a committee with the authors of a paper presented on the 12th ICAAR in Beijing [11] as members.

As for the 1996-version, the 2004 version of NB21 states that concrete shall be considered secure against AAR if at least one of the following conditions is fulfilled:

- The aggregate is documented to be non-reactive;
- The binder has a composition that prevents AAR at the actual alkali content;
- The concrete will serve under dry exposure conditions.

NB21 is a key element in the Norwegian system for preventing alkali aggregate reactions. The system also includes:

- Descriptions of the actual test methods;
- Certification of producers of aggregates and concrete;
- Certification of test laboratories;
- Round robin tests for test laboratories;
- A committee of experts to be used for interpretation of the regulations in cases of uncertainty or dispute.

The system in Norway for preventing AAR is considered to represent the same security level as corresponding systems for securing against durability damage from corrosion and frost.

6. CONCLUSIONS

From the Norwegian research project (2000-2003) concerning field experience from investigation of about 160 concrete structures (mainly bridges) with respect to alkali aggregate reactions (AAR), the following conclusions may be drawn:

The Norwegian petrographic method appears to be appropriate as a screening engineering tool in order to classify alkali reactive aggregates. The degree of variation in the method should be set to ± 5vol%-point. However, recommendations are made for further development and strengthening of the method, including advanced image analysis systems. This will enhance the value of the method as an engineering tool to screen certain types of potentially reactive aggregates.

Several of the investigated structures (mainly bridges) have map cracking. However, laboratory analyses have shown that alkali aggregate reactions are not the cause of damage for all the map-cracked structures. Also other mechanisms, e.g. drying shrinkage and temperature movements are present.

For 20 of the 46 structures investigated in detail in the laboratory (with age from about 20-45 years) AAR is documented to be one of the main causes for the observed map cracking. However, the visual inspections showed in general a rather small extent of damage, with rather small crack widths varying from about 0.05-0.15 mm. The maximum crack width was > 0.35 mm for only 3 of the about 80 structures (3.8 %) of which cores were drilled out. For 9 of the 20 structures with documented AAR expansions are most likely present.

The project has succeeded in developing a technical and economical feasible method for separating the sand- and coarse aggregate fractions from the drilled cores, and thus made it possible to perform petrographical analyses in a similar way as for “virgin material”. It was also possible to “link” most of the aggregates to geological areas and known deposits. This would not have been possible only by use of a traditionally structure analysis of the concrete cores.

The project has also succeeded in characterising the degree of damage in the drilled cores by introducing a so-called “Crack Index” (CI), based on counting of 3 crack parameters in the plane polished sections.

The moisture content within the concrete structures (in depths from about 200-300 mm) is in general very high. The degree of water saturation varied from about 83-100 %, with a mean value of about 91 %.

A good correlation was found between the "Crack Index" in the plane polished sections, the degree of water saturation and the presence of AAR. These findings are also verified by statistical analyses. With one exception the degree of water saturation of the concretes is higher than 90vol% for all the concrete with presence of AAR.

No good correlation was found between the observed damage due to AAR (i.e. measured CI) and the water/binder ratio or the air content of the concrete, respectively.

A reasonable correlation was found between the content of reactive rock types in an aggregate and the "Crack Index". It seems likely that coarse aggregates lead to more damage (i.e. is more severe) than the sand fractions. Thus, more strict requirements are suggested to a coarse aggregate compared to sand aggregate.

The overall experience gained in the research project was that the results obtained with the three Norwegian laboratory test methods correlates satisfactory with field experience, under supposition that some of the critical limits are changed. Thus, based on the results from the research project, specific suggestions were given for revision of the Norwegian guidelines for production of durable concrete given by the Norwegian Concrete Association (NB publication No. 21 - 1996, [2]).

ACKNOWLEDGEMENTS

This research project was initiated in 2000. SINTEF Civil and Environmental Engineering, Department for Cement and concrete (now named: SINTEF Technology and Society, Concrete), managed the whole project, while ERGO Engineering Geology Ltd (by Børge Johannes Wigum, now employed at Hönnun Consulting Engineers) was in charge of the steering committee. Total budget was about NOK 7 millions (included man-hours within the different participating companies). Among these the Norwegian Research Council funded NOK 1.5 millions, while the Norwegian road authorities funded most of the laboratory investigations.

The national society for aggregate producers in Norway (PGL) hosted the research project, in which aggregate-, precast concrete- and concrete producers, cement producer NORCEM, road- and railroad authorities, the Control Council for Concrete Products, the Norwegian Concrete Association and the Norwegian army corps of engineers all participated. This work would not have been possible without financial support by these members, and the Norwegian Research Council.

REFERENCES

1. Lindgård J., Dahl P.A., Jensen V., "Rock composition – reactive aggregates: Test methods and requirements to laboratories", SINTEF report no. STF70 A93030, Trondheim, 1993, 9 pp. (In Norwegian).
2. Norwegian Concrete Association, NB: "Durable concrete containing alkali reactive aggregates", NB Publication No. 21, Oslo, 1996, 5 + 27 pp including appendices. (In Norwegian).
3. Lindgård, J, and Wigum, BJW: "Alkali Aggregate Reaction in Concrete – Field experiences", SINTEF report no. STF22 A02616, Trondheim, 2003, 127 pp + appendices. (In Norwegian).
4. Wigum, B.J., Haugen, M., Skjølsvold, O. and Lindgård, J., "Norwegian Petrographic Method – Development and Experiences During a Decade of Service", paper presented at the 12th ICAAR Conference, Beijing, October, 2004.
5. Grattan-Bellew, "Laboratory evaluation of alkali-silica reaction in concrete from Saunders Generating Station", ACI Materials Journal, V. 92, March-April 1995.
6. Haugen, M., Skjølsvold, O., Lindgård, J. and Wigum, B.J., "Cost effective method for determination of aggregate composition in concrete structures", paper presented at the 12th ICAAR Conference, Beijing, October, 2004.
7. Lindgård, J., Haugen, M., Skjølsvold, O., Hagelia, P. and Wigum, B.J., "Experience from evaluation of degree of damage in fluorescent impregnated plane polished sections of half-cores based on the "Crack Index Method"", paper presented at the 12th ICAAR Conference, Beijing, October, 2004.
8. Jensen, V., "Alkali Aggregate Reactions in Southern Norway", Doctor Technical Thesis, the Norwegian Institute of Technology, University of Trondheim, 1993, 262 pp + Appendices.
9. Norwegian Committee for Standardization, NS-EN 206-1:2001, "Concrete Part 1: Specification, performance, production and conformity", (Amendment (in Norwegian) prA1:2003 incorporated), 2003, 90 pp.
10. Norwegian Concrete Association, NB: "Durable concrete containing alkali reactive aggregates", NB Publication No. 21, Oslo, September 2004, 22 + 12 pp including appendices. (In Norwegian).
11. Dahl, P.A., Lindgård, J., Danielsen, S.W., Hagby, C., Kompen, R., Pedersen, B. and Rønning, T.F., "Specifications and guidelines for production of AAR resistant concrete in Norway", paper presented at the 12th ICAAR Conference, Beijing, October, 2004.
12. Norwegian Concrete Association, NB: "Alkali aggregate reactions in concrete. Test methods and requirements to laboratories", NB Publication No. 32, Oslo, September 2004. (In Norwegian).
13. RILEM Recommended Test Method TC-106-1 (now AAR-1): "Detection of potential alkali-reactivity of aggregates: Petrographic method, Final Committee Draft" (not yet published).
14. Nixon, P.J. (Chairman), 2000, RILEM TC 106-AAR: Alkali-aggregate reaction – Recommendations – A-TC106-2 (now AAR-2): "Detection of potential alkali-reactivity of aggregates – The ultra-accelerated mortar-bar-test", Materials & Structures, Vol. 33, No. 229, pp 283-289.

On the plastic behaviour of multi directional epoxy-bolted CFRP laminates

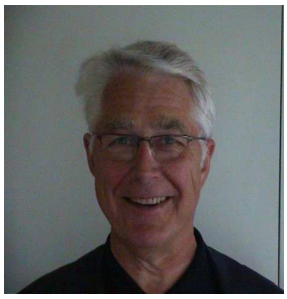

Aage P. Jensen
Ph.D., Associate Professor
Technical University of Denmark Building 118, DK-2800 Lyngby
aapj@byg.dtu.dk

Ervin Poulsen
Professor Emeritus of C.Eng.
8 Skovbrynet, Nodebo DK-3480 Fredensborg
ervin-poulsen@get2net.dk

ABSTRACT

The second generation of CFRP laminate has recently been developed. It is a multi directional CFRP laminate, i.e. a laminate with carbon fibres having several directions other than the first generation. The paper describes the laboratory tests carried out in order to develop anchorage devices for such multi directional CFRP laminates which are epoxy-bonded and bolted or nailed to the concrete substrate for the purpose of strengthening against failure caused by bending. The tests were carried out at the Technical University of Denmark, IABM and BYG · DTU.

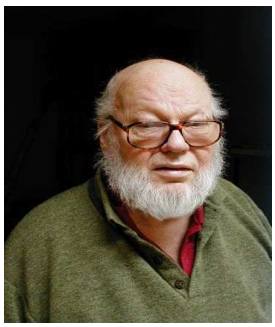

Key words. Multi directional CFRP laminates. Anchorage by bolts. Test methods.

1. INTRODUCTION

Strengthening of RC structures by means of external bonded reinforcement has been used for many years. However, it was the use of carbon fibre reinforced polymer laminates which really accelerated the application.

The first CFRP laminates used as external bonded reinforcement were composed of uni directional fibres bonded together with epoxy or vinyl ester resin. These CFRP laminates have a smooth surface and are produced in widths of 40 mm to 120 mm. The thickness is typically 1.2 mm to 1.4 mm. These CFRP laminates have a very high tensile strength, but since the fibres are parallel, the tensile strength perpendicular to the longitudinal axis is very low. Thus, they cannot be anchored with bolts or nails to the concrete substrate. Therefore, special anchoring devices have to be developed, cf. *Poulsen* [1].

2. NEW CFRP COMPOSITES OF TRADECC

The anchoring of the first generation of CFRP laminates by special anchoring devices is rather time consuming and expensive. Therefore, TRADECC has developed new CFRP laminates which contain fibres in the plus and minus 45° direction, besides the longitudinal direction. These CFRP laminates are manufactured on request in a width of 50 mm to 600 mm and an effective thickness of 1.0 mm to 30 mm. The length is available according to request. A scrim cloth (peel tape) protects both surfaces, cf. Figure 1. The packing depends on the length and thickness of the laminates.

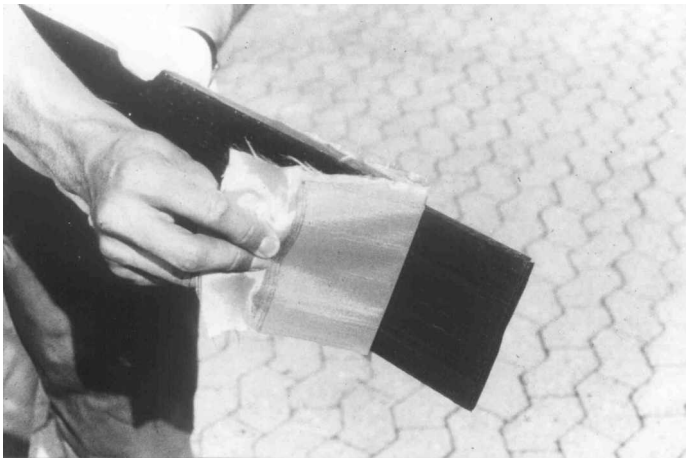

Figure 1 - A scrim cloth (peel tape) protects the surface of the CFRP laminate.

2.1 PC CarboComp Plus laminates

The laminates described above are PC CarboComp Plus and have the following advantages:

- They can be anchored to the concrete substrate with bolts and nails. The stresses in the bored longitudinal fibres are transferred to the adjoining fibres by the fibres in the plus and minus 45° direction. The anchoring increases the bearing capacity and allows a higher load than the first generation CFRP laminates, all other being equal, since the embedded strength of the anchoring bolts have a plastic failure, cf. Figure 2 and 3. Therefore, the partial safety factor is considerable lower than that of a brittle failure; cf. *DS 411:1999* [2].
- They are produced in the width of the beam so the contact surface is maximum and only one laminate is required.
- They have a rough, clean surface (the scrim cloth is easily peeled of), cf. Figure 1, so there is no need for high pressure blasting or degreasing before gluing.

The width of a standard PC CarboComp Plus laminate is 100 mm and the effective thickness of the laminate is 1.0 mm.

Figure 2 - Shear failure of CFRP laminate.

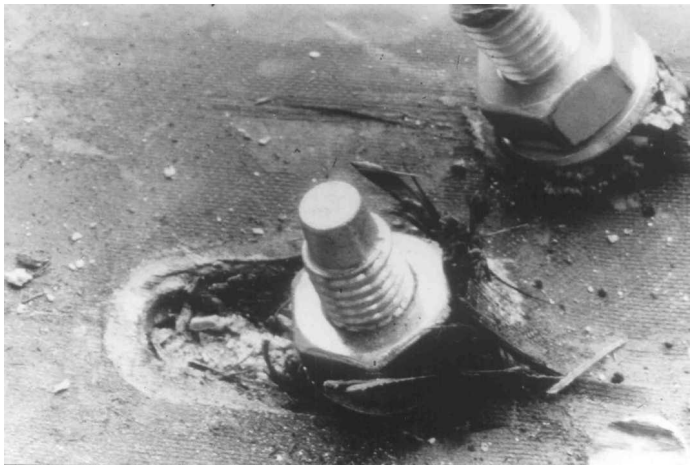

Figure 3 - Plastic failure of bolts after testing the beam.

2.2 Properties of PC CarboComp Plus laminates

The main properties of PC CarboComp Plus laminates are as shown in Table 1.

Table 1 - Properties of PC CarboComp Plus laminates

Properties	Values
Tensile strength	> 2850 MPa
Modulus of elasticity	> 175 GPa
Maximum elongation	≈ 1.65 %
Density	≈ 1600 kg/m^3
Water absorption	< 0.1 %
Application temperature	From – 40 ^{O}C to + 130 ^{O}C

3 EXPERIMENTAL DATA

In order to study the anchorage of PC CarboComp Plus laminates to concrete substrate by means of epoxy and bolts, tests were carried out at the Technical University of Denmark, IABM DTU. From earlier tests on bolted connections of multi directional CFRP laminates it was expected that the failure of bolted connections due to fail of the embedded strength had a plastic behaviour, cf. *Croes et al.* [3] and *Turvey et al.* [4]. The following presentation is based upon work of *Beck & Jacobsen* [5].

3.1 Single bolt test set-up

The aim of these tests was to determine the embedded strength of the multi directional CFRP laminates (the bearing failure) versus the diameter of the bolt and the distance from the bolt to the end of the CFRP laminate, applying two widths of the laminates, 100 mm and 50 mm.

The bolt was fixed in a predrilled hole of the laminate. Various versions of the joint were pre-tested before the final selection of the joint. Then, the tests were carried out by prestressing the bolts by means of a nut and washer on both sides of the laminates, applying a controlled torque of 10 kpm. This arrangement was necessary in order to keep the laminate in a plane position as is the case when glued and bolted to the concrete substrate. The tensile force was transmitted through the bolt to the CFRP laminates by means of a U-shaped fork.

3.2 Failure of embedded strength

The PC CarboComp Plus used had an effective thickness of 1.0 mm and a width of 50 mm and 100 mm. The distance from the bolt to the end of the CFRP laminate was 25 mm, 50 mm, 75 mm and 100 mm. There was no significant influence of the width and the distance from the bolt to the end of the laminate. There was an excellent plastic behaviour of the failure. However, in order to achieve a decent long plastic behaviour it was concluded that the minimum distance from the bolt to the end of the laminates ought to be 50 mm. Tests results are shown in Table 2. It may be detected that the characteristic value (i.e. 5 % fractile) is approx. 1000 MPa, almost independent of the diameter of the bolts in these tests, i.e. from ∅ 10 mm to ∅ 24 mm.

Table 2 – Embedded strength of CFRP laminates loaded by embedded bolts vs. bolt diameter.

Properties	Units	∅10 mm	∅16 mm	∅20 mm	∅24 mm
Nos. of tests	Nos.	36	27	21	20
Mean value	MPa	1514	1328	1687	1830
Deviation	MPa	242	194	418	331
5 % fractile	MPa	1023	967	1039	1186

3.3 Tests of PC CarboComp Plus laminates bolted to concrete substrate

To study the interaction of an epoxy-bolted PC CarboComp Plus laminate the test set-up shown in Figure 4 was used. Tests results showed that the embedded failure of the laminate is plastic while the failure of concrete is brittle. It was also documented that the HILTI design of bolts embedded in concrete could be used.

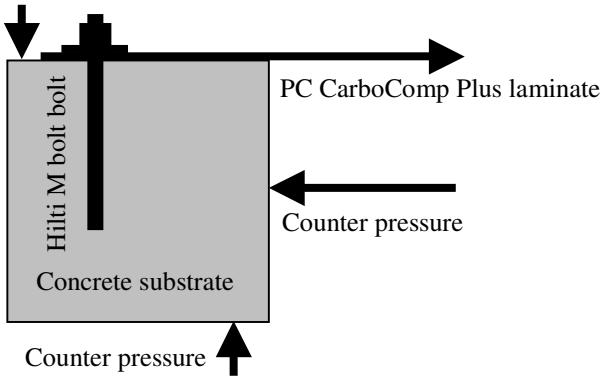

Figure 4 – Test set-up for a single bolt anchored to the concrete.

4 CONCRETE BEAMS

In concrete beams strengthened by an external bonded carbon fibre laminate, debonding of the laminate usually takes place at a sudden when the beam is loaded by an increasing load. The sudden debonding is caused by an unstable crack between the laminate and the substrate, cf. *Neubauer et al.* [6]. The debonding results in an undesirable drop in the bearing capacity of the beam and ways to avoid it should be looked for.

One way to escape the drop in the bearing capacity might be to use a CarboComp Plus laminate anchored to the beam by bolts as demonstrated above. When debonding takes place it is supposed that the bolts will assure a continuation of the connection between laminate and

substrate and since the laminate 'yields' under a constant load it might be expected that the load on the beam also will be constant even for considerable deflections.

In order to test such an idea and to obtain information about the influence of the bolt pattern and the number of bolts necessary a number of 10 beams were tested. Two of the beams were tested in a pre-testing series.

In simple supported beams strengthened by e.g. a Sika CarboDur laminate the laminate is supposed to be self-anchored by extended ends of the plate, cf. *Neubauer* [7]. With such a focus on the end of the plate and with the conception that debonding often starts at the ends of the plate it was decided to place all bolts at the ends of the laminate and only vary the number of bolts.

4.1 The pre-testing beams

Testing was carried out of 2 Nos. 3000 mm long RC beams, cross-section 300 × 300 mm, each strengthened by a single 100 × 2.0 mm multi directional laminate from TRADECC in Belgium. The beams were tested by an Amsler beam test rig. The beams were simply supported and loaded by two equal forces at the middle of the span. The strengthening of the beams was as follows:

- The CFRP laminate of one of the beams was, besides being glued to the substrate by epoxy adhesive anchored to the substrate by five HILTI stainless steel bolts, ∅ 10 mm M bolts, in one end of the CFRP laminate and seven bolts in the other. The bolts were placed into holes ∅ 12 mm, drilled into the substrate and injected with a HILTI adhesive. Each nut was tightened by a torque of 5 kpm.
- The CFRP laminate of the other beam was, besides being glued to the substrate by epoxy adhesive anchored to the substrate by 37 HILTI stainless steel nails, ∅ 3.7 mm Kwik DNH, in both halves of the CFRP laminate. The laminate was predrilled with a ∅ 5 mm drill and fixed by means of powder actuated nails.

Epoxy bonded CFRP Laminate Anchored by Bolts. According to the evaluation the used method of design has been satisfactory in coordination with the observations made. The load-deflection diagram showed a remarkably long plastic branch (with a constant load bearing capacity) so that it is possible to count on a warning, plastic failure. Due to the test set-up the anchorage was not loaded to failure.

The beam was designed so the anchorage was the weakest link. The failure mode of the anchorage was a 'yielding' of the anchorage, yielding of the embedded bolts and 'yielding' as a result of the embedded strength of the CFRP laminate. The test was cut off by a deviation of the anchorage of approx. 40 mm compared to the substrate.

This testing documents that it is possible to obtain a plastic failure (with warning) of an epoxy-bonded anchorage, bolted to the substrate. This means, that it is possible to harmonize a strengthening of a RC beam (or a RC slab) with epoxy-bolted multi directional laminates so that it is not necessary to use a high partial safety factor against a brittle failure (a speciality of the Danish Code of Practice) for the reason of a tension failure in the concrete or the CFRP laminate. A low safety factor may be used, when a ductile failure is decisive.

Epoxy bonded CFRP Laminate Anchored by Powder Actuated Nails. According to the evaluation the used method of design has been satisfactory in coordination with the observations made. The load-deflection diagram was monotonously increasing with the deflection until a

brittle failure took place (i.e. an unwarning failure).

This failure occured as a sliding failure of the concrete, following a plane just below the tips of the nails. It is the plan to consider if it is possible to obtain a plastic failure by other types of nails, another thickness of the CFRP laminate or combinations.

Epoxy-nailed CFRP laminates have their advantages in the mounting. Thus, it is justified to study if it is possible to obtain a 'plastic' failure.

5. BEAM TESTS

5.1 Test specimens

A test program consisting of 8 test beams of length 4.5 m was carried through by students, cf. *Olsen et al*. [8] under supervision of the authors. The beams had all the same dimensions and were reinforced by two rebars, 2 ∅16 mm as shown in Figure 5. Despite one beam all beams were also reinforced by an externally bonded multi directional CFRP plate 1×100 mm. The plate was in its full length glued to the beam by an epoxy adhesive and further fixed to the beam by a number of bolts, ∅10 in both ends. To secure that failure took place at end (A) two more bolts were added in end (B) than in end (A). The bolts in end (A) were placed in the laminate in accordance with the pattern shown in figure 2 starting next to the end of the laminate. The bolts were placed into holes ∅12 mm, drilled into the concrete and injected by an adhesive. A torque of 5 kNm tightened each nut. In the beam with 3 bolts the laminate was further fixed by a number of powder – actuated stainless nails, ∅3.7 mm.

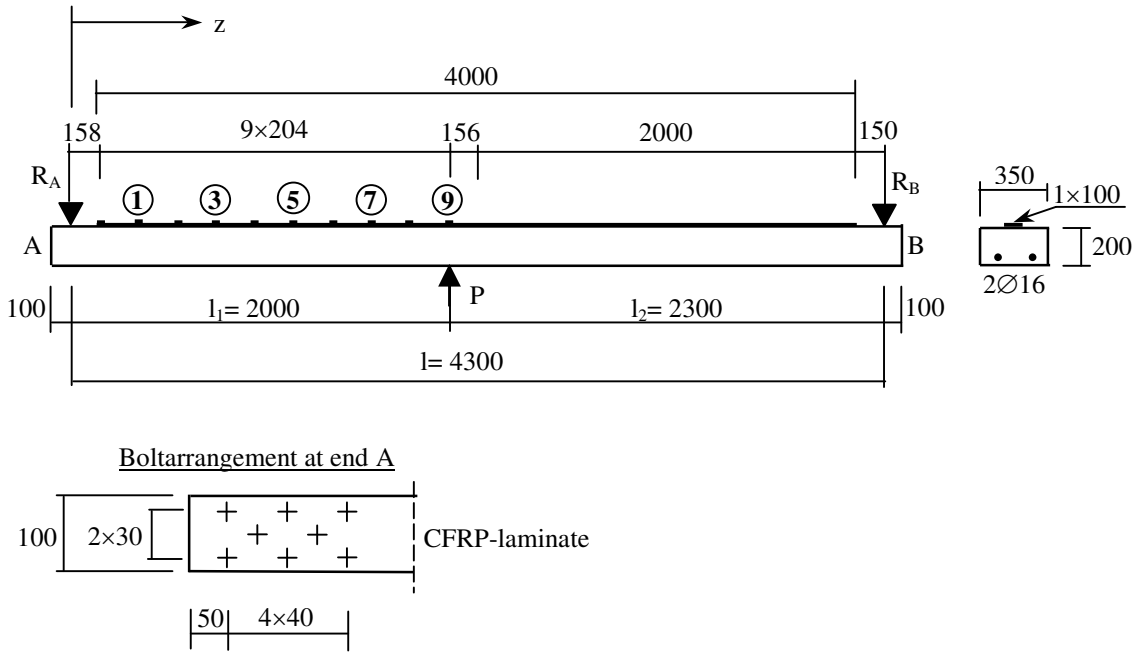

Figure 5 – Test specimen with placement of load P, CFRP-laminate and strain gauges shown. Bolts at end B(right end) are not shown.

The concrete had a compressive strength of 31 MPa. The beams were labelled no.x.x where the first digit designates the number of CFRP plates and the second digit the number of bolts at end

(A). A reference beam with no plate and no bolts is labelled no. 0.0 while the rest are labelled from no.1.0 to no.1.5 and no.1.8.

Figure 6 – Test set-up of the test beam.

5.2 Test set-up

The beams were tested in an Amsler beam test rig, cf. Figure 6. The beams were simply supported at both ends and loaded by a single force P displaced 150 mm from the middle of the beam towards end 'A' to promote failure to take place at this end. The beams were tested upside down with a load speed of 2 kN/min until debonding of the laminate and then with a speed of 1 kN/min.

The strains in the laminate were monitored by 10 strain gauges (Nos. 0 - 9) placed along the one halve part (A) of the beam, see figure 5. The deflections of the beam were monitored at both ends and at the mid-point besides at two more points in between. All tests were performed at room temperature.

5.3 Test results

The first beam to be tested was the beam with no external plate (no. 0.0). The beam behaved as expected, but the test was stopped unintentionally when yielding of the rebars started for a displacement of the mid-point of approximately 50 mm. All other beams were loaded until the deflection of the mid-point reached a value of approximately 100 mm.

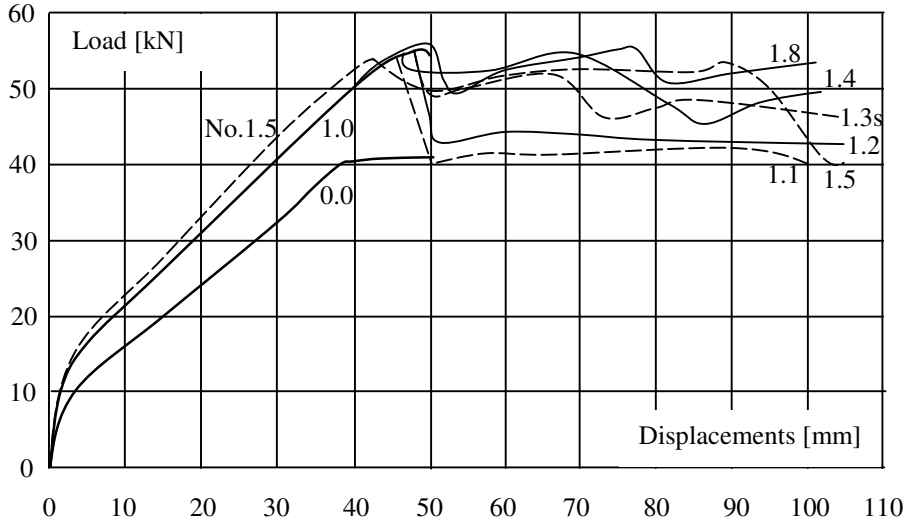

Figure 7 – Load-deflection diagrams for all test specimens.

All beams reinforced with a CFRP-laminate behaved in the same way independently of the number of bolts until debonding took place. Vertical cracks due to bending developed smoothly as expected for the increasing load the distance between two such consecutive cracks being about 70 mm in mean.

Debonding of the plates had the form of a crack in the concrete just below the plates starting from the middle of the beam and in all cases but one running towards the end 'A'. In the beam with no bolts (no. 1.0) the crack developed at a sudden with no warning while in beams with bolts at the ends debonding had a stable character in the very beginning.

In figure 7 deflections of the mid-point of the beam is shown as function of the load *P*. It is observed that:

- The maximum load is increased from 40.9 kN for the reference beam (no.0.0) to 54.7 kN for beam no.1.0 with one bonded plate and no bolts.
- The maximum load 54.7 kN is (almost) independent of the number of the bolts.
- After maximum load is reached and debonding takes place the load drops to a lower and more or less constant level depending of the number of bolts. The drop has a tendency to decrease with the increasing number of bolts.

Thus the multi directional CFRP laminate increases the maximum load on the beam with more than 30% while bolts placed at both ends of the plate have no effect. After debonding at maximum load bolts have a varying effect on the bearing capacity but the chosen bolt pattern is in all cases inadequate to keep the load at maximum level after debonding.

During loading strains along the mid axis of the plate were recorded with time intervals of 20 or 10 seconds. It turned out that even a 10 seconds interval was insufficient to catch all details of the strain distribution when debonding was about to take place at maximum load.

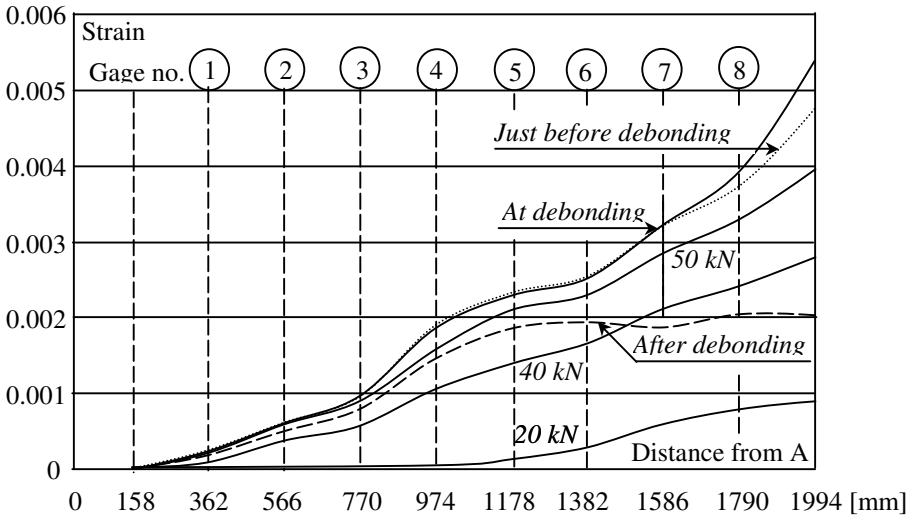

Figure 8 – Strain distribution in the plate at different load levels for beam no.1.5.

As a representative example the strain distribution for beam no.1.5 is shown in Figure 8 for different load levels. In this case the strains are recorded every 10 seconds. It is seen that independent of the load level the strains increase towards the centre of the beam as long as debonding has not started. It is further observed that the strain gradient changes along the beam and increases with the load over most parts of the beam. At debonding the strain gradient reaches its maximum next to the centre of the beam probably due to yielding of the rebars. After debonding the strains drop dramatically to an almost constant level over large parts of the beam. In several cases the plate debonds completely and is in such cases only fixed to the beam by the bolts, which carry same residual load.

In general the strain distribution before debonding is as expected. The almost linear strain distribution next to the end of the beam indicates a state with no bending-cracks in contrast to the central part of the beam where the increasing strain gradient indicates yielding of the rebars. In the transition zone between the two parts the strain gradient reaches an unaccountable level.

Since debonding is crucial for strengthening of any beam with a CFRP laminate it is of great importance to create a model that can handle the onset of debonding. A model based on fracture mechanics is proposed by *Neubauer et al*. [6], but it has a drawback with respect to simplicity.

In this study debonding always takes the form of a crack in the concrete why the reason is that the strength parameters of the concrete must govern the onset of debonding. Thus a working hypothesis might be as simple as a shear failure between the plate and the substrate and the model propose itself and takes the form illustrated in Figure 9.

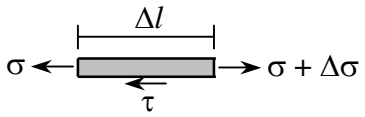

Figure 9 – Plate element of length Δl with stresses.

At two consecutive sections in the plate Δl apart, the normal stresses are σ and $\sigma + \Delta\sigma$ respectively. As long as debonding of the plate has not yet taken place the difference in the normal stresses is equilibrated by a shear stress τ along the bottom of the plate. For an even stress distribution equilibrium takes the form:

$$\Delta\sigma \times t \times b = \tau \times \Delta l \times b \tag{1}$$

or

$$\tau = t \times \frac{\Delta\sigma}{\Delta l} = t \times E \times \frac{\Delta\varepsilon}{\Delta l} \;\Rightarrow\; t \times E \times \frac{d\varepsilon}{dl} \quad \text{for } \Delta l \to 0 \tag{2}$$

where
- t is the thickness of the plate,
- b is the width of the plate,
- E is the modulus of elasticity for the laminate.

In Table 3 the maximum strain difference between two consecutive strain gauges for each beam at failure is given. It is observed that the maximum strain difference has a tendency to increase with the number of bolts with the beam without bolts as an exception. In average the strain difference $\Delta\varepsilon = 0.00130$ over a length $\Delta l = 204$ mm.

Table 3 – Maximum strain difference at failure

Beam no.	Gauge no.	Strain difference
1.0	6-7	0.00158
1.1	7-8	0.00069
1.2	7-8	0.00102
1.4	8-9	0.00110
1.5	8-9	0.00144
1.8	6-7	0.00197
Average		0.00130

Inserting into the formula above one finds that in average the maximum shear stress at debonding is:

$$\tau_{average} = 1 \times 175000 \times \frac{0.00130}{204} = 1.12 \text{ MPa} \tag{3}$$

The values of thickness t and the modulus of elasticity E are effective and minimum values respectively. The strain difference $\Delta\varepsilon$ over the length Δl represents the slope of the chord line, which is less than the maximum slope of the tangent, so for this reasons the calculated value of the average shear stress at debonding must be a minimum value, i.e. $\tau_{\text{average}} > 1.12$ MPa.

The shear strength of the concrete is difficult to access but if it is put equal to the tension strength one has according to the Danish code *DS 411:1999* [2]

$$\tau_{\max} = \sqrt{0.1\, f_c} = \sqrt{0.1 \times 31} = 1.76 \text{ MPa} \tag{4}$$

Even though there is a marked difference between the value of the average shear stress $\tau_{average}$ and the maximum shear stress τ_{max} they do not contradict each other and they are of the same order.

7. CONCLUSION

This study neither confirm nor discard the simple model proposed for the onset of debonding but show that more detailed studies are needed.

With respect to the hoped for plasticity-like behaviour of the beams after debonding the study demonstrates that a group of bolts at the ends of the plate has some effect but also that the beam soften and looses some carrying capacity after debonding. The study might indicate that a different placement of the bolts could influence the behaviour of the beam so for this reason further studies are also needed.

8. ACKNOWLEDGEMENT

The authors acknowledge the support by TRADECC, the Danish Prefab Assn., PL Beton, Spæncom, Condor Kemi, Condor Entreprise, HILTI, Germann Instruments, the staff of the laboratories of IABM and BYG·DTU at the Technical University of Denmark and the students involved.

REFERENCES

1. Poulsen. On the Anchorage of Uni Directional CFRP Laminates. *XVIII Symposium on Nordic Concrete Research.* Helsingør Denmark 2002.
2. DS 411:1999. Norm for betonkonstruktioner (Code of Practice for the structural use of concrete (in Danish but an English edition is available)). Dansk Standard. Ordrup Denmark.
3. Croes, Cuypers, Wastiels, de Roover & Vantomme. Study of Bolted Joints in Sandwich Elements With Cementious Composite Faces for Civil Applications. Composites in Constructions. Figueiras et al. Swets & Zeitinger. Lissabon Portugal 2001.
4. Turvey & Wang. Effects of temperature on the structural integraty of bolted joints in pultrusions. Composites in Constructions. Figueiras et al. Swets & Zeitinger. Lissabon Portugal 2001.
5. Beck & Jacobsen. Bolteforankring af kulfiberbånd (Anchorage of CFRP laminates by bolts (in Danish)). Bachelor Thesis, the Technical University of Denmark IABM. Copenhagen 2002.
6. Neubauer & Rostásy. Debonding mechanism and model for CFRP-plates as external reinforcement for concrete members. Composites in Constructions. Figueiras et al. Swets & Zeitinger. Lissabon Portugal 2001.
7. Neubauer. Verstärken von Betonbauteilen mit geklebte CFK-Lamellen Sika CarboDur - Einführung und Berechnungsbeispiele-. Fachseminar, Gladbeck 13 Juni 1997.
8. Olsen & Jørgensen. Forstærknning af betonplader med pålimet kulfiberbånd (Strengthening of concrete slabs by bonded CFRP laminates (in Danish)). *Bachelor Thesis, the Technical University of Denmark IABM*. Copenhagen 2003.

Replacement of Cement by Limestone Filler: The Effect on Strength and Chloride Migration in Cement Mortars.

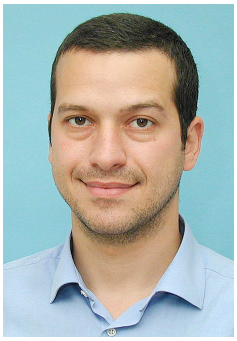

Dimitrios Boubitsas
M.Sc.Civ.Eng., Ph.D., Student
SP Swedish National Testing and Research Institute
Lund Institute of Technology
P.O. Box 118
SE-221 00 Lund
E-mail: dimitrios.boubitsas@byggtek.lth.se

ABSTRACT
This paper describes studies carried out to examine the effect on 28-day strength and chloride migration of cement mortar when a certain amount of the cement is replaced as binder by limestone filler. Fillers produced from three different calcareous carbonates were used, and three different mean particle sizes of the same type of filler were included in the study. The amount of replacement of cement with filler varied between 12 and 24 weightpct. of the total binder, and mortars with different water/binder-ratios were used.

Key words: chloride migration, efficiency, k-value, limestone filler, strength.

1. INTRODUCTION

Use of limestone filler in combination with Portland cement is common practice in many European countries, in the interest of technical, economical and ecological benefits.

The substitution of parts of the cement by limestone filler have shown to have several effects on the properties of paste, mortar and concrete. In studies of pure compounds of clinker, various authors have reported that the C_3S hydration rate is accelerated when the amount and fineness of $CaCO_3$ is increased [1]. Although limestone filler has no pozzolanic properties, several studies indicate that even non-hydraulic fillers enhance the hydration of the major cement phases at early ages [2, 3]. This is due to the fact that they generate a large number of nucleation sites for precipitation of the hydration products [1]. Calcium carbonate may also react with C_3A to form calcium carboaluminates [4].

The enhanced degree of hydration at an early age has also been reflected by the early age strength. It has been shown that the use of limestone filler as a replacement for cement may improve the strength of both mortars and concretes at early ages (3 and 7 days), but this improvement seems to be less pronounced or has completely disappeared at a later age (28 days) [5, 6].

Most of the research investigations have emphasised on the effect of limestone filler on the hydration reaction and strength development. There are, however, very few references describing the durability effects of limestone addition.

One of the major durability problems of concrete structures is the diffusion of chloride ions through the normal thicknesses of concrete cover causing corrosion of the reinforcing bars. The measuring technique used by most workers to study chloride penetration is the steady-state cell diffusion test, and the samples used are often thin specimens of paste. It is well known that penetration of chlorides is strongly affected by their chemical and physical interaction with the C-S-H phases in the hydrated cement paste. In a steady-state test, most of the interactions will be completed, and their effect on chloride transport will be reduced. During an unsteady-state experiment, these interactions take place and slow down the ion penetration.

In cell diffusion tests of thin mortar specimens, in which cement had been replaced by limestone filler but in which the W/C-ratio had been kept constant (i.e. a reduction of the bulk water), the chloride diffusion coefficient was found to be lower for blended mortars [7]. Cochet et. al. [8] found, also with cell diffusion tests, that the diffusion of chloride ions in mortars with blended cement was equivalent to that of mortars with Portland cement without mineral additions, provided that the cements considered are in the same strength grade.

In pounding tests, where the specimens were immersed in artificial sea water, Moukwa [9] has shown that the addition of limestone filler led to a much higher chloride penetration than in the reference mortar with only OPC.

The objective of the study described in this paper is to determine the coefficient of efficiency (k-value) for mortars with limestone filler addition, based on strength and chloride penetration. The coefficient of efficiency for mineral additions defines how many parts by weight of normal Portland cement that can be replaced by one part of a specified mineral addition without changing the concrete properties. Normally, the k-value is used only for EN 206-1 Type II additions [10], i.e. reactive additions such as most fly ashes, silica fume and vitrified blast furnace slags. In this paper, however, the k-value concept is used also for limestone filler in order to be able quantitatively to compare the efficiency of different types of qualities of limestone.

In most cases, the W/C-ratio is assumed to be the dominant factor defining the concrete properties; for example, when strength and permeability are concerned. When additions are used in concrete, the equivalent water/cement-ratio $(W/C)_{eq}$ is used instead of W/C. The equivalent water/cement-ratio is calculated by using the equation:

$$(W/C)_{eq} = W/(C+kR) \qquad (1a)$$

where:

W = water content by weight (kg/m^3)
C = cement content (kg/m^3)
R = content of addition (kg/m^3)
k = k-value.

The k-value is used for calculating $(W/C)_{eq}$ which in turn is used, among other things, for predicting the long-term performance of concrete structures in respect of strength, frost resistance, reinforcement corrosion and other durability properties. A problem is that almost all k-values given in regulations and standards are based on results from strength testing of 28-day-old concrete. These values are, therefore, probably not relevant for predicting the long-term performance and durability of concrete structures. More representative values can be obtained only from results derived from durability testing. This article presents such results for chloride

permeability (chloride migration), and compares them with k-values obtained from traditional compressive strength testing.

The project described in this paper is part of a larger program investigating the efficiency of fillers in concrete. Another part of the program deals with the influence of type I additions on early strength development under winter conditions. Results from that part of the program has previously been published in Nordic Concrete Research [11].

2. MATERIALS AND METHODS

2.1 Materials

The physical and chemical properties of the materials used throughout the experimental program, as given by the producers, are shown in Tables 1 and 2. The aggregate used was CEN standard sand in accordance with EN 196-1 [12], and the cement was a CEM I 52.5 R product conforming to ENV 197-1 [13].

The natural calcium carbonate types used as fillers in this investigation can be divided into chalk, limestone and marble. Chalk originates from the shells of fossil protozoans. It comes from the most recent geological deposits formed in the Cretaceous era, and has very fine crystals. Limestone is also of biogenic origin, but more compact than chalk. Its constituents are seashells and coral, which have been subjected to pressure and were formed in the Carboniferous era. The size of the crystals ranges between that of chalk and marble. Marble is formed when chalk or limestone recrystallise under high heat and pressure and form coarse crystals.

Fillers produced from three different qualities of natural calcium carbonate (CH, LL and MA) were used in this study, see Table 2. Type LL is a calcium carbonate powder manufactured from a high-purity white limestone from France, which were supplied in three different particle sizes (LL, LLF and LLC). Type MA is a white marble powder with high purity from Austria, while type CH filler is a Danish calcium carbonate powder from a more recent origin than the two others, and can be defined as a fine microcrystalline sedimentary chalk. The calcium carbonate content of all three limestone qualities was ≥ 98% by mass.

All materials were received in single bulk deliveries and stored in airtight containers to prevent deterioration with time.

Table 1 - Properties of the cement

Chemical composition	(%)	Mineralogical composition	(%)
CaO	64.1	C_3S	62.8
SiO_2	20.9	C_2S	12.4
Al_2O_3	3.8	C_3A	5.5
Fe_2O_3	2.7	C_4AF	8.3
SO_3	3.4		
MgO	2.8		
K_2O	1.1		
Na_2O	0.3		
Cl	0.02		

Table 2 - Physical characteristics of the cement and limestone fillers used

Material	Designation	Mean particle size (μm)	Specific Surface, BET (m^2/kg)
Cement	CEM	8	1760
Limestone (fine)	LLF	0,44	15000
Chalk	CH	2,3	2200
Limestone (medium)	LL	5,5	1000
Marble	MA	7,0	1500
Limestone (coarse)	LLC	22,0	700

Blaine fineness of the cement: 550 m^2/kg

2.2 Test program

Five different mortar mixtures were cast with Cement I 52.5 R as the only binder and a range of water/binder-ratios between 0.4 and 0.8. Another seven different mortar mixtures were cast where a part of the Cement was replaced with limestone filler (binder = cement + limestone). The mixture compositions are shown in Table 3.

The aim was to reach about the same consistency for all the mixtures, which was accomplished by keeping the water content fairly constant and altering the cement content. The consistency was measured in accordance with European Standard test method EN 1015-3 [14]. The mortars were produced in accordance with European standard EN 196-1 [12], with some modifications (see Table 3). The first modification was that, in some cases, the water/cement-ratio differed from EN 196-1, which specifies a constant 0.5 ratio. The second modification was that the mortar batches were much larger than in EN 196-1. The third modification was that, in those cases where the water/binder ratio was not 0.5, the proportions by mass in the mix differed from those given in the standard (one part of cement, three parts of standard sand and one half part of water).

The air contents are relatively high, as a result of the fine-grained aggregate and the high paste volume. The air content was measured in accordance with Swedish Standard SS 13 71 24 [15]. However, the variation between the different mixtures was small, with the air contents varying from 4.8% to 6.0%. This indicates that variations of the air contents between the mixes do not influence the test results very much.

Table 3 – Mortar mix proportions used in the experimental study

Mortar	W/B	W/C	Cement (kg/m^3)	Limestone filler (kg/m^3)	Water (kg/m^3)	Aggregate (kg/m^3)	Air (%)	Consistence (mm)
Cement								
OPC-0.4	0.40	0.40	702		281	1263		169
OPC-0.5	0.50	0.50	500		250	1500	4.9	170
OPC-0.6	0.60	0.60	413		248	1593		176
OPC-0.7	0.70	0.70	345		242	1666		168
OPC-0.8	0.80	0.80	319		255	1654		172
Cement and limestone filler								
LLF24-0.5	0.50	0.66	380	120	250	1500	4.8	135
CH24-0.5	0.50	0.66	380	120	250	1500	4.8	173
LL12-0.5	0.50	0.57	440	60	250	1500	5.0	175
LL24-0.5	0.50	0.66	380	120	250	1500	4,7	180
LL24-0.7	0.70	0.92	262	83	242	1666	5.4	164
MA24-0.5	0.50	0.66	380	120	250	1500	6.0	178
LLC24-0.5	0.50	0.66	380	120	250	1500	4.8	165

2.3 Determination of the k-value

The k-value for mineral additions can be calculated by using Equation (1a), which gives:

$$k = (W/(W/C)_{eq}-C)/R \quad (1b)$$

$(W/C)_{eq}$ can be calculated by using empirical relationships between the studied property (i.e. strength or chloride permeability) and W/C for OPC mixtures, and comparing this relationship with results obtained for mortars containing limestone filler: see Figure 1. By using the known values of C, R and W, and the value of $(W/C)_{eq}$, the k-value can be calculated using Equation (1b).

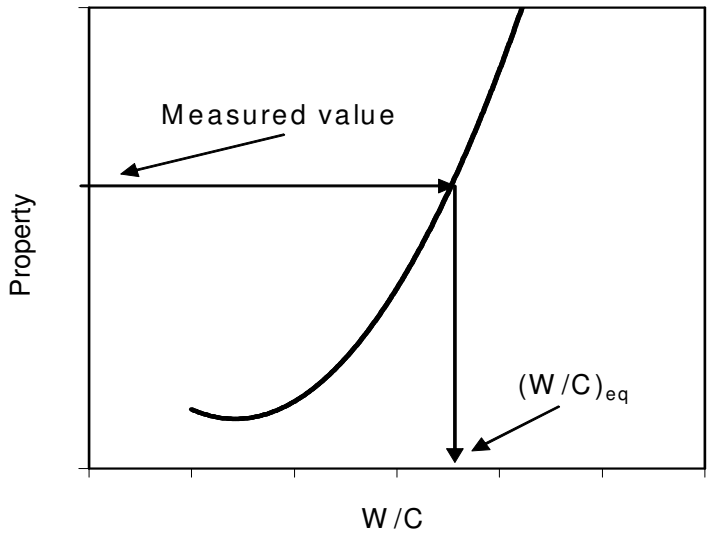

Figure 1- The relation between the w/c-ratio and a defined property (strength, migration coefficient, etc.) for Ordinary Portland Cement. This relation is used for determining the value of $(W/C)_{eq}$ for concrete and mortar containing mineral additions.

2.4 Strength test

Prismatic mortar specimens (40 mm x 40 mm x 160 mm) were cast and water-cured for 28 days. By the end of this period, the flexural and compressive strengths were determined in accordance with European Standard EN 196-1.

2.5 Chloride permeability test

This paper uses the migration coefficient for defining the chloride permeability properties. Migration is the movement of ions under the influence of an external electrical field, while diffusion is the movement of ions as the result of a concentration gradient. Normally, the value of the migration coefficient determined using this method is very similar to the diffusion coefficient. A detailed investigation of the relationship between migration and diffusion is presented in [16]. Chloride migration testing was performed in accordance with Nordtest Method NT BUILD 492 [17], which is a non-steady-state method. An external electrical potential was applied axially across the specimen and forced the chloride ions on the outside to migrate into the specimen. After a certain test duration, specified in the standard, the specimen was axially split and a silver nitrate solution was sprayed on to one of the freshly split sections. The chloride penetration depth can then be measured from the visible white silver chloride precipitation, after which the chloride migration coefficient can be calculated from this penetration depth as specified in the standard.

450 mm long cylinders with a diameter of 100 mm, were cast in steel moulds. After demoulding, the cylinders were stored under water until the time for testing at 28 days. Immediately before testing, 50 mm thick specimens were sawn from the cylinders, cutting off 50 mm at each end of the cylinders.

After sawing, any burrs were brushed and washed away from the surfaces of the specimens and excess water was wiped off. When the specimens were surface-dry they were placed in a dessiccator for vacuum treatment. The vacuum (1-5 kPa) was maintained for three hours and then, with the vacuum pump still running, the container was filled with saturated $Ca(OH)_2$ solution until the specimens were immersed. The vacuum was maintained for another hour before air was allowed to re-enter the container. The specimens were then kept in the solution for 18 ± 2 hours, after which testing started.

3. RESULTS

3.1 Compressive strength

The results from the compressive strength tests are summarized in Table 4. Each value is the mean result of six specimens. The table also shows the mean values for the k-value, calculated as described in Section 2.3.

Table 4 – Results from compression tests

Binder	W/B	Replacement	Compressive strength, f_c	Standard deviation, f_c	k-value	Standard deviation, k
		% by weight	(MPa)	(MPa)		
Cement						
OPC-0.4	0.40		82.4	1.9		
OPC-0.5	0.50		66.7	1.7		
OPC-0.6	0.60		48.5	1.5		
OPC-0.7	0.70		42.2	1.5		
OPC-0.8	0.80		33.2	1.3		
Cement and limestone filler						
LLF24-0.5	0.50	24	51.9	1.1	0.38	0.06
CH24-05	0.50	24	49.8	1.1	0.26	0.06
LL12-0.5	0.50	12	62.3	0.8	0.85	0.08
LL24-0.5	0.50	24	48.6	1.0	0.20	0.05
LL24-0.7	0.70	24	31.1	1.3	0.40	0.1
MA24-0.5	0.50	24	47.3	1.4	0.14	0.07
LLC24-0.5	0.50	24	49.9	1.0	0.27	0.04

The results from the compressive strength tests are also shown in Figure 2 for the mortars with Portland Cement as binder. There is a linear relationship, with good correlation, between compressive strength and 1/(W/C), i.e. Bolomey´s Formula [18]. This relationship is used in this investigation for determining the k-values for the mortars containing limestone filler.

Figure 3 shows the case where type LL limestone filler is used, and the only variation is the amount of replacement. It can be seen that the amount of replacement has a significant effect on the compressive strength. 12 % replacement gives a k-value of 0.85, while the corresponding value for 24 % replacement is 0.2. The same tendency was observed by Lundgren [11], although the effect was less pronounced. It seems, however, that there is a tendency for limestone filler content to have an effect; at least in the interval studied here. It should be observed that a limestone filler content of 24 % is very high. In practice, the content is normally below 20 %, and typical contents are 12-16 %.

However, most of the tests in this investigation have been performed with mortars containing 24 % limestone. This may have had a negative influence on the reported k-values, and one must be aware of this fact when the results are analysed.

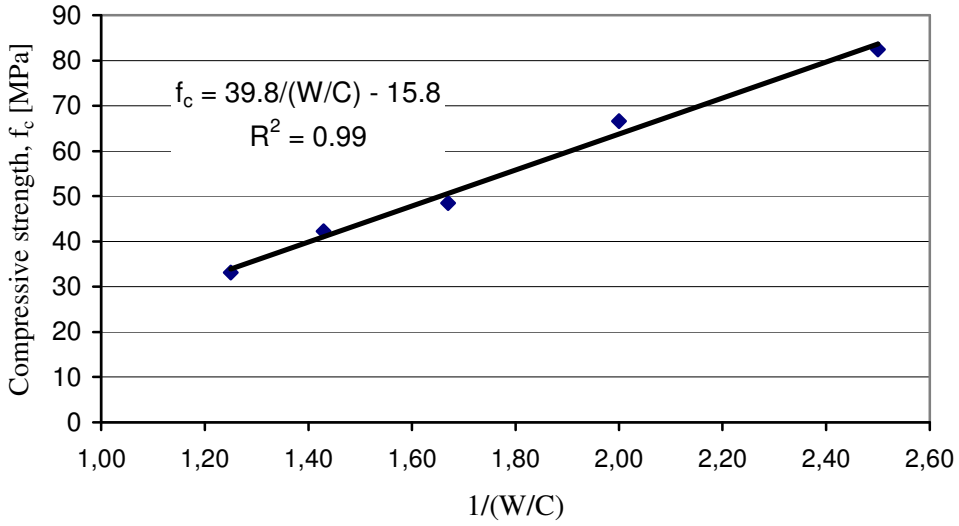

Figure 2 – The 28 days compressive strength, f_c as a function of 1/(W/C) for mortar with Portland Cement as binder.

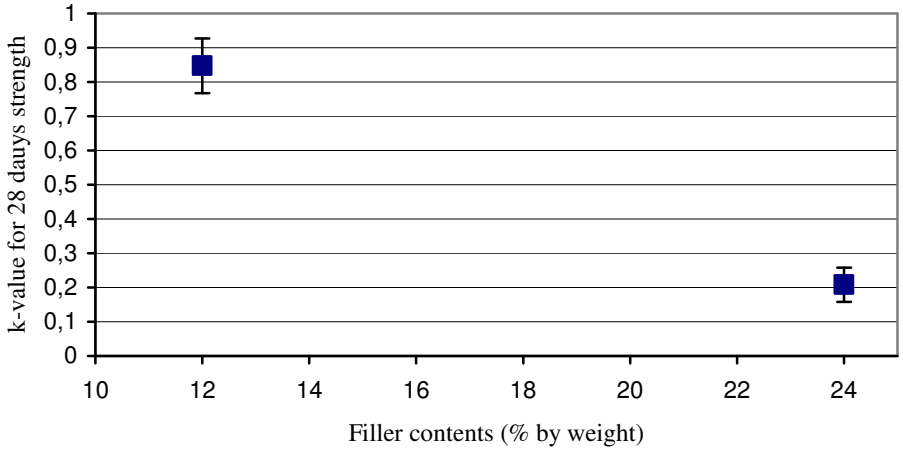

Figure 3 – The k-value for 28 days compressive strength versus the amount of cement substituted by limestone filler (% by weight of total binder). The results are relevant for mortars with W/B-ratios of 0.5, and for a filler quality of LL.

Figure 4 shows the compressive strength as a function of the mean particle size of type LL filler. The results do not indicate any tendency for the k-value to vary as a function of the fineness, except perhaps for the very fine fraction, which has a slight tendency to give a higher k-value. Regardless of the fineness of the filler, the k-values seem to be relatively small, between 0.2 and 0.4.

Similar results were reported by Lundgren [11] for tests performed after curing for seven days at 20 ºC. However, according to Lundgren, the influence of the fineness on the compressive strength is much greater for lower temperatures and shorter curing times.

Figure 5 shows compressive strength results for fillers produced from different types of calcareous carbonates. There is a very weak tendency for fillers produced from younger materials

with smaller crystals (chalk) to produce a slightly higher efficiency than fillers from older materials with larger crystals (marble). The tendency is very weak and cannot be regarded as significant if based on the results in this investigation.

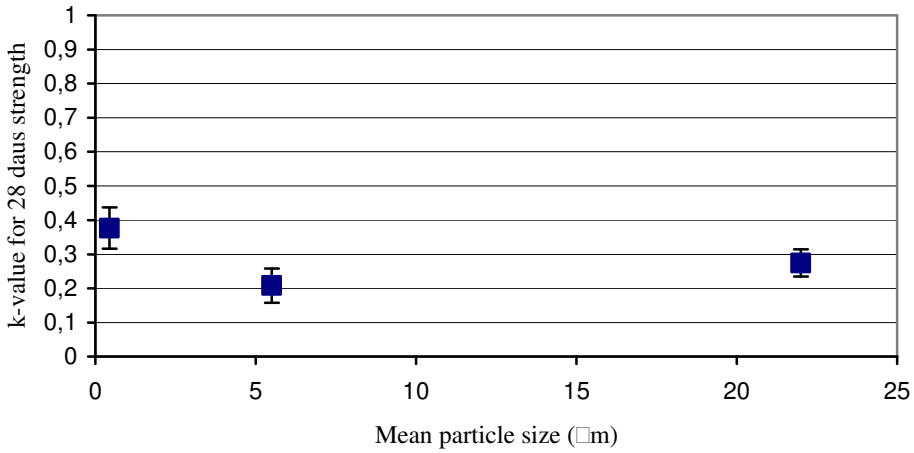

Figure 4 – The k-value for 28 days compressive strength, as a function of the mean particle size for type LL limestone filler. The results are relevant for mortars with W/C-ratios of 0.5.

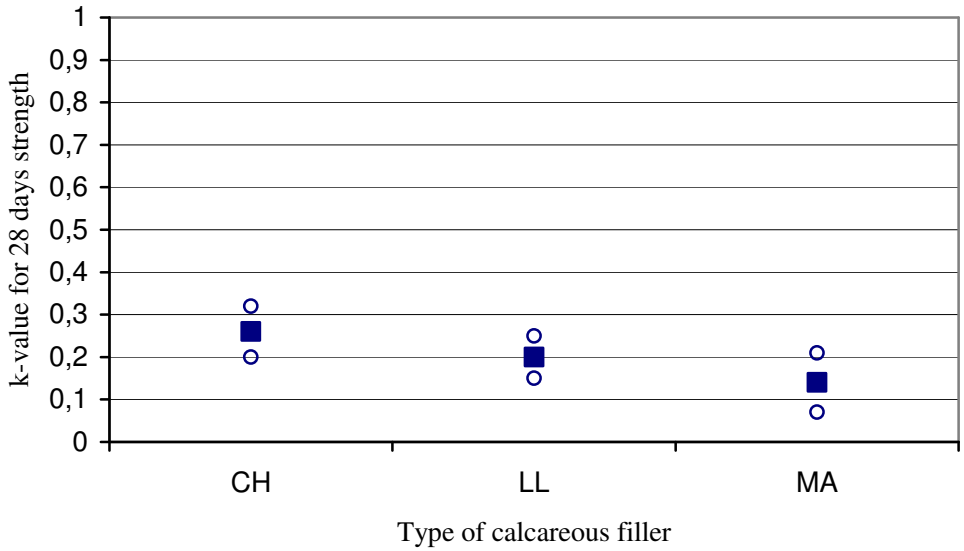

Figure 5 – The k-value for 28 days compressive strength plotted against the different calcium carbonate types. The results are relevant for mortars with W/C-ratios of 0.5.

3.2 Chloride migration

The results from the chloride migration tests are summarized in Table 5. Each value is the mean result of tests on three specimens. The table also shows the mean values for the coefficient of efficiency, together with the standard deviation.

Table 5 – Results from chloride migration test

Binder	W/B	Replacement (% by weight)	Migration coefficient, D_m ($*10^{-12}$ m^2/s)	Standard deviation, D_m ($*10^{-12}$ m^2/s)	k-value	Standard deviation, k
Cement						
OPC-0.4	0.40		8.3	0.6		
OPC-0.5	0.50		11.9	0.1		
OPC-0.6	0.60		15.4	0.9		
OPC-0.7	0.70		20.4	0.3		
OPC-0.8	0.80		24.2	0.6		
Cement and limestone filler						
LLF24-0.5	0.50	24	23.0	0.4	-0.47	0.03
CH24-0.5	0.50	24	24.5	1.2	-0.60	0.09
LL12-0.5	0.50	12	14.4	0.8	0.10	0.25
LL24-0.5	0.50	24	23.3	1.2	-0.49	0.10
LL24-0.7	0.70	24	38.5	0.2	-0.56	0.01
MA24-0.5	0.50	24	22.7	0.7	-0.44	0.06
LLC24-0.5	0.50	24	19.9	0.6	-0.17	0.06

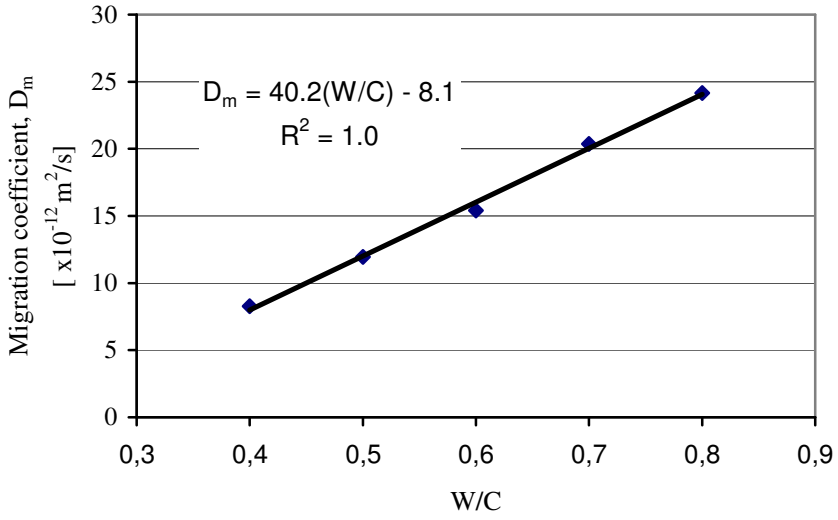

Figure 6 – Chloride migration coefficient as a function of W/C for mortars with ordinary Portland cement as binder.

The migration coefficient (D_m) for the mortars with Ordinary Portland Cement as the only binder are plotted in Figure 6 as function of the W/C-ratio. There is a linear relationship between D_m and W/C. This relationship is used in this investigation for determining the k-values in accordance with the method described in Section 2.3 for the mortars containing limestone filler.
Figure 7 shows the k-values for chloride migration for two different amounts of limestone filler in mortar. The scatter is relatively wide, but the tendency is the same as for compressive strength, i.e. the k-value is much higher for 12 % substitution than for 24 % substitution of the cement by

limestone filler. The values, however, are much lower for chloride migration than for compressive strength; 0.1 compared to 0.85 for 12 %, and -0.5 compared to 0.2 for 24 % replacement. This indicates that efficiency values based on strength tests are unusable for predicting chloride penetration for concrete qualities containing limestone filler.

It must be noted that the k-values for chloride migration obtained in this investigation are very low. The k-value for 12 % filler contents is 0.1, which means that the filler has almost no effect at all. This is not completely unexpected, as limestone fillers are normally assumed to be more or less chemically inert. On the other hand, the value for 24 % replacement is surprisingly low at -0.5. A negative value in fact means that the chloride permeability for 24 % replacement is higher than for a situation where 24 % of the cement is removed from the mortar without any replacement.

The results from the tests reported in this paper cannot explain the very low and negative k-values for higher limestone contents. Additional work is required.

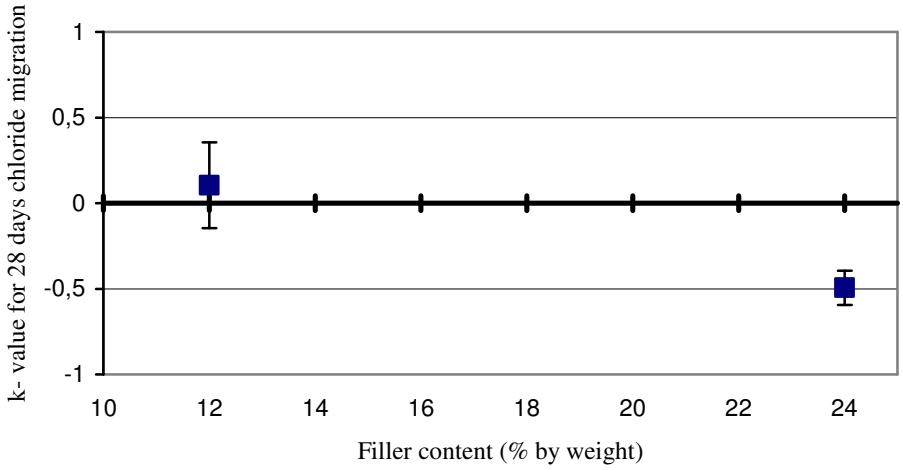

Figure 7 – Compressive strength versus the amount of filler (% by weight of total binder). The results are relevant for mortars with W/B-ratios of 0.5 with type LL filler quality.

Figure 8 shows the k-value for migration as a function of the mean particle size of type LL limestone filler. All the values are negative, with the highest value being observed for the coarsest filler (LLC). This contradicts the results for compressive strength, where there is a tendency for the finest filler to give the highest k-value.

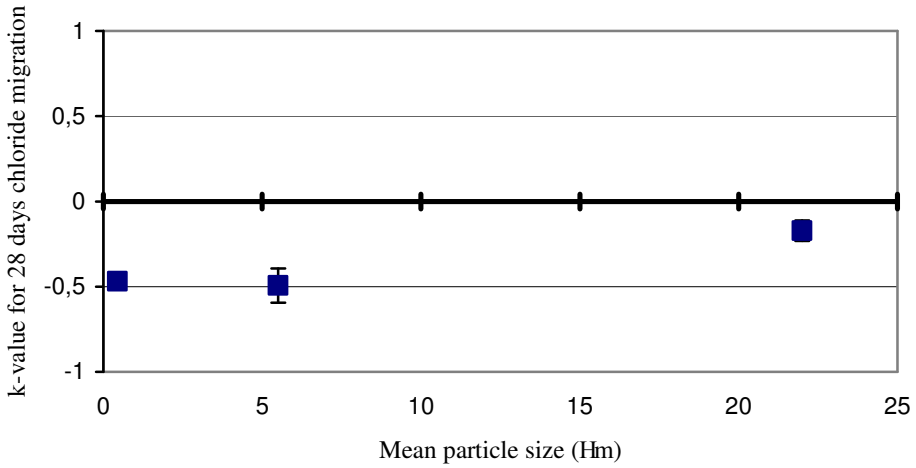

Figure 8 – k-values for the Chloride migration coefficient, as a function of the mean particle size of the limestone filler used in the mortars. The results are relevant for mortars with W/B-ratios of 0.5 and type LL filler.

Figure 9 shows the k-value for migration as function of the W/B-ratio. The values are similar, about -0.5, for the two ratios tested, W/B = 0.5 and W/B = 0.7.

Figure 10 shows the k-value for the migration coefficient for fillers produced from different calcareous carbonates. All the values are negative and there is a tendency for marble (MA) to have a slightly higher value and chalk (CH) to have a somewhat lower value. This contradicts the results from the strength tests, where CH gave the highest values and MA the lowest values. It must, however, be observed that the tendencies are weak, both in respect of migration and of strength.

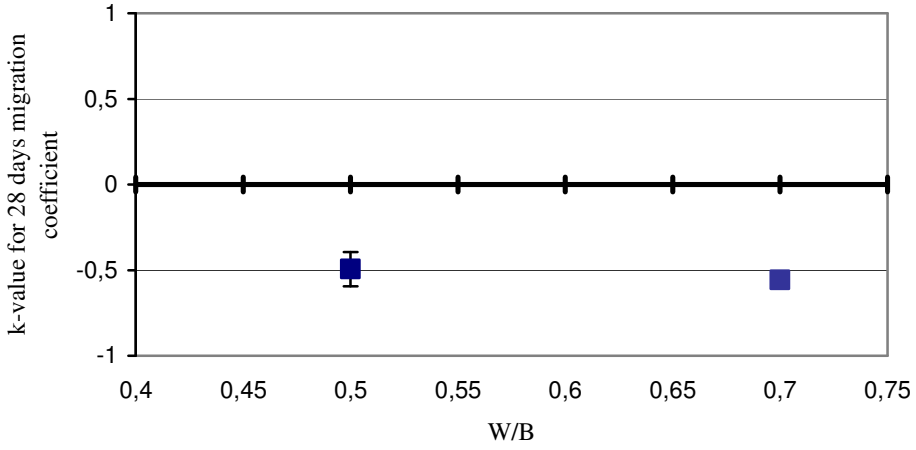

Figure 9 – The k-value for 28 days chloride migration coefficient, plotted against the water /binder ratio for the mortar mixes with type LL filler.

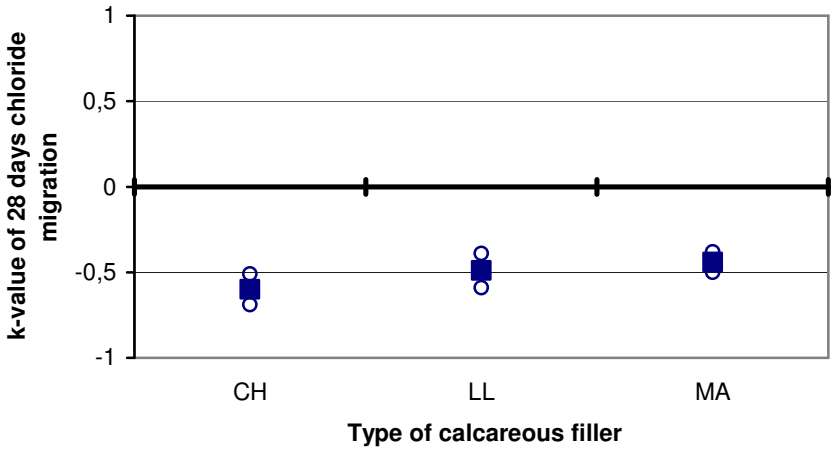

Figure 10 – The k-value for 28 days compressive strength, plotted against the different calcium carbonate types.

4 Conclusions

The results presented in this paper are relevant for the constituent materials used and where the limestone fillers are added to the mortar directly in the mixer. Other materials or other ways of using limestone fillers, such as a part of the cement, may lead to other results. It must also be emphasized that uncertainties can occur in the results, because in some cases the results are only based on a few measurement points.

Based on the test results presented in this paper, the following conclusions can be drawn:

- The efficiency of limestone filler as replacement for cement in mortar and concrete is higher for moderate replacements, 12 %, than for higher replacements, 24 %. This is relevant both for 28 days compressive strength and for chloride migration
- The k-values for 28 days compressive strength for the limestone fillers used in this investigation are in the interval 0.2 to 0.9, while the corresponding interval for chloride migration is -0.6 to 0.1. This means that the efficiency for compressive strength, when expressed (for example) as a k-value, cannot be used for estimating the efficiency as far as chloride migration is concerned. It is reasonable to believe that the k-value for the limestone filler, as well as for other additions, is unique also for other material properties of mortar and concrete.
- The mean particle size of limestone filler has little effect on the k-value. There is a tendency, as far as 28 days compressive strength is concerned, for the filler with the finest mean particle size (0.44 μm) to be slightly more efficient than the coarser fillers. The opposite, however, is the case for chloride migration, for which the coarsest filler is the most efficient (or, in other words, has the least negative effect on the migration properties).
- There is a slight tendency for fillers produced from older calcareous carbonates with large crystals (marble) to be less efficient where 28 days strength is concerned than is the case when the filler has been produced from younger materials with finer crystals (chalk). However, the situation seems to be the opposite for chloride migration, i.e. marble is slightly more efficient than chalk.

REFERENCES

1. RAMACHANDRAN, V.S. and CHUN-MEI, Z., "Dependence of Fineness of Calcium Carbonate on the Hydration behavior of Tricalcium Silicate," *Durability of Building Materials*, Vol. 4, 1986, pp. 45-66.
2. Husson, S., Gullhot, B., and Pera, J. "Influence of Different Filler on the Hydration of C_3S," Proceedings, 9th International Congress on the Chemistry of Cement. India 1992,vol. IV. pp. 83-89.
3. Walter.A.Gutteridge and Dalziel, J.A., "Filler Cement: the effect of the Secondary Component on the Hydration of Portland Cement," *Cement and Concrete Research*, Vol. 20, 1990, pp. 778-782.
4. Bonavetti, V.L., Rahhal, V.F., and Irassar, E.F., "Studies on the Carboaluminate formation in Limestone Filler-Blended Cements," *Cement and Concrete Research*, Vol. 31, 2001, pp. 853-859.
5. Bonavetti, V.L., et al., "Limestone Filler Cement in Low W/C Concrete: A rational use of energy," *Cement and Concrete Research*, Vol. 33, 2003, pp. 865-871.
6. Soroka, I. and Stern, N., "Calcareous Fillers and the Compressive Strength of Portland Cement," *Cement and Concrete Research*, Vol. 6, 1976, pp. 367-376.
7. Hornain, H., et al., "Diffusion of Chloride Ions in Limestone Filler Blended Cement Paste and Mortars," *Cement and Concrete Research*, Vol. 25, 1995, pp. 1667-1678.
8. Cochet, G. and Jesus, B., "Diffusion of Chloride Ions in Portland Cement-Filler Mortars," Proceedings, Blended Cements in Construction, Sheffield,UK 1991. pp. 365-375.
9. Moukwa, M., "Penetration of Chloride Ions from Sea Water into Mortar under Different Exposure Conditions," *Cement and Concrete Research*, Vol. 19, 1989, pp. 894-904.
10. EN206-1, Concrete-Part 1: Specification, performance, production and conformity. *European standard,* 2000.
11. Lundgren, M., "Limestone Filler as Addition in Cement Mortars: Influence on Early-Age Strength Development at Low Temperature." *Nordic Concrete Research*, no.31, 2004, pp 50-63.
12. EN 196-1, Methods for testing cement-Part 1: Determination of strength, *European standard,* 1994.
13. EN 197-1, Cement-Part 1: Composition, specification and conformity criteria for common cements. *European standard,* 2000.
14. EN 1015-3, Methods of test for mortar for masonry- Part 3: Determination of consistency of fresh mortar (by flow table).
15. SS 13 71 24, Concrete testing-Fresh concrete-Air content (pressure method), Swedish standard, 1989.
16 Luping, T., "Evaluation of the rapid test method for measuring the chloride diffusion coefficients of concrete." SP Report 1998:42, SP Swedish National Testing and Research Institute, 1998.
17 NT BUILD 492, "Concrete, Mortar, and Cement-based Repair Materials: Chloride Migration Coefficient from Non-steady-state Migration Experiments." *Nordtest methods,* 1999.
18. Bolomey, J., "Deterermination de la resistance a la compression des mortiers et betons". Bulletin technique de la Suisse romande, 1925.

Relaxation of prestressing steel – Comparison between virgin strands and strands exposed to long-term loading

Thomas Roth
M.Sc., Tekn. Lic.
Royal Institute of Technology
Dept. of Civil & Architectural Engineering
SE-100 44 Stockholm, Sweden
E-mail: Thomas.roth@byv.kth.se

Johan Silfwerbrand
Professor
Royal Institute of Technology
Dept. of Civil & Architectural Engineering
President
Swedish Cement and Concrete Institute
SE-100 44 Stockholm, Sweden
E-mail: Johan.Silfwerbrand@cbi.se

ABSTRACT

The prestressing force in concrete structures is successively reduced by steel relaxation, concrete shrinkage, and concrete creep. A temperature increase from 20 to 40°C may double the relaxation. In nuclear reactor containments, the temperature is often considerably above 25°C. However long term measuring series indicate, that the losses are less dramatic than anticipated. In order to investigate how long-term exposure to real conditions influence strength and relaxation properties, 7 thirty years old wires from Forsmark nuclear power plant were tested in the laboratory and compared with 7 virgin wires of similar type. The test results indicate that the strength is slightly reduced due to the long term exposure. For new wires, a relaxation of 2 % was determined after 5 days at 22°C and 4 % at 55°C. The old wires were, however, resistant to renewed loading and did not show any noticeable relaxation. This means that it is likely that the prestressing forces at Forsmark will not be reduced further if the temperature during a limited time would be increased to 55°C.

Key words: concrete structures, prestressing steel, reactor containment, tensile force loss.

1. INTRODUCTION

The prestressing force in concrete structures like prestressed bridges and nuclear power reactor containments is successively reduced due to relaxation of the steel and shrinkage and creep of the concrete. These force losses have to be considered in design. According to the Swedish concrete handbook BBK 94 [1], the relaxation is estimated as 12 % after 50 years and at least 15 % after 100 years providing the average temperature is a maximum of 25°C. The relaxation is increased at elevated temperatures and at increased stress ratios (defined as the ratio between stress and strength). A temperature increase from 20 to 40° may lead to twice as high relaxation values (Figure 1, [2]).

For Swedish reactor containments, this temperature influence may cause a problem since the temperature often exceeds 25°C. However, long measuring series of prestress losses in Swedish nuclear reactor containments indicate that the temperature influence may be exaggerated. Consequently, this urgently requires investigation, both through continuation of the measuring series and by testing prestressing wires in the laboratory. Two questions that may be raised are: (i) how does the real environment with varying temperature during 30 years influence the strength and (ii) how does it influence the relaxation properties for renewed loading at room and elevated temperature?

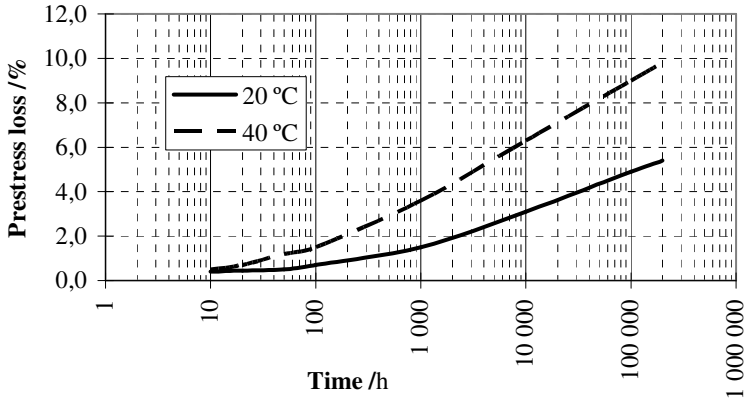

Figure 1 – Difference in steel relaxation between room and elevated temperature. From Petersson & Sundquist [2].

2. AIM

The current tests aim at answering the two questions in the previous chapter, i.e., determine the strength and relaxation properties of prestressing strands taken from a nuclear reactor containment and compare these results with tests on virgin strands of similar type.

3. TEST METHODS

The test methods used for determining tensile strength and relaxation of prestressing steel followed, as far as possible, the standard SS-EN ISO 15630-3:2002 [3], section 5 and 8, respectively.

3.1 Test specimens

The test specimens were from two different origins: (i) new prestressing strands and (ii) prestressing strands taken from Forsmark nuclear power plant, which have carried service loads for more than 30 years. The service load equalled approximately 70 % of the ultimate load and the average temperature was approximately 45°C. The strands were taken from horizontal cable No. 55a. The prestressing cables at Forsmark consist of 19 strands Φ 13 mm according to the Swedish Standard then in force, i.e., SIS 21 36 20 of SIS steel 1757-08 [4]. The strand consists in turn of seven wires with a diameter Φ = 4.4 mm. The cables were manufactured by Bridon Wire Limited in 1975 or 1976. The new strands were made of the same steel quality. The test specimens taken were the straight central wire of the prestressing strands.

The number of test specimens was computed by multiplying the number of origins, the number of temperature conditions, and the number of tests at each combination according to the following:

Number of origins: $n_1 = 2$ (old, new)
Number of temperature conditions: $n_2 = 2$ (room temperature, elevated temperature)
Number of tests for determining tensile strength: $n_3 = 3$.
Number of tests for determining relaxation: $n_4 = 2$.
Number of test specimens: $N = n_1 \times n_3 + n_1 \times n_2 \times n_4 = 2 \times 3 + 2 \times 2 \times 2 = 6 + 8 = 14$.

3.2 Test setup – tensile strength

For determining tensile strength the MTS universal testing machine placed in the laboratory hall of The Swedish Cement and Concrete Research Institute (CBI) was used.

3.3 Test setup – relaxation

For determining relaxation the MTS machine was reused (Figure 2). Two wires were placed after each other in a series. The load will be the same, but this setup enables testing two wires at each test in order to save time and money. The wires were provided with gages in order to register the length difference over a measuring length of L_0. ISO 1560-3:2002, section 8, states that $L_0 \geq 200$ mm, preferably $L_0 = 1000$ mm. Here, $L_0 = 400$ mm was used.

In order to keep a constant temperature around the test specimens, an insulating cover was constructed outside the testing machine. At room temperature (+20°C), a cling film was used to prevent temperature drops due to opening of the laboratory doors. At elevated temperature (+55°C), an insulating box was constructed to keep a constant temperature.

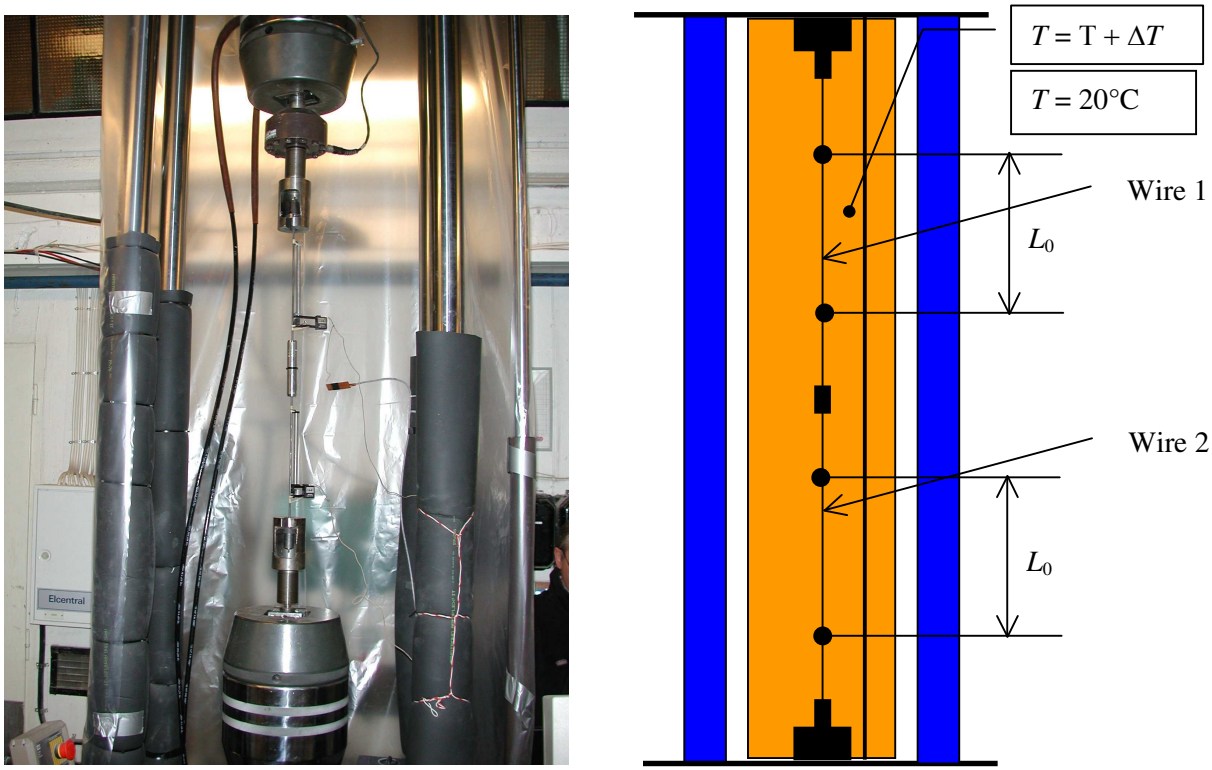

Figure 2 – Test setup at relaxation test under room temperature.

3.4 Method description

a) Three previously unloaded and three wires from Forsmark were loaded to failure in order to determine the tensile strength according to ISO 15630-3:2002, section 5. The average value $F_{m,m}$ for both the types was calculated.

b) Two previously unloaded and two wires from Forsmark were tested in the testing MTS machine by applying a tensile force $F = 0{,}7 \times F_{m,m}$ to the wire mainly according to ISO 1560-3:2002, section 8. The wires were placed after each other in a series and the load would thus be equally high in both wires. The loading up to F was soft and continuous following the scheme in the standard. The deformation ΔL_0 over a measuring length of L_0 = 400 mm was measured. The load should subsequently be constant with a variation $\Delta F/F$ less than 0.005 ‰ and the difference between two consecutive measurements should not exceed 0,050 ‰. The temperature should be kept constant at T = 20°C. The load should continue during 120 hours (5 days). Load, deformation and temperature were measured. Measurements should be done after 1, 2, 4, 8, 15, 30 and 60 minutes, after 2, 4, 6, 24 hours, and after 2, 3, 4 and 5 days.

c) Item b) was repeated twice for another four wires but at the elevated temperature $T = T + \Delta T$ = 55°C.

d) The eight wires loaded in items b) and c) were finally loaded to failure to determine their tensile strength according to item a).

3.5 Summary of the extent of the measurements

Tensile strength tests on 14 wires. Relaxation tests with 4×2 wires during 5 days totalling 20 days or four weeks.

3.6 Deviation from standard

The largest deviation between standard and testing concerns the type of loading under the relaxation tests. Here, a constant load was used instead of a constant deformation. The reason was a need of simplicity. The relaxation X may, however, be estimated through the measured creep ratio ϕ according to the following relationship:

$$X = 1 - \frac{1}{1+\phi} \approx \phi \tag{1}$$

Where, the creep ratio $\phi(t)$ is measured as

$$\phi(t) = 1 - \frac{\varepsilon(t)}{\varepsilon_0} = 1 - \frac{\Delta L(t)}{\Delta L_0} \tag{2}$$

Where, ΔL_0 and $\Delta L(t)$ is instant length change and length change at time t, respectively.

In a laboratory hall used not solely for the current test, it is always difficult to keep a constant temperature, since the laboratory doors have to be opened letting in outdoor air. The room temperature was about +22°C, i.e., somewhat higher than the intended value. During the testing time of five days the temperature variation was limited to 2 degrees with the exception of a few short periods (Figure 3). During the relaxation tests with elevated temperature, the temperature variation was also limited to 2 degrees with an average close to the intended +55°C.

During performance of the standard test method, the load should not vary more than ±20 ‰ (for load $F > 1000$ kN, here the load was $F \approx 1400$ kN). In the tests performed at room temperature the load variation was 40 and 50 ‰ for the new and old wire, respectively (Figure 4). The load control was considerably improved in the tests at elevated temperature and the load variation was limited to 2.5 ‰. Consequently, the load variation demand was fulfilled for the tests performed at elevated temperature, but not for the tests at room temperature.

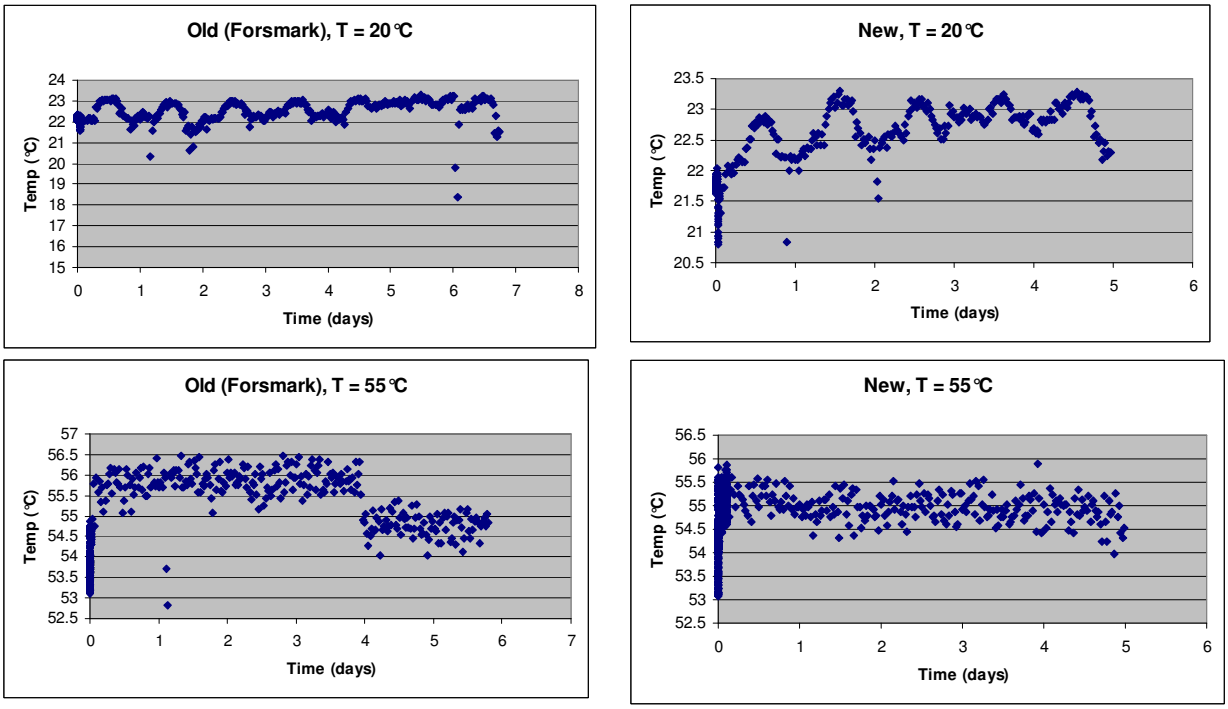

Figure 3 – Measured temperature variations during the relaxation tests.

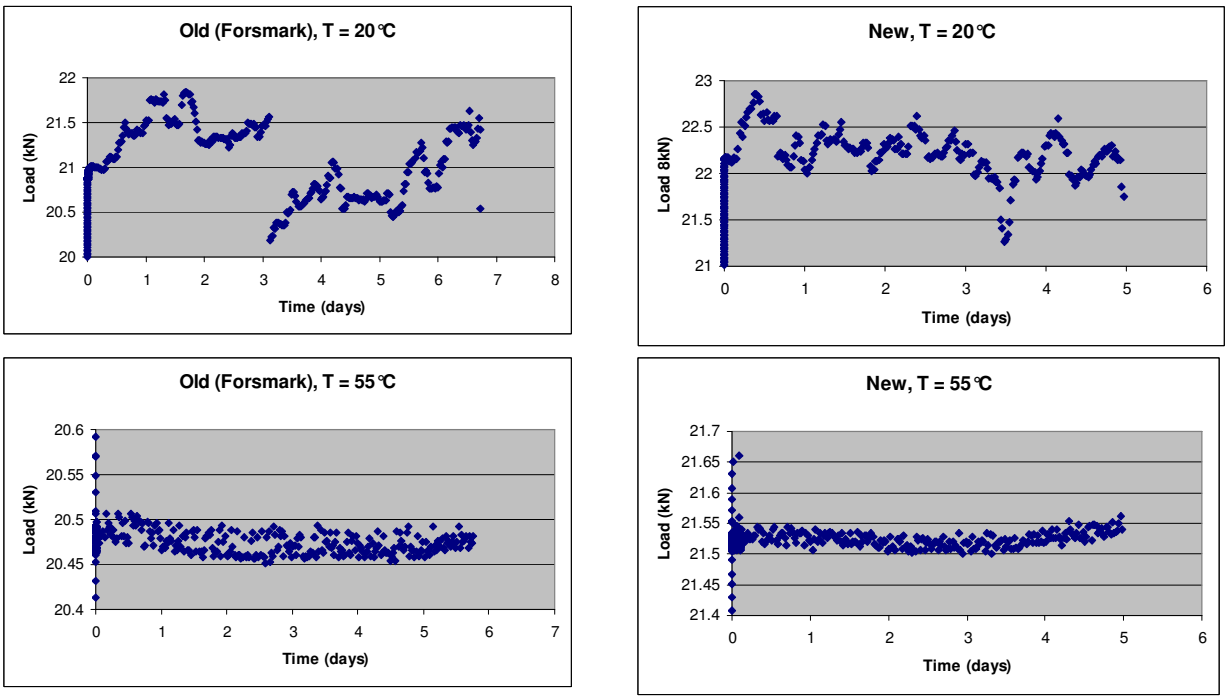

Figure 4 – Measured load variations during the relaxation tests.

4. TEST RESULTS

4.1 Tests on tensile strength

The results of the tensile strength tests are summarized in Table 1. The table covers both new wires and old wires previously exposed to loading during 30 years in Forsmark. Besides the

tests to determine tensile strength of the two categories, tensile tests were also performed on the wires after the relaxation tests.

The average ultimate strength was 1950 MPa for the old wires and about 2000 MPa for the new ones. After exposure to relaxation tests, the measured tensile strength was somewhat reduced. The strength drop was, however, hardly larger than the scatter (cf. obtained standard deviation of 0.3 to 1.1 % with obtained strength drops between 0.1 and 1.3 %). Neither the 70 % load level nor the elevated temperature seems to have any detrimental impact on the strength of the prestressing wires. This statement is valid both for the new and the old ones.

Table 1 – Tests on tensile strength

Origin of test specimen	Test specimen No.	Relaxation tested?	Average diameter (mm)	Ultimate force (kN)	Ultimate tensile strength (MPa)		Strength drop* (%)
					Single value	Average [Std dev (%)]	
Forsmark	1	No	4.379	29.08	1931	1948	
	2	No	4.378	29.23	1942	[1.08]	
	3	No	4.377	29.67	1972		
	4	Yes (22°C)	4.379	28.85	1915	1923	1.30
	5	Yes (22°C)	4.378	29.06	1930		
	6	Yes (55°C)	4.377	28.94	1923	1946	0.13
	7	Yes (55°C)	4.376	29.60	1968		
New	1	No	4.415	30.74	2008	2013	
	2	No	4.412	30.88	2020	[0.30]	
	3	No	4.412	30.76	2012		
	4	Yes (22°C)	4.414	30.52	1995	2001	0.62
	5	Yes (22°C)	4.415	30.73	2007		
	8	Yes (55°C)	4.413	30.35	1984	1994	0.96
	9	Yes (55°C)	4.412	30.64	2004		

*Strength drop is defined as the relative difference expressed in percent between the average ultimate tensile strengths of a test series subjected to a relaxation test and the series that is not subjected to relaxation.

4.2 Relaxation tests

The strain development of the wires exposed to sustained loading was measured continuously. Figure 5 shows the development of strain during two of the tests. There is only a minor strain increase during the 5 days testing time.

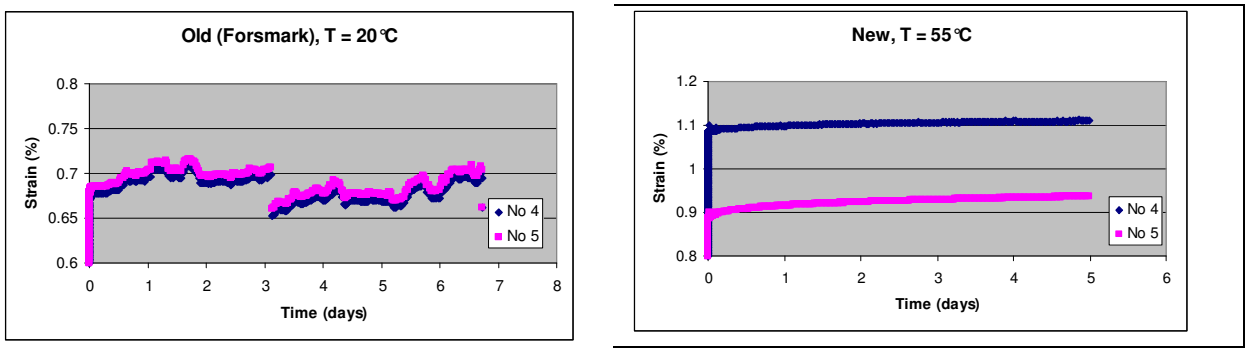

Figure 5 – Strain development for two relaxation tests.

Determination of the creep ratio had to be compensated because load was not constant and since the creep was fairly low during the limited testing time (5 days). The method used utilizes the

fictitious modulus of elasticity E^* defined as $E^* = E/(1 + \phi)$, where E is the modulus of elasticity and ϕ is the creep ratio. Using Hooke's law between stress and strain, we know that $\varepsilon(0) = \sigma(0)/E$. If σ is $\sigma(0)$ = constant, we obtain $\varepsilon(t) = \sigma(0)/E^*$. This may be approximately correct even if σ varies slightly around a certain mean value. Consequently, $E^* = \sigma/\varepsilon(t)$. If the load F varies slightly, both σ and ε will vary simultaneously without substantially affecting the creep. We may write $\sigma(t) = F(t)/A$ and $\varepsilon_{el}(t) = F(t)/EA$, where A is the area of the cross section of the wire and $\varepsilon_{el}(t)$ is the elastic part of the strain. The total strain is the sum of the elastic strain and the creep strain, i.e., $\varepsilon(t) = \varepsilon_{el}(t) + \varepsilon_{cr}(t)$. During short time loading, $\varepsilon_{el}(t) >> \varepsilon_{cr}(t)$. We may now be able to determine a value of the creep ratio ϕ minimizing the influence of a varying load by the following equations:

$$\phi(t) = \frac{E}{E^*(t)} - 1 = \frac{\dfrac{\sigma(0)}{\varepsilon(0)}}{\dfrac{\sigma(0)}{\varepsilon_{el}(t) + \varepsilon_{cr}(t)}} - 1 \approx \frac{\dfrac{\sigma(0)}{\varepsilon(0)}}{\dfrac{\sigma(t)}{\varepsilon_{el}(t) + \varepsilon_{cr}(t)}} - 1 = \frac{\dfrac{P(0)/A}{\varepsilon(0)}}{\dfrac{P(t)/A}{\varepsilon_{el}(t) \cdot \left(1 + \dfrac{\varepsilon_{cr}(t)}{\varepsilon_{el}(t)}\right)}} - 1 \approx \tag{3}$$

$$\approx \frac{\dfrac{P(0)}{\varepsilon(0)}}{\dfrac{P(t)}{\varepsilon(t)}} - 1$$

Since $\varepsilon_{cr}(t)/\varepsilon_{el}(t) << 1$. The benefit is that the influence of the load variation can be minimized since the equation contains the quota $P(t)/\varepsilon_{el}(t)$ = constant.

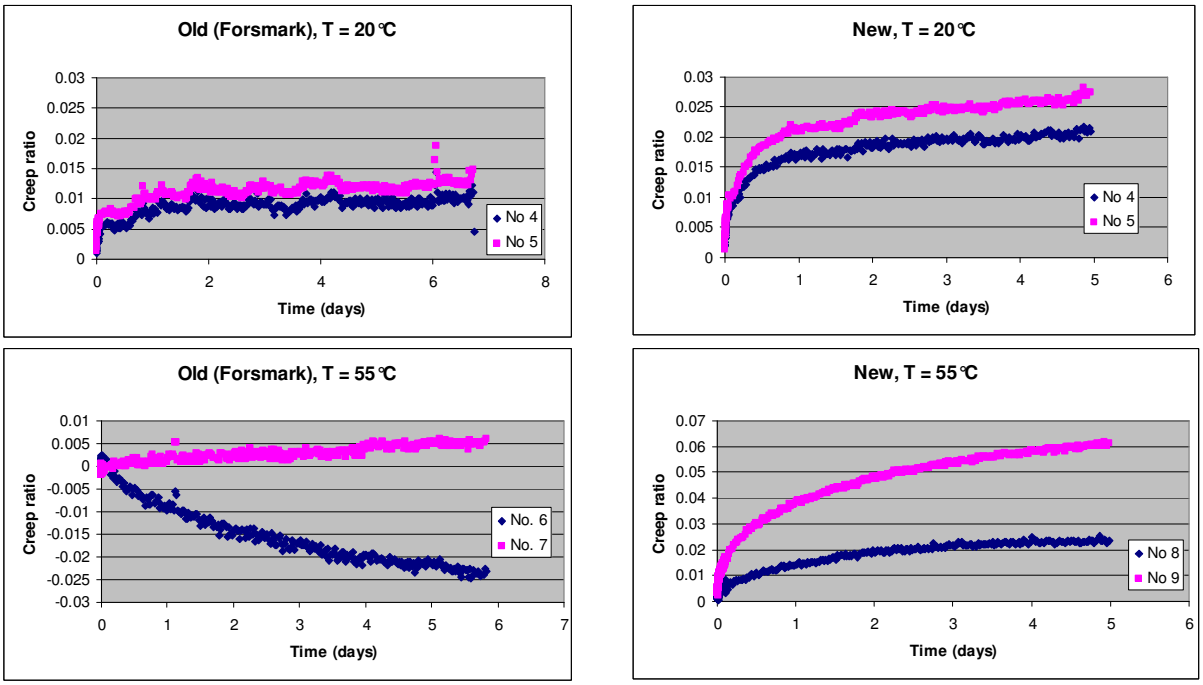

Figure 6 – Measured creep coefficient for the four relaxation tests.

The test results contain several interesting facts, Figure 6. First, the previous observation that the temperature has an important impact on the relaxation is supported. A temperature increase from

22°C to 55°C leads to a doubled relaxation, from 2 to 2.5 % after 5 days to 4 % or slightly more. These results agree with the results presented by Petersson & Sundquist [2] (Figure 1) even if these new values are higher. The second observation concerns the relaxation of the old wires previously exposed to loading during 30 years. Here, it can be seen that the relaxation is much lower than the relaxation of the new wires or even negligible. At normal temperature, the measured relaxation is limited to 1 %. At an elevated temperature, the measured relaxation is less than 0.5 %. On one of the wires, a negative creep was measured. Theoretically, it means that the strain has diminished during the testing time. This is, of course, not physically possible; as such materials do not exist. However, the measured values are very small and the unexpected results are likely to be devoted to measuring errors. However, no measuring errors could be observed during the test. The practical conclusion from the tests is that prestressing strands that have carried load during a long time are likely to withstand a sudden force or temperature increase without developing any substantial relaxation.

5. CONCLUDING REMARKS

Tensile and relaxation tests have been carried out to investigate if strength and relaxation properties of prestressing strands change with time. From the tests, the following conclusions can be drawn:

- The ultimate strength of the 30 year old wires was 2.5 % lower than the strength of new ones of similar type. It has not been possible to discern whether this small difference is due to a minor deterioration or to natural scatter.
- Exposure to elevated temperature and load levels equal to 70 % of the ultimate load during 5 days does not impair the tensile strength of the wires. The obtained strength decrease was less or equal to 1 %.
- The relaxation of new wires is doubled if the temperature is increased from 22 to 55°. During the testing time of 5 days, relaxation values equal to 2 and 4 %, respectively, were obtained. The results are in consistence with previous research.
- The relaxation of wires previously exposed to loading during more than 30 years in a nuclear power plant was limited to 1 % or negligible both at room and elevated temperature.
- The final conclusion is that the prestressing strands used in a typical Swedish nuclear power plant have practically the same strength as at the time of installation and that the prestressing forces will not be reduced further if the temperature during a limited time would be increased to 55°C.

ACKNOWLEDGEMENT

Financial support from KTH and The Swedish Nuclear Power Inspectorate is gratefully acknowledged. The authors wish to thank Mr. Stefan Trillkott and Mr. Claes Kullberg of the Structural Engineering Laboratory, KTH, for carrying out the laboratory tests.

REFERENCES

1. BBK 94. "Boverkets handbok om betongkonstruktioner. Band 1 - Konstruktion" (”Swedish Concrete Handbook. Part 1 – Structural Design”). The National Board of Housing, Building and Planning and AB Svensk Byggtjänst, Karlskrona and Solna, respectively, 1994, 185 pp. (In Swedish).
2. Petersson T & Sundquist H. “Spännbetong” (”Prestressed Concrete”). Compendium in Concrete Structures and Structural Design and Bridges. *Report* No. 46, 2nd Edition, Department of Structural Engineering, KTH, Stockholm, 1999, 212 pp. (In Swedish).
3. Swedish Standard SS-EN ISO 15630-3:2002. ”Armeringsstål och stål för spännarmering – Provningsmetoder Del 3: Spännarmering.” (”Steel for the Reinforcement and Prestressing of Concrete – Test Methods – Part 3: Prestressing Steel”). SIS Förlag AB, Stockholm, 2002, 27 pp. (In Swedish).
4. Berglund L-E, Forsmarks Kraftgrupp AB, Östhammar, Sweden. Personal communication, August 10, 2004.

Moisture in Self-levelling Flooring Compounds. Part I. Water Vapour Diffusion Coefficients

Anders Anderberg
M.Sc., Dr.-student
Div. Building Materials, Lund University
P.O. Box 118, 221 00 Lund, Sweden
E-mail: anders.anderberg@byggtek.lth.se

Lars Wadsö
Dr., Senior researcher
Div. Building Materials, Lund University
P.O. Box 118, 221 00 Lund, Sweden
E-mail: lars.wadso@byggtek.lth.se

ABSTRACT

Diffusion coefficients of three self-levelling flooring compounds (SLC) and water vapour resistance of a primer have been measured with the cup method. The results show that the diffusion coefficient is dependent not only on the vapour content (relative humidity), but also on the absolute moisture content, i.e., there is a hysteresis effect on moisture transport. At RH lower than approximately 90 %, SLC have higher diffusion coefficients than a standard concrete (w/c 0.7 OPC), but the opposite is true at higher RH. This can be explained by the fact that SLC have different pore structure than concrete. The latter may also be an effect of the high amount of polymer in SLC that form a film throughout the material and thereby limits capillary moisture transport.

Key words: moisture transport, water vapour, self-levelling flooring compound, cup method, diffusion coefficient.

1. INTRODUCTION

During the last decades there has been an increasing interest in the possible connections between indoor air quality and health, and it has been found that dampness is a risk factor for health effects in the airways, as well as tiredness and headache [1]. This seems to be true irrespectively of whether the dampness is measured as condensation on windowpanes, water damage or smell/odour. However, the connection between dampness and health effects is not known. Two discussed possibilities are emissions from degraded building materials and emissions from microbiological growth. Both chemical degradation processes and microbiological growth increase with increasing moisture content (or relative humidity) as the molecular mobility of chemical reactants and microbial nutrients then increases [2].

Cementitious materials are often considered to contribute to healthy indoor environments, as they are stable inorganic materials. However, their very alkaline nature can give rise to problems as many other modern building materials, like adhesives, sealants, flooring materials and paints, are based on polymers, some of which are not stable under alkaline conditions. A common problem in Sweden is PVC flooring bonded to concrete floors with a water-based adhesive. As long as the concrete is dry the construction works well, but if the moisture level becomes too high the alkaline pore solution will come in contact with the adhesive, possibly degrading it by hydrolysis [3]. The degradation products are often strongly odorous alcohols like 2-ethyl-hexanol and butanol that diffuse through the PVC flooring into the indoor environment.

The above-mentioned problems can occur in older buildings if the moisture level in a concrete floor increases, for example because of leakage. It can also occur in new buildings if the concrete has not been dried enough before flooring materials are laid. Different solutions have been proposed to make it possible to build the above type of constructions without risk of degradation:

- The use of alkali resistant polymers in adhesives.
- The placement of a thin low-alkali flooring compound between the concrete and the adhesive.
- The use of self-desiccating concrete and flooring compounds.

These solutions and combinations of them have been tested with good results, both in laboratories and in buildings [3-6].

Self-levelling flooring compounds (SLC) are normally laid in 1-30 mm layers on concrete or other substrates to give a horizontal and smooth surface for flooring materials. When used on concrete they may also act as a barrier to alkalis between the concrete and the flooring, thus giving the flooring and adhesive a less aggressive environment. Usually a polymer primer is applied on the substrate before the SLC is laid. The primer gives a better and more uniform bonding between substrate and SLC, prevents air from the concrete to give rise to bubbles on the SLC surface and also prevents excessive amounts of water from the fresh SLC to be absorbed by the substrate.

This paper reports a study of water vapour diffusion coefficients of three commercial SLC measured with the cup method. Although several workers have measured diffusion coefficients of concrete and mortars, we know of only one previous study on a flooring compound (non self-levelling) [7]. The present study, together with measurements of sorption isotherms and scanning curves [8], can be used to predict the moisture state of flooring constructions. This is of interest, e.g., for prediction of:

- The long-term moisture state of the flooring adhesive.
- The distribution of the water from a water based adhesive applied on an SLC.
- The transport of hydroxide ions (OH^-) from the usually more alkaline concrete to the flooring adhesive and other sensitive materials.

SLC consist of binder, filling materials, polymer and admixtures. The binders are normally a mixture of calcium aluminate cement (CAC), Portland cement (PC) and calcium sulphate in the forms of anhydrite and hemihydrate. Filling materials are sand and finely ground mineral materials like limestone. A polymer powder is added to improve abrasion resistance and the flexural and tensile strength of the otherwise brittle cement matrix. The polymer particles

coalesce and form a film [9] throughout the material that can be described as an interspersed secondary binder system [10]. The admixtures control for example setting time, curing time, flowing characteristics, air entrainment and separation. A more detailed description of SLC is given by Harbron [10].

The moisture state of a material can be presented in different ways. In this paper we have chosen to work with vapour content v (g vapour per m^3 air). This can be seen as the vapour state in the pores of the material and is convenient as the same potential can also be used in the gas phase outside the material. The vapour content is the product of the relative humidity (expressed as a fraction) and the saturation vapour content, which can be found tabulated as a function of temperature.

Moisture can be transported by vapour diffusion, surface flow and capillary flow. Since it normally is of no interest to separate the effects of different kinds of transport processes, the total moisture flow is usually determined. The moisture transport properties of a material are then described with one coefficient, the diffusion coefficient D. For most materials the diffusion coefficient is a function of the vapour content (or, at isothermal conditions, the relative humidity, RH).

2. MATERIALS AND METHOD

2.1 Materials

The three tested commercial products were based on Portland cement, calcium aluminate cement, calcium sulphate and small amounts of silica fume. A typical composition of the mineral part of an SLC is shown in Table 1.

Table 1 – Typical composition of the mineral part (excluding admixtures) of an SLC, partly adapted from [11].

Portland cement	around 3 %
Calcium aluminate cement	around 17 %
Calcium sulphate	around 7 %
Limestone filler (calcite)	around 30 %
Sand (siliceous)	40-50 %
Silica fume	less than 3 %

The three tested products were:

A. Normal SLC with water to binder ratio of about 1.0. This product is generally used in non-industrial constructions.
B. Rapid-drying SLC, which is similar to the above product, but is used with lower water to binder ratio (about 0.7) to give the product a higher degree of self-desiccation. This product is mainly used in renovation as one can walk on it in 1-2 hours and apply final covering in 1 day.
C. SLC for industrial floors, containing slag as a binder and a larger amount of polymer to increase the abrasion resistance [9]. The water to binder ratio is about 0.6. The final product allows medium heavy rolling equipment.

The products were mixed according to the manufacturers guidelines and left to hydrate, the first 24 hours in open air, approximately 20 ºC and 50 % RH, and after that in sealed plastic bags. Measurements were made when the specimens were 2-6 months old, except the dried and resaturated specimens for hysteresis measurements that were 8-11 months old.

Influence of the amount of mixing water was tested in flooring compound A by using 10 % more and 20 % less mixing water than required by the manufacturer's guideline. The effects of hysteresis on the diffusion coefficient due to desorption or absorption was also tested by drying and wetting test specimens of flooring compound A before testing. These dried and wetted specimens had been used in the main measurement series. While still attached to the cups, they were either dried at 25 % RH and 30 ºC, or resaturated with liquid deionised water.

The diffusion resistance of a primer was measured by applying it on test specimens of product A. The primer was a dispersion consisting of styrene acrylate in water. The fraction of styrene acrylate used in the dispersion depends on the substrate. In these tests the primer contained about 12 % styrene acrylate.

2.2 Cup method

The cup method was used to determine diffusion coefficients. In this method two different constant humidity levels are created at each side of a test specimen. Normally the specimen is placed as a lid on a cup containing a saturated salt-solution. The internal RH is controlled by the salt solution and the external RH is that of the room where the cup is placed. The mass flow rate is measured by weighing the cup regularly, thus registering the weight change of the cup.

Fick's law of diffusion is:

$$q = -D\frac{dv}{dx} \tag{1}$$

where q (g/(m^{2}s)) is the moisture flow, D (m^2/s) the diffusion coefficient and dv (g/m^3) the difference in vapour content over the distance dx (m). An integrated form of Fick's law can then be used to calculate the diffusion coefficient:

$$q = \overline{D}\frac{v_2 - v_1}{L} \tag{2}$$

Here, $\overline{D}$ (m^2/s) is the average diffusion coefficient in the interval v_1 to v_2 and L (m) is the thickness of the specimen. A complication for a cup measurement is that the measured flow rate is not only a function of the diffusion resistance within the material, but also depends on external mass transfer resistances at both sides of the specimen, Z_i and Z_e (s/m). Inside the cup Z_i is normally equal to the diffusion resistance of the stagnant air in the gap between the salt solution and the specimen. Outside the cup, where there always are air movements, Z_e is a boundary layer mass transfer resistance. The total flow can thus be described as follows:

$$q = \frac{1}{L/\overline{D} + Z_i + Z_e}(v_2 - v_1) \tag{3}$$

The diffusion cups (Fig. 1) used in this study, were designed and previously used by Hedenblad [12]. The cups were made of polypropylene and the sealing was made with a polyurethane sealant (Marine Adhesive Sealant 5200, 3M, St Paul MI, USA). The tightness of the cups was validated with aluminium specimens. The leakage was 0.5 mg per day over a 300-day period with an internal RH of 100 % and an external RH of 55 % at 20 ºC. This leakage corresponds to less than 1 % of the moisture flow in all present measurements.

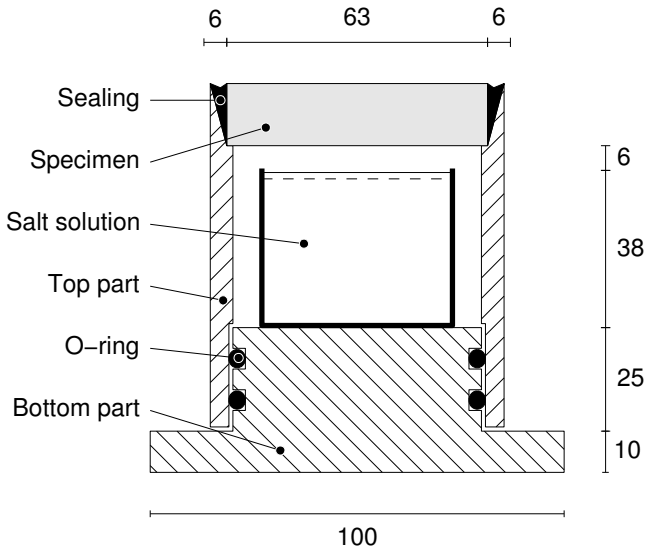

Figure 1– Schematic picture of the cup used.

The experiments were carried out with focus on higher RH, as this is the most interesting area related to indoor environment. The diffusion coefficients were mainly determined at 20±1 ºC with an outer climate of 55±2 % RH. The RH inside the cups were as follows [13]:

75.5 % (NaCl)	85.1 % (KCl)	94.6 % (KNO_3)
97.6 % (K_2SO_4)	100 % (H_2O)	

Tests were also performed at 5±1 ºC in a climate box. The outer climate had an RH of 63.5 %, (NaBr) and the RH inside the cups were as follows [13]:

75.6 % (NaCl)	87.7 % (KCl)	96.3 % (KNO_3)
98.5 % (K_2SO_4)	100 % (H_2O)	

Measurements were started with specimens standing in a climate room with low air velocity, approx. 0.05 m/s. To minimise the influence of the external mass transfer resistances, the air velocity above the specimens was increased with a fan to about 2 m/s. This gave a slightly higher flow rate for specimens with the highest diffusion rate, but did not influence the results of the other specimens.

All tests were performed with triple or quadruple specimens of 8±1 mm thickness and 63±1 mm diameter. Individually measured values of thickness and diameter were used in the evaluation. An analytical method [14] for correction of edge effects has been used in these evaluations, as the moisture flow is not perfectly one-dimensional at the edges of our specimens.

3. EVALUATION

The isothermal cup measurements have been made with one external climate and five different internal climates. The aim of the evaluation is to calculate the diffusion coefficient as a function of the moisture state. We have assumed that the internal mass transfer resistance, Z_i, is equal to the resistance of stagnant air in the air gap between the salt solution and the specimen and that the external mass transfer resistance is negligible. In the present evaluations the vapour content at the internal side of the specimen was calculated as the vapour content of the salt solution minus the vapour content difference over the air gap. The external vapour content used was that of the ambient climate. Constant condition on one side of the specimen is a prerequisite for the evaluation method outlined below.

Equation 2 can be rewritten:

$$qL = \overline{D}(v_2 - v_1) \tag{4}$$

All cup measurements of a certain material and in a certain vapour content range will have the same product of mass flow rate and specimen thickness. Rewriting Eq. 1 and integrating gives:

$$\int_0^L q\,dx = -\int_{v_1}^{v_2} D(v)\,dv \tag{5}$$

The left hand side integral is qL (Eq. 4). Therefore:

$$\overline{D} = \frac{\int_{v_1}^{v_2} D(v)\,dv}{v_2 - v_1} \tag{6}$$

If two cup measurements are made with the same external climate v_0, but with two different internal climates v_1 and v_2, it is possible to calculate the mean diffusion coefficients in two intervals: D_{01} and D_{02}. Here, Eq. 4 is written for these two measurements and for a hypothetical measurement in the interval v_1 to v_2, see Fig. 2:

$$q_m L_a = \overline{D}_{02}(v_2 - v_0) \tag{7}$$

$$q_m L_b = \overline{D}_{01}(v_1 - v_0) \tag{8}$$

$$q_m L_c = \overline{D}_{12}(v_2 - v_1) \tag{9}$$

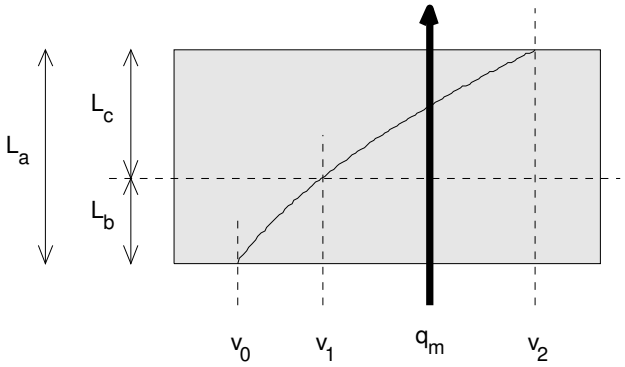

Figure 2 – A schematic drawing of a cup measurement made with a specimen of thickness L_a between vapour contents v_0 and v_2. Also shown is the division of the specimen into two specimens of thickness L_b and L_c and how one will get the same flow as with the thicker specimen by making measurements in the interval v_0 to v_1 and v_1 to v_2, respectively.

Note that these three measurements have the same flow rate and that $L_a=L_b+L_c$. From Eqs. 7-9 one can write the following expression for D_{12}:

$$\overline{D}_{12} = \frac{\overline{D}_{02}(v_2 - v_0) - \overline{D}_{01}(v_1 - v_0)}{v_2 - v_1} \tag{10}$$

As this equation does not include q or L, it is a general expression valid also for specimens that do not conform to the limitations of Fig. 2 (same q and $L_a=L_b+L_c$). Equation 10 can thus be used to calculate mean diffusion coefficients in difference-intervals not directly measured.

Measurements were made with one external climate v_0 and five different internal climates v_1-v_5. D_{01}, D_{02}... D_{05} can directly be calculated with Eq. 4 and D_{12},... D_{45} can be calculated with Eq. 10, i.e., the diffusion coefficient is obtained as a function of the moisture state. Other similar methods for evaluation have been proposed, e.g., by Chang et al. [15] and Bažant et al. [16].

4. RESULTS AND DISCUSSION

4.1 Diffusion coefficients

The results are presented in Figs. 3-5. As can be seen in Figs. 3 and 4, the rapid drying SLC B with lower water to binder ratio has a slightly lower diffusion coefficient than SLC A. When compared with normal concrete, w/c 0.7 [7], SLC A and B both have higher diffusion coefficients up to about 90 % RH. At higher RH, diffusion coefficients for concrete are significantly higher. A possible explanation of these differences may be the different pore structures of concrete and SLC. Other influential factors may be the higher aggregate content of concrete and the polymer in the SLC that forms an interspersed secondary binder system in the hydrated product (which may limit the capillary flow that dominates the moisture transport at high RH). The influence from the transition zone between aggregate and paste may also differ between concrete and SLC.

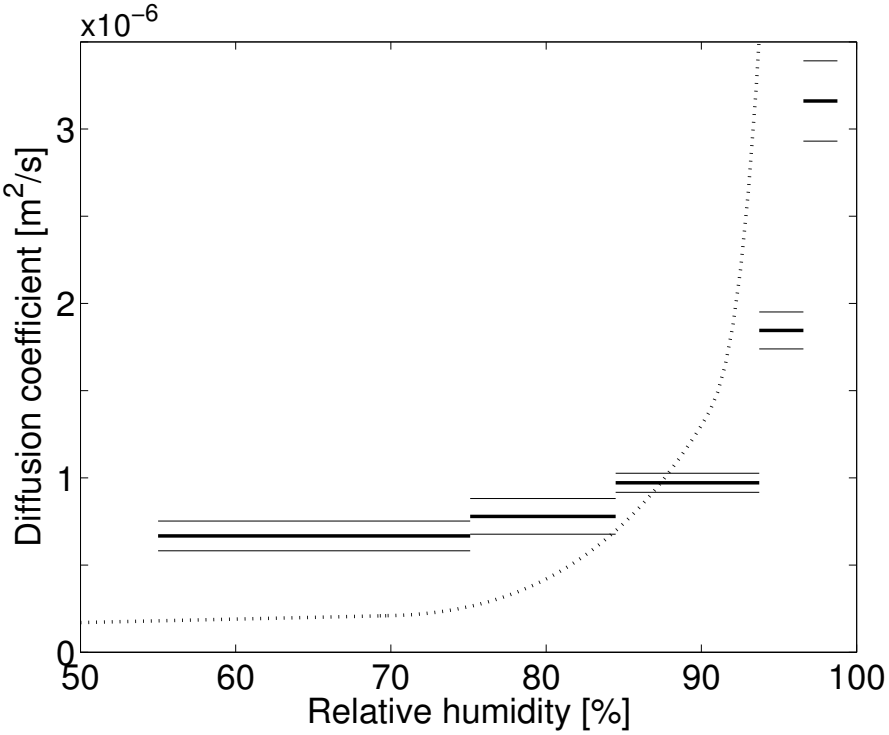

Figure 3 – Diffusion coefficient for SLC A. Thick line is the mean value in the shown interval. Thin lines indicate one standard deviation. As a comparison, a curve fit of a diffusion coefficient for concrete with water to cement ratio 0.7 [7] is given as a dotted line.

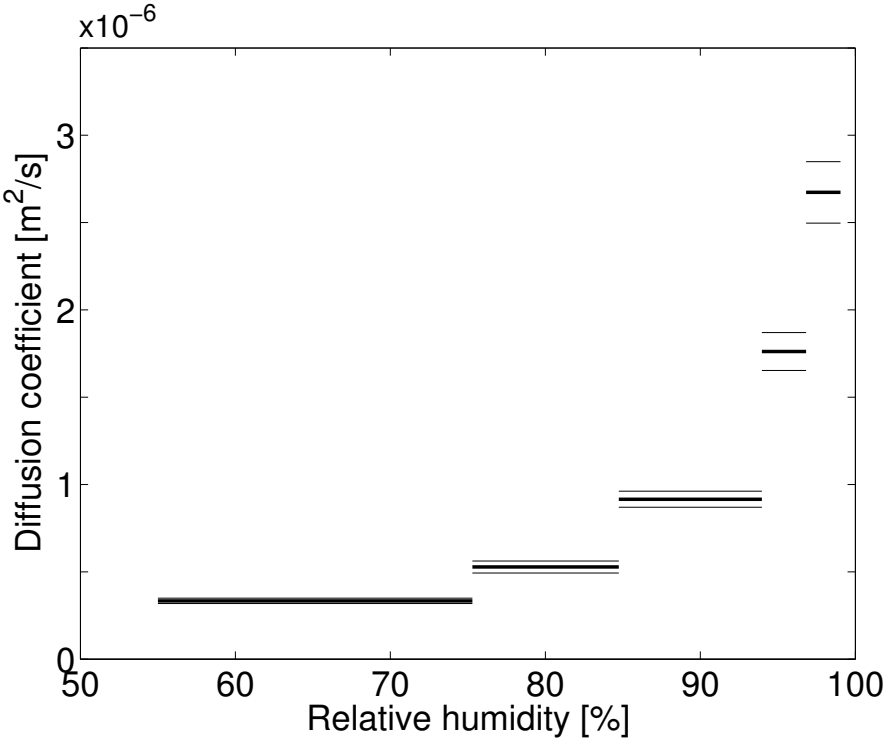

Figure 4 – Diffusion coefficient for SLC B. Thick line is the mean value in the shown interval. Thin lines indicate one standard deviation.

SLC C (Fig. 5) for industrial floors has a lower diffusion coefficient than the other two SLC (note the different scale on the y-axis in Fig. 5). This may be an effect of the higher polymer content in the industrial flooring material, the lower water to binder ratio and the slag content. Although microstructures of slag cement pastes are similar to those of Portland cement, the permeability is normally lower in slag cement pastes [18].

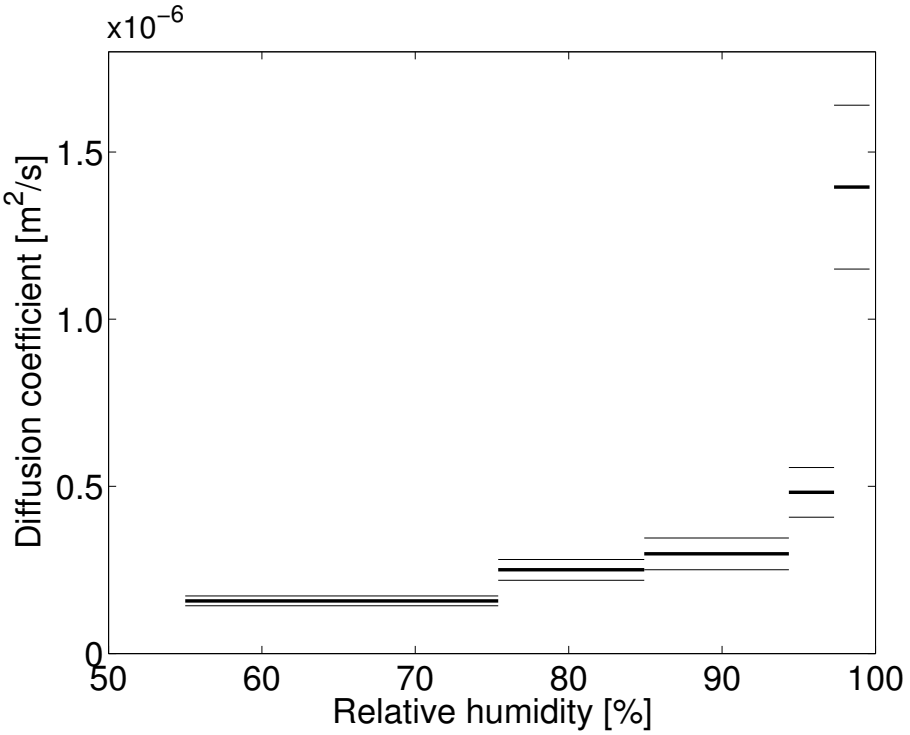

Figure 5 – Diffusion coefficient for SLC C. Thick line is the mean value in the shown interval. Thin lines indicate one standard deviation.

4.2 Influence of water/binder ratio

As can be seen in Table 2, the diffusion increases with increasing water to binder ratio.

Table 2 – Mean diffusion coefficients and standard deviations for samples of product A made with different amounts of mixing water. Four replicates were measured in each sample.

Sample	RH-interval %	Diffusion coefficient 10^{-6} m^2/s
Normal	55-85.1	0.70 ± 0.02
	55-97.6	0.84 ± 0.03
+ 10 % mixing water	55-85.1	0.85 ± 0.03
	55-97.6	0.93 ± 0.02
- 20 % mixing water	55-85.1	0.47 ± 0.03
	55-97.6	0.59 ± 0.03

4.3 Influence of hysteresis

Most materials have sorption hysteresis as they have different isotherms for desorption (drying) and absorption (humidification). At a certain RH a drying specimen contains more water than a specimen absorbing water vapour. The influence of this on the diffusion rate has been studied by measurements of diffusion coefficients with specimens in absorption and desorption mode, respectively, Table 3. The results indicate that specimens undergoing desorption, i.e., contains more water, have higher diffusion coefficients.

Table 3 – Mean diffusion coefficients and standard deviations for samples of product A in absorption and desorption mode. Each sample included three replicates. Note that these test specimens were older than the other test specimens and the results can therefore not directly be compared with the other results in this article.

Sample (Product A)	RH-interval %	Diffusion coefficient 10^{-6} m^2/s
Absorption	55-75.5	0.59 ± 0.05
Desorption	55-75.5	0.78 ± 0.01
Absorption	55-97.6	0.71 ± 0.05
Desorption	55-97.6	0.90 ± 0.05

4.4 Influence of temperature

A direct comparison between measurements at 20 and 5 °C was not possible to make, as the saturated salt solutions used do not generate the same RH at different temperatures. An estimation is however possible to make and this shows that the diffusion coefficient at 5 °C is about 60 % of the diffusion coefficient at 20 °C, see Table 4.

Table 4 – Mean diffusion coefficients and standard deviations at 20 and 5 °C for product A. Samples measured at 20 °C included four replicates and samples measured at 5 °C included three replicates.

Temperature ºC	RH-interval %	Diffusion coefficient 10^{-6} m^2/s
20	55-75.5	0.67 ± 0.09
20	55-94.6	0.77 ± 0.04
20	75.5-94.6	0.97 ± 0.13
5	63.5-75.6	0.40 ± 0.07
5	63.5-96.3	0.47 ± 0.05
5	75.6-96.3	0.58 ± 0.11

4.5 Influence of polymer primer

Results of measurements with and without primer (not given here) show that the resistance of the primer was in the order of 5000 s/m at 75 % RH. This corresponds to the resistance of about

4 mm of SLC A at 75 % RH. The amount of applied primer was 0.4 kg solution per m^2, i.e., 0.05 kg (solid)/m^2. A dependence of thickness could also be seen, where an increased amount of primer applied gave a higher resistance.

4.6 General discussion

A survey of sources of uncertainty and errors in the cup method was done by Hansen and Lund [19]. The main sources of uncertainty described were surface and air space resistances, changes in barometric pressures, RH oscillations and boundary effects. In the present study, long-term measurements minimised the influence of barometric pressure changes and RH oscillations. Surface and air space resistances and boundary effects are described earlier in this paper.

When evaluating diffusion coefficients with Eq. 10, values from measurements are used both when evaluating diffusion coefficients in the measured interval and in the next interval with higher RH. This means that measurement errors in one interval also influence the calculated diffusion coefficients of the next higher interval and that the uncertainty for these calculated values increases. This can be seen in Table 4, where the last diffusion coefficients are calculated from the first two values.

Carbonation occurs in all cement-based materials. Carbonation in ettringite systems [20] and calcium aluminate cement [21] leads to a slightly more open material. Consequently, materials exposed to air should have higher diffusion coefficients than less carbonated materials. Materials in these experiments were hydrated in sealed plastic bags, but exposed to air when measurements were performed.

Evaluation of measurements with Eq. 10 requires that the material is homogeneous. Carbonation, as discussed above, can give the material slightly different properties, as the carbonation front moves from the surface and inwards into the specimen. There may also be a higher concentration of polymer in the surface region as a consequence of bleeding in the fresh mortar. Water transported from the fresh mortar to the surface may carry polymers, which then accumulates in the surface region, while the water evaporates. This higher concentration of polymers in the surface may influence the moisture transport properties and therefore give a slightly inhomogeneous material.

Measurements of moisture transport properties together with measurements of moisture storage capacities (sorption isotherms) [8] makes it possible to calculate and predict drying times, moisture loads, ion transport etc. This is important because it is well known that other materials may take harm in contact with cementitious materials under high moisture loads.

5. CONCLUSIONS

This study reports moisture diffusion coefficients of self-levelling flooring compounds (SLC). Moisture diffusion in SLC was found to be higher than in normal concrete at RH lower than approximately 90 %, but lower than normal concrete (w/c 0.7) at higher RH. A temperature dependence on moisture diffusion was found where the moisture diffusion coefficient at 5 ˚C was about 60 % of the moisture diffusion coefficient at 20 ˚C. Sorption hysteresis influences the moisture diffusion so that, at the same RH, a drying material has higher moisture diffusion coefficient than a material absorbing water vapour.

6. ACKNOWLEDGEMENTS

We thank Bo Johansson for helping us with the measurements.

REFERENCES

1. Bornehag, C-G., et al., "Dampness in Building and Health Nordic Interdisciplinary Review of the Scientific Evidence on Associations between Exposure to "Dampness" in Buildings and Health Effects (NORDDAMP)." *Indoor Air*, Vol. 11, 2001, pp. 72-86.
2. Fennema, O.R., "*Water and Ice"*, in *Food Chemistry*, O.R. Fennema, Editor. 1985, Marcel Dekker Inc. New York and Basel. pp. 23-67.
3. Sjöberg, A., "*Secondary emissions from concrete floors with bonded flooring materials - effects of alkaline hydrolysis and stored decomposition products"* P-01:2, Department of Building Materials. Chalmers University of Technology: Göteborg. 2001, 188 pp.
4. Wengholt Johnsson, H., "Flooring materials on concrete substrate - Field measurement of drying times and emissions in Gärdsrådet, Umeå (In Swedish)". NCC Teknik Göteborg. 1998, 27 pp.
5. Björk, F., et al., "Degradation of Components in Flooring Systems in Humid and Alkaline Environments." *Construction and Building Materials*, Vol. 17, 2003, pp. 213-221.
6. Alexanderson, J., "Emissions from alkali attack on adhesives and floor coverings." *Concrete*, Vol., 2001, pp. 18-19.
7. Hedenblad, G., "Material data for moisture transport calculations (In Swedish)". Byggforskningsrådet: Stockholm. 1996, 53 pp.
8. Anderberg, A. and Wadsö, L., "Moisture in Self-levelling Flooring Compounds. Part II. Sorption Isotherms." *Nordic Concrete Research*, No. 32, 2004
9. Hoffman, A., "Effect of Redispersible Powders on the Properties of Self-Levelling Compounds". Technical paper, Wacker Polymer Systems, 20 pp.
10. Harbron, R. "*A General Description of Flow-Applied Floor Screeds-An Important Application for Complex Formulations Based on CAC". Proceedings,* International Conference on Calcium Aluminate Cements. Edinburgh, Scotland 2001. pp. 597-604.
11. Scrivener, K.L., et al. "*Effect of CO2 and humidity on the Mechanical Properties of a Formulated Product Containing Calcium Aluminate Cement". Proceedings,* Ibausil. Weimar, Germany 1997,vol. 1. pp. 745-752.
12. Hedenblad, G., "Moisture permeability of some porous materials". *Report* TVBM-7068, Building Materials, Lund Technical University. 1993, 5 pp.
13. Greenspan, L., "Humidity Fixed Points of Binary Saturated Aqueous Solutions." *Journal of Research of the National bureau of Standards-A. Physics and Chemistry*, Vol. 81A, No. 1, 1976, pp. 89-96.
14. Claesson, J., Hagentoft, C.-E., and Wadsö, L., "Masked Edge Effects When Measureing Diffusion Coefficients With the Cup Method." *Polymer Engineering and Science*, Vol. 34, 1994, pp. 821-826.
15. Chang, S.C. and Hutcheon, N.B., "*Dependence of Water Vapor Permeability on Temperature and Humidity"*. 1956, Trans. ASHRAE, 62. p. 437-450.
16. Bažant, Z.P. and Najjar, L.J., "Nonlinear water diffusion in nonsaturated concrete." *Materials and Structures*, Vol. 5No 25, 1972, pp. 3-20.

17. Nilsson, L.-O., "Long-term moisture transport in high performance concrete." *Materials and Structures*, Vol. 35, 2002, pp. 641-649.
18. Taylor, H.F.W., "Cement Chemistry". 2nd edition. Thomas Telford, London, 1997, 437 pp.
19. Kielsgaard Hansen, K. and Lund, H.B. "*Cup method for determination of water vapour transmission properties of building materials. Sources of uncertainty in the method". Proceedings,* Proceedings of the 2nd symposium "Building Physics in the Nordic Countries"1990. pp. 291-298.
20. Scrivener, K.L. "*Historical and Present Day Applications of Calcium Aluminate Cements". Proceedings,* International Conference on Calcium Aluminate Cements. Edinburgh, Scotland 2001. pp. 3-23.
21. Gaztañaga, M.T., Gonñi, S., and Guerrero, A. "*Accelerated Carbonation of Calcium Aluminate Cement Paste". Proceedings,* Calcium Aluminate Cements. Edinburgh, Scotland 2001. pp. 349-358.

Moisture in Self-levelling Flooring Compounds. Part II. Sorption Isotherms

Anders Anderberg
M.Sc., Dr.-student
Div. Building Materials, Lund University
P.O. Box 118, 221 00 Lund, Sweden
E-mail: anders.anderberg@byggtek.lth.se

Lars Wadsö
Dr., Senior researcher
Div. Building Materials, Lund University
P.O. Box 118, 221 00 Lund, Sweden
E-mail: lars.wadso@byggtek.lth.se

ABSTRACT

Moisture sorption in self-levelling flooring compounds was investigated by using a sorption balance. Results are presented as sorption isotherms. Influence of temperature, age, water to binder ratio and carbonation are also presented. An increased temperature and increased water to binder ratio gives lower moisture sorption. Results from scanning curves indicate that, when changing sorption mode, even a minute change in moisture content may result in a significant change in relative humidity in the material.

Key words: sorption isotherm, water vapour, self-levelling flooring compound, sorption balance.

1. INTRODUCTION

Recently, the connection between the indoor environment and occupants health has gained an increased interest. Moisture has been shown to be an important factor as it promotes chemical reactions and biological growth. This is further discussed in the first paper [1] of this series of two papers dealing with moisture properties of self-levelling flooring compounds.

Moisture in materials has different properties and is of different interest depending on how hard the water molecules are bound to the surface and the structure of the material. This is important as not all water inside materials contribute to the processes that may influence the indoor environment. The weakest bound water is here the most interesting as it supports biological growth, transport of substances, etc. [2].

The strongest bound water in a cementitious material is chemically bound as reaction products in the hardened cement paste and is part of the solid structure of the material. As this water is

strongly bound in the structure and does not leave the material under normal circumstances it is of no interest concerning indoor environmental aspects.

Physically bound water stands in equilibrium with the water vapour in the surrounding atmosphere. The amount of water in a material, excluding chemically bound water, is normally given as a sorption isotherm, i.e., the relation between the moisture content (the mass of water per mass of dry material) and the relative humidity (RH) at equilibrium.

Physically bound water can either be adsorbed to surfaces, absorbed in the structure of the material or capillary condensed in pores. The first layer of adsorbed water is the strongest bound, most immobile and remains non-frozen at -55 ºC [3]. This water behaves as part of the solid and corresponds to the monolayer moisture content [2]. A monolayer can be seen as when all of the dry matter is covered with one layer of water molecules [4]. Further added water is more mobile. When sufficiently abundant part of this water may allow for chemical reactions and microbial growth.

In porous materials water is bound not only due to adsorption, but also due to capillary condensation. Water molecules then condense on concave water menisci. Pores with radii less than a certain critical radius are then completely water filled. The curvature of the menisci corresponds to a certain equilibrium RH. A smaller radius corresponds to a lower equilibrium RH. When a material is in equilibrium with low RH, only small water menisci can exist, i.e., only small pores can be completely water filled. At higher RH, larger water menisci can exist and pores with larger pore radii can thus be water filled. In a fine porous material, capillary condensed water is the dominant contributor to transport processes, chemical reactions and microbial growth.

A consequence of capillary condensation is sorption hysteresis [4], i.e., a material will contain different amounts of water in equilibrium with a certain RH, depending on whether the material is drying or taking up moisture, Fig. 1. A material taking up moisture never contains more water than a drying material at the same RH.

As can be seen in Fig. 1, a sorption isotherm contains two main curves, one for desorption and one for absorption. If a previously desorbing material starts to absorb moisture it follows a scanning curve from the desorption isotherm towards the absorption isotherm and vice versa. A result of this is that a small increase in moisture content may lead to a large increase in RH. The consequence of this for moisture related processes is not fully known, but it is probable that RH is not the only parameter describing the rate of chemical and biological processes [2] and that moisture content also may be important, which has been seen for microbial growth on food stuffs [5].

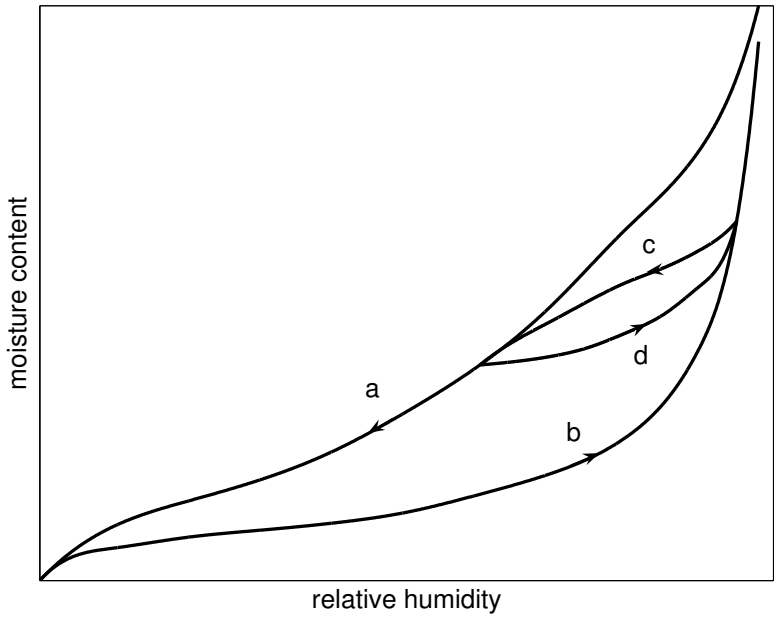

*Figure 1 – Example of a sorption isotherm, where **a** is a desorption isotherm, **b** an absorption isotherm, **c** a scanning curve from the absorption isotherm to the desorption isotherm and **d** a scanning curve from the desorption isotherm to the absorption isotherm.*

The sorption isotherm is, as the name indicates, only valid at a certain temperature. An increase in temperature at constant moisture content results in an increase in RH [2, 6], opposite to the behaviour of air, where an increase in temperature results in lower RH. For concrete, variations of the sorption isotherm within normal temperature ranges are generally neglected, although studies by for example Nilsson [7] show a temperature dependence of about 0-0.4 % RH per ºC depending on moisture condition. An increase in temperature normally increases the rate of chemical reactions [8].

Chemical degradation reactions are dependent on transport properties, as reactants have to come in contact with each other. The critical RH limits at which processes start to take place are somewhat diffuse. A practical value often used in Sweden for concrete slabs with bonded PVC-flooring is 85 % RH. Generally an RH of at least 80 % is needed for biological growth, although some species can grow at lower RH [2, 9].

This paper deals with physically bound water in the RH-range of 10-95 %. Measuring moisture at higher RH levels than 98 %, requires other measurement techniques, see e.g. [10-13]. Measuring moisture down to 0 % RH gives incorrect values for self-levelling flooring compounds (SLC) as chemically bound hydrate water from ettringite is partly non-reversibly released. This has been observed during vacuum drying and drying over desiccants [14] and drying at temperatures above 60 °C [15]. We have noted a significant decrease in mass when drying specimens from 10 % to 0 % RH (not shown in this paper). This mass decrease corresponded to more than 5 % moisture content, i.e., more than the total sorption capacity between 10 % and 95 % RH.

2. MATERIALS AND METHOD

2.1 Materials

Sorption isotherms of three different types of commercial SLC were tested. The three tested commercial products were based on Portland cement, calcium aluminate cement, calcium sulphate and small amount of silica fume. The three tested product were:

A. Normal SLC with water to binder ratio of about 1.0. This product is generally used in non-industrial constructions.
B. Rapid-drying SLC, which is similar to the above product, but is used with lower water to binder ratio (about 0.7) to give the product a higher degree of self-desiccation. This product is mainly used in renovation as it allows foot traffic in 1-2 hours and final covering in 1 day.
C. SLC for industrial floors, also containing slag as a binder and a higher amount of polymer to increase the abrasion resistance [16]. The water to binder ratio is about 0.6. The final product allows medium heavy rolling equipment.

The products were mixed according to the manufacturers guidelines and left to hydrate, the first 24 hours in open air, approximately 20 ºC and 50 % RH, and after that in sealed glass jars. Small amounts of water were added to the specimens in the jars to keep the RH at 100 %. Test specimens were cut from the centre of cast cylinders to avoid edge effects and carbonation. Specimens had hydrated for a minimum of 12 months prior to testing, if not otherwise stated. The side lengths of the specimens were in the order of 4x4x3 mm^3 with masses in the order of 100 mg. Carbonated specimens were exposed to atmospheric conditions for three months. Validation of carbonation was made in parallel measurements (not on the tested specimens).

2.2 Method

A sorption balance (DVS 1000, Surface Measurements Systems, London, UK) was used to determine sorption isotherms and scanning curves. This type of instrument has previously been used in the study of sorption on various materials, for example, food stuffs [17], plant material [18] and inorganic building materials [19]. With this instrument it is possible to measure sorption when the RH is changed in steps and as ramps. A flow of dry nitrogen gas is divided into two gas streams of which one is saturated with water vapour and the other left dry, see Fig. 2. By mixing different proportions of the gases, RH between 0 and 100 % can be generated, although for practical reasons, the upper limit is 98 % RH.

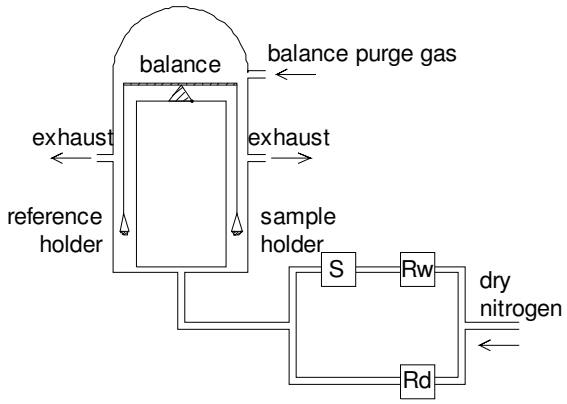

Figure 2 – Schematic picture of the DVS 1000 sorption balance. A flow of dry nitrogen gas is divided into two gas streams where one is saturated with water vapour, by bubbling through liquid water (S) and one is kept dry. The flow rates are controlled by two mass flow regulators (Rw and Rd). By mixing different proportions of the two gases, the desired RH can be generated.

Test cycles with several measurement steps and ramps have been used in the present measurements, Fig. 3. The test specimen is exposed to these relative humidities and the mass change of the specimen is continuously measured. A normal test cycle for one specimen lasted 8-12 days in the present study. The environment in the sorption balance was free from carbon dioxide during the measurements. The trueness (precision) was ±1.0 % RH and the balance resolution was 0.1 μg.

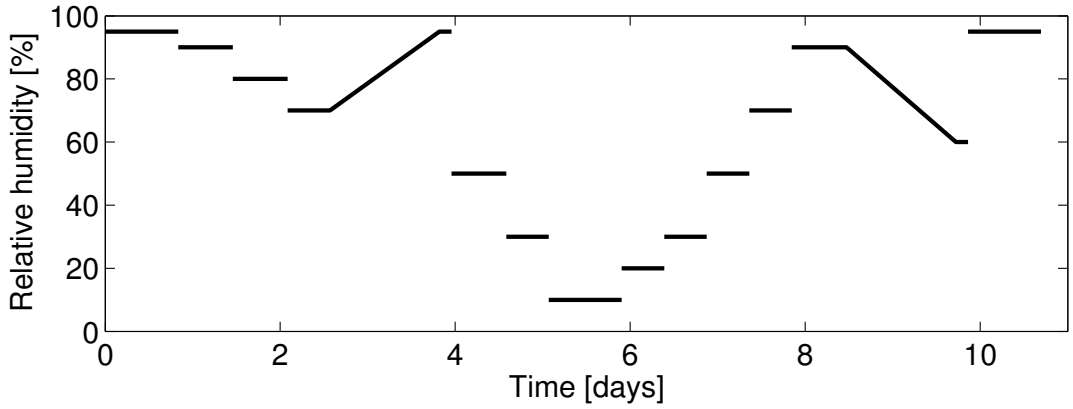

Figure 3 – Typical RH test cycle used in the present study. The test cycle starts and ends at 95 % RH and includes two ramps for scanning curves, one from desorption to absorption and one from absorption to desorption.

Scanning ramp rates were about 100 minutes per % RH. After each scanning ramp, the relative humidity was kept at the final ramp value for 120 minutes validating that each scan was close to equilibrium. The change in mass during these 120 minutes corresponded to less than 0.03 % moisture content.

2.3 Performed tests

Sorption isotherms for the three self-levelling flooring compounds described above were measured with the sorption balance. The influence of different amounts of mixing water, different temperatures, age and carbonation were also measured.

2.4 Evaluation

Steady state measurements were made until the specimens had almost reached equilibrium. The final part of the curve was then curve-fitted and extrapolated with the equation

$$m(t) = m_0 + (m_f - m_0)e^{-k(t-t_0)} \quad (1)$$

where $m(t)$ is the mass at time t, m_0 is the initial mass at the start of the curve-fitting, m_f is the final mass, k is a constant and t_0 is the initial time at the start of the curve-fitting, see Fig. 4. The curve fitting was done in MATLAB 6.5 with a least square method. The correction never corresponded to more than 6 % of the total mass change in each time step. The final sorption isotherms shown in the figures are curve fitted between the measurement points with a general spline function.

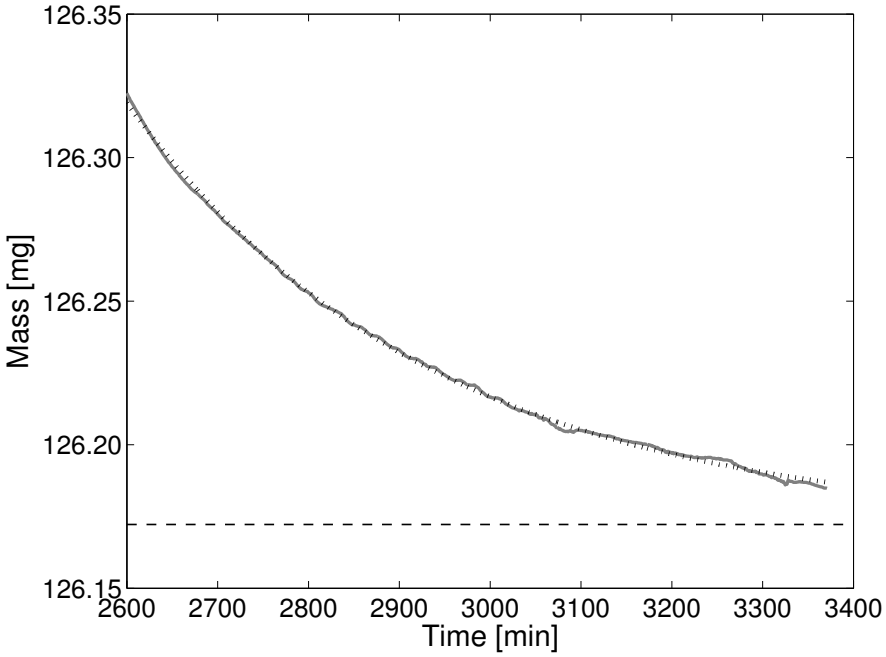

Figure 4 – Extrapolation of the final part of a measurement step in the sorption balance. Solid line is measured values, dotted line curved fitting of measured values and dashed horizontal line extrapolated equilibrium value used in evaluations.

For one material, SLC A, two measurements were performed with specimens casted at different occasions, but with material from the same batch. The mean relative difference in moisture content between the two measurements was 5 %.

3 RESULTS AND DISCUSSION

3.1 Sorption isotherms

Results of measurements of SLC A-C are presented in Figs. 5-7. Results are given as moisture content (relative to mass at 10 % RH, here called dry weight) as a function of RH. SLC B has a higher moisture sorption than SLC A. This may be an effect of the lower water to binder ratio of SLC B (see subsection 3.2), but also due to the larger amount of paste in SLC B. The sorption isotherm of SLC C for industrial floors has a different appearance than the sorption isotherms for SLC A and B. This might be an effect of the slag content and the lower water to binder ratio.

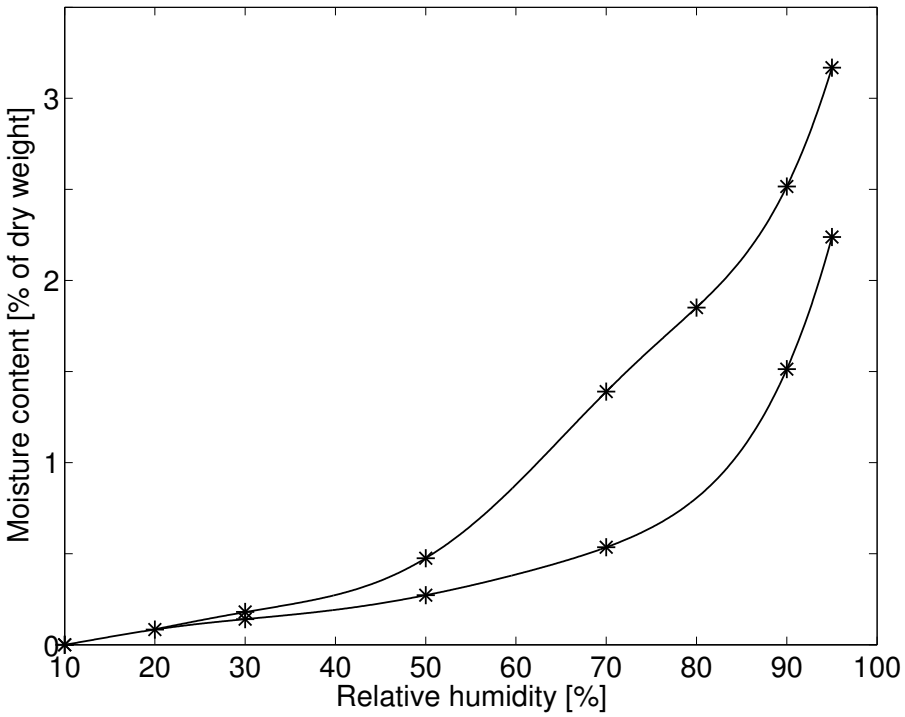

Figure 5 – Sorption isotherm of flooring compound A. Stars are measured values.

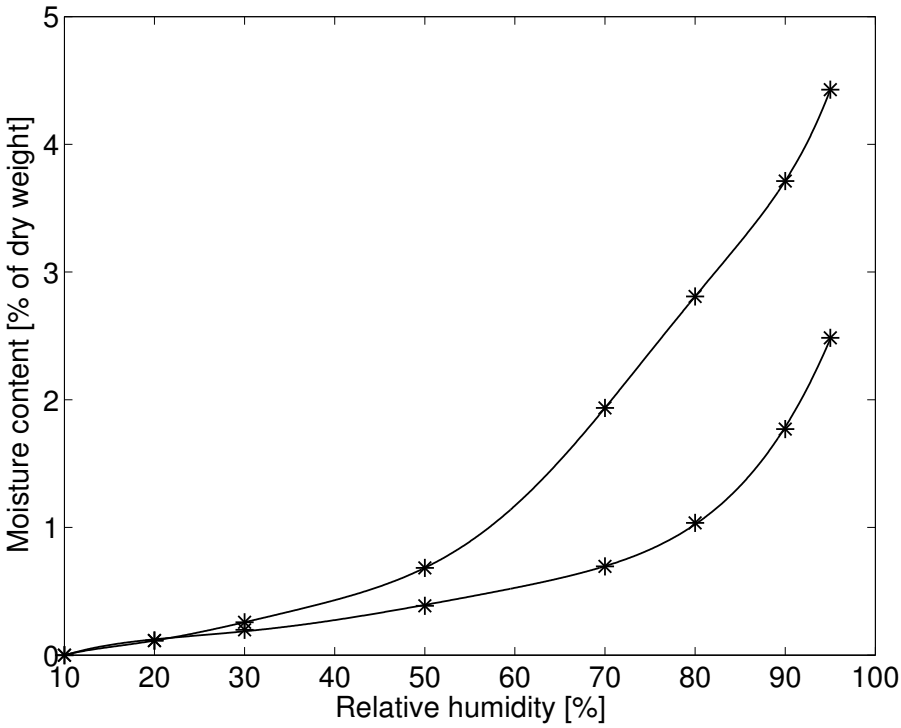

Figure 6 – Sorption isotherm of flooring compound B. Stars are measured values.

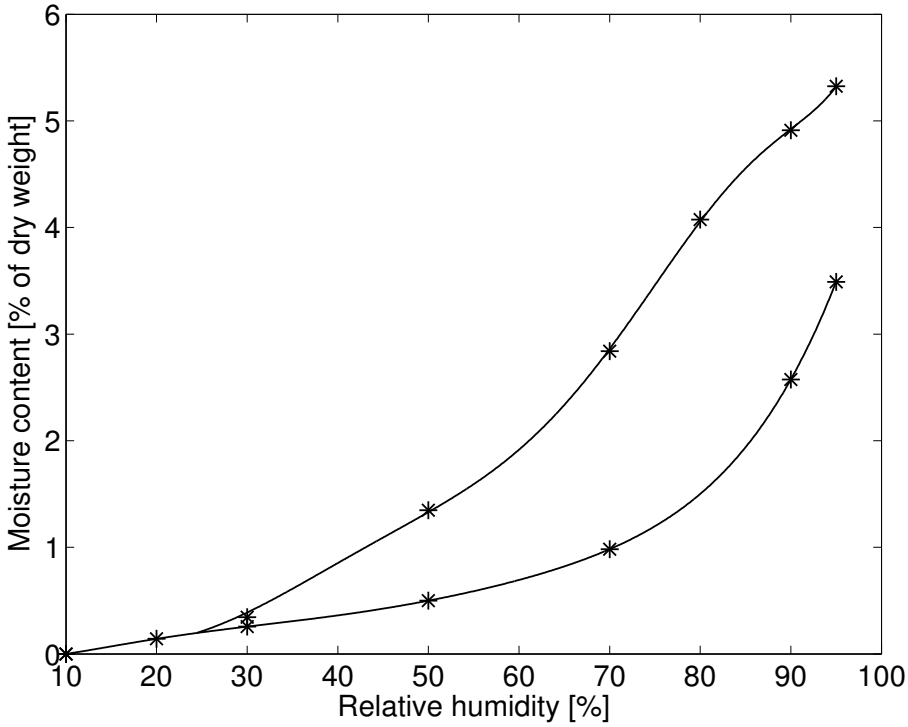

Figure 7 – Sorption isotherm of flooring compound C. Stars are measured values.

3.2 Influence of water to binder ratio

The influence of water to binder ratio was investigated by casting specimens of product A with 20 % less and 10 % more mixing water than recommended. The result indicates that a higher water to binder ratio results in lower sorption, although no difference was seen for normal and +10 % mixing water in absorption. A decrease in water to binder ratio results in lower pore volume and a different pore size distribution with a larger amount of smaller pores. A smaller pore has a relatively larger surface area and will be water filled at lower RH than larger pores. As a result specimens casted with lower water to binder ratio will contain more moisture at the same RH in the hygroscopic range.

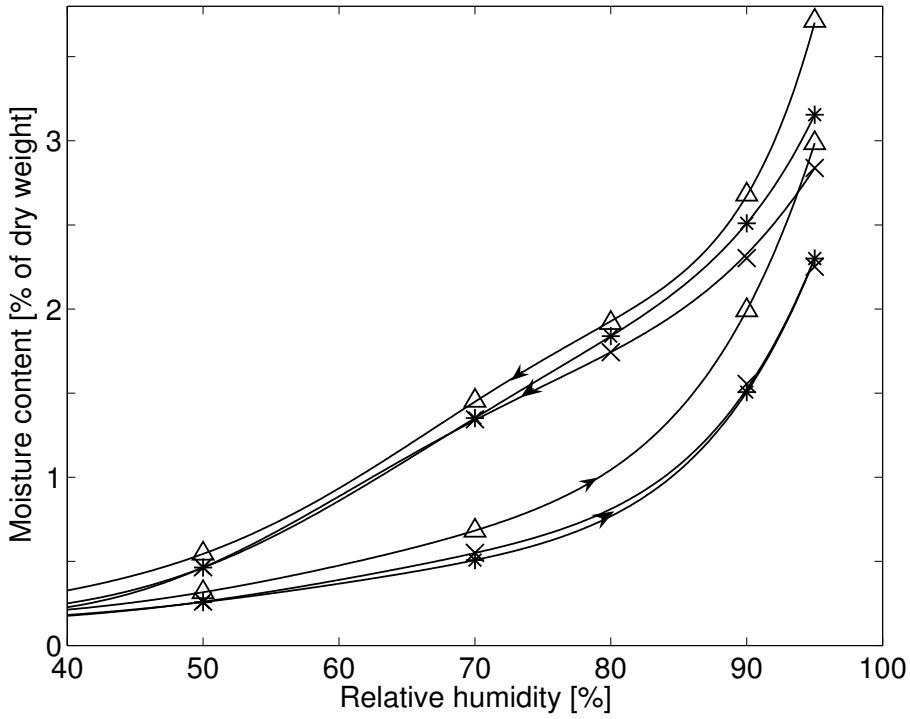

Figure 8 – Sorption isotherms of SLC A casted with normal amount of mixing water (stars), 10 % more mixing water than recommended (x-marks) and 20 % less mixing water than recommended (triangles). Measurement values below 40 % RH showed only small differences.

3.3 Influence of temperature

The influence of temperature on moisture sorption was studied by measurements at 10, 20 and 40 ºC. As can be seen in Fig. 9, the moisture sorption capacity is lower at higher temperature, that is, an increase in temperature results in an increase in RH at constant moisture content. This behaviour is in qualitative agreement with the Clausius-Capeyron equation [20].

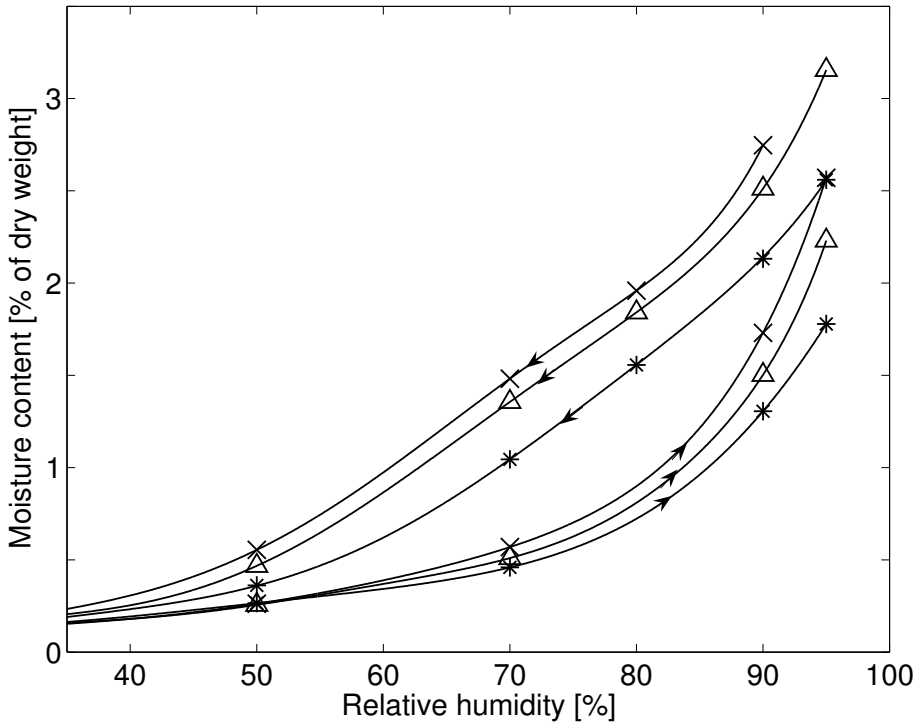

Figure 9 – Sorption isotherms of SLC A at the following temperatures: 10 ºC (x-marks), 20 ºC (triangles) and 40 ºC (stars). Measurement values below 40 % RH showed only small differences.

3.4 Influence of age

The structure of the material gradually develops with time until hydration has stopped. As the measurements of sorption isotherms in the sorption balance are relatively fast, it is a suitable instrument for determining sorption isotherms on not completely hydrated materials. Sorption isotherms for SLC A presented in Fig. 10 were determined at 1, 3 and 12 months of age. A difference due to hydration can be seen, but the major part of the sorption isotherm was already developed after one month. The RH in a young material will thus decrease, even if moisture cannot leave the material. Note that specimens in this investigation hydrated at 100 % RH.

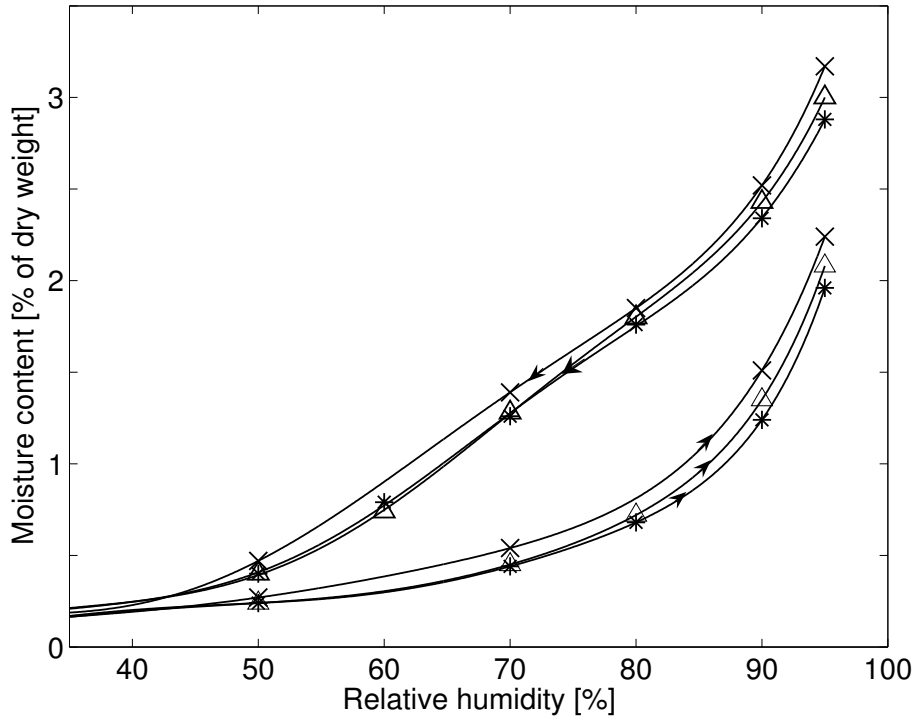

Figure 10 – Sorption isotherm of SLC A at 1 month (stars), 3 months (triangles) and 12 months (x-marks) of age. Measurement values below 40 % RH showed only small differences.

3.5 Scanning curves

Knowledge of scanning curves makes it possible to do more accurate predictions of RH in materials changing sorption modes. As seen in Figs. 11 and 12 a small change in moisture content results in a large change in RH. The consequences of this for chemical reactions and biological growth is however somewhat unclear, as discussed in section 1.

The following scanning curves for SLC A, are presented in Figs. 11 and Fig. 12.

- absorption 70-90 % RH after desorption (Fig. 11)
- desorption 90-70 % RH after absorption (Fig. 11)
- absorption 60-95 % RH after desorption (Fig. 12)
- desorption 95-70 % RH after absorption (Fig. 12)

The results show, e.g., that a sample that has dried to 70 % RH and then absorbs moisture corresponding to a moisture content increase of 0.1 %, will have a final RH of about 80 %. If a calculation had been made with only one curve of the isotherm the final RH would have been about 73 % RH, i.e., only slightly higher than 70 %. The scanning effect will therefore act as a lever, giving large increases in RH for small increases in moisture content.

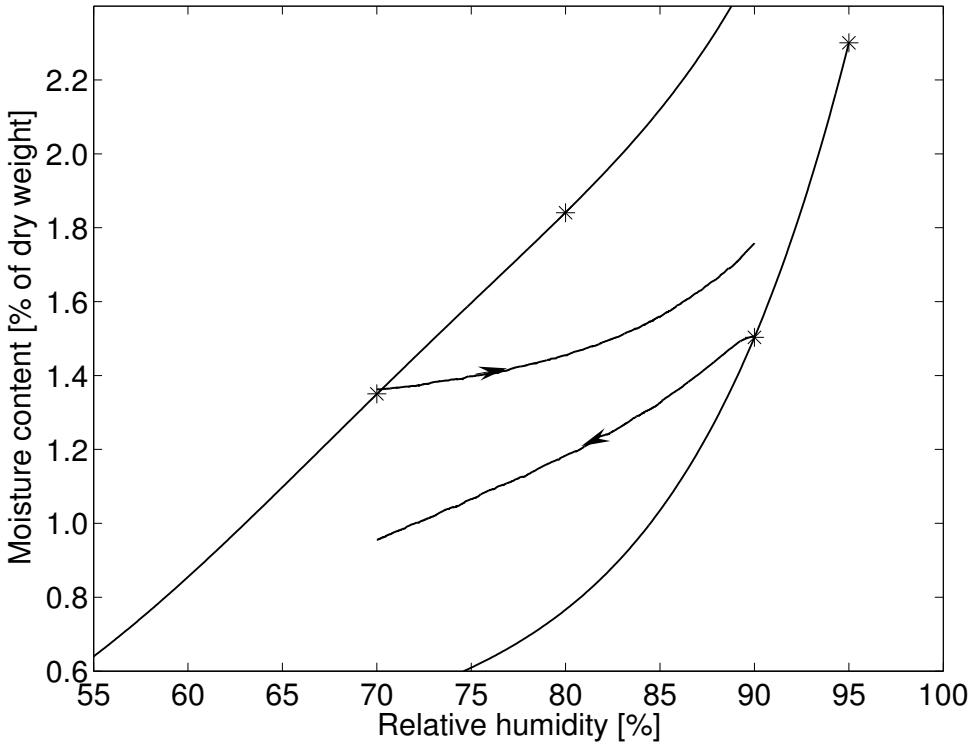

Figure 11 – Scanning curve for SLC A, absorption from desorption mode (70 to 90 % RH) and desorption from absorption mode (90 to 70 % RH).

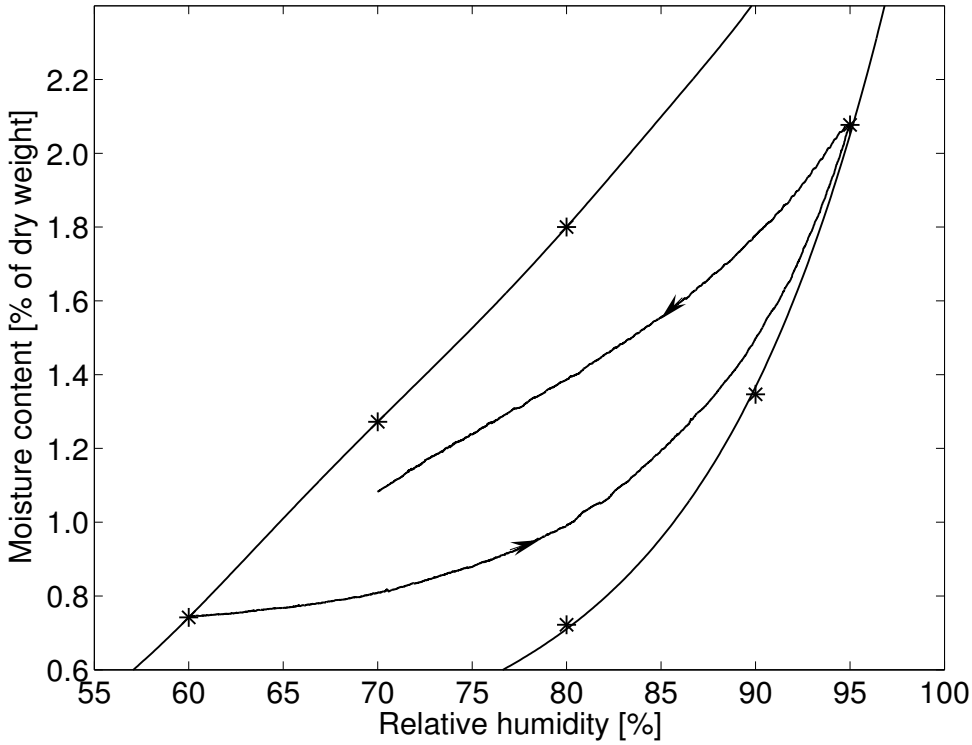

Figure 12 – Scanning curve for SLC A (three months old), absorption from desorption mode (60 to 95 % RH) and desorption from absorption mode (95 to 70 % RH)

3.6 Carbonation

Carbonation is the process where carbon dioxide from air dissolves in the pore solution and reacts with components in the material. Carbonation of ettringite [21] and calcium aluminate cement based materials [22] leads to a slightly more open material, while carbonation of Portland cement based materials results in a denser material [23]. Measurements on carbonated and non-carbonated specimens of SLC A are presented in Fig. 13. Only minor differences where seen.

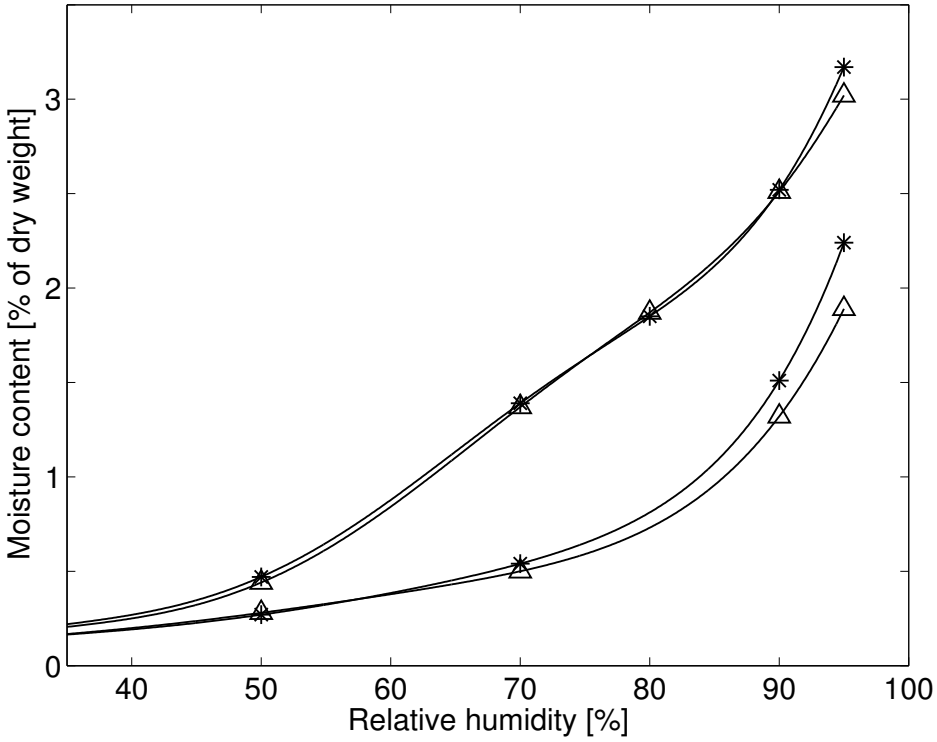

Figure 13 – Measurements performed on carbonated (triangles) and non-carbonated (stars) specimens of SLC A.

4 CONCLUSIONS

This study shows that self-levelling flooring compounds have a pronounced sorption hysteresis. Measured scanning curves indicate that when changing sorption mode, for example when adding water to a drying material, a small change in moisture content may result in a large change in RH. Normally RH is believed to be the index best describing critical levels for moisture related processes, such as chemical degradation and biological growth. However, for materials showing large hysteresis it may be necessary to also consider the influence of moisture content.

REFERENCES

1. Anderberg, A. and Wadsö, L., "Moisture in Self-levelling Flooring Compounds. Part I Diffusion Coefficients." *Nordic Concrete Research*, No. 32, 2004.
2. Fennema, O.R., "*Water and Ice"*, in *Food Chemistry*, O.R. Fennema, Editor. 1985, Marcel Dekker Inc. New York and Basel. pp. 23-67.
3. Bager, D.H. and Sellevold, E.J., "Ice formation in hardened cement paste, Part I - Room temperature cured pastes with variable moisture contents." *Cement and Concrete Research*, Vol. 16, 1986, pp. 709-720.
4. Adamson, A.W., "Physical Chemistry of Surfaces". 5th. John Wiley & Sons, Inc., 1990, 777 pp.
5. Labuza, T.P., Cassil, S., and Sinskey, A.J., "Stability of intermediate moisture foods. 2. Microbiology." *Journal of Food Science*, Vol. 37, 1972, pp. 160-162.
6. Bažant, Z.P. and Najjar, L.J., "Nonlinear water diffusion in nonsaturated concrete." Materials and Structures, Vol. 5No 25, 1972, pp. 3-20.
7. Nilsson, L.-O. "Temperature effects in relative humidity measurements on concrete - some preliminary results". Proceedings, Building physics in the Nordic countries. Lund 1987. pp. 456-462.
8. Jones, L. and Atkins, P., "Chemistry Molecules Matter and Change". 4th edition. W. H. Freeman and Company, New York, 2002., 998 pp.
9. Fog Nielsen, K., "Mould growth on building materials Secondary metabolites, mycotoxines and biomarkers" The Mycology group, Biocentrum-DTU. Technical University of Denmark: Lyngby. 2002, 80 pp.
10. Fagerlund, G., "Determination of pore size distribution by suction porosimetry." Materials and Structures, Vol. Vol. 6, No 33, 1973, pp. 191-201.
11. Fagerlund, G., "Determination of pore size distribution from freezing-point depression." Materials and Structures, Vol. Vol. 6, No 33, 1973, pp. 215-225.
12. Krus, M. and Kießl, K., "Determination of the moisture characteristics of porous capillary active materials." Materials and Structures, Vol. Vol. 31, 1998, pp. 522-529.
13. Janz, M., "Techique for Measuring Moisture Storage capacity at High Moisture Levels." Journal of Materials in Civil Engineering, Vol. September/October, 2001, pp. 364-370.
14. Zhang, L. and Glasser, F.P., "Critical examination of drying damage to cement pastes." Advances in cement research, Vol. 122, 2000, pp. 79-88.
15. Shimida, Y. and Young, J.F., "Structual changes during thermal dehydration of ettringit." Advances in cement research, Vol. 132, 2001, pp. 77-81.
16. Hoffman, A., "Effect of Redispersible Powders on the Properties of Self-Levelling Compounds". Technical paper, Wacker Polymer Systems, 20 pp.
17. Hébrard, A., et al., "Hydration properties of durum wheat semolina: influence of particle size and temperature." Powder Technology, Vol. 130, 2003, pp. 211-218.
18. Caro, Y., et al., "Plant Lipases: Biocatalyst Aqueous Environment in relation to Optimal Catalytic Activity in Lipase-Catalyzed Synthesis Reactions." Biotechnology and Bioengineering, Vol. 776, 2002, pp. 693-703.
19. Janz, M. and Johannesson, B.F., "Measurement of the Moisture Storage Capacity Using Sorption Balance and Pressure Extractors." Thermal Envelope & Building Science, Vol. 244, 2001, pp. 316-334.
20. Atkins, P.W., "Physical Chemistry". Sixth edition. Oxford University Press, 1998, 1014 pp.
21. Scrivener, K.L. "Historical and Present Day Applications of Calcium Aluminate Cements". Proceedings, International Conference on Calcium Aluminate Cements. Edinburgh, Scotland 2001. pp. 3-23.

22. Gaztañaga, M.T., Gonñi, S., and Guerrero, A. "Accelerated Carbonation of Calcium Aluminate Cement Paste". Proceedings, Calcium Aluminate Cements. Edinburgh, Scotland 2001. pp. 349-358.
23. Taylor, H.F.W., "Cement Chemistry". 2nd edition. Thomas Telford, London, 1997, 437 pp.